1-D Simulations of EGR on a Marine Diesel Engine using GT-Power

Author(s):
Cavadini, Matteo

Publication date:
2014

Permanent link:
https://doi.org/10.3929/ethz-a-010441353

Eidgenössische Technische Hochschule Zürich
Swiss Federal Institute of Technology Zurich

Laboratorium für Aerothermochemie und Verbrennungssysteme
Aerothermochemistry and Combustion Systems Laboratory

Master Thesis

1-D Simulations of EGR on a Marine Diesel Engine using GT-Power

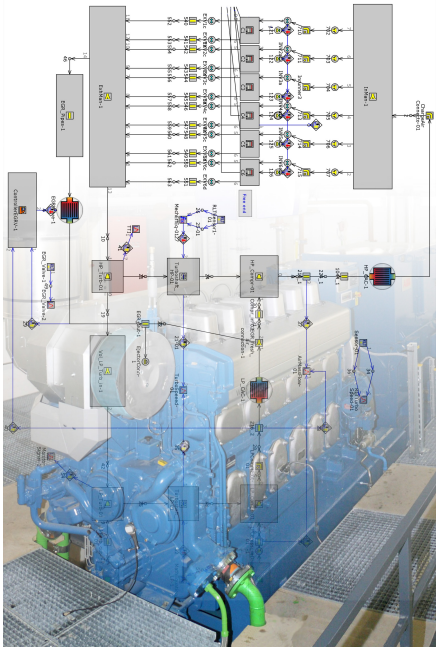

Aerothermochemistry and Combustion Systems Laboratory
Swiss Federal Institute of Technology (ETH) Zurich

Matteo Cavadini

FS 2014

Advisor:
Prof. Konstantinos Boulouchos

Supervisor:
Panagiotis Kyrtatos

Eidgenössische Technische Hochschule Zürich
Swiss Federal Institute of Technology Zurich

Institut für Energietechnik
LAV
Laboratorium für Aerothermochemie und Verbrennungssysteme
Prof. Dr. Konstantinos Boulouchos

STUDENT THESIS PROPOSAL SPRING SEMESTER 2013

1-D Simulations of EGR on a Marine Diesel Engine using GT-Power

Gaseous emissions such as nitrogen oxides (NO_x) from ship propulsion and power generation are becoming ever more important, due to environmental issues and corresponding government legislation. Past and ongoing experimental research on marine diesel engines has shown the possibility to reduce NO_x emissions through the combination of Miller valve timing, two-stage turbocharging and Exhaust Gas Recirculation (EGR).

The main aim of this project is to simulate different configurations for the EGR system on a 6-cylinder, two-stage turbocharged Wärtsilä medium speed diesel engine, and compare them in terms of overall engine efficiency, flexibility and projected component durability/wear. The simulations are to be performed using the 1-D simulation tool GT-Power, in which a full model of the engine setup without the EGR systems is available.

TASKS / GOALS

- Run GT-Power model to obtain target turbocharger efficiencies to be used.
- Change GT-Power model to add the different EGR configurations/paths.
- Simulate the different GT-Power configurations and compare them in terms of engine efficiency, engine/EGR rate flexibility and projected component wear
- Compare the simulation results to engine meaurements

THESIS TYPE AND DURATION

- ST/BT/MT
- Duration: 1 semester / 6 months

REQUIREMENTS

- Knowledge and understanding of IC engines is required
- Ability for independent research
- Knowledge of GT-Power is a plus

CONTACT

Panagiotis Kyrtatos
Institut für Energietechnik, ML 23
Sonneggstrassse 3, CH-8092 Zürich
+41 (44) 632 2475
kyrtatos@lav.mavt.ethz.ch

Acknowledgments

During this very interesting Master Thesis I had as usual some moments where I alone could not proceed straight forward as wished. Exactly then my supervisor, Panagiotis Kyrtatos, helped me to overcome these problems, giving me more precise explanations and deeply stimulating inputs to continue researching solutions and alternatives. Therefore I would like to address him special thanks.

A warm thank you also goes to my ex-colleagues from the internship at ABB Turbo Systems Ltd. (ZTA division, Baden) who have kindly allowed me to use their layout to represent the various engine, turbocharger and EGR path topologies simulated.

An important role also has played my whole family, without whom all this would not have been possible, supporting me during all Master semesters.

Least but not last I would like to send a big thank to my girlfriend to withstand my constant delays and my "I don't have time today, sorry, I'm working hard at my thesis." explanations.

You all have given me a beautiful intense 6 months of work.

Contents

List of Figures

List of Tables

Abstract

Actual Large Diesel Engines will not meet the always stricter imposed emissions regulations if not modified. A possible solution to reduce pollutant emissions would be given by the combination of Miller valve timing, two-stage turbocharging and Exhaust Gas Recirculation (EGR) technologies.

The scope of this project was to simulate and evaluate different EGR paths applied on a 6-cylinder, two-stage turbocharged Wärtsilä medium speed diesel engine and validate the results through matching of test bench engine runs measurements. Engine efficiencies, turbocharger efficiencies, engine and EGR rate flexibility as well as projected component wear were important key parameters that have been analyzed. 1-D simulations were carried out with the use of the Gamma Technologies vehicle simulation software GT-POWER®, part of the GT-SUITE®, the industry standard for engine simulations.

In this proposal 5 EGR configurations were examined:

- Semi-Short Route
- 1 Donor Cylinder Semi-Short Route
- 2 Donor Cylinders Short Route
- EGR Blower Short Route
- EGR Turbocharger Short Route

Simulation results shows that NO_x emissions can be effectively lowered through the implementation of an EGR system. This reduction will be obviously cost in terms of increased fuel consumption, increased thermal stress on the HP turbine as well as increased mechanical stress due to higher peak pressures in the cylinders. Varying the EGR path configuration and optimizing the TC components and specifications different results can be achieved with peculiar advantages and disadvantages for each choice. These results are consistent with existing literature and were confirmed by test bench measurements.

This research has a great importance because shows a fair and complete comparison between the performance of today most used and some of the new coming EGR technologies. Through simulations of different EGR paths, variation of key parameters, load and EGR rates the NO_x reduction potential has been highlighted and confirmed. All the benefits and drawbacks of each single EGR configuration is investigate and compared with each other and with the standard engine setup without EGR. A "best choice" configuration is finally pointed out and supported through exhaustive explanations.

Symbols

Symbols

B	Cylinder bore	$[m]$
c	Concentration	$[mol/mol]$
c_m	Mean piston speed	$[m/s]$
c_p	Heat Capacity	$[J/(g \cdot K]$
dS/dt	Entropy flow	$[W/K]$
E	Energy	$[J]$
EGR	EGR Rate	$[\%]$
F	Force	$[N]$
F_{prop}	Vehicle propulsion force	$[N]$
g	Acceleration due to gravity	$[m/s^2]$
H_l	Lower heating value	$[J/kg]$
HRR	Heat Release Rate	$[J/^\circ CA]$
m	Mass	$[kg]$
m_f	Fuel mass	$[kg]$
$\dot{m}_f$	Fuel mass flow	$[kg/s]$
N_z	Engine type parameter (two/four stroke)	$[-]$
p	Pressure	$[Pa]$
p_{me}	Mean effective pressure	$[Pa]$
p_{mf}	Fuel effective pressure	$[Pa]$
$p_{m,loss}$	Losses effective pressure	$[Pa]$
P	Power	$[W]$
P_e	Mechanical engine power	$[W]$
P_V	Vehicle propulsion power	$[W]$
q	Displacement	$[-]$
q	Volumetric flow	$[m^3/s]$
r	Radius	$[m]$
S	Cylinder stroke	$[m]$
SOI	Start Of Injection	$[^\circ CA\ bTDC]$
t	Time	$[s]$
T	Time	$[s]$
T	Torque	$[Nm]$
v	Velocity	$[m/s]$
V	Velocity	$[m/s]$
V_d	Displacement volume	$[m^3]$

z	Number of cylinders	$[-]$
γ	Gear ratio	$[-]$
η	Efficiency coefficient	$[-]$
η_m	Mechanical efficiency	$[-]$
$\eta_T C$	Turbocharging efficiency	$[-]$
Θ	Moment of inertia	$[-]$
Π	Pressure Ratio	$[kg/m^3]$
ρ_{air}	Density of air	$[kg/m^3]$
ω	Angular velocity	$[rad/s]$

Indices

0	Nominal
air	Air
C	Compressor
Com	Compression
$comp$	Compressor
eng	Engine
Exp	Expansion
f	Final
f	Fuel
$full$	Full Load Conditions
i	Inlet
HP	High Pressure
i	Initial
ICE	Internal Combustion Engine
$loss$	Losses
LP	Low Pressure
m	Motor
max	Maximal
min	Minmal
o	Outlet
T	Turbine
$turb$	Turbine
TC	Turbocharger
tot	Total

Acronyms and Abbreviations

a	after
b	before
BDC	Bottom Dead Center
BMEP	Brake Mean Effective Pressure
BSFC	Brake Specific Fuel Consumption
C	Compressor
CCEM	Competence Center Energy and Mobility
CIMAC	Conseil International Des Machines A Combustion
CO	Carbon Oxide
CO_2	Carbon Dioxide
ECA	Emission Control Area
EGR	Exhaust Gas Recirculation
EPA	Environmental Protection Agency
ETH	Eidgenössische Technische Hochschule
EURO	European Emissions Standards
FC	Fuel Consumption
FEM	Full Engine Model
FMEP	Friction Mean Effective Pressure
FRM	Fast Running Model
GPS	Global Positioning System
HFO	Heavy Fuel Oil
HP	High Pressure
ICE	Internal Combustion Engine
IMEP	Indicated Mean Effective Pressure
IMO	International Maritime Organization
LAV	Laboratorium für Aerothermochemie und Verbrennungssysteme
LERF	Large Engine Research Facility
LP	Low Pressure
MEP	Mean Effective Pressure
NO	Nitric Oxide
NO_2	Nitrogen Dioxide
NO_x	Nitrus Oxides
O_2	Oxygen
OECD	Organisation for Economic Cooperation and Development
PM	Particulate Matter
PR	Pressure Ratio
PSI	Paul Scherrer Institute
SCR	Selective Catalytic Reduction
T	Turbine
TDC	Top Dead Center
TTI	Temperature Turbine Inlet
VIC	Variable Inlet Valve Closure
VTG	Variable Turbine Geometry
VVT	Variable Valve Timing

Chapter 1

Introduction

1.1 Project Motivation

Internal Combustion Engines are today the preferred choice for electricity generation and for propulsion of many vehicles, from small light cars or motorbikes to large vessels. Due to an increasing environmental awareness pollutants emissions of these engines are constantly reduced in oder to meet the always stricter imposed regulations (e.g. EURO and EPA emissions limits for passenger cars and trucks, etc.).

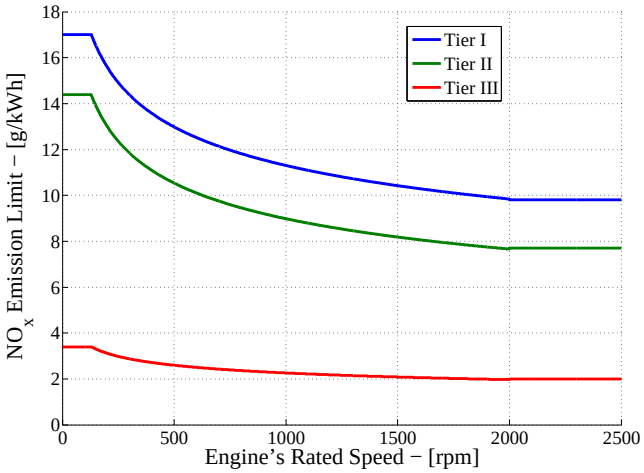

Figure 1.1: Nitrogen Oxides (NO_x) - IMO Tier Regulation.

In the marine technology field the new regulation IMO Tier III starting from 2016 will drastically reduce the allowable total weighted cycle NO_x emissions limits (i.e. about 80% lower emissions levels with respect to the Tier I limit, see Figure 1.1). The NO_x control requirements will apply to installed marine diesel engine of over 130 kW output power other than those used solely for emergency purposes irrespective of the tonnage of the ship onto which such engines are installed [25]. Different levels (Tiers) of control apply based on the ship construction date and within any particular Tier the actual limit value is determined from the engine's rated speed (as specified in Table 1.1). The Tier III controls apply only to the specified ships while operating in Emission Control Areas (ECAs) established to

limit NO_x emissions, outside such areas the Tier II controls apply.

Tier	**Ship construction date on or after**	**Total NO_x emission limit (g/kWh) n = engine's rated speed (rpm)**		
		$n < 130$	$130 < n < 1999$	$n \geq 2000$
I	1 January 2000	17.0	$45 \cdot n^{-0.20}$	9.8
II	1 January 2011	14.4	$44 \cdot n^{-0.23}$	7.7
III	1 January 2016[1]	3.4	$9 \cdot n^{-0.20}$	2.0

Table 1.1: Nitrogen Oxides (NO_x) - IMO Tier Regulation.

Actual large diesel engine technology is not capable to reduce the emissions levels enough in order to stay within these limits. Possible solutions to reduce emissions would be given by the use of an after-treatment system or by the combination of Miller valve timing, two-stage turbocharging and Exhaust Gas Recirculation (EGR) technologies.

Reducing NO_x emissions through an after-treatment system means developing and assemble a Selective Catalytic Reduction (SCR) complex which will need a considerable amount of space and logistics. This would probably restrict this choice to stationary power plants. Exhaust Gas Recirculation (EGR) systems present a much compacter solution for NO_x reduction, which could lead to be the preferred choice for mobile applications like marine and traction.

Because of the near in the future deadline of the new IMO Tier III emission limits, engine manufacturer and engineering teams in this sector are working hard to develop on one hand cleaner engines and on the other hand EGR solutions which could cut down NO_x concentration in the exhaust without loosing too much in terms of efficiency and therefore fuel consumption.

Past and ongoing experimental research on marine diesel engines has shown the possibility to reduce NO_x emissions through the combination of Miller valve timing, two-stage turbocharging and Exhaust Gas Recirculation (EGR) [13, 34, 39, 43]. This well known trade-off between engine pollutant emissions, efficiency and fuel consumption rends the task very challenging and hard to solve. Because in these large diesel engines a positive scavenging pressure (the intake pressure is higher than the exhaust pressure) is needed in order to cool the critical component of the exhaust valve, the recirculation of the exhaust gases needs a pumping device to overcome the pressure difference between exhaust and intake manifold. Thus many possible layouts of the EGR path can be implemented, inserting another variable into the problem. In order to demonstrate the validity of this technology, in its many ways, and to compare various possible configurations in terms of efficiency, durability and flexibility this master thesis has been originated. For these and other legitimate reasons it makes sense to look closely at EGR technology for NO_x reduction and their potential.

[1] Subject to a technical review to be concluded 2013 this date could be delayed, regulation 13.10

1.2 Project Overview

1.2.1 Competence Center Energy And Mobility Project

The following master thesis is part of the contribution given by the ETH Zurich to the project named "In-cylinder emission reduction in large diesel engines (NO_x-Reduction)" actually on-going at the Competence Center Energy and Mobility (CCEM) facility center.

The vision of the Competence Center Energy and Mobility (CCEM-CH) is a more sustainable energy system, which provides the energy services required for economic growth with strongly reduced primary energy input. The system meets the societal demand for services in an economically affordable and environmentally compatible manner, thereby preserving the earth's climate. The 2000 Watt society[2] is a metaphor for such a system.

The mission of the Center is a contribution towards reducing the CO_2 emissions of the Swiss energy system, and to enhancing security of supply by decreasing the dependence on imported fossil energy carriers. For targeting a significant impact on society, projects will be designed together with stakeholders, and will strengthen the competitiveness of Swiss industry by development of new and innovative systems, products, and services.

Institutions and laboratories from the ETH Domain and the Universities of Applied Sciences form alliances with industrial partners to engage in large projects targeting a measurable impact in the areas of Mobility, Electricity Production, and the Heat and Buildings sector.

Within the transportation sector, high growth rates are associated with important environmental impacts and an almost exclusive dependence on liquid fossil fuels. Therefore, the following themes have been selected:

- Low carbon fuels - methane from biomass with over 60% efficiency at competitive cost, and hydrogen produced CO_2-free and more economically than with the present renewable benchmark, complemented by electricity for purely electric battery-powered propulsion.
- Clean freight transport approaching the "zero impact" limit.
- Efficient passenger transport - hybrids based on advanced storage systems (4 times improved specifications) and internal combustion engines or fuel cells that lower the fleet fuel consumption towards the core target of 3 liters equivalent per 100 km.

Part of the second point listed above is the project "In-cylinder emission reduction in large diesel engines (NO_x-Reduction)".

As primary outcome of this collaborative effort the project team expects a significant technological progress towards an efficient, clean burning diesel engine that does not require exhaust gas after treatment to further reduce NO_x or particulate emissions.

[2]The 2000 W Society is a vision promoted by the Board of the Swiss Federal Institutes of Technology aiming at a sustainable society regarding eco-logical, economic as well as societal aspects. It postulates a total primary energy use of some 65 GJ per capita and year within the second half of this century, which equals an average power consumption of 2000 W per capita. Today the average Swiss citizen has a total primary energy use of about 5000 W.

One goal is set in the thorough comprehension of the physiochemical processes involved governing the NO_x and soot formation under the combined application of Miller inlet valve timing with 2-stage turbocharging and EGR, water-in-fuel emulsions and pilot injections.

This understanding will yield a second key deliverable, namely a fast numerical algorithm based on phenomenological models incorporating the new technological approach and having good predictions for NO_x and soot.

The Large Engine Research Facility (LERF) at Paul Scherrer Institute (PSI) has been successfully established as a research platform for testing the NO_x reduction potential when using Miller valve timing in combination with serial 2-stage turbocharging (MT/S2TC). In past research, a significant NO_x reduction potential using this technology has been confirmed. It also became clear, however, that the stringent legislative limits set to enact in 2016 by the International Maritime Organization (IMO) cannot be reached using this technology alone and that additional measures are needed. The current project aims at combining additional measures with the already implemented approach to further reduce specific NO_x emissions towards the required limit, while maintaining low CO_2 emissions and close-to-zero soot emissions.

The team has conceived three different technological advancements to be tested individually and combined in conjunction with Miller timing and 2-stage turbo charging.

The main technological building block will focus on the arrangement of Exhaust Gas Recirculation (EGR) together with MT/S2TC. This combination has the largest potential for meeting the NO_x emission limits, but it is also expected to generate significantly increased particulate emissions.

The second technological building block involves using water-in-fuel emulsions (WFE), which has positive effects on both NO_x and particulate emissions.

The third building block uses multiple fuel injections as means to shorten the ignition delay and thus reduce the amount of premixed combustion, a need for which has been highlighted in prior research concerning extreme Miller valve timing to allow further reduction of NO_x emissions.

Due to the generic nature of the problem, industry-relevant results from the LERF must be anchored on a fundamental understanding of the underlying mechanisms. To achieve this, the individual technological building blocks will be studied experimentally in different setups as well as computationally.

Besides the 6-cylinder engine at PSI we will investigate the new technologies on a 1-cylinder MTU engine at ETHZ and at the newly refurbished constant volume combustion cell (HTDZ) at PSI. Using the three platforms the team is able to cover the complex system behavior and address system integration issues on the 6-cylinder engine, study processes in a more controlled environment on the 1-cylinder engine, and obtain fundamental understanding of the modified combustion through optical access to the flame at the HTDZ.

In parallel, 3D simulation work based mainly on results from the HTDZ will allow the in-depth investigation of spray and combustion characteristics. All experimental and simulation results will be used to create an industry-relevant, fast phenomenological model for NO_x and particulate formation/oxidation which in turn will aid the optimization towards an efficient, clean burning and low emission diesel engine for the future.

In the project, two worldwide leading companies (ABB Turbo Systems, Wärtsilä FI) will participate with additional funding and significant resources and are ex-

pected to substantially profit from the planned developments. If successful, this research effort will allow for the first time to perform fast, predictive modeling of efficiency and emissions of large diesel engines when using a variety of promising future technologies. [2, 24]

1.2.2 Thesis Project

The scope of this project was to simulate and evaluate different EGR paths applied on a 6-cylinder, two-stage turbocharged Wärtsilä medium speed diesel engine (see Section 1.3) and validate the results through matching of test bench engine runs measurements. Engine efficiencies, turbocharger efficiencies, engine and EGR rate flexibility as well as projected component wear were important key parameters that have been analyzed. 1-D simulations were carried out with the use of the Gamma Technologies vehicle simulation software GT-POWER®, part of the GT-SUITE®, the industry standard for engine simulations.

A theoretical background part at the beginning of the thesis report (see Chapter 2) permit to explain to the reader the important basic knowledge concerning NO_x emissions and the technologies used to reduce them, i.e. EGR, two-stage Turbocharging, Miller Timing, SCR.

Starting point of the thesis was an already existing GT-POWER® engine model with fully implemented geometry, i.e. engine parameters, piping geometry, TC configurations and maps, etc. were taken from the actual test bench setup and applied in the simulation model (see Section 3.1). The existing model reflected the starting test bench situation, which did not include any EGR solution.

For simulation time reasons the full model has been then simplified (see Section 3.2) to a Fast Running Model (FRM) leading to a radical increase in computational speed. After recalibration, this model has been taken as the basis to create the various models with different EGR configurations and EGR rates (between 10% and 30% by mass).

In this proposal 5 EGR configurations were examined (see Section 3.3):

- Semi-Short Route
- 1 Donor Cylinder Semi-Short Route
- 2 Donor Cylinders Short Route
- EGR Blower Short Route
- EGR Turbocharger Short Route

Except for the EGR Blower, which needs a mandatory rematch in order to run, and the EGR Turbocharger Short Route configuration, which needs a challenging control strategy, all the other EGR paths were simulated with the current engine & turbocharging configuration (standard). After that an optimization at full load condition has been performed for all EGR configurations. The TC specifications (both Low Pressure and High Pressure Turbochargers) were changed in order to get minimal BSFC keeping in mind important constrains given by the HP turbine inlet temperature (maximum 540 $°C$) and the target EGR rate chosen for optimization (25% EGR by mass). All the configurations were compared with each other, with

their optimized case and with the case without EGR.

For the Semi-Short and EGR Blower configuration an additional study has been carried out for the full load condition. Here the Split (the ratio of low pressure and high pressure compressor ratio) has been varied, once by holding the intake pressure constant and once by keeping the HP turbine inlet temperature at the maximal allowable value. The Turbocharging Efficiency has been then calculated and the corresponding curves were compared and analyzed.

The Semi-Short configuration could be compared with the test bench measurements because they were implemented in the time period of the thesis. These measurements were used partly to calibrate the simulation model and partly to validate the simulation's results.

After becoming aware of each configuration's advantages and disadvantages the 1 Donor Cylinder Semi-Short solution has been adopted on the test bench for further runs. To check the engine overall performance and constrains additional simulation has been done for the newly chosen key parameter values (like TC maps).

Lastly a brief NO_x emissions analysis was carried out (see Section 3.4). After a simple model calibration various simulations were used to check the predicted value of pollutant emissions for different load points, EGR rates, injection rail pressure and injection timing. Due to the lack of measurements points, the difficulty and the time expensive task of a good NO_x model calibration results only in the ability to estimate NO_x reduction (relative) but not in absolute values.

Results from the simulations, comparisons and NO_x modeling analysis have been summarized in the Chapter 4.

Simulation results show that NO_x emissions can be effectively lowered through the implementation of every one of these solutions. At high load conditions, in case of EGR rates over 20% about 75% NO_x reduction is expected. A very important result is that by the implementation of one of the EGR solution on the Wärtsilä test engine experimented through simulations, the IMO Tier III limitation can be fulfilled.

This NO_x reduction results in increased fuel consumption (about $2 - 5\ g/kWh$ at full load), increased thermal stress on the HP turbine as well as increased mechanical stress due to higher peak pressures in the cylinders. Varying the EGR path configuration and optimizing the TC components and specifications different results can be achieved with specific advantages and disadvantages for each choice.

A further adjustment of the rail pressure and of the injection timing would lead to a lower fuel consumption increasing minimally the NO_x emissions. Concluding using this strategy has been shown that a part of the BSFC increase due to the use of an EGR system could be regained paying only though a very small increase in emissions. These results are consistent with existing literature and were confirmed by the first set of test bench measurements.

1.3 Test Bench Setup

The test engine used in the laboratory exercise is a 6-cylinder, two-stage turbocharged medium speed diesel engine, a Wärtsilä 6L20 characterized by the following data:

Combustion System	Direct Injection Diesel 4-Stroke
Cylinders Arrangement	In-Line
Number of Cylinders	6 [–]
Firing Order	$1-5-3-6-2-4$
Bore	200 $[mm]$
Stroke	280 $[mm]$
Connecting Rod Length	510 $[mm]$
Compression Ratio	16 [–]
TDC Clearance Height	12 $[mm]$
Displacement Volume	8.796 $[L]$
Clearance Volume	0.586 $[L]$
Nominal Speed	1000 $[rpm]$
Rated BMEP	24.60 $[bar]$
Rated Power	1080 $[kW]$
Rated Mean Piston Speed	9.333 $[m/s]$
Max. Cylinder Pressure	180 $[bar]$
Max. HP TTI	540 $[°C]$
Fuel Injection System	L'Orange Common Rail
Fuel Injection Pressure	$1000-1500$ $[bar]$
Number of Injector Orifices	9 [–]
Air Charging	Two-Stage Turbocharging
Turbocharging System	Based on ABB Turbo Systems
LP Turbocharger	TPS 52-E
HP Turbocharger	TPS 44-F
Valve Train System	Wärtsilä variable inlet valve closure (VIC)
Valves per Cylinder	4 [–]
Inlet Valve Closing (IVC)	69.0 (70.0)[3] $[°bBDC]$
Inlet Valve Closing (IVC) (Miller)	28.8 (84.4)[3] $[°aBDC]$
Inlet Valve Opening (IVO)	11.4 (6.6)[3] $[°bTDC]$
Exhaust Valve Opening (EVO)	42.2 (36.0)[3] $[°bBDC]$
Exhaust Valve Closing (EVC)	22.8 (22.0)[3] $[°aTDC]$
Exhaust System	Single-pulse / 3-pulse

Table 1.2: Specification of the research diesel engine at the test bench.

The test engine allows also the modification of cam profile which was simulated during this research. Additionally are used all the required sensors in order to measure the data concerning the engine, like engine speed, engine torque, engine power, air and fuel consumption, various temperatures and pressures, in-cylinder pressure, injection timing and pressure, and concerning the exhaust gas, like O_2, CO_2, NO_x, Soot concentration sensors. For the Turbochargers' components their speed is measured. All the important measured values can be found in the Appendix A.

More information on the test-bed setup and measurement equipment and techniques can be found in [32], [31] and [51].

[3]Values for M80 Cam Profile.

The experiments were set as follows: running the engine at constant rated speed of 1000 rpm and changing:

- Load: from 10% to 100% (maximal 90% load for EGR Setup, because 100% load can not run for security reasons, critical temperature limits are reached).
- EGR Rate: between 0% (no EGR) and 35% EGR by mass fractions.
- Start Of Injection: from 2 to 15 $°CA\ bTDC$ depending on the engine load.
- Rail Pressure: between 1000 and 1500 bar depending on the engine load.

For each combination of these variations all values are recorded. With the measurement of the cylinder pressures the Heat Release Rate (HRR) can be evaluated. After the data have been recorded and stored, it is possible to look for relationships between them and determine the trade-off between emissions and efficiency.

A single type of conventional diesel fuel was used throughout the experimental procedure. Data for the fuel are shown in Table 1.3.

Density at 15°C	kg/m^3	836.1
Viscosity at 40°C	mm^2/s	2.576
Cetane Number	$-$	51
Distillation Analysis:		
at 180°C	$Vol.\%$	0.9
at 250°C	$Vol.\%$	37.8
at 340°C	$Vol.\%$	95.4
at 350°C	$Vol.\%$	98.4
Distillation Start	°C	171
10% Temperature	°C	208
50% Temperature	°C	266
90% Temperature	°C	323
95% Temperature	°C	338

Table 1.3: Diesel Fuel Analysis Results.

Chapter 2

Theoretical Background

2.1 NO_x Emissions

2.1.1 Nature Of The Problem

Diesel engines are a well-known source of air pollution. Engine exhaust gases contain:

- Oxides of Nitrogen: nitric oxide NO, and small amounts of nitrogen dioxide NO_2, collectively known as NO_x.
- Oxides of Carbon: carbon monoxide CO and carbon dioxide CO_2.
- Organic Compounds: unburned or partially burned hydrocarbons HC.
- Particulate Matter: small particulate emissions ($-0.1\ \mu m$ diameter) particles which consists primarily of soot with some additional absorbed hydrocarbon material.

The relative amounts depend on the engine design and operating conditions, but for the case of a marine engine limitations are imposed as follow [1, 25]:

- NO_x: engine's rated speed dependent following the IMO Tier limitations illustrated in the Figure 1.1 and Table 1.1 from Section 1.1.
- HC: for Tier II and later engines is 2.0 $[g/kWh]$.
- CO: for Tier II and later engines is 5.0 $[g/kWh]$.
- PM: no standards apply for this engine's category, PM emissions must be measured for certification testing and reported.

In the diesel engine, the fuel is injected into the cylinder just before combustion starts, so throughout most of the critical parts of the cycle the fuel distribution is nonuniform. The pollutant formation processes are strongly dependent on the fuel distribution and how that distribution changes with time due to mixing.

Figure 2.1 illustrates how various parts of the fuel jet and the flame affect the formation of NO_x, unburned HC, and soot (or particulate matter) during the "premixed" and "mixing-controlled" phases of diesel combustion in a direct-injection engine with swirl.

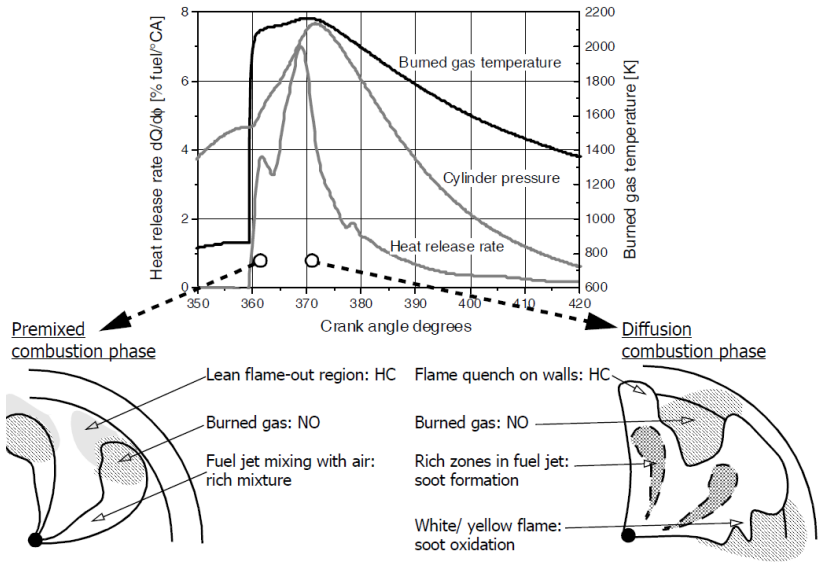

Figure 2.1: Pollutant emissions formation in direct-injected diesel engines for both premixed and diffusion combustion phase [30].

Soot forms in the rich unburned-fuel-containing core of the fuel sprays, within the flame region, where the fuel vapor is heated by mixing with hot burned gases. Soot then oxidizes in the flame zone when it contacts oxygen, giving rise to the yellow luminous character of the flame.

Hydrocarbons and aldehydes originate in regions where the flame quenches both on the walls and where excessive dilution with air prevents the combustion process from either starting or going to completion.

Nitric oxide forms in the high-temperature burned gas regions, but temperature and fuel/air ratio distributions within the burned gases are now nonuniform and formation rates are highest in the close-to-stoichiometric regions. Effects of this pollution sure are very harmful; firstly NO_x reacts to create photochemical smog, which can cause damages to the lungs, then the reaction of NO_x with water (see following Equations 2.1 - 2.3) create nitric acid (HNO_3) which are responsible for the acid rain and lastly NO_x contributes to the ozone depletion.

$$2\ NO_2 + H_2O \rightarrow HNO_2 + HNO_3 \tag{2.1}$$

$$3\ HNO_2 \rightarrow HNO_3 + 2\ NO + H_2O \tag{2.2}$$

$$4\ NO + 3\ O_2 + 2\ H_2O \rightarrow 4\ HNO_3 \tag{2.3}$$

For some pollutant species, e.g., carbon monoxide, organic compounds, and particulate matter, the formation and destruction reactions are intimately coupled with the primary fuel combustion process. Thus an understanding of the formation of these species requires knowledge of the combustion chemistry. For nitrogen oxides and sulfur oxides (emissions coming from the sulfur content present in very small amount in almost all heavy fuel oil used in marine engines), the formation and destruction processes are not part of the fuel combustion process. However, the reactions which produce these species take place in an environment created by the combustion reactions, so the two processes are still intimately linked. [22]

2.1.2 Kinetics Of NO_x Formation

Nitric oxides (NO_x) form throughout the high-temperature burned gases behind the flame through chemical reactions involving nitrogen and oxygen atoms and molecules, which do not attain chemical equilibrium. The higher the burned gas temperature, the higher the rate of formation of NO_x. As the burned gases cool during the expansion stroke the reactions involving NO_x freeze, and leave NO_x concentrations far in excess of levels corresponding to equilibrium at exhaust conditions (see Figure 2.2).

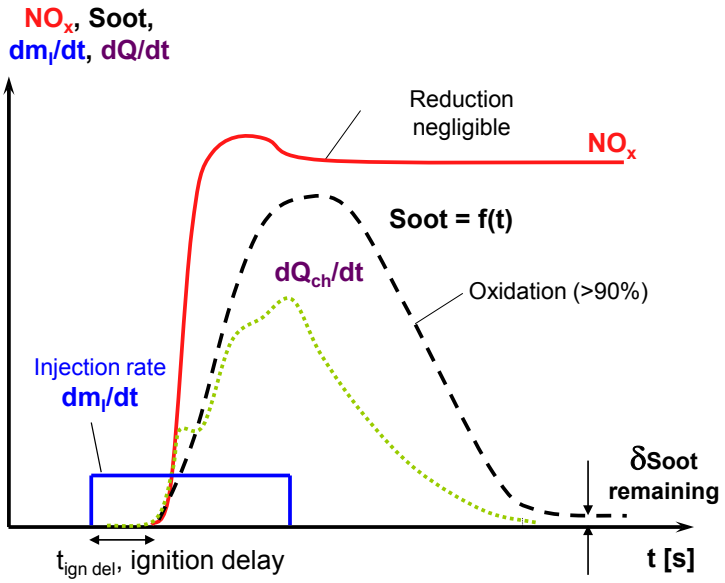

Figure 2.2: The freezing process consequently keep high NO_x emissions, while soot after been produced is almost completely oxidized [30].

While nitric oxide (NO) and nitrogen dioxide (NO_2) are usually grouped together as NO_x emissions, nitric oxide is the predominant oxide produced inside the engine cylinder. The principal source of NO is the oxidation of atmospheric (molecular) nitrogen. However, if the fuel contains significant nitrogen, the oxidation of the fuel nitrogen-containing compounds is an additional source of NO.

The most important NO formation mechanisms can be resumed into four categories:

1. Thermal NO (also called Zeldovich mechanism)
2. Prompt NO (also called Fenimore mechanism)
3. Nitrous NO (from N_2O)
4. Fuel NO

The first two mechanisms are very important and principal source of NO emissions in marine diesel engines. The third mechanism becomes important in the case where the first two produce only very low levels of NO emissions. The last mechanism becomes very important in coal combustion or in the combustion of heavy fuel oils with nitrogen content over 0.4% in mass [50].

Thermal NO Formation

The mechanism of NO formation from atmospheric nitrogen has been studied extensively. The so-called extended Zeldovich mechanism is the most used model to describe thermal NO formation (and its destruction). The denomination "thermal" comes from the very high activation energy needed for the reactions to brake the triple N_2-bond, which means that sufficiently fast production rates are achievable only at very high temperatures (above 2000 K).

Zeldovich was the first to suggest the importance of reactions 2.4 and 2.5. Lavoie et al. added reaction 2.6 to the mechanism, which contributes significantly to the correct estimation of NO emissions.

$$O + N_2 \overset{k_1}{\longleftrightarrow} NO + N \tag{2.4}$$

$$N + O_2 \overset{k_2}{\longleftrightarrow} NO + O \tag{2.5}$$

$$N + OH \overset{k_3}{\longleftrightarrow} NO + H \tag{2.6}$$

Each of these elementary chemical equations have a reaction rate constant that should be determinate experimentally. Some of the usual values present in the literature are presented in the Table 2.1.

Reaction i	$\boldsymbol{k_{i,r}}$ $\boldsymbol{[cm^3/(mol \cdot s)]}$	**Author**
1	$1.8 \cdot 10^4 \cdot exp\left(-\frac{38400}{T}\right)$	[5]
	$0.544 \cdot 10^{14} \cdot T^{0.1} \cdot exp\left(-\frac{38020}{T}\right)$	[45]
	$0.76 \cdot 10^{14} \cdot exp\left(-\frac{38000}{T}\right)$	[22]
2	$6.4 \cdot 10^9 \cdot T \cdot exp\left(-\frac{3150}{T}\right)$	[6]
	$9.0 \cdot 10^9 \cdot T \cdot exp\left(-\frac{3280}{T}\right)$	[45]
	$1.48 \cdot 10^8 \cdot T^{1.5} \cdot exp\left(-\frac{2860}{T}\right)$	[41]
3	$3.0 \cdot 10^{13}$	[6]
	$3.36 \cdot 10^{13} \cdot exp\left(-\frac{195}{T}\right)$	[45]
	$4.1 \cdot 10^{13}$	[22]

Table 2.1: Forward reactions coefficients for the Zeldovich mechanism.

The NO formation rate is obtained from the reaction equations 2.4 to 2.6 and

gives:

$$\begin{aligned}\frac{d[NO]}{dt} &= k_{1,r} \cdot [O][N_2] + k_{2,r} \cdot [N][O_2] + k_{3,r} \cdot [N][OH] \\ &\quad -k_{1,l} \cdot [NO][N] - k_{2,l} \cdot [NO][O] - k_{3,l} \cdot [NO][H]\end{aligned} \tag{2.7}$$

And for the time dependent change in nitrogen concentration the following applies:

$$\begin{aligned}\frac{d[N]}{dt} &= k_{1,r} \cdot [O][N_2] - k_{2,r} \cdot [N][O_2] - k_{3,r} \cdot [N][OH] \\ &\quad -k_{1,l} \cdot [NO][N] + k_{2,l} \cdot [NO][O] + k_{3,l} \cdot [NO][H]\end{aligned} \tag{2.8}$$

If the instantaneous NO concentration is below the equilibrium concentration at the corresponding temperature, as it is in most cases for the engine combustion, the forward reaction has a significant impact on total product. Only when the instantaneous NO concentration is above the equilibrium concentration at the corresponding temperature, the total revenue is largely determined by the reverse reaction. However, in engines, this situation occurs mostly to the end of the expansion stroke when the temperature has already fallen far under the freezing temperature (temperature under which no reactions occur).

The rate constants for the forward reactions show that the formation of NO via the reaction 2.4 is much slower than by the reactions 2.5 and 2.6. This slow reaction, which will be the rate-determining step, needs high enough temperature to break the N_2 triple bond, therefore the "thermal" designation.

Because of this strong temperature dependence, the NO formation process is called a kinetically controlled formation. This means that the chemical reaction kinetics, at the temperatures present in the combustion chamber, are slow compared to the physical time-scale of the flow field and that the chemical equilibrium cannot therefore be achieved.

The reaction kinetics of the two forward reactions 2.5 and 2.6 are clearly faster than reaction 2.4, thus the N produced in the first step will immediately react to other NO as described in the second and third step. This leads to the simplification of quasi-steady N concentration during the whole process, i.e.:

$$\frac{d[N]}{dt} \approx 0 \tag{2.9}$$

Consequently the Equations 2.7 and 2.8 can be rewritten to:

$$\frac{d[NO]}{dt} = 2 \cdot k_{1,r} \cdot [O][N_2] - k_{1,l} \cdot [NO][N] \tag{2.10}$$

For a simplified estimation of the NO production, the backward reaction can be neglected due to the freezing process typic for internal combustion engines. Equation 2.10 will then be:

$$\frac{d[NO]}{dt} = 2 \cdot k_{1,r} \cdot [O][N_2] \tag{2.11}$$

This simplified equation should be seen only as a rough approximation of NO emissions, since it predicts a too high concentration. Reason is that the (although slightly) reverse reactions of Equations 2.4 to 2.6 slow down the actual NO production and towards the end of the working cycle, can even cause a slight decrease in NO concentration.

Prompt NO Formation

The formation of Prompt-NO in the flame front itself is much more complicated than the Thermal-NO formation, because this process is very closely associated with the formation of the CH-radicals, which can react in many different ways. The so-called Prompt-NO formation was first described by Fenimore [15]. In the rate-limiting step reacts intermediate formed CH with N_2 to HCN (Hydrogen Cyanide) and then quickly replaced by NO further,

$$CH + N_2 \xrightarrow{k_9} HCN + N \rightarrow ... \rightarrow NO \tag{2.12}$$

with

$$k_{9,r} = 4.4 \cdot 10^9 \cdot exp\left(-\frac{11060}{T}\right) \quad \left[\frac{m^3}{kmol \cdot s}\right] \tag{2.13}$$

Ethyne (acetylene, C_2H_2) as the precursor of the CH-radicals is formed only under fuel-rich conditions in the flame front, hence the term "Prompt-NO". Because of the relatively low activation energy of the reaction, the Prompt-NO formation already takes place at temperatures of about 1000 K. For the oxidation of HCN and CN are the following reactions

$$HCN + O \xrightarrow{k_{10}} NCO + H \tag{2.14}$$

$$CN + O_2 \xrightarrow{k_{11}} NCO + O \tag{2.15}$$

$$HCN + OH \xleftrightarrow{k_{12}} CN + H_2O \tag{2.16}$$

with the rate-limiting production rate coefficients

$$k_{10,r} = 2.3 \cdot 10^4 \cdot T^{1.71} \cdot exp\left(-\frac{3521}{T}\right) \quad \left[\frac{m^3}{kmol \cdot s}\right] \tag{2.17}$$

$$k_{11,r} = 8.7 \cdot 10^9 \cdot exp\left(\frac{216}{T}\right) \quad \left[\frac{m^3}{kmol \cdot s}\right] \tag{2.18}$$

$$k_{12,r} = 4.7 \cdot 10^9 \cdot exp\left(-\frac{5174}{T}\right) \quad \left[\frac{m^3}{kmol \cdot s}\right] \tag{2.19}$$

$$k_{12,l} = 7.4 \cdot 10^9 \cdot exp\left(-\frac{3715}{T}\right) \quad \left[\frac{m^3}{kmol \cdot s}\right] \tag{2.20}$$

Because the follow-up reaction (of NCO to NO) is in comparison relatively fast, it approximately applies for the Prompt-NO formation

$$\frac{d[NO]}{dt} = k_{10,r} \cdot [HCN][O] + k_{11,r} \cdot [CN][O_2] \tag{2.21}$$

Basically, the information available in the literature regarding the reaction constant $k_{9,r}$, the rate-limiting reaction 2.12 are still inconsistent [50]. Therefore, the calculation of Prompt-NO formation is also associated with a much greater uncertainty than the calculation of the Thermal-NO. However, on the basis of an estimation of the products of reaction 2.12 shows that the Prompt-NO in contrast to the Thermal-NO, see reaction 2.4, is not as strongly temperature dependent (due to a lower activation temperature), but for CH and HCN strongly dependent on the local fuel concentration.

In the combustion engines about $5\% - 10\%$ of nitrogen oxides occurs over the Fenimore mechanism (Prompt-NO) and $90\% - 95\%$ over the Zeldovich mechanism (Thermal-NO).

Nitrous NO Formation

This reaction mechanism is then of importance when lean fuel-air mixtures suppress the formation of CH and so less Prompt-NO is formed and if persistently low temperatures suppress the formation of Thermal-NO.

N_2O is formed analogously to the first and rate-limiting reaction of the Zeldovich mechanism,

$$N_2 + O + M \longrightarrow N_2O + M \tag{2.22}$$

The stabilization is done by a molecule M, so that N_2O and not NO is produced. The NO formation is then carried out by oxidation of corresponding N_2O

$$N_2O + O \longrightarrow NO + NO \tag{2.23}$$

Because the N_2O is formed only in a three-body collision reaction, this reaction preferably proceeds at high pressures. Low temperatures barely slow down this reaction. the NO formed over the reaction of N_2O is the major NO source for lean premixed combustion in gas turbines. This mechanism, however, is also to be observed for lean burning Otto engines.

Fuel NO Formation

One of the major sources of NO production from nitrogen-bearing fuels such as certain coals and heavy fuel oils, is the conversion of fuel bound nitrogen to NO during combustion [8]. During combustion, the nitrogen bound in the fuel is released as a free radical and ultimately forms free N_2, or NO. Fuel-NO is formed at temperatures around 1100 K mainly in the flame front and can contribute as much as 50% of total emissions when combusting oil and as much as 80% when combusting coal.

Although the complete mechanism is not fully understood, there are two primary paths of formation.

The first and major source of Fuel-NO_x involves the oxidation of volatile nitrogen species during the initial stages of combustion. During the release and prior to the oxidation of the volatiles, nitrogen reacts to form several intermediaries which are then oxidized into NO. If the volatiles evolve into a reducing atmosphere, the nitrogen evolved can readily be made to form nitrogen gas, rather than NO.

The second path involves the combustion of nitrogen contained in the char[1] matrix during the combustion of the char portion of the fuels. This reaction occurs much more slowly than the volatile phase. Only around 20% of the char nitrogen is ultimately emitted as NO, since much of the NO that forms during this process is reduced to nitrogen by the char, which is nearly pure carbon.

NO_2 Formation

Chemical equilibrium considerations indicate that for burned gases at typical flame temperatures, NO_2/NO ratios should be negligibly small. While experimental data show this is true for spark-ignition engines, in diesels NO_2 can be 10% to 30% of the total exhaust oxides of nitrogen emissions. A plausible mechanism for the persistence of NO_2 is the following: NO formed in the flame zone can be rapidly converted to NO_2 via reactions such as

[1] Charring is a chemical process of incomplete combustion of certain solids when subjected to high heat. The resulting residue matter is called char.

$$NO + HO_2 \rightarrow NO_2 + OH \tag{2.24}$$

Subsequently, conversion of this NO_2 to NO occurs via

$$NO_2 + O \rightarrow NO + O_2 \tag{2.25}$$

unless the NO_2 formed in the flame is quenched by mixing with cooler fluid. This explanation is consistent with the highest NO_2/NO ratio occurring at high load in diesels, when cooler regions which could quench the conversion back to NO are widespread.

It is customary to measure total oxides of nitrogen emissions, NO plus NO_2, with a chemiluminescence analyzer and call the combination NO_x. It always important to check carefully whether specific emissions data for NO_x are given in terms of mass of NO or mass of NO_2 which have molecular weights of 30 and 46, respectively. [22]

2.1.3 GT-Power NO_x Model For Combustion

To predict NO_x emissions during combustion GT-POWER has already an integrated NO_x model that can be simply switched on in case of interest in values of this kind of pollutant gas.

The NO calculation is based on the extended Zeldovich mechanism, which tells that the governing equations for NO production are the N_2 oxidation rate equation (see Equation 2.4), the N oxidation rate equation (see Equation 2.5) and the OH reduction rate equation (see Equation 2.6) already described in Section 2.1.2.

The reaction rate coefficients were already presented in Table 2.1. The choice of the GT-POWER programmers between the available proposals is reported here mainly because of the addition of some tuning parameters that allow the user to calibrate the NO_x model in order to match engine measurements data. k_1, k_2, and k_3 are the rate constants that are used to calculate the reaction rates of the three equations, these are presented here in the same way has implemented into the simulation software:

$$k_1 = F_1 \cdot 7.6 \cdot 10^{10} \cdot exp\left(-\frac{38000 \cdot A_1}{T_b}\right) \tag{2.26}$$

$$k_2 = F_2 \cdot 6.4 \cdot 10^{6} \cdot T_b \cdot exp\left(-\frac{3150 \cdot A_2}{T_b}\right) \tag{2.27}$$

$$k_3 = F_3 \cdot 4.1 \cdot 10^{10} \tag{2.28}$$

$$\tag{2.29}$$

Where:

- F_1 is the N_2 Oxidation Rate Multiplier.
- F_2 is the N Oxidation Rate Multiplier.
- F_3 is the OH Reduction Rate Multiplier.
- A_1 is the N_2 Oxidation Activation Temperature Multiplier.
- A_2 is the N Oxidation Activation Temperature Multiplier.
- T_b is the Burned Sub-Zone Temperature in Kelvin.

The units of k_1, k_2, and k_3 are all in $m^3/(kmol \cdot sec)$. Internally the concentration terms are in units of $kmol/m^3$, and there are two first order concentration terms per reaction so overall reaction rates are in units of $kmol/(m^3 \cdot sec)$. Using these units with the numbers above would give the same answer as using the units and numbers used in the Table 2.1, where the pre-exponent units are $cm^3/(mol \cdot sec)$, concentration units are mol/cm^3, and overall rate units are $mol/(cm^3 \cdot sec)$.

The results of this model are very sensitive to the equivalence ratio (availability of oxygen) and temperature. Therefore, trapped cylinder mass (i.e. engine airflow, EGR fraction, trapping ratio), fuel-to-air ratio, and combustion rate all must be reasonable values before any reasonable NO prediction can be expected. Therefore, always confirm that the simulated values for these results compare well before comparing the NO simulation to measurements. In case of a measured combustion rate, compare also maximum cylinder pressure and crank-angle at maximum cylinder pressure.

NO is ultimately very sensitive to maximum cylinder temperature, and therefore a two zones temperature in the combustion model has been used, because the single zone temperature calculation does a very poor job of capturing the maximum cylinder temperature. Two zones model indicates that temperature and composition will be independently calculated for the burned and unburned gases in the cylinder chamber. This model is recommended for most simulations and must be used to achieve meaningful NO_x emissions results.

For a calibration of the NO_x model, some tuning parameters are available. Here a short explanation is given on which influence each of them will have on the prediction of NO_x emissions:

- NO_x Calibration Multiplier: Multiplier to the predicted net rate of NO_x formation, where the net NO formation rate is the total NO formation rate minus the NO dissociation rate. This value may be set to "def", which will set this multiplier to 1.0.
- N_2 Oxidation Rate Multiplier: Multiplier to the N_2 oxidation rate equation (see 2.4). ("def" = 1.0)
- N_2 Oxidation Activation Energy Multiplier: Multiplier to the activation energy multiplier of the N_2 oxidation rate equation. Values less than one will typically cause the total NO formation rate to increase, and values greater than one will cause the rate to decrease. For most simulations, the predicted NO is very sensitive to this multiplier, and so caution should be used when changing this value. ("def" = 1.0)
- N Oxidation Rate Multiplier: Multiplier to the N oxidation rate equation (see 2.5). ("def" = 1.0)
- N Oxidation Activation Energy Multiplier: Multiplier to the activation energy multiplier of the N oxidation rate equation. ("def" = 1.0)
- OH Reduction Rate Multiplier: Multiplier to the hydroxyl reduction rate equation (see 2.6). ("def" = 1.0)

In this master thesis the NO_x emissions were predicted using this model. The calibration process, which can take very long time, has been drastically reduced for time reasons and consists in the use of the NO_x Calibration Multiplier only.

2.2 NO_x Emissions Reduction Strategies

The reduction of NO_x emissions is nowadays very important and focus of many researches. This great effort putted into the research of cleaner combustion engines allows to reduce NO_x emissions in various different ways. Principally the strategies that can be adopted divides into two main categories:

- In-Cylinder NO_x Reduction: consisting in technologies that modifies the combustion process, trying generally to reduce the adiabatic flame temperature.
- Exhaust After-treatment Systems for NO_x Reduction: consisting in various types of catalytic converter, depending on the burning fuel, that converts the NO content to not harmful gases.

The technologies belonging to these two categories are now explained in the following Sections.

2.2.1 In-Cylinder NO_x Reduction

The in-cylinder reduction of NO_x emissions bases on three different physical principles, all with the goal of reducing the adiabatic flame temperature, thus high combustion temperatures are the main cause of high NO_x emissions, as shown in the previous Section 2.1.2. The usual technologies are now categorized with respect to their principles:

- Change in composition:
  - Nitrogen enrichment.
  - Exhaust Gas Recirculation (EGR).
  - Air humidification.
- Reduction of the reactant temperature:
  - Miller timing.
  - Charge air cooling.
  - Reduced compression ratio.
- Cooling of the flame:
  - Direct water injection.
  - Water-fuel emulsions.

In the next Sections a brief description of each technology is given and for a deeper understanding is referred to the corresponding relevant literature.

Nitrogen Enrichment

Dilution of the cylinder charge with inert gases is one method of lowering the peak cylinder temperatures. Nitrogen is an obvious diluent. Advantages are a reduced amount of oxygen in the intake and therefore a reduced combustion rate and lower adiabatic flame temperature. Major disadvantage is the need of an extra supply of nitrogen or an oxygen filter. [33, 36, 40, 42]

Exhaust Gas Recirculation

An effective way to reduce the NO_x emissions is given by the increase of inert concentration in the combustion chamber. Nitrogen enrichment is one of this solution, but similar to nitrogen enrichment there is the exhaust gas recirculation, i.e. EGR. The exhaust gases are approximately composed out of N_2, CO_2 and H_2O, all inert gases, therefore have a high heat capacity and only a very small amount of oxygen, leading to lower peak temperature and consequently to lower NO_x emissions.

The main advantage of this technology is that using exhaust gas which is readily available avoid the implementation of additional devices for inert gas enrichment. This fact rends a first realization of an EGR system very simple. But some disadvantages have to be taken into account, like an increase in soot emissions due to lower oxygen availability to oxidize soot, the limitation to amount of EGR used due to excessive CO and UHC emissions. All the major problems through the use of recycled exhaust to dilute the engine intake mixture, lowering the NO levels, comes form a deteriorated combustion quality.

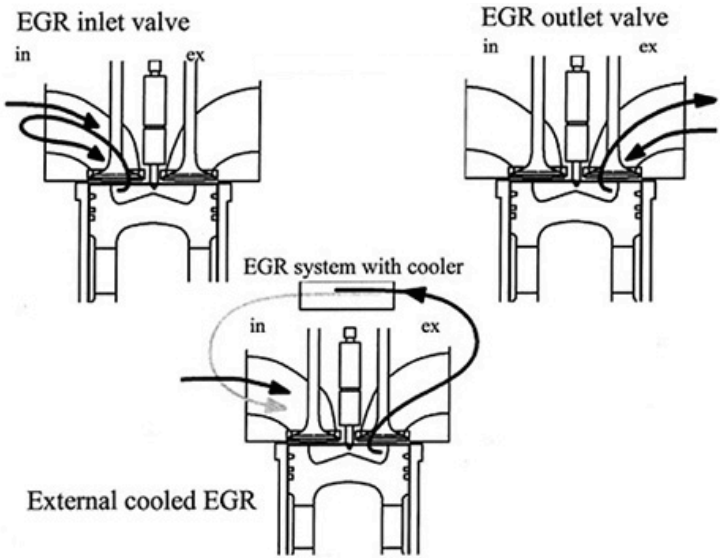

Figure 2.3: EGR Internal and External Configuration [14].

EGR Systems can be divided into three categories depending on the path choose for recirculate the exhaust gases from the exhaust side to the fresh intake side:

- Internal EGR: here the exhaust gases are retained into the combustion chamber through an appropriate valve timing, either the inlet valve as the exhaust valve. This configuration does not require any additional piping or devices, but it also does not achieve acceptable results in the mitigation of NO_x emissions (see upper part of Figure 2.3).

- HP-EGR (Short Route): the exhaust gases are recirculated from the exhaust receiver, before the turbine, directly into the intake receiver after the compressor (see Figure 2.4, right). The EGR flow is normally separately cooled and then throttled to the wished EGR rate then merged and mixed with the fresh air coming from the previous compressor stage.

- LP-EGR (Long Route or Semi-Short Route): this is another solution of recirculation path, where the exhaust gases are expanded in the turbine (or throttled in a separate route), cooled and merged with mixing before the compressor stage. In case of a two-stage turbocharging solution this path is normally recirculated in the volume between the two compressors, thus this is called "Semi-Short Route" (see Figure 2.4, left). For the single-stage turbocharging the recirculation will goes into the volume before the only one compressor, thus a "Long Route".

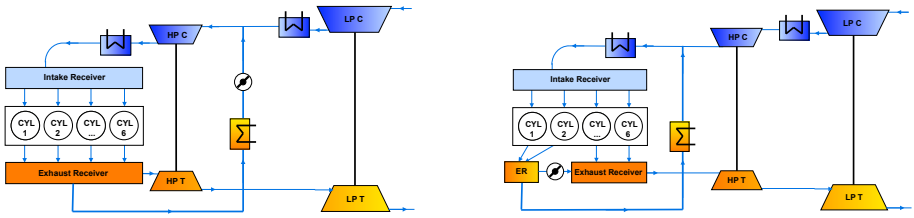

Figure 2.4: External EGR - Semi-Short Route (left) and Short Route (right). [3]

All the external EGR paths uses the pumping energy coming from different elements of the engine system. In this report the five configurations for the EGR path that were investigated are all external and use pumping from four different elements as follow:

- Semi-Short Route: from the HP Compressor.
- 1 Donor Cylinder Semi-Short Route: from one of the engine pistons and the HP Compressor.
- 2 Donor Cylinders Short Route: from two of the engine pistons.
- EGR Blower Short Route: from the crankshaft driven dedicated blower.
- EGR Turbocharger Short Route: from a dedicated turbocharger.

These EGR configurations are analyzed and compared in detail throughout this report, but for additional literature on the EGR working principles is referred to [4, 13, 39, 53].

Air Humidification

Artificially increasing the humidity of the intake air causes a beneficial increase of its heat capacity. This is due to the higher value of heat capacity for water ($c_p = 4.181$ $[J/(g \cdot K)]$ at $25°C$) with respect to that of air ($c_p = 1.005$ $[J/(g \cdot K)]$ at $25°C$). The problems here are the complex system that has to be implemented for humidify air and, more important in case of a turbocharged engine, is the limited amount of water that can be introduced due to saturation which could damage the compressors wheels. [23, 54]

Miller Timing

Miller timing is one of the few measures that can be applied in an internal combustion engine to simultaneously reduce NO_x emissions and fuel consumption - a fact that engine builders are acknowledging by introducing it practically on every

modern engine, which are operated today with at least moderate Miller timing.

The basic principle underlying the Miller process is that the effective compression stroke can be made shorter than the expansion stroke by suitable shifting of the inlet valve timing. When both the engine output and boost pressure are kept constant, this will reduce the cylinder filling and the pressure and temperature in the cylinders will be lower, having a positive effect to minimize NO_x formation.

The drawback is that ever-higher boost pressures are necessary for a constant engine output (due to a lower charging efficiency), i.e. increasing demands are made on the turbocharging system. Normally a significant reduction of NO_x emissions is achieved only though the simultaneous adoption of a 2-stage turbocharging system. Then it is also hampered the start-up and low load operation due to fuel ignition issues at low temperatures.

If only ideal processes are considered, then the overall efficiency of the Miller process is worse than that of the process with conventional valve timing. The reason is that the part of the positive "gas exchange loop" lying between the compression curve and the BDC (see Figure 2.5) is cut off. This loss, referred to in the following as "Miller loss", can lead to a reduction in engine efficiency of up to 0.5%.

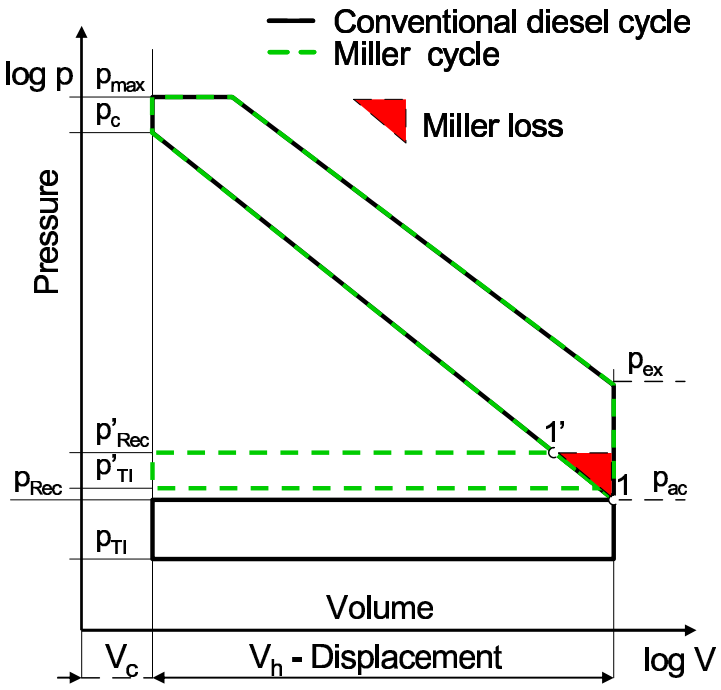

Figure 2.5: Ideal Process with and without Miller Timing [11].

In a real process it can be expected that when the pressure behaves in the same way in the high-pressure section, more output at higher efficiency will be achieved since the gain from the lower heat losses will more than compensate for the Miller loss. If the output and all other process parameters are kept constant, the pressure level will be generally lower, thus improving the efficiency of the high-pressure process. The lowering of the peak pressure has, as a rule, the effect of freeing up some of the engine's mechanical potential for a further improvement in efficiency.

This improvement can take the following forms:

- An increase in air/fuel ratio.
- An increase in compression ratio.
- An increase in the combustion pressure rise due to earlier injection.

The Miller process has then a very high potential with regard to improvement of emissions and engine efficiency. This potential can be even increased by introducing Miller timings that produce far more Miller effect than is usual today. However, this requires very high boost pressures and therefore a 2-stage turbocharging system. [11, 12, 28, 47]

Charge Air Cooling

For turbocharged engines a very common way to increase the power density is to include in the intake system a charge air cooler which reduces the temperature of the intake air. This is not only beneficial to the overall engine efficiency, but also for the NO_x emissions. Unfortunately this simple and quite cheap way of reducing emissions is limited and dependent on the environmental temperature (intake air cannot be cooled further than the ambient temperature) and leads to very poor gains in terms or NO_x reduction. [21]

Reduced Compression Ratio

The engine compression ratio is an important geometrical parameter which influence the combustion process and thus the engine output power and the emissions. Reducing this value means reduce the effective compression stroke and it will cause a lower reactant end temperature (at TDC). This choice is to avoid if possible because of its intrinsic reduction in thermodynamic efficiency (which increase for increasing compression ratio) and, as for the case of Miller timing, for hampered the start-up and low load operation due to fuel ignition issues at low temperatures. [49]

Direct Water Injection

The direct injection of water is an alternative to the humidification of the charge air. This solution avoid the risk of damaging a turbocharging system though water condensation, but needs an extra injector and requires then a redesign of the combustion chamber. This major changes make this option very costly. In spite of that this solution is very effective and localized, it cools the flame directly using water, achieving good results in NO_x reduction. [7, 23]

Water-Fuel Emulsion

A promising technology for NO_x reduction especially for heavy-duty diesel engines and mainly large scale ones is the addition of water to the combustion chamber to reduce, by cooling the flame directly, peak combustion temperature that obviously affects NO_x formation. The use of a water-fuel emulsion permits to cool the flame while the burning process is happening. A part of the combustion heat is used to evaporate the water content of the fuel instead for work. The fast water evaporation during the injection enhances although mixing and increases the soot

oxidation, generating a solution to two of the major emissions problem for diesel engines at once. As a drawback this technology shows a very unstable water-fuel mixture, which will separate without the use of additives. Consequently this leads to a difficult control of the amount of water content in the fuel. Nevertheless recent studies on this topic shows that the NO_x reduction is higher when using water-fuel emulsion compared to water injection in the intake manifold for the same water percentage and still trust this promising solution. [23, 49]

2.2.2 Exhaust After-treatment Systems For NO_x Reduction

Another solution for NO_x reduction is given by the use of an exhaust after-treatment system. Catalysts are the most expensive solution but they can effectively reduce NO_x emissions (as well as other pollutant emissions) to very low values. Other disadvantage is the place needed by such devices, thus this is mostly likely to be found on stationary power generation where the dimensions restrictions are less severe than for marine applications. The use of an exhaust after-treatment system can be as a replacement of all in-cylinder NO_x reduction technologies or joined together for a further reduction and cleaning process of the exhaust gases.

Urea Selective Catalytic Reduction

For diesel engines the leading solution in the field of exhaust after-treatment systems is the so-called Selective Catalytic Reduction (SCR) Catalyst. Scope of this catalyst is to convert nitrogen oxides into harmless diatomic nitrogen (N_2) and water (H_2O) through a chemical reaction with the aid of an additional reactant (i.e. this reactant agent should be tanked beside the fuel increasing the operational costs). A gaseous reductant, typically anhydrous ammonia, aqueous ammonia or urea, is added to a stream of exhaust gas and reacts on the catalyst surface. Carbon dioxide (CO_2) is a reaction product when urea is used as the reductant. Commercial selective catalytic reduction systems are typically found on large diesel engines for power generation purpose.

Before the reduction of NO_x can take place the exhaust gases are mostly treated by an oxidizer catalyst to oxidize the unburned hydrocarbons, CO and NO (see Equations 2.30 to 2.32) and by a particulate filter to eliminate the soot (See Figure 2.6).

$$C_xH_y + (x + y/4)\ O_2 \rightarrow x\ CO_2 + y/2\ H_2O \tag{2.30}$$

$$CO + 1/2\ O_2 \rightarrow CO_2 \tag{2.31}$$

$$2NO + O_2 \rightarrow 2NO_2 \tag{2.32}$$

The NO_x reduction reaction takes place as the gases pass through the catalyst chamber. Before entering the catalyst chamber the ammonia (NH_3), or other reductant (such as urea, $CO(NH_2)_2$), is injected and mixed with the gases. Several reductants are currently used in SCR applications including anhydrous ammonia, aqueous ammonia or urea. All those three reductants are widely available in large quantities. Pure anhydrous ammonia is extremely toxic and difficult to safely store, but needs no further conversion to operate within an SCR. Aqueous ammonia must be hydrolyzed in order to be used, but it is substantially safer to store and transport than anhydrous ammonia. Urea is the safest to store, but requires conversion to

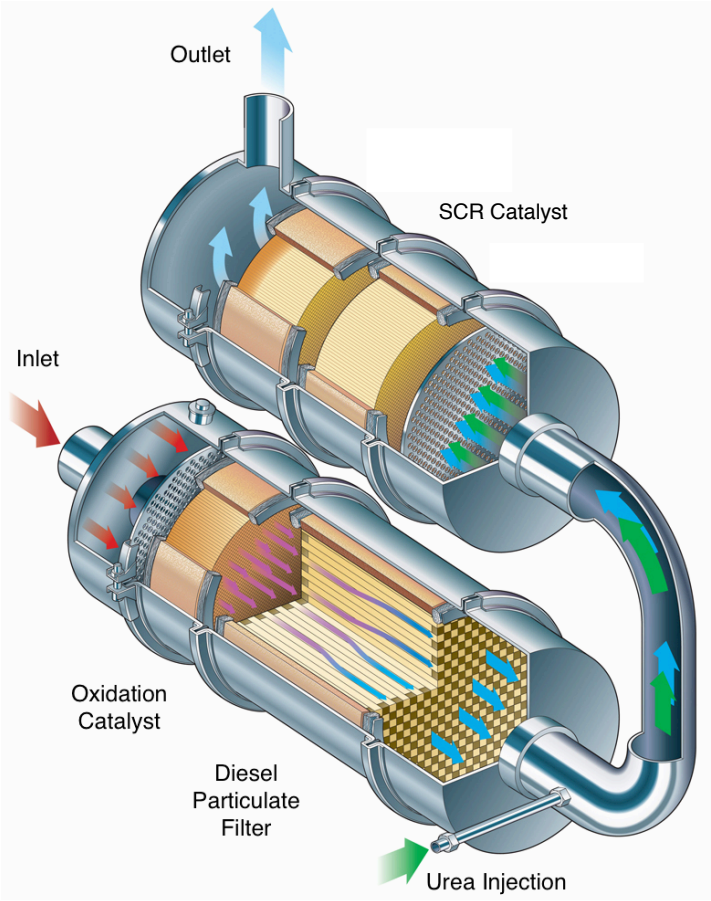

Figure 2.6: Exhaust after-treatment system for NO_x reduction including a SCR catalyst [38].

ammonia through thermal decomposition in order to be used as an effective reductant. The conversion of urea to ammonia take place through Equation 2.33 at the entry of the SCR catalysts.

$$CO(NH_2)_2 + H_2O \rightarrow 2NH_3 + CO_2 \tag{2.33}$$

The actual NO_x reduction occurs following the chemical equation for a selective catalytic reduction process:

$$4NO + 4NH_3 + O_2 \rightarrow 4N_2 + 6H_2O \tag{2.34}$$
$$2NO + 2NO_2 + 4NH_3 \rightarrow 4N_2 + 6H_2O \tag{2.35}$$
$$3NO_2 + 4NH_3 \rightarrow 3.5N_2 + 6H_2O \tag{2.36}$$

Equation 2.34 is called the standard SCR-Reaction but through the use of the oxidation catalysts the faster reaction (called also fast SCR-Reaction) is promoted (see Equation 2.35). A less important reaction, but that still reduces NO_x, is the slow NO_2-SCR-Reaction of Equation 2.36.

Like every catalyst several unwanted secondary reactions could happen, some of the more important are here reported:

$$4NH_3 + 3O_2 \rightarrow 2N_2 + 6H_2O \quad (2.37)$$
$$2NH_3 + 2O_2 \rightarrow N_2O + 3H_2O \quad (2.38)$$

These reactions oxidize a part of the useful NH_3 to, in the best case, N_2, causing only a waste of urea (but increasing the urea consumption and therefore the costs) and in the worst case forming N_2O emissions which are currently the most important ozone-depleting substance.

Other disadvantages of this technology is the need of a minimal operating temperature (of about 220°C) in order to successfully reduce the NO, under this temperature the catalysts does not work as desired. This means that the cold start emissions control will be an issue. After that the presence of small ammonia concentrations in the after catalyst exhaust gases (ammonia slip) cannot be excluded, this because not all the ammonia injected may react properly.

The ideal reaction has an optimal temperature range between 630 and 720 K, but can operate from 500 to 720 K with longer residence times. The minimum effective temperature depends on the various fuels, gas constituents, and catalyst geometry.

SCR catalysts are made from various ceramic materials used as a carrier, such as titanium oxide, and active catalytic components are usually either oxides of base metals (such as vanadium, molybdenum and tungsten), zeolites, or various precious metals. Each catalyst component has advantages and disadvantages. [20, 29]

Chapter 3

Results

In this chapter the different developed simulation models for each EGR configuration tested in the thesis are shown. Important parameters are figured out and compared between configurations to better understand pro and contra of the analyzed EGR technologies.

3.1 Full Engine Model (FEM)

The starting point of this thesis is given by an already existing engine model, given as a simulation model in GT-POWER (see Figure in the Appendix B.2). This model is a so-called Full Engine Model (FEM), where the topography is detailed represented, all the different piping and other devices are implemented taking the informations from the engine manufacturer. Many physical models used by the simulation program (like heat transfer models, pressure drop models, etc.) were used directly as given with some adjustments of the key parameters, tuning variables used in the calibration process. An important fact that has to be kept on mind is that during this master thesis no combustion model is implemented. Instead of a combustion model the measured heat release rate (available thanks to the test bench sessions) is implemented. This means that for each load point and later (for the EGR configurations) for each EGR rate an heat release rate profile is given as an input reproducing the combustion phase as measured from the engine. This procedure leads to more accurate results for the defined engine load point but limits radically the possibility to simulates other load points, meaning that with this method only loads with available HRR can be simulates.

Such detailed models should give the best results in terms of accuracy and allows to analyze different variables in every point of interest. Unfortunately, for each component added to describe the engine model (i.e. a pipe section, junction, cooler, etc.) the number of nodes increases as well as the computational burden. Of course the computational time is also dependent on the machine which is running the program. The calculation time could then not be a problem if the simulation program is running on a very powerful computer (or a supercomputer), but for normal laptops this could increase drastically, especially if an optimization process has to be carried out. A solution to this time problem is explained in Section 3.2.

3.1.1 Without EGR

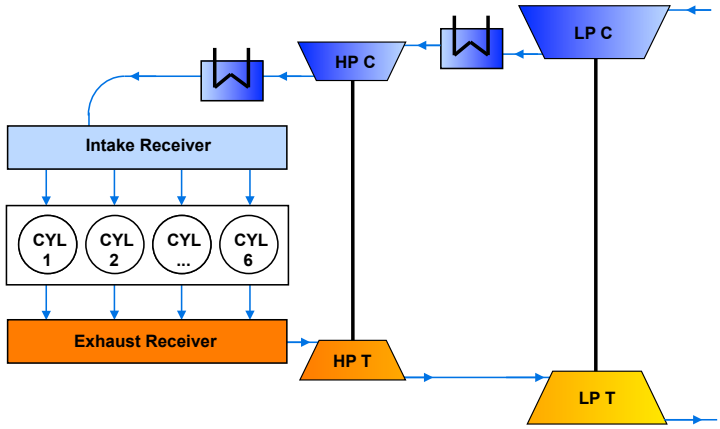

Figure 3.1: Topology of the two-stage turbocharged engine without EGR. [3]

First step of the part of simulation of the thesis was to check the already existing FEM engine model, which reflect the original engine configuration without EGR path implemented. The engine is, has shown in Figure 3.1, two-stage turbocharged with double intercooler, one after each compressor stage.

The engine characteristics as well as the turbochargers specifications and maps are incorporated in the simulation model, the boundary and initial conditions (taken from the measurements sessions) and the chosen load curve (10%-25%-33%-40%-48%-50%-66%-70%-75%-85%-99%-100% load) are integrated into the case setup folder.

The simulation takes about 10 minutes per load case to complete the calculations. The results of this model should already have been correctly calibrated with existing measurement data.

Calibration

For completeness a recalibration check is carried out, the only parameters that have changed during the calibration process are friction multipliers and heat transfer multipliers in order to match pressure drops and temperatures at the measuring locations.

The calibration's objective was to have the best possible match between measured values and simulation results for the high load points, especially for the 99% load. For this point the important variables which are compared are following:

- Pressures and Temperatures at different locations:
  - Point 1,LP: Low Pressure Compressor Intel.
  - Point 2,LP: Low Pressure Compressor Outlet.
  - Point 1,HP: High Pressure Compressor Intel.
  - Point 2,HP: High Pressure Compressor Outlet.
  - Point 3: Intake Manifold.

  - Point 4: Exhaust Manifold.
  - Point 5: High Pressure Turbine Outlet.
  - Point 6: Low Pressure Turbine Outlet.
- Maximal Cylinder Pressure.
- Air Massflow.
- Turbocharger Rotational Speeds.
- Brake Specific Fuel Consumption.
- Useful Exhaust Energy.

The calibration shows a good corresponding overall (see Figure 3.2) with a mean error of ca. 1.16%. The intake side shows very good simulated values, while the exhaust side, still reaching very good results, has a bit more variation, especially after the high pressure turbine. BSFC is only slightly overestimated (less than 2%) but more than acceptable. Greater differences can be seen for the rotational speed of the high pressure turbocharger and for the useful exhaust energy. For the first a measurement offset on the test bench is the cause of this discrepancy, therefore the measurement should not be trusted. For the useful exhaust energy a different definition between the measured value and the simulated one causes a not corresponding estimation. In the measurement the exhaust energy is calculated as the part of energy wasted, i.e. not used by the turbines, while for the simulation the "useful" exhaust energy already indicates that is counting the power turbines too. The two values were compared with the same definition and results shows a good corresponding with acceptable errors around 5%.

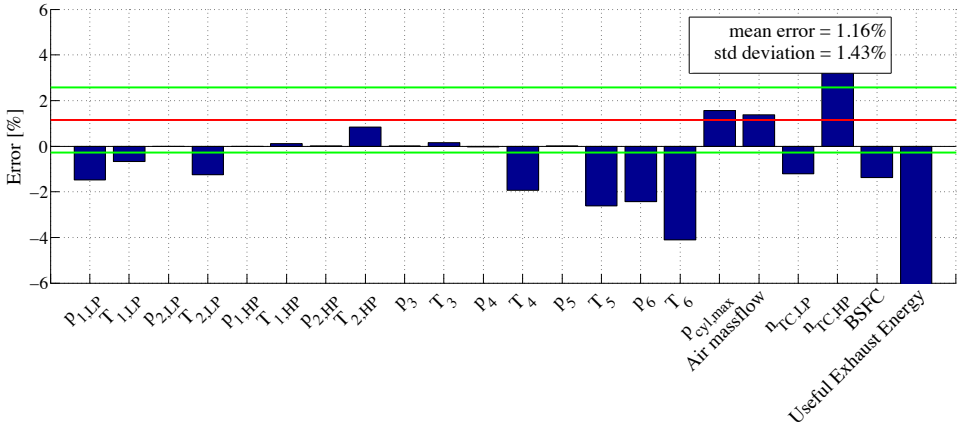

Figure 3.2: Comparison between measured and simulated values - 99% Power Case.

This configuration has been already optimized in terms of minimize the BSFC through the correct choice of the two turbochargers. With this configuration the fuel consumption curve presented in Figure 3.5 is expected and confirmed my measurements. These values will be the best achievable for this engine configuration and they will be taken as target to compare the efficiency of others models with the EGR path implemented.

3.1.2 Semi-Short EGR Configuration

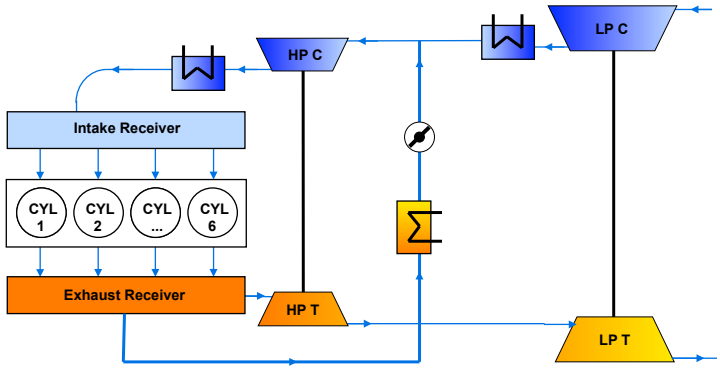

Figure 3.3: Topology of the two-stage turbocharged engine with a Semi-Short EGR Route. [3]

As first EGR configuration that has been tested is the semi-short route (see Figure 3.3). This is the simplest method to implement EGR because there is no need of additional pumping devices (the HP compressor will pump the EGR flow) and the piping results to be very simple.

The EGR flow is taken out from the exhaust manifold and feed through the EGR piping setup. A dedicated EGR cooler cools the recirculated gases to a defined temperature (set to 70°C). The correct amount of EGR that is needed is ensured by an EGR valve actuated by a simple PID EGR controller, which will tends to close the valve for reducing the EGR flow and opens it for increasing this flow. The EGR rate is defined throughout this report as a mass ratio between flows:

$$EGR = \frac{\dot{m}_{EGR}}{\dot{m}_{air}} \cdot 100 \ [\%] \tag{3.1}$$

Calibration

This configuration was already implemented on the test bench and was running as the thesis has started, allowing to calibrate the EGR model too, thus measurements were available. At the test bench EGR rates of 20% and 25% were experimented for loads varying from 10% up to 75% load. Because the turbocharger components are matched to fit the engine configuration without EGR, the higher load points in this case cannot be run thus the engine constrain limits - cylinder peak pressure and HP turbine inlet temperature - are reached. Therefore the chosen calibration point is the one with measurements available with the highest possible load (i.e. 75% load) and with 25% EGR rate.

The calibration results shows a good matching with an overall error of ca. 1.32% (see Figure 3.4). With respect to the calibration without EGR some major differences can be highlighted. The HP compressor inlet temperature presents an important difference between measure and simulation, this is because the thermocouple used to measure the temperature is located in a pipe section where probably the mixing process between EGR and fresh air flow is not complete. The other temperatures and the EGR temperature itself had some discrepancy, but they remain in limits (notice that the difference is calculated in percentage for temperatures registered in degrees Celsius and not in Kelvin, which in absolute values will increase

the error by four or more times). All the simulated values shows deviations which are in the same order of magnitude to the ones registered in the model without EGR, only the BSFC is now slightly underestimate, but still within reasonable limits (less than 3.5%). Similar results are obtained for other loads (apart from very low loads) and lower EGR rates, concluding that the calibration of the EGR model was satisfyingly good.

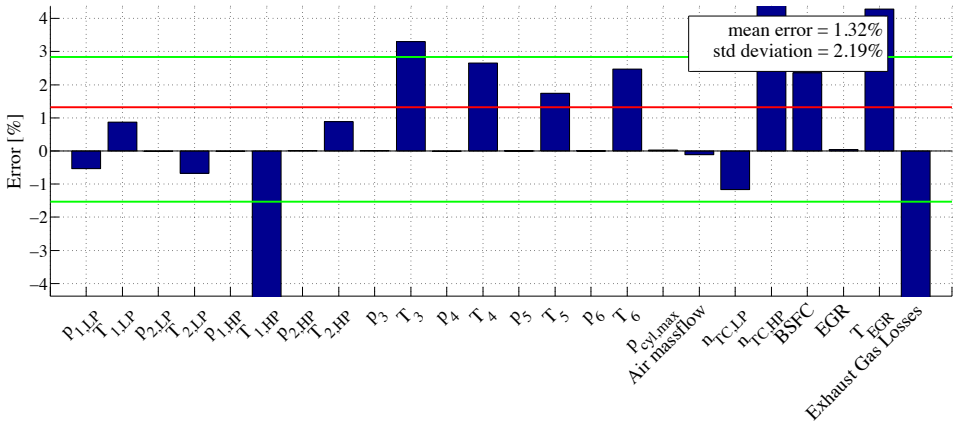

Figure 3.4: Comparison between measured and simulated values - 75% Power Case and 25% EGR.

The following Figure 3.5 shows that implementing EGR to an engine without changing any components will reduce markedly the efficiency of the system.

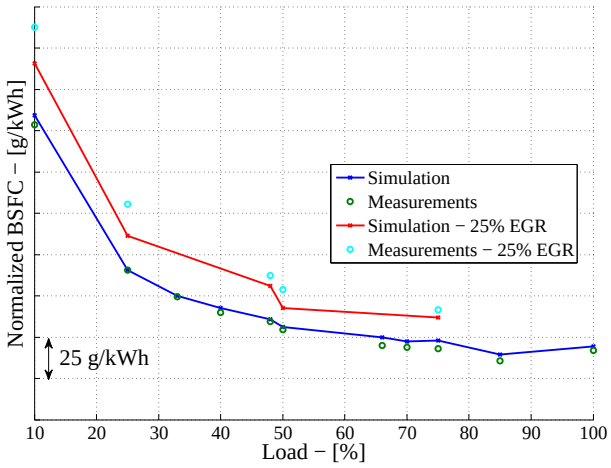

Figure 3.5: Brake Specific Fuel Consumption for the engine model without and with 25% EGR.

A last note has to be made: for this simulation model with implemented EGR path the heat release rates used are the same as the one for load points without EGR. The HRR of a load point without EGR is obviously different to the one with EGR, especially if the EGR rate is significant. This is because the increased amount of inert gases (introduced in the combustion chamber by the EGR route) leads to a slower combustion with lower peak temperatures and therefore a different HRR

profile. The different combustion length does not count for the simulation, thus the program will scale the HRR curve ("stretch" the time axis) in order to meet the desired engine output power. What really can affect the results is the profile itself of the HRR curve, but this one does not differ too much from that from measurements without EGR. Of course implementing the correct HRR curve will increase the results accuracy, this step has been then made for the other engine model setups.

3.2 Fast Running Model (FRM)

For reducing the computational time burden a valid solution is given by the Fast Running Model (FRM). This model reduces the fidelity, by lumping volumes together, to enable larger time steps and solve fewer subvolumes. The detailed cylinders remain in the model, as well as modeled heat transfer from cylinders.

For the used engine model pipes were, if possible, lumped to larger volumes and heat transfer devices (like coolers) were simplified. The Figure in Appendix B.4 shows the reduced model. Here all the intake pipes has been replaced by an intake manifold as a volume which correspond to the sum of all single components' volume. The same procedure is done for the exhaust manifold, the intermediate volume between the two turbines, the EGR path and the pipes between the two compressors. During this operation the heat transfer multiplier is adjusted in order to correctly simulate the different volume to area ratio. The pressure drops between lumped volumes is also checked and re-calibrate.

3.2.1 Calibration

During the calibration process of the FRM the well known pressure and heat transfer multipliers were corrected in order to get the best match with the available measurements data. After that also the engine friction multipliers were adapted for better results. To notice is that for this model the new heat release rate curves for the EGR cases are implemented, which will decrease the differences between simulation model and real results.

Important values regarding the engine, like the cylinder maximal peak pressure and the airflow rate, are very good calibrated for the 75% load case (see Figures in the Appendix C.1.1), compressors side the powers needed by both is more than good estimated and (apart from the problematic HP turbocharger) the rotational speed too. Turbines side the generated power corresponds for the high loads to the measured values. The same can be said for the inlet temperatures, especially for the important limiting HP turbine inlet temperature (constrain).

Unique drawback of this calibration procedure is that the BSFC estimated through simulation does not correspond perfectly with the measured one (see Figure 3.6) for both tested EGR cases. The deviations are considered small and acceptable, but has to be kept in mind throughout the thesis results, that the BSFC simulated will underestimate the real one of about 3%. Although most important in this research are not the absolute value of BSFC, but the possible gain or lose in the comparisons between EGR configurations (therefore an offset will then not count, because it will cancel out).

3.2.2 Comparison Between FEM And FRM

For a double check that during the conversion from the fully detailed engine model to the fast running one, with the lumped volumes, a comparison between these two model results has been done. Often is considerate a detailed model the best choice to have very accurate simulations, which is also true, but the power and accuracy of a FRM is generally understated. The following Figure 3.6 should be only as one example of the achievable fidelity by the FRM with respect to the FEM e.g. the BSFC.

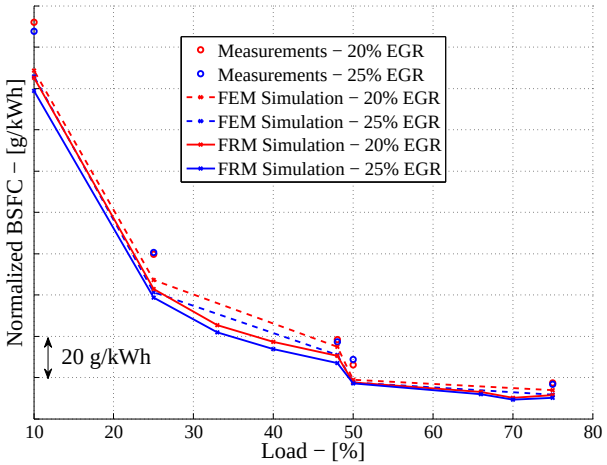

Figure 3.6: Brake Specific Fuel Consumption for the FEM and the FRM with 20% and 25% EGR compared with the measurements.

3.3 Exhaust Gas Recirculation Setups

3.3.1 Semi-Short Configuration

This engine with implemented EGR path configuration is the same that has been already discussed in the previous Sections 3.1.2, 3.2.1 and 3.2.2.

Non-Optimized

The implementation of the EGR path was done merely through the setting up of a semi-short route, without any changes to the engine parameters or to the turbochargers specifications. This procedure leads to a bad use of the turbocharging system, because the exhaust flow that will go through the turbines is now reduced (exhaust gases minus the recirculated ones) while the flow going through the compressors is increased (fresh air plus the recirculated exhaust gases). A certain unbalance is introduced to the system, which reacts consequently reducing its efficiency and increasing its fuel consumption (as already shown in Figure 3.5). At 75% engine load the BSFC increase for 25% EGR is remarkably high (ca. 12.1 g/kWh).

A re-matching of the turbocharging components is needed in order to reduce the deficit in BSFC caused by the EGR path.

Optimized

The re-matching of the turbochargers specifications started with the optimization process with the goal of minimize the BSFC. This optimization procedure had as tuning parameter the turbine mass multiplier. This parameter permits the user to fictitiously increase/decrease the capability of the turbine to manage more/less exhaust flow. Physically the variation of this parameter reflects the change in the turbine nozzle diameter, increasing/decreasing turbine mass multiplier consists in a reduction/increment in the turbine nozzle ring.

Firstly both nozzle ring diameters (for LP and HP turbine) were changed in order to get the minimal BSFC. Some limitations (constrains) are given, these were the EGR rate (the optimization is carried out for an EGR rate of 25%) and the maximal HP turbine inlet temperature, which should not overcome the critical value of 580°C.

After some iterations it was clear that good results could be achieved through the adjustment of the HP turbine nozzle ring diameter, while the LP turbine nozzle diameter has almost no influence on reducing the BSFC and therefore discarded.

The optimization process was carried out for three different EGR rates: 20%, 25% and 30%. The HP turbine nozzle diameter was varied for each EGR rate and for each load point (simulating the behaviour of a variable turbine geometry VTG). Thus the best possible fuel re-gain with respect to the non EGR simulation setup can be achieved. The results of the optimizations show the BSFC reduction obtained though re-matching of the HP turbine and the effects on the constrain given by the HP turbine inlet temperature (see Table 3.1).

For increasing load the HP turbine inlet temperature tends to increase, which is meaningful, due to the higher overall thermal load. The same can be seen also of increasing EGR rate, this is because for these cases the intake pressure is not

held constant, i.e. for increasing EGR rate the intake pressure will drop increasing the HP TTI. Very interesting is that the BSFC that can be re-gained through a re-matching of the HP turbine nozzle ring lies on average over all loads between ca. 10.1 g/kWh and 16.4 g/kWh depending on the EGR rate case.

Because a VTG turbine nozzle ring would not be installed on the test bench during the master thesis duration, a single turbine mass multiplier has been chosen between the ones that gave the best fuel consumption overall, giving during the choice more importance at the 25% EGR case. The choice was of a much smaller turbine nozzle ring (turbine mass multiplier 1.5). This configuration would lead to good BSFC reductions with respect to the non-optimized case (still between ca. 8.0 g/kWh and 12.9 g/kWh depending on the EGR rate case) but holding some security margin on the HP turbine inlet temperature, which does not overcome the limit of 580°C for every load at 25% EGR (see Table 3.2 and Figures 3.7, 3.8).

TARGET		bsfc				
Power	EGR	Δ abs	Δ %	TTI	EGR	HPT
100%	20%	12.96	6.24%	562.50	20.03%	2.08
85%	20%	8.48	4.22%	517.26	20.01%	1.57
75%	20%	10.95	5.17%	553.92	20.02%	1.93
70%	20%	9.46	4.49%	561.50	20.02%	1.93
66%	20%	9.58	4.49%	562.95	20.02%	1.93
50%	20%	7.63	3.51%	520.94	20.01%	1.57
48%	20%	22.86	9.92%	450.76	20.04%	2.49
40%	20%	20.03	8.45%	444.18	20.02%	1.93
33%	20%	20.47	8.35%	438.25	20.01%	1.93
25%	20%	22.23	8.47%	421.46	20.01%	1.93
10%	20%	35.74	9.78%	321.74	20.00%	2.49
	AVERAGE	16.40	6.64%		AVERAGE	1.98
					MEDIAN	1.93
TARGET		bsfc				
Power	EGR	Δ abs	Δ %	TTI	EGR	HPT
100%	25%	9.68	4.71%	583.83	25.03%	1.93
85%	25%	5.69	2.85%	557.03	25.01%	1.57
75%	25%	8.04	3.82%	591.57	25.03%	1.93
70%	25%	6.91	3.30%	565.41	25.01%	1.57
66%	25%	7.02	3.30%	567.06	25.01%	1.57
50%	25%	5.53	2.54%	568.18	25.01%	1.57
48%	25%	18.67	8.22%	478.44	25.04%	2.49
40%	25%	16.45	7.03%	470.11	25.02%	1.93
33%	25%	16.86	6.97%	463.20	25.02%	1.93
25%	25%	18.25	7.05%	443.55	25.01%	1.93
10%	25%	29.44	8.20%	331.85	24.99%	2.48
	AVERAGE	12.96	5.27%		AVERAGE	1.90
					MEDIAN	1.93
TARGET		bsfc				
Power	EGR	Δ abs	Δ %	TTI	EGR	HPT
100%	30%	6.98	3.41%	601.00	30.02%	1.64
85%	30%	3.86	1.93%	601.61	30.01%	1.57
75%	30%	6.07	2.88%	601.05	30.01%	1.57
70%	30%	3.57	1.71%	564.65	30.00%	1.20
66%	30%	3.72	1.75%	566.11	30.00%	1.20
50%	30%	2.79	1.28%	551.02	30.00%	1.09
48%	30%	15.39	6.83%	511.07	30.05%	2.46
40%	30%	14.19	6.10%	498.69	30.03%	1.99
33%	30%	14.21	5.92%	489.58	30.03%	1.93
25%	30%	15.35	5.98%	467.44	30.02%	1.93
10%	30%	25.29	7.13%	335.85	30.00%	2.49
	AVERAGE	10.13	4.08%		AVERAGE	1.73
					MEDIAN	1.64

Table 3.1: Optimization process by varying HP turbine mass multiplier - VTG similar.

TARGET		bsfc				
Power	EGR	Δ abs	Δ %	TTI	EGR	HPT
100%	20%	10.47	5.05%	530.33	20.00%	1.50
85%	20%	7.63	3.79%	520.78	20.01%	1.50
75%	20%	9.47	4.47%	520.67	20.01%	1.50
70%	20%	8.39	3.99%	527.00	20.00%	1.50
66%	20%	8.50	3.99%	528.62	20.01%	1.50
50%	20%	6.73	3.10%	524.78	20.01%	1.50
48%	20%	15.32	6.65%	455.54	20.01%	1.50
40%	20%	15.77	6.65%	434.52	20.00%	1.50
33%	20%	15.84	6.46%	434.69	20.00%	1.50
25%	20%	17.55	6.69%	413.07	20.00%	1.50
10%	20%	26.24	7.18%	307.30	20.00%	1.50
	AVERAGE	12.90	5.27%			

TARGET		bsfc				
Power	EGR	Δ abs	Δ %	TTI	EGR	HPT
100%	25%	8.02	3.90%	560.30	25.01%	1.50
85%	25%	4.89	2.44%	561.48	25.01%	1.50
75%	25%	7.00	3.32%	561.02	25.01%	1.50
70%	25%	6.09	2.91%	569.36	25.01%	1.50
66%	25%	6.17	2.90%	571.19	25.01%	1.50
50%	25%	4.75	2.18%	571.91	25.01%	1.50
48%	25%	13.26	5.84%	464.69	25.01%	1.50
40%	25%	13.12	5.60%	459.03	25.01%	1.50
33%	25%	13.57	5.61%	450.49	25.01%	1.50
25%	25%	14.75	5.70%	430.71	25.01%	1.50
10%	25%	21.02	5.86%	325.54	25.00%	1.50
	AVERAGE	10.24	4.21%			

TARGET		bsfc				
Power	EGR	Δ abs	Δ %	TTI	EGR	HPT
100%	30%	5.86	2.86%	601.57	30.01%	1.50
85%	30%	3.05	1.52%	607.42	30.01%	1.50
75%	30%	5.12	2.43%	607.92	30.01%	1.50
70%	30%	3.74	1.78%	617.69	30.01%	1.50
66%	30%	3.86	1.82%	619.47	30.01%	1.50
50%	30%	2.80	1.28%	625.40	30.01%	1.50
48%	30%	11.07	4.91%	499.38	30.02%	1.50
40%	30%	11.00	4.73%	491.79	30.02%	1.50
33%	30%	11.35	4.73%	481.34	30.02%	1.50
25%	30%	12.70	4.95%	453.63	30.01%	1.50
10%	30%	17.54	4.95%	338.51	30.00%	1.50
	AVERAGE	8.01	3.27%			

Table 3.2: Optimization process by varying HP turbine mass multiplier - Fixed value.

For comparison the 75% engine load and 25% EGR case is used (as in the previous non-optimized case): here the increase in BSFC with respect to the standard case without EGR is of about 5.6 g/kWh. The increase in efficiency permits to recover almost 50% of the BSFC deficit caused by the introduction of an EGR path. The 30% EGR case will be critical regarding the temperatures in the higher load points with the Miller timing activated. This will only cause a limiting EGR fraction usable for higher loads to up to 25% EGR and not more, without going into further problematics.

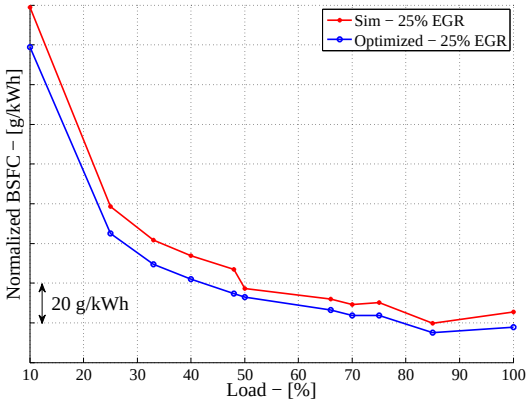

Figure 3.7: Optimization Semi-Short Route - BSFC reduction.

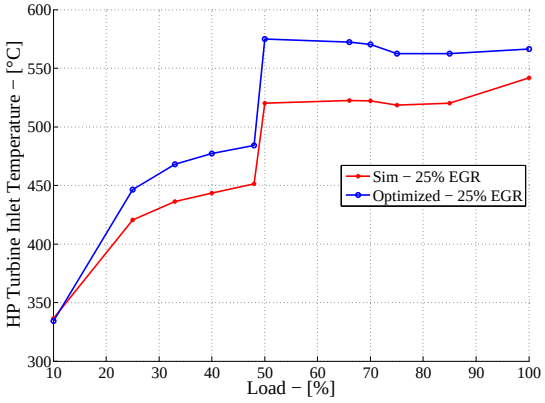

Figure 3.8: Optimization Semi-Short Route - HP turbine inlet temperature increase.

A big disadvantage of this technology is that the EGR flow must firstly throttle down from the exhaust pressure to the intermediate stage pressure, and then recompressed by the HP compressor to the intake pressure. Doing so a waste of energy occurs. The optimization process allows to reduce this throttling loss, through a more suitable choice of the intake pressure and consequently of the exhaust pressure (see Figures 3.9 and 3.10).

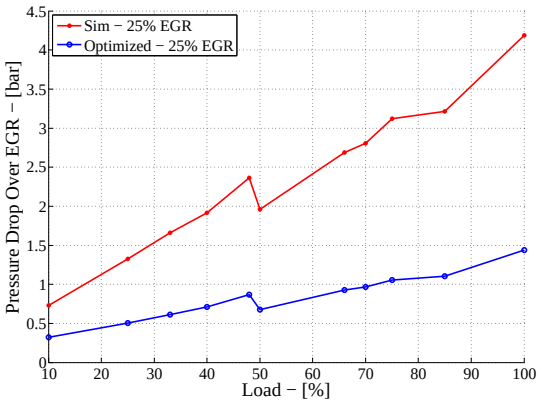

Figure 3.9: Optimization Semi-Short Route - Decrease of the throttling over the EGR valve.

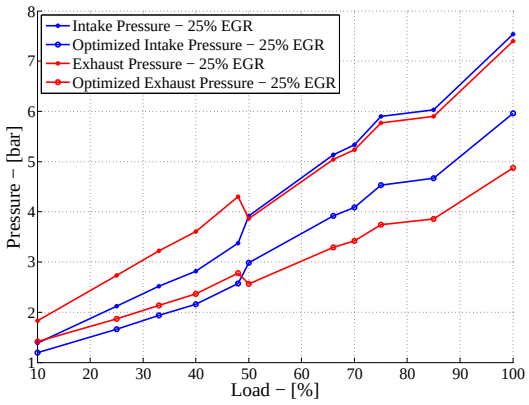

Figure 3.10: Optimization Semi-Short Route - Intake and exhaust pressures.

Reducing this loss gives also another advantage, namely the compression power

of the HP stage required is less than before (as can be seen in Figure 3.11) and the overall turbines power also drastically decreases (see Figure 3.12). Only disadvantage of reducing the intake pressure is that the scavenging effect is reduced (as shown in the Figure **??** in the Appendix C.2.1), with the consequent increase in HP turbine inlet temperature. With this configuration the HP stage is compressing less than in the non-optimized case while the LP stage will have a slightly increase in pressure ratio. This fact will shift the usual PR curves for a two-stage turbocharged engine, which they will not cross themselves anymore for low loads (as depicted in the Figure 3.13 with the simulation results and simplified in the Figure 3.14 for an illustrative purpose only), meaning that the LP stage will always deliver more power than the LP stage. In the optimal case the intermediate pressure is equal tho the exhaust pressure (meaning no throttling losses), in order to match the exhaust pressure the LP compressor must have a PR that will be always be higher than the one of the HP compressor, this "switch" is the consequence.

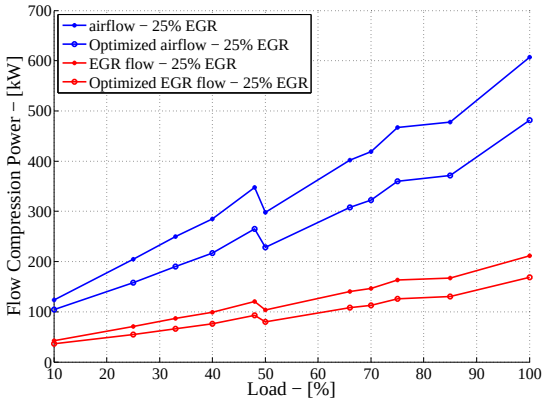

Figure 3.11: Optimization Semi-Short Route - Decrease of the HP compression power.

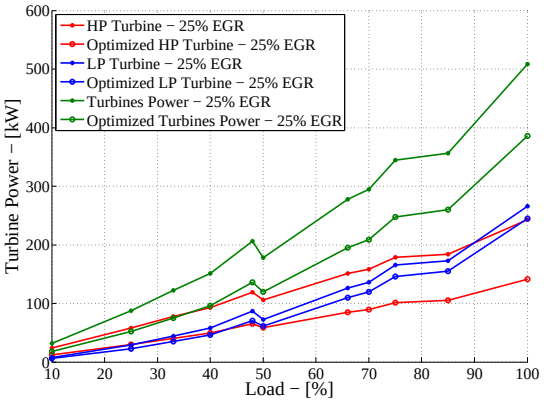

Figure 3.12: Optimization Semi-Short Route - Turbines power.

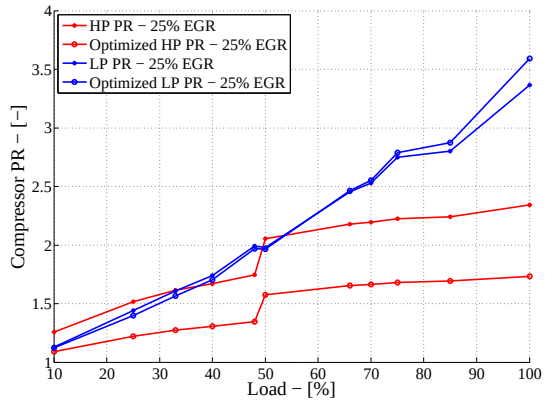

Figure 3.13: Optimization Semi-Short Route - Pressure Ratios.

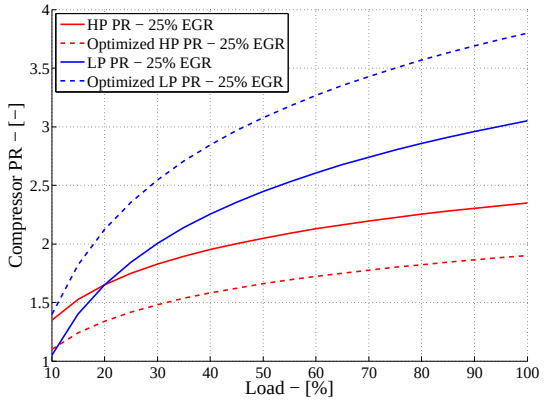

Figure 3.14: Optimization Semi-Short Route - PR simplified illustrative.

This analysis shows the best possible re-gain in terms of BSFC achievable through the optimization process. This is not feasible on the engine for all loads and EGR

rates of interest because of exceeded constrains like maximal cylinder peak pressure and HP turbine inlet temperature. A more moderate optimization permits to lay in a secure operation for the points of interest but still reducing the BSFC with respect to the non-optimized case of about -7.6 g/kWh. The absolute difference at full load for this configuration is then only 3.3 g/kWh higher than in the case without EGR.

Constant Intake Pressure And Constant HP Turbine Inlet Temperature Analysis

The optimization process shown before has the goal to reduce as much as possible the brake specific fuel consumption without taking care of eventual change in conditions that would be kept constant in case of a fair comparison. Exactly for this reason, a fair comparison of the optimized with the non-optimized model, the following analysis has been carried out.

As constrains were chosen two key parameters: once the intake receiver pressure (also called boost pressure) and once the HP turbine inlet temperature. These two separated ways of analyze the optimization process should give a better understanding on the origin of this BSFC reduction and thus of this efficiency increase. For the optimization two supplementary models were created with once a PID boost pressure controller and once with a TTI targeting process implemented. In both cases the turbochargers components were substituted by so-called "simple components". These components do not use any maps, but they have a fixed efficiency, allowing to change operational point without taking into account a variation in compressor and turbine efficiency. Such choice allows to fairly compare the simulation results. The efficiencies chosen are the ones of the actual engine model configuration used as a starting point:

- $\eta_{LP,comp} = 76.56\%$
- $\eta_{HP,comp} = 78.38\%$
- $\eta_{LP,turb} = 85.30\%$
- $\eta_{HP,turb} = 76.50\%$

Of course for changing turbocharger efficiencies the results of this analysis will be different.

The starting point of the optimization is the 100% load point with 25% EGR which shows a turbocharger pressure ratio split of 1.44. The split value is defined as the ratio of the compressors pressure ratios as follow:

$$Split = \frac{PR_{LP,comp}}{PR_{HP,comp}} \tag{3.2}$$

This value can be seen as a parameter describing from which turbocharger stage is delivered the compression power, if this value is low means that the HP stage is delivering more power, while for increasing values the LP stage gain importance in the process of creating the desired boost pressure.

During this analysis the split has been varied for both cases changing the nozzle ring diameter for both the two turbines. Doing this it allows to have a wide range of split values to analyze, approximately for both cases from $Split = 1$ to $Split = 4.5$.

The results concerning the BSFC are shown in Figure 3.15. The best fuel consumption reduction that can be obtained in case of holding the intake pressure constant is of about −2.2 g/kWh at a split of 3.51. While with variable intake pressure but holding the TTI the expected fuel consumption reduction is of ca. −9.2 g/kWh at a split of 3.84.

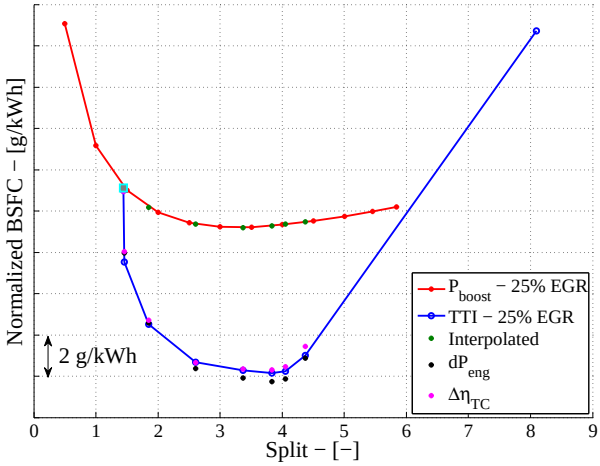

Figure 3.15: Optimization Semi-Short Route - BSFC for split variation in case of constant P_{boost} and constant TTI.

The reduction of split to lower values than already implemented is counterproductive, because it will decrease the intermediate pressure and increase the exhaust pressure causing an augmented EGR flow throttling and a consequently increased work to be done by the HP compressor to re-compress the flow. On the contrary for increasing split more work is done by the low pressure stage, reducing the difference between the exhaust pressure and the intermediate pressure, causing a lower throttling loss over the EGR valve.

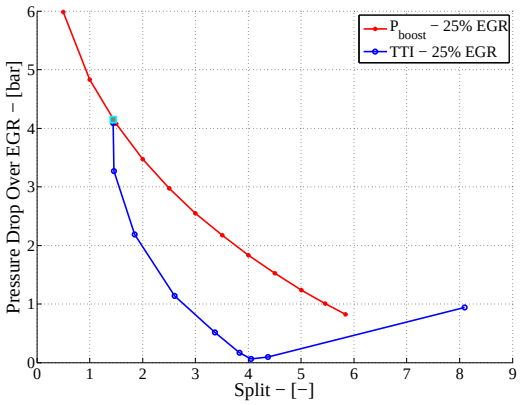

Figure 3.16: Optimization Semi-Short Route - Decrease of the throttling over the EGR valve.

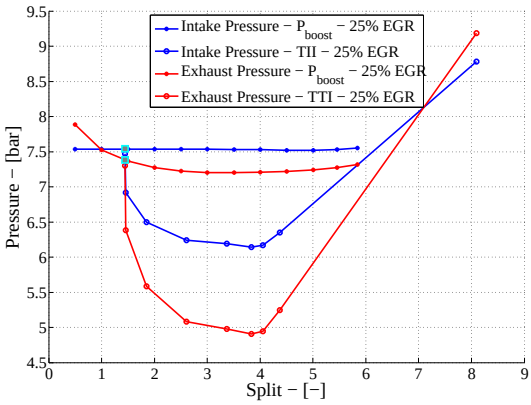

Figure 3.17: Optimization Semi-Short Route - Intake and exhaust pressures.

For constant intake pressure a constant overall compressors power is needed, with

varying the split this power is simply differently handled by the two compressors. By allowing a lower intake pressure (keeping TTI constant) the overall compressors (and also turbines) power is reduced (see Figures 3.18 and 3.19).

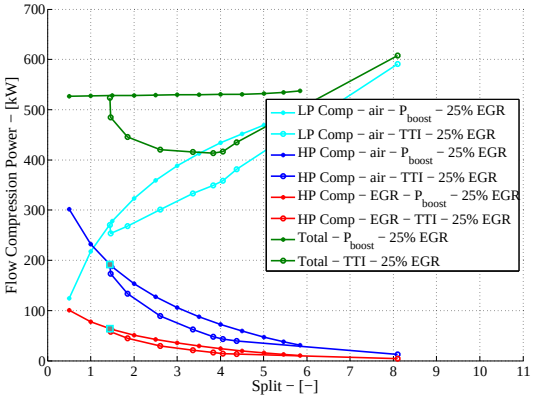

Figure 3.18: Optimization Semi-Short Route - Compressors Power.

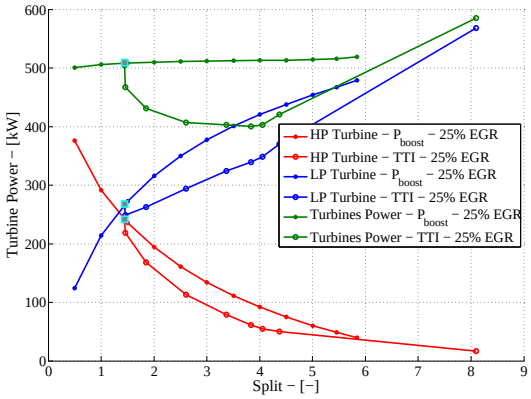

Figure 3.19: Optimization Semi-Short Route - Turbines Power.

As already mentioned the efficiency of the single turbocharger's components is a key factor for the results of this optimization process. The fact that the EGR flow could be expanded less reducing the EGR throttling losses is a first reason of the reduced BSFC. This should lead to a split value for the best efficiency where almost no expansion of the EGR flow occurs, which is not the case at least for the constant pressure case. This is because influencing is also the way in which the turbines power is managed by the two compressors.

A way to understand this gain in efficiency through a better handling of the turbochargers power is given by the turbocharging equivalent efficiency $\eta_{TC,eq}$. This value gives an assessment of the overall system treated as a black box, where the two-stage unit is considered as a single unit and the efficiencies are calculated across the boundaries of this single unit, with both turbochargers, crossover flows and cooling devices taken into account. Equation 3.3 shows how to calculate it following the CIMAC recommendations [9]:

$$\eta_{TC,eq} = \frac{\dot{m}_{Co,HP} \cdot \Delta h_{Com}\left(T_{Ci,LP}, \frac{p_{Co,eq,HP}}{p_{Ci,eq,LP}}\right)}{\dot{m}_{Ti,HP} \cdot \Delta h_{Exp}\left(T_{Ti,HP}, \frac{p_{Ti,eq,HP}}{p_{To,eq,LP}}\right)} \tag{3.3}$$

This efficiency could be also splitted into four single contributions as explained in the Equation 3.4:

$$\eta_{TC,eq} = \eta_{TC,m} \cdot \eta_{\Delta Tcool,TC} \cdot \eta_{\Delta Teta,TC} \cdot \eta_{\Delta p,TC} \tag{3.4}$$

Where the single efficiencies have the following meaning:

- $\eta_{TC,m}$: Average turbocharger's efficiency, which takes into account the performance of the turbocharger proportionately, but not the crossover flows or the intermediate cooling.
- $\eta_{\Delta Tcool,TC}$: Influence of the intermediate cooling between the compressors (normally is $\eta_{\Delta Tcool,C} > 1$) and the temperature drop between the turbines ($\eta_{\Delta Tcool,T}$).

- $\eta_{\Delta Teta,TC}$: Influence of the previous stage's efficiency at the outlet of stage's temperature - compressor's side ($\eta_{\Delta Teta,C}$) and turbine's side ($\eta_{\Delta Teta,C}$).
- $\eta_{\Delta p,TC}$: Influence of the pressure drop between the compressors ($\eta_{\Delta p,C}$) and between the turbines ($\eta_{\Delta p,T}$).

Using the definition of the turbocharging efficiency the following Figure 3.20 is resulted, regarding the simulations that has been carried out.

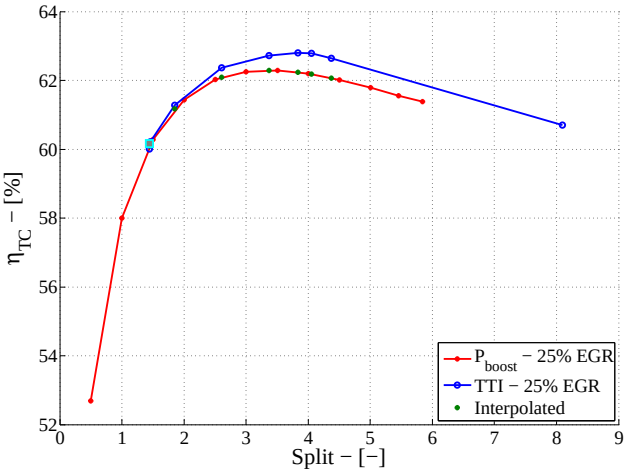

Figure 3.20: Optimization Semi-Short Route - Turbocharging efficiency for split variation in case of constant P_{boost} and constant TTI.

Simulations show that the fuel consumption is directly related with the turbocharging efficiency, namely the lowest values for BSFC corresponds to the highest for the turbocharging efficiency. The minimal difference present between the two cases in the turbocharging efficiency is not reflected in the BSFC curves, where the difference is evidently greater. This is caused by the fact that only a minimal part of the BSFC reduction is coming from this increase, while the rest is coming from the advantageous pressure difference over the engine (phenomenon already mentioned in [10]). This contribution can be calculated approximately through the Equation 3.5:

$$BSFC_{new} = BSFC_{old} \cdot \left(1 - \frac{\Delta p_{eng,new} - \Delta p_{eng,old}}{BMEP}\right) \tag{3.5}$$

Where the pressure difference over the engine is defined as:

$$\Delta p_{eng} = p_{intake} - p_{exhaust} \tag{3.6}$$

Subtracting the contribution in the BSFC reduction of the favorable pressure difference over the engine remains only a smaller gain as shown in the turbocharger efficiency graph and in the Figure 3.15 as the difference between the black asterisks and the pink ones. For a confirmation of this fact and to highlight the correlation between increase in turbocharging efficiency and BSFC reduction the following Figure 3.21 should be helpful.

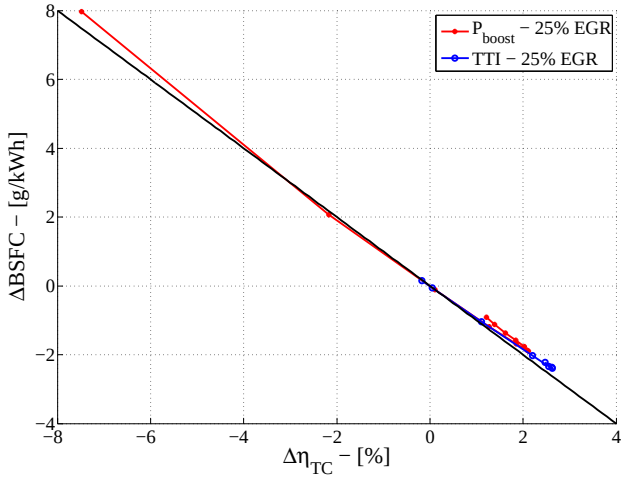

Figure 3.21: Optimization Semi-Short Route - BSFC reduction relation with the turbocharging efficiency of the system for all the simulated points.

This graph shows a linear relation between the two values, the slope is of about -1 g/kWh as expected from the corresponding literature sources the know-how gained through experience. Remember that for the constant TTI case only the BSFC reduction due to the efficiency increase is showed, without the pressure difference over the engine effect.

This analysis shows, in a fair comparison, that the efficiency of a semi-short EGR solution can be optimized regaining up to 9.2 g/kWh depending on the chosen constrain, rending this solution very attractive.

3.3.2 1 Donor Cylinder Semi-Short Configuration

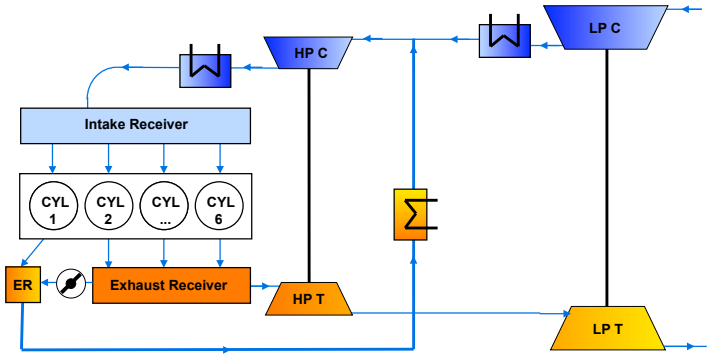

Figure 3.22: Topology of the two-stage turbocharged engine with 1 Donor Cylinder EGR Semi-Short Route. [3]

Another configuration for the EGR path tested in this master thesis is the 1 Donor Cylinder Semi-Short Route. This solution is using the work generated by one cylinder to pump the EGR flow to the intermediate pressure. This cylinder is donating its BMEP for this purpose therefore is called “donor”. Of course some changes

has to be made to the engine and to the piping: not only a new piping, like in the semi-short route solution, for the EGR flow has to be set up, but also a new exhaust receiver for the donor cylinder. Eventually a separation of the exhaust receiver is also possible.

This principle leads to a constant EGR rate, namely all the flow that is coming from the donor cylinder will be recirculated. In case of a six cylinders engine this would mean an EGR rate of approximately 1/6, i.e. 16.67%. This EGR rate cannot be influenced in any ways, is uncontrolled. For have some more flexibility to the system the two exhaust receivers can be connected together through a pipe with a valve. The pressure on the main exhaust receiver will be always higher than the one on the donor cylinder exhaust receiver, opening the EGR valve between the two receivers will let some of the exhaust gases flow from the main exhaust receiver into the donor cylinder exhaust receiver increasing therefore the overall EGR rate. Doing this way this solution is not anymore a genuine one donor cylinder configuration but more an hybrid one, because using the work from one cylinder and some of that from the other five. Through the implementation of such a valve the EGR rate can be now controlled, but only marginally, to be specific from a minimal EGR rate of 16.67% (which can not be controlled) to EGR rates over 30%.

Existing literature claims that this solution will be very promising [13], for this reason a deeper look is taken in the following Sections and the results are compared with the semi-short solution.

Non-Optimized

After setting up the engine model the simulations were carried out with a constant EGR rate of 25% and a load variation between 10% and 100%.

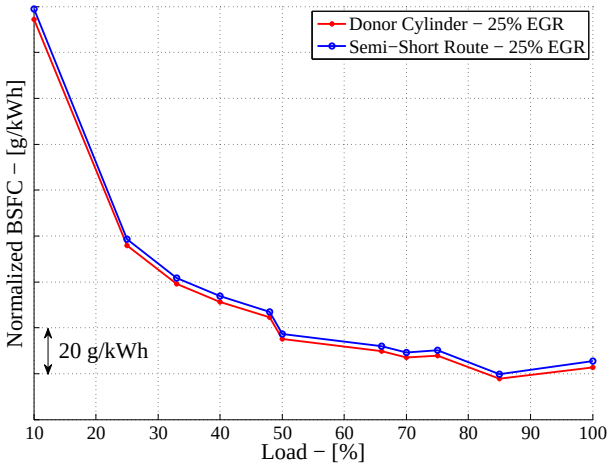

Figure 3.23: Brake Specific Fuel Consumption for the non-optimized one donor cylinder solution with respect to the semi-short route.

Without any optimization this configuration shows effectively already a lower BSFC for all the loads, which consists in −2.6 g/kWh with respect to the semi-short case at full load (see Figure 3.23). This advantage comes from the absence of

throttling losses and therefore lower compression power needed by the system (see Figures 3.24 and 3.25).

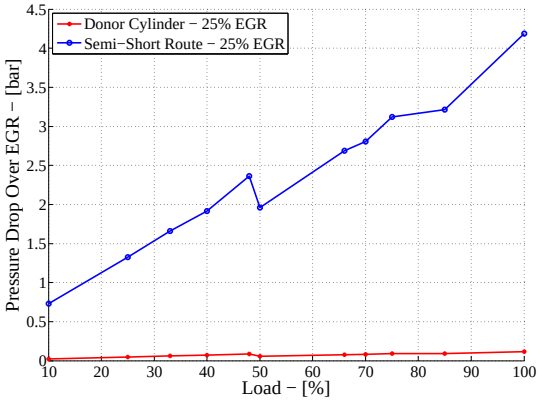

Figure 3.24: 1 Donor Cylinder Semi-Short Route - Pressure drop over the EGR valve.

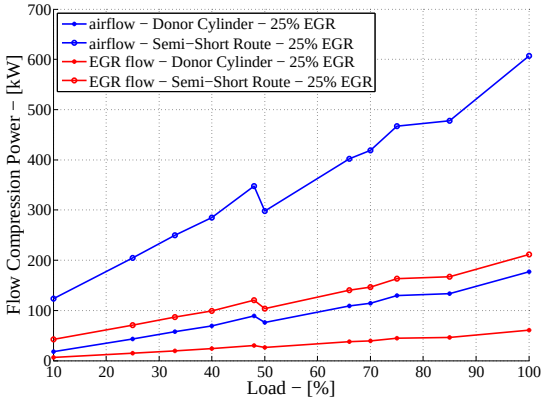

Figure 3.25: 1 Donor Cylinder Semi-Short Route - HP Compressor Power.

The drawbacks are given by an increase in HP turbine inlet temperature of about 18°C, while the donor cylinder shows a thermal load relief of almost −90°C (see Figure 3.26) and a very positive pumping mean effective pressure for the donor cylinder, causing also unbalancing in the engine operation.

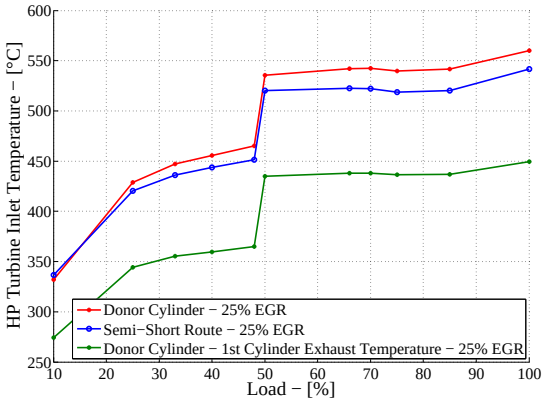

Figure 3.26: 1 Donor Cylinder Semi-Short Route - HP turbine inlet temperature.

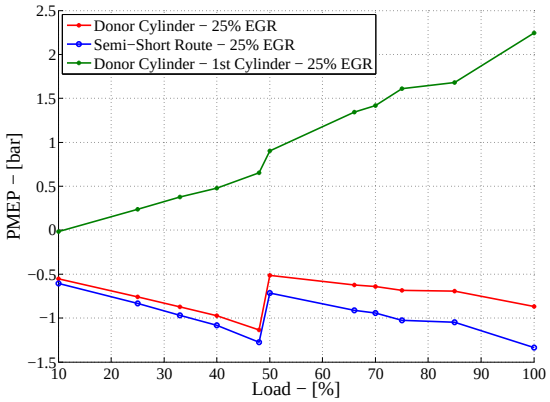

Figure 3.27: 1 Donor Cylinder Semi-Short Route - Pumping mean effective pressure.

Because the engine efficiency compared to the case without EGR is still too low (BSFC at 75% load is increased by ca. 9.7 g/kWh) a re-matching is carried out.

Optimized

As for the optimization process in Section 3.3.1 here the HP turbine mass multiplier has been varied to find a BSFC optimum. This best value is after the optimization process equal to 1.5. The optimization results in almost exactly the same BSFC

curve as for the optimized case for the semi-short route configuration (see Figure 3.28). The actual optimized BSFC at full load shows an increase of 3.2 g/kWh with respect to the case without EGR. Through optimization the BSFC has been reduced by −5.1 g/kWh.

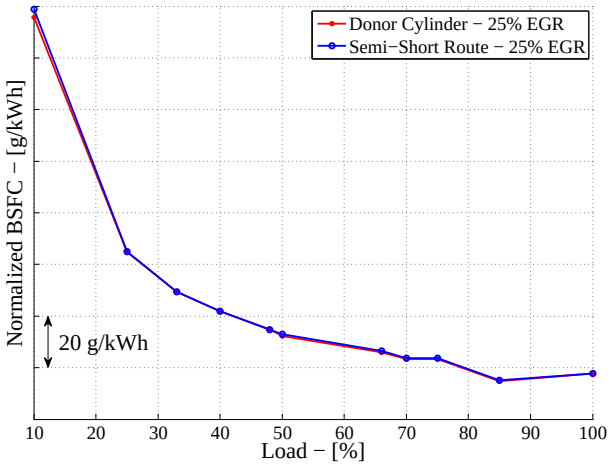

Figure 3.28: Brake Specific Fuel Consumption for the optimized one donor cylinder solution with respect to the semi-short route.

This process allows to reduce the unbalance of the engine given by the higher pumping mean effective pressure showed by the donor cylinder of about 1.5 bar (see Figure 3.30). For the unbalance advantage there is as expected an increase of the thermal load on the HP turbine (reaching the same values as for the semi-short case) and also for the donor cylinder (which will remain only marginally under the 550°C limit) as shown in Figure 3.29.

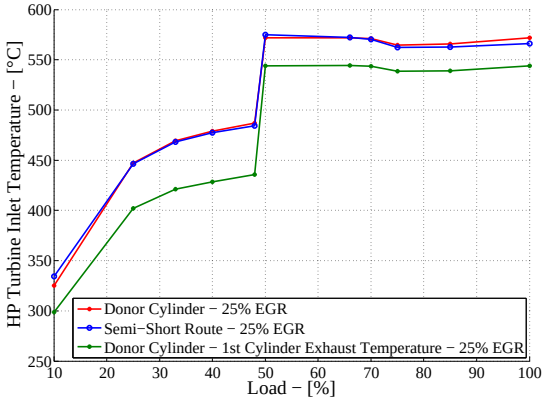

Figure 3.29: Optimization 1 Donor Cylinder Semi-Short Route - HP turbine inlet temperature.

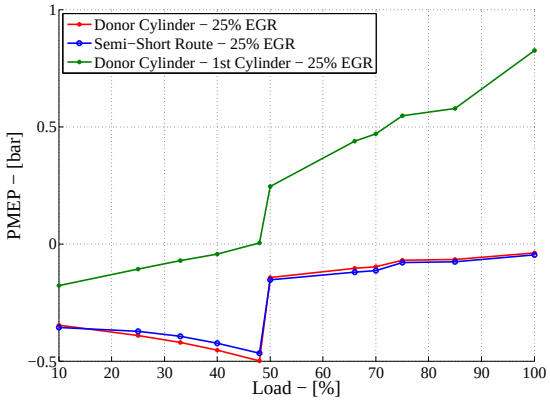

Figure 3.30: Optimization 1 Donor Cylinder Semi-Short Route - Pumping mean effective pressure.

Concluding can be said that the one donor cylinder EGR path gives equivalent results as the semi-short route if both optimized. For the solution presented in this Section the EGR rate is limited downwards by the physical fact that one cylinder

(at least) will always pump EGR flow to the intake producing a minimal value of 16.67%. This limitation will count as a disadvantage with respect to the semi-short route, where a desired EGR rate can be set acting on the EGR valve in a range from 0% up to over 30%.

M80 Cam Profile

During the master thesis there has been a close collaboration with ABB Turbochargers Ltd., supplier of the turbochargers for the test engine. The ABB engineers have proposed a new cam profile for the donor cylinder to improve the BFSC in the case of a 1 donor cylinder EGR configuration. This new cam profile has been implemented and tested for the non-optimized case and the optimized one.

The valve system of this engine allows variations in the timing and in the shape of the opening and closing events. The inlet valve has a variable timing, depending on the engine load, one of the two inlet valve profiles is switched on. For low loads (up to 48% load) a normal intake profile is used (green curve in Figure 3.31). The variable valve timing will switch to a Miller cam timing and profile for loads from 50% to 100% (red curve). The exhaust valve timing and profile is kept constant for all loads (blue curve).

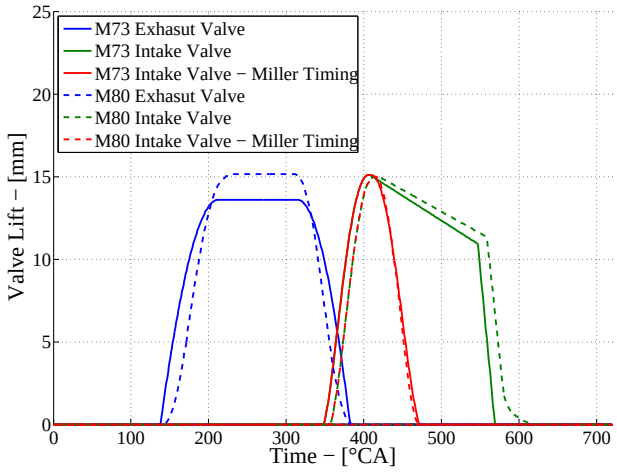

Figure 3.31: Cam Profiles used in the simulations - M73 and M80.

The actual cam profile (called M73, solid lines) showed in the Figure 3.31 has been substituted by a new profile (called M80, dashed lines). The difference consists mainly in a higher exhaust valve lift, but a lower overlap and a slightly delayed inlet valve closing timing for the case without Miller.

The results of this solution, for both optimized and non optimized cases, are shown in Figures 3.32 and 3.33 (the 85% and 50% load did not converged). For the standard case the adoption of the new cam will effectively reduce the BSFC for the Miller cases of up to -2.5 g/kWh for full load conditions with respect to the M73 cam profile. This advantage is coming through an improved gas exchange phase, paid by an higher thermal stress. The advantage is then lost after the optimization, where then the BSFC improvement is reducted to almost see no difference compared

with the old cam profile M73. To eventually recuperate part of the benefits of the M80 cam profile a new cam profile for the optimized engine model should be found, keeping in mind the higher thermal load on the HP turbine and on the cylinders.

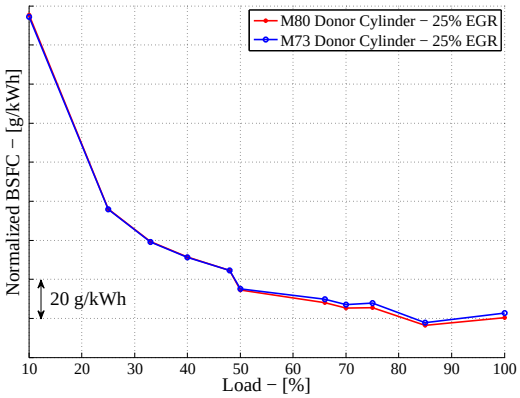

Figure 3.32: 1 Donor Cylinder Semi-Short Route - BSFC reduction through new M80 Cam profile.

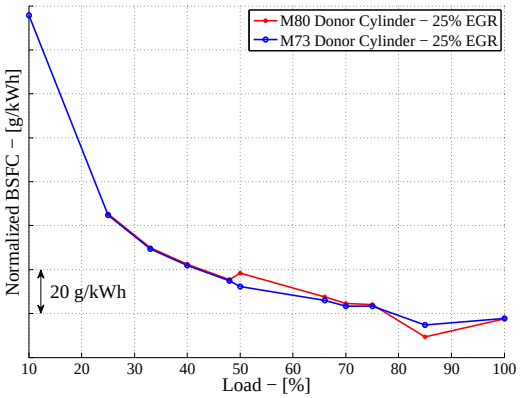

Figure 3.33: Optimization 1 Donor Cylinder Semi-Short Route - BSFC with new M80 Cam profile.

The actual M73 cam profile works with optimal results in case of a rematching of the turbocharger system components, therefore a change of the cam timing is not recommended. Besides this the M80 Cam case requires, if optimized, to a rematch of the LP compressor, which is during the simulation working in surge region (values are extrapolated).

3.3.3 2 Donor Cylinders Short Configuration

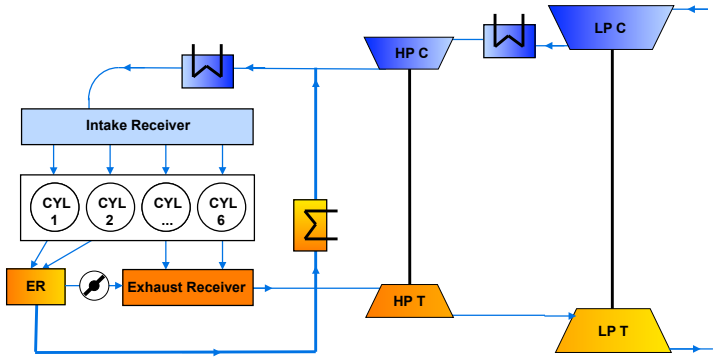

Figure 3.34: Topology of the two-stage turbocharged engine with 2 Donor Cylinders EGR Short Route. [3]

Another way to use the principle of the donor cylinder is given by this configuration: the 2 Donor Cylinders Short Route. In this case the number of donor cylinders is augment to two and the EGR flow is then recirculated directly in the second turbocharging stage after the HP compressor. The two donor cylinders will be used for pumping the EGR flow into the intake manifold. The exhaust gases of these two cylinders are collected in a separate exhaust manifold creating here also a fixed

EGR rate of 2/6, i.e. 33.33%. As for the one donor cylinder configuration is here the EGR rate constant until the two exhaust manifolds are connected to each other. An EGR vale will then convoy some of the exhaust gases coming from the two donor cylinders to the main exhaust manifold (which have a lower pressure than the one of the donor cylinders) creating a flow in the opposite direction respect to the single donor cylinder and thus reducing the actual EGR rate. Namely this case in limited upwards defining an EGR rate range between 0% and 33.33% EGR.

Non-Optimized

With this configuration implemented a simulation run has been run and the obtained results in terms of BSFC are compared with the solution of one single donor cylinder EGR path.

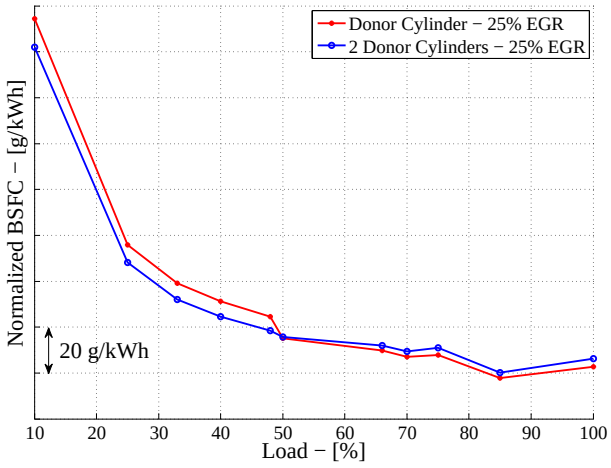

Figure 3.35: Brake Specific Fuel Consumption for the non-optimized two donor cylinders solution with respect to the one donor cylinder.

Figure 3.35 shows that this solution gives an interesting trend regarding the BSFC compared with the single donor cylinder one. For high loads (with the Miller cam timing) the fuel consumption is increased (e.g. up to 3.5 g/kWh more than the single donor cylinder at full load), while for lower loads, where the Miller timing is deactivated, this solution gives a remarkable lower fuel consumption (over -5 g/kWh). Attention should be paid to the fact that for these lower loads the EGR rate is not the desired 25%, but 33% instead. This is causes by a too low intake pressure that leads to a lower donor cylinders exhaust receiver pressure with respect to the the one of the other cylinders inverting the flow over the EGR valve (which would therefore increasing the EGR rate) To avoid this fact the EGR valve is completely closed for these cases and the engine runs with an EGR rate of about 33%.

The great advantage of this solution is given by the lower thermal stress on the HP turbine (see Figure 3.36) and a much more balanced engine run. The positive pressure drop over the engine is lower then for the single donor cylinder keeping the PMEP negative which is negative for the overall power extracted by the engine (see Figure 3.37) but it is advantageous for the balance of the engine.

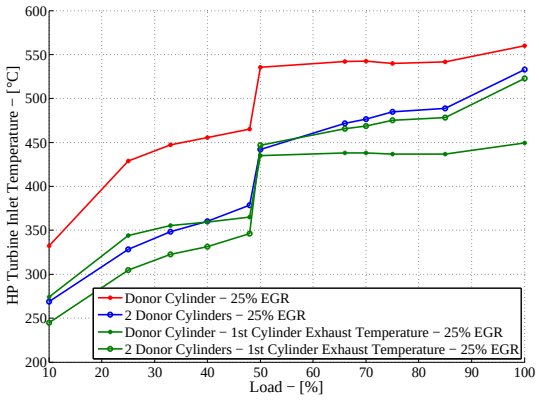

Figure 3.36: 2 Donor Cylinders Short Route - HP turbine inlet temperature.

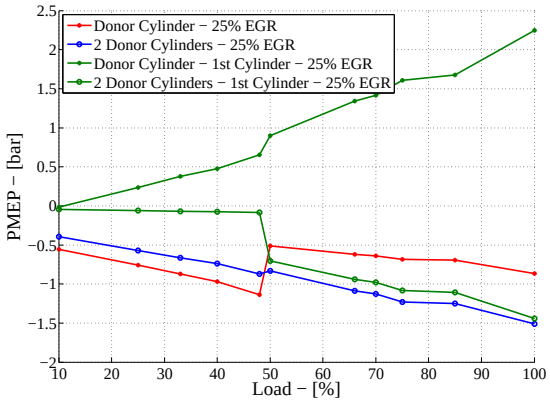

Figure 3.37: 2 Donor Cylinders Short Route - Negative PMEP for the donor cylinders.

Attention should be also paid to the fact that for this configuration the HP compressor is working in the surge region, while the LP compressor works over the choke line. Both the compressors should be rematched in order to handle well the new reduced mass flow (EGR short route will cut out from both compressors an important amount of flow).

Optimized

The optimized case has been ruined with the HP turbine mass multiplier increased from the default value of 1.0 to 1.5, scaling thus the mass flow axis for the turbine map. This configuration leads to an improved high load behaviour as depicted in Figure 3.38 where the BSFC is matching the one registered for the single donor cylinder optimized case.

This improvement does not affect the already present advantageous BSFC curve at lower loads where the Miller timing is deactivated (EGR rate still of 33% instead of 25%). At full load the fuel consumption simulated is increased by ca. 1.0 g/kWh compared to the 1 donor cylinder, while for all other loads a reduction can be achieved.

The thermal stress, normally increasing through the optimization process, is in this case increased only for the donor cylinders while is reduced for the inlet temperature at the HP turbine (see Figure 3.39). The advantage of a positive PMEP (work is done during the pumping stroke) shown by the single donor cylinder case is for the two donor cylinders optimized case completely lost, increasing therefore slightly the overall BSFC but still remaining at the same levels as the other solution (see Figure 3.40).

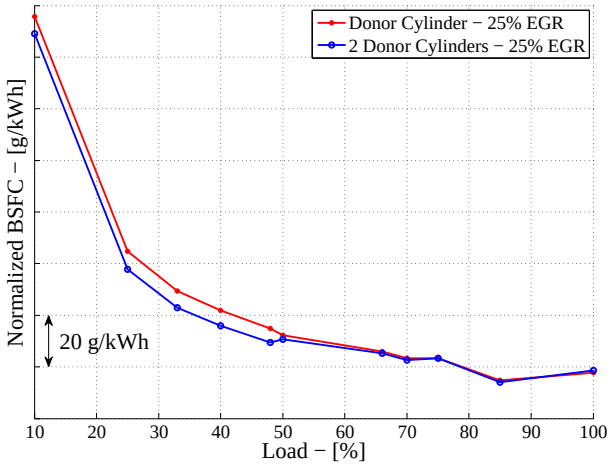

Figure 3.38: Brake Specific Fuel Consumption for the optimized two donor cylinders solution with respect to the one donor cylinder.

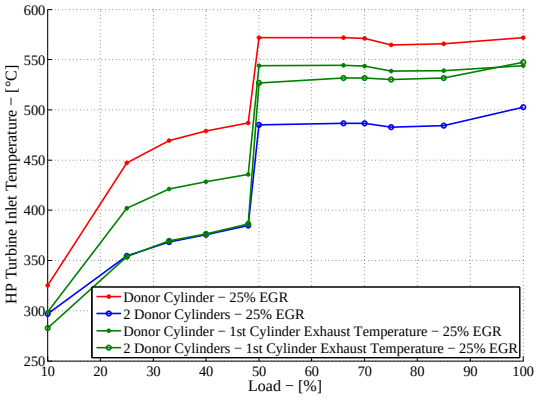

Figure 3.39: Optimization 2 Donor Cylinders Short Route - HP turbine inlet temperature.

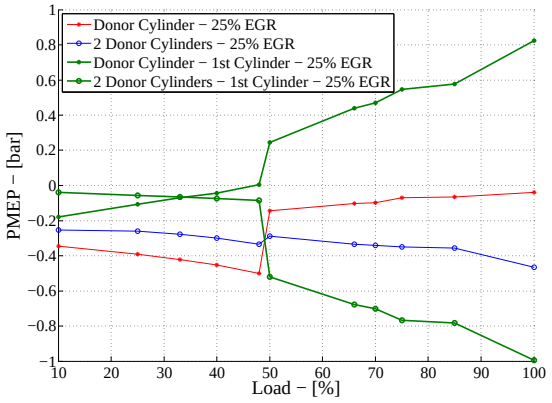

Figure 3.40: Optimization 2 Donor Cylinders Short Route - Negative PMEP for the donor cylinders.

The two donor cylinders would be advantageous with respect to the single donor cylinder solution under many aspects: the BSFC simulated is always lower (apart for full load, minimally for Miller cases, while remarkably for other cases) compared with the single donor cylinder and the semi-short route configuration. The fact that the thermal stress is lower on this solution and that no EGR with a short route configuration will flow through the compressor wheel (which can be problematic) rends the two donor cylinders EGR path a valid and competitive technology.

3.3.4 EGR Blower Configuration

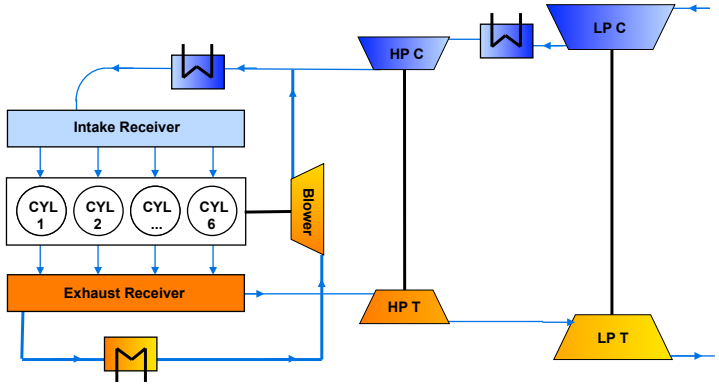

Figure 3.41: Topology of the two-stage turbocharged engine with EGR Blower Short Route. [3]

This configuration for the exhaust gases recirculation to the intake manifold (short route) uses normally an electrically driven blower which is used to pump the exhaust gases overcoming the pressure gradient. Like a turbocharger has a compressor side (blower) but the turbine side is replaced by a mechanical (connected through a gear to the engine crankshaft) or an electrical drive. Of course a motor-gearbox configuration will increases weight, complexity, space requirements and costs. The electrically driven bower needs very high speeds, such machines are nowadays very expensive. But the advantage of this configuration is given by the higher flexibility of the system, since the EGR blower can be controlled independently of the engine speed and higher turbocharging efficiencies eliminating the turbine side (see results shown in Section 3.3.4).

For this optimization again a simple components model has been developed, where the two turbochargers were substituted like in Section 3.3.1. For the EGR Blower a compressor map of an actual model of EGR Blower developed by ABB Turbosystems Ltd. has been used, this map implemented in GT-Power is shown in the following Figure:
In the next Sections the non-optimized case is not presented because for this EGR configuration the engine will not perform as desired. Thus the solution following two cases are analyzed instead:

- EGR Blower externally driven: energy is considered “for free”.
- EGR Blower driven by the engine crankshaft: the blower acts as auxiliary torque attached on the engine.

Then, considering the engine model with the energy for the EGR blower taken from the engine crankshaft, an additional analysis holding some constrains parameters constant is carried out as in the Section 3.3.1. This will allow to fairly compare the full load point with the solution given by the semi-short route configuration.

Optimized

In this case with simple components the mass multiplier (which in reality would reflect the turbine nozzle ring diameter) is not present anymore for the optimization

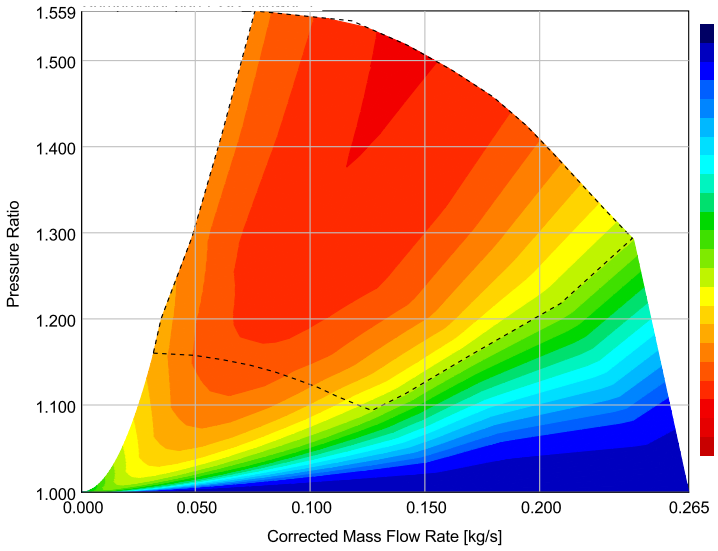

Figure 3.42: Compressor Map for the EGR Blower.

process. Instead of this variable directly the turbine nozzle ring diameter should be given in and will be therefore become the optimization tuning parameter.

Through a calibration procedure using the standard case (not optimized) the following values for the turbines nozzle rings have been found:

- Low Pressure Turbine: 67.43 mm.
- High Pressure Turbine: 44.99 mm.

After have found these values the HP turbine nozzle ring diameter has been optimized with the goal of minimize the BSFC at full load. The results for both cases, externally electrically driven and crankshaft driven, gives obviously different values, thus the second case should produce more power in order to cover the requirement of the blower. The resulting HP turbine nozzle ring diameters are:

- Electrically driven - Optimized High Pressure Turbine: 58.36 mm.
- Crankshaft driven - Optimized High Pressure Turbine: 56.64 mm.

This means that for both cases a bigger nozzle ring is needed to reduce the BSFC, i.e. lowering the intake pressure (see Figure 3.46). The BSFC curves are shown in Figure 3.43.

The fuel consumption in the electrically driven case is clearly very low (the lowest ever simulated, corresponding to -2.8 g/kWh compared to the case without EGR). The two curves are actually equivalent, the difference correspond to the additional fuel consumption needed to drive the EGR blower. At full load this BSFC penalty is of ca. 4.8 g/kWh. Adding this difference the BSFC still remains low, with only 2.0 g/kWh more than the case without EGR). The increase of total engine power output in order to drive the EGR blower has been calculated and is at full load of ca. 25 kW which corresponds to about 2.5% of the total engine (see Figure 3.44). Similar values has been already experimented in other researches and are consistent with existing literature [13].

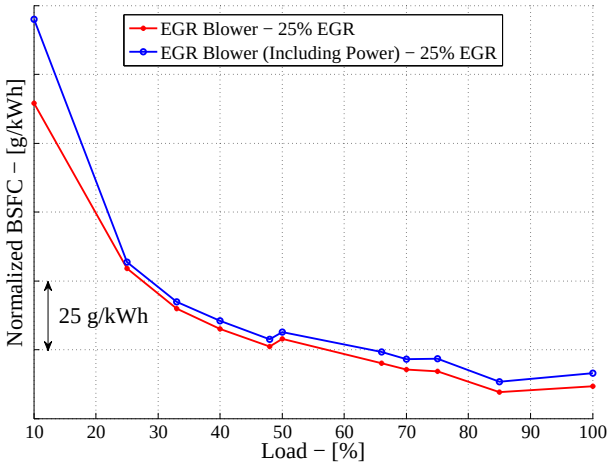

Figure 3.43: Brake Specific Fuel Consumption for the optimized EGR Blower solutions.

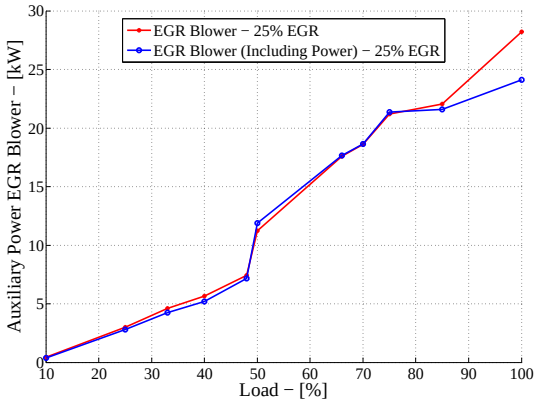

Figure 3.44: Optimization EGR Blower Short Route - EGR Blower power.

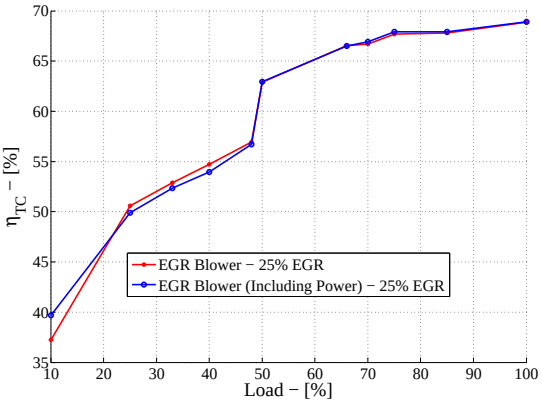

Figure 3.45: Optimization EGR Blower Short Route - Turbocharging efficiency.

This solution permits to reduce the BSFC also through the increase in turbocharging efficiency gaining over 6% points with respect to the semi-short configuration (see Figure 3.45). The limiting HP turbine inlet temperature shows also benefits, because all values (although the electrically driven case at 50% load becomes critical) remains lower than the ones for the optimized semi-short route case (compare Figure 3.8 with Figure 3.47).

This solution represents the best under many aspects, the BSFC is reduced drastically, the thermal stress is high but still not critical. Only disadvantage is that this is one of the most expensive solution to be implemented.

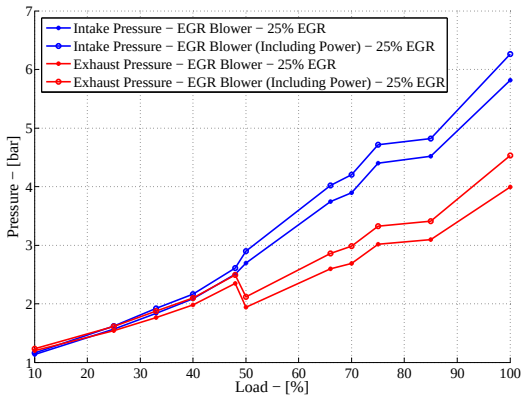

Figure 3.46: Optimization EGR Blower Short Route - Intake and exhaust pressures.

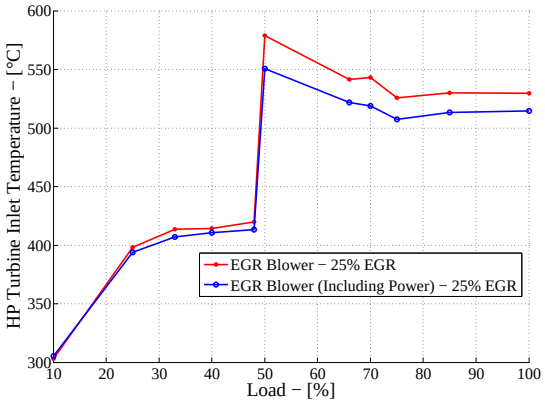

Figure 3.47: Optimization EGR Blower Short Route - HP turbine inlet temperature.

Constant Intake Pressure And Constant HP Turbine Inlet Temperature Analysis

After the search of maximal BSFC improvement the following analysis has been carried out in order to fairly compare this solution with the semi-short one. The same turbochargers configuration as in Section 3.3.1 is obviously chosen. The achieved Split variation is for both constrains cases in a range between 0.5 and 4.0.

The BSFC reduction curves through the variation of split shown in Figure 3.48 remarks the lower achievable fuel consumption (especially for the constant boost pressure case). The fact that the optimum by the EGR blower solution is found by lower splits. This would mean that both turbochargers will have a similar dimension and a smaller one with respect to the solution of the semi-short case, where the split goes up beyond 3.0 (i.e. the LP compressor will do three times more pressure ratio compared to the HP stage).

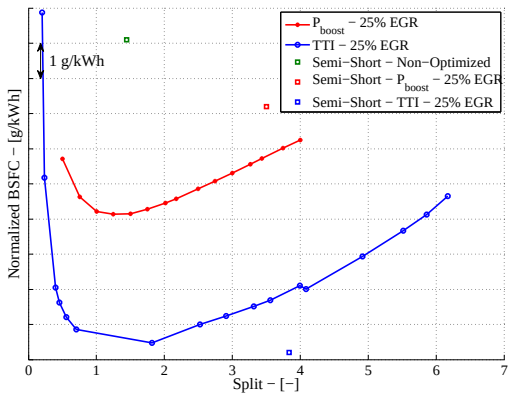

Figure 3.48: Optimization EGR Blower Short Route - BSFC for split variation in case of constant P_{boost} and constant TTI.

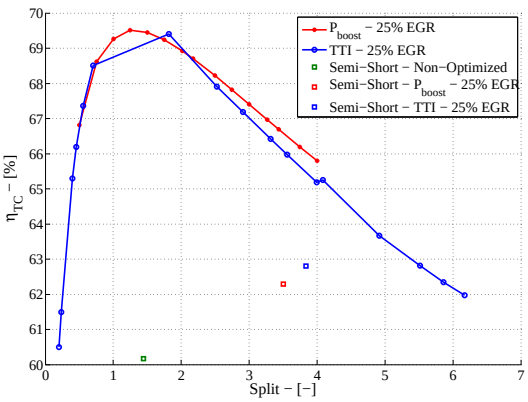

Figure 3.49: Optimization EGR Blower Short Route - Turbocharging efficiency for split variation in case of constant P_{boost} and constant TTI.

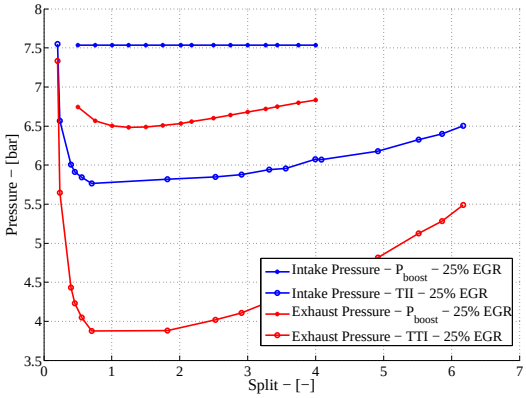

Figure 3.50: Optimization EGR Blower Short Route - Intake and exhaust pressures for split variation in case of constant P_{boost} and constant TTI.

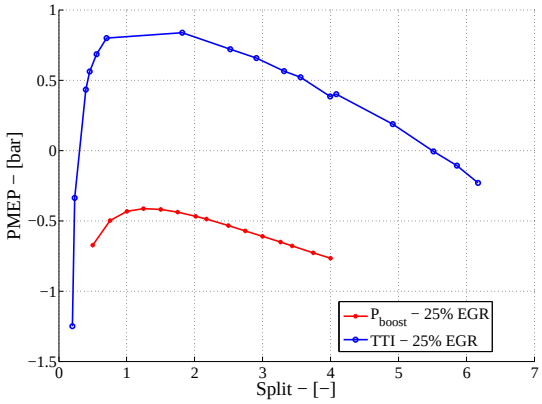

Figure 3.51: Optimization EGR Blower Short Route - PMEP for split variation in case of constant P_{boost} and constant TTI.

The Figure 3.49 shows the big improvement in turbocharging efficiency with respect to the semi-short route solution. The introduction of an EGR blower also increase the pressure drop over the engine (allowing a much higher intake pressure compared to the low exhaust pressure) increasing the corresponding benefits of the optimization in terms of BSFC as explained by the Equation 3.5 in Section 3.3.1.

The EGR blower solution shows in a fair comparison an effective advantage for the constant boost pressure case compared for the results obtained for the semi-short EGR path. For the case of constant HP turbine inlet temperature the results are similar in terms of BSFC, but the more complicate and cost intensive solution represented by the EGR blower would then be discarded promoting the semi-short route solution.

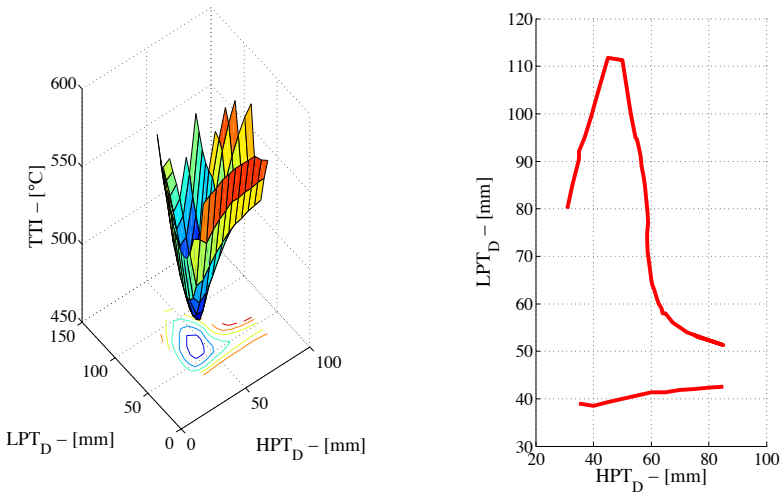

Figure 3.52: Optimization EGR Blower Short Route - TTI effects of the variation of the HP and LP turbine nozzle ring diameters.

An additional analysis with the constant HP turbine inlet temperature has been done to better understand the variation's effects of both turbines nozzle rings. Figure 3.52 shows the temperature profile and on the right the iso-line for a turbine inlet temperature of 540°C. The TTI is decreasing for lower values of HP, and for moderate LP, turbine nozzle rings diameters.

The following two Figures depicts other two important parameters that are changing with this variation of nozzle rings diameters: the Split and the BSFC. Obviously is of interest to get the lowest possible fuel consumption, which is done through increasing both turbine nozzles diameters. This is not possible because the inlet turbine temperature limit will be overcome.

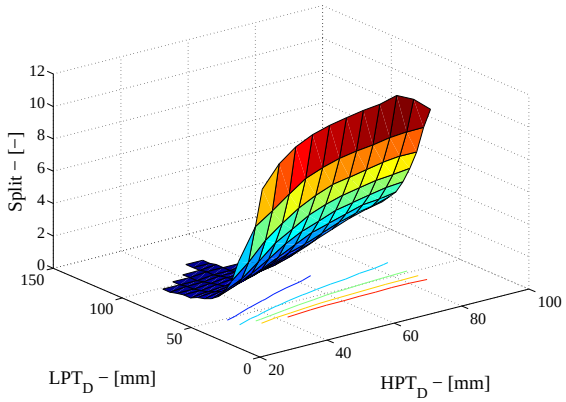

Figure 3.53: Optimization EGR Blower Short Route - Split effects of the variation of the HP and LP turbine nozzle ring diameters.

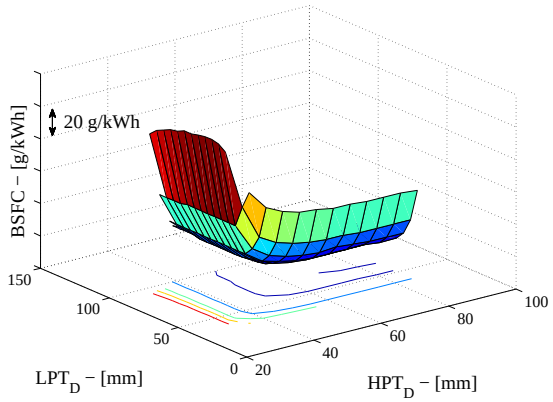

Figure 3.54: Optimization EGR Blower Short Route - BSFC effects of the variation of the HP and LP turbine nozzle ring diameters.

Superposing the iso-line of the inlet turbine temperature to the graph of the BSFC as in Figure 3.55 rends clear that the optimization process for lowest BSFC is limited for different reasons.

The lowest BSFC values would be reached by increasing both turbine nozzle ring diameters, but this is limited by the increasing inlet HP turbine temperature. This increased is actually caused by the lowered boost pressure, effect given by the increase of the nozzle ring diameters of both turbines. Exactly the opposite reason that is limiting the optimization process is present if, holding a constant LP turbine nozzle ring diameter, the HP turbine nozzle ring diameter is continuously reduced. This will drastically increase the boost pressure, up to values where fuel has to be burned in order to create the necessary boost required by such a turbocharger specification. Doing the opposite as before, holding a constant HP turbine nozzle ring diameter and reducing the LP turbine nozzle ring diameter continuously, an increase in BSFC is expected. This increase can be understood as follow: decreasing the LP turbine nozzle ring diameter means increasing the intermediate pressure, thus - for the blower case - more fuel is needed in order to move the blower to compress the exhaust gases to this higher intermediate pressure, while - for the semi-short route case - the throttling losses are increased reducing the overall turbocharging efficiency.

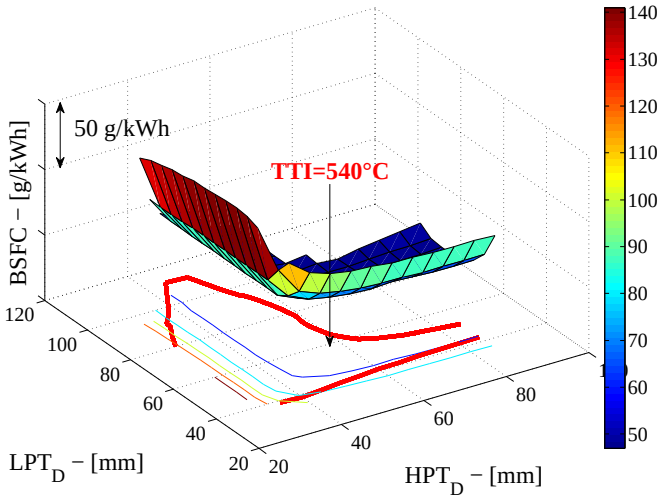

Figure 3.55: Optimization EGR Blower Short Route - TTI iso-line on the BSFC effects of the variation of the HP and LP turbine nozzle ring diameters.

3.3.5 EGR Turbocharger Configuration

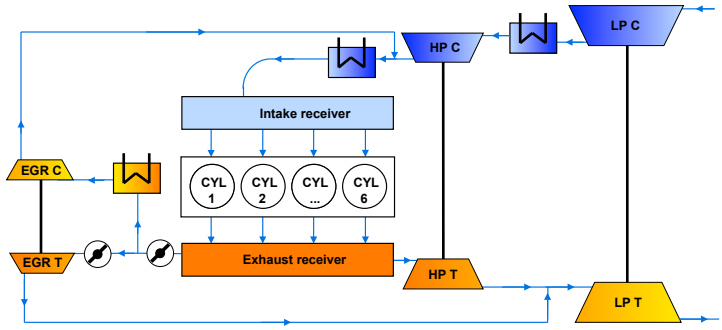

Figure 3.56: Topology of the two-stage turbocharged engine with EGR Turbocharger Short Route. [3]

This configuration is from the layout point of view the most complicated one. The EGR path is recirculated through a short route connection between the exhaust and the intake manifold, but instead of the electrically driven blower, an additional small turbocharger is used to pump the EGR flow. Two EGR valves have to be used in order to control the EGR rate (see Figure 3.57):

- The first: used to reduce the overall EGR flow through the dedicated turbocharger, this is normally open for high load points (apart the full load where the exhaust gas flow is too high and will exceed the limiting EGR turbine inlet temperature).
- The second: actually simulated directly through a variable turbine geometry (VTG) used to create the correct pressure ratio to pump the EGR flow.

One of this two vales can be substituted by a wastegate valve reducing the difficult control strategy that has to be implemented in order to drive this EGR configuration. But adopting this solution the efficiency will drop slightly because some of

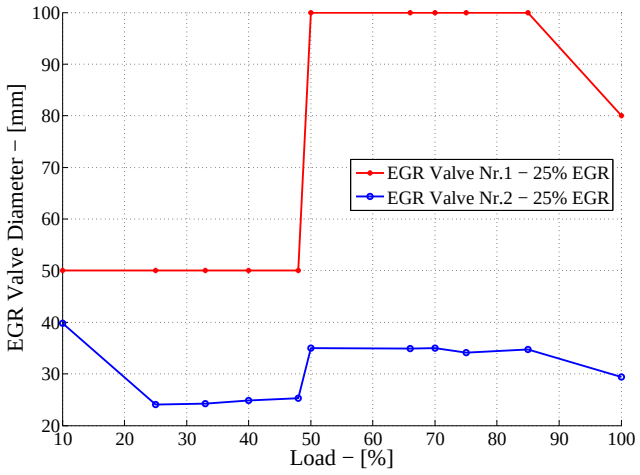

Figure 3.57: Optimization EGR TC Short Route - EGR Valves diameter

the exhaust flow energy will be only used by the LP turbine.

Optimized

In order to run this configuration an optimization process has been carried out as already done also in the other cases. The non-optimized case will not run without any adaption of the turbocharging system.

The turbochargers (HP, LP and EGR TC) are simple components, meaning that they will always maintain a constant efficiency over the whole operation map. This allows changes of the specification comparing the improvements in a fair way. The efficiencies of the two main turbochargers are the same as listed in Section 3.3.1, while for the EGR TC an efficiency of $\eta_{EGR,C} = \eta_{EGR,T} = 60\%$ has been chosen as mentioned in [13].

The optimization consists in the variation of both LP and HP tubing nozzle ring diameters to get the lowest possible fuel consumption. Doing this the EGR rate will be adjusted by a controller that will act on the second EGR valve, while the first EGR valve is actuated in an feed-forward control, based on previous simulation's results. The best solution has to be excluded because not capable to run at all loads (but only full load), therefore an optimization for the critical 50% load was done taking into account to not penalize too much the higher load points. This optimizations gives the following results for the tuning parameters:

- Optimized High Pressure Turbine nozzle ring diameter: 47.36 mm.
- Optimized Low Pressure Turbine nozzle ring diameter: 55.94 mm.

For the EGR valves diameters is referred to the Figure 3.57 shown before.

The BSFC curve of Figure 3.58 shows that although the optimization process has been done for the 50% load point, for all other loads the fuel consumption is reduced compared to the semi-short configuration too. This fact confirms that the EGR TC solution is a valid solution that gives high efficiency at all loads for the

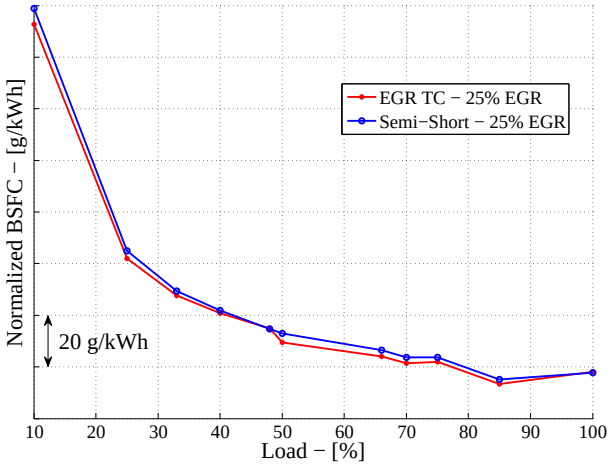

Figure 3.58: Brake Specific Fuel Consumption for the optimized EGR Turbocharger solution.

configuration tested. Other advantage is the lower thermal load on both the HP and the EGR turbine (see Figure 3.59).

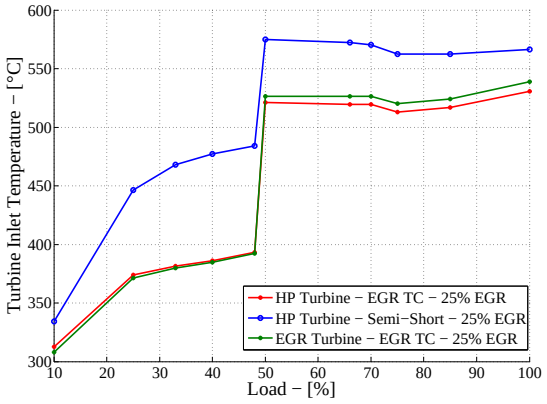

Figure 3.59: Optimization EGR TC Short Route - HP and EGR turbine inlet temperature.

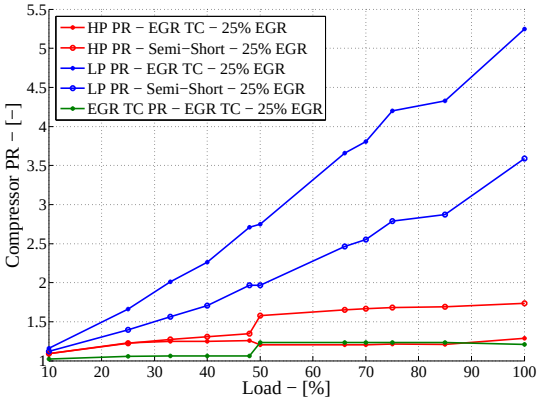

Figure 3.60: Optimization EGR TC Short Route - Pressure Ratios.

A very interesting fact is that the optimization process tends to equalize the intermediate pressure with the exhaust pressure, for this limiting case the best efficiency is registered. But for the limiting case where this two pressures are equal, then the EGR TC will have to pump the exhaust gases to the intake manifold, doing exactly the same pressure ratio of the HP turbocharger (as in this optimized case, see Figure 3.60). Then a much simpler solution, without loosing any efficiency, would be to simply connect the exhaust manifold to the intermediate stage manifold, i.e. use the semi-short route configuration, making unnecessary an additional EGR TC.

This configuration is very promising because of the reduced BSFC penalty and the lower HP turbine inlet temperature (although the higher temperature will be then registered at the first of the two throttle valves), but the high costs caused

by an additional turbocharger, the maintenance of this unit, the complex control strategy, the increased space needed for the devices and the pipings compared to a simple semi-short route will reduce the attractiveness of this solution.

3.3.6 1 Donor Cylinder Semi-Short Test Bench Configuration

At the end of the master thesis one of this simulated configurations has decided to be implemented on the test bench in order to analyze it experimentally. The choice has fallen on the 1 Donor Cylinder Semi-Short Route EGR Path.

To modify the actual EGR configuration from a simple semi-short route to a one donor cylinder configuration a separation of the exhaust manifold should be made. This test engine has an exhaust manifold which consists in six separate parts (one for each cylinder) connected together forming the whole manifold. This allows to insert a plate in the exhaust manifold to divide the exhaust gases of any of the cylinders. On the test bench a fixed EGR rate will be used. To create this rate a plate with a fixed orifice diameter will be inserted (instead of a valve with variable controllable diameter).

The three EGR rates of 20%, 25% and 30% are simulated in order to find the expected orifice diameter for each one. The resulting three orifice diameters are:

- Diameter for 20% EGR = 0.1234 mm
- Diameter for 25% EGR = 13.99 mm
- Diameter for 30% EGR = 21.41 mm

The results in terms of BSFC of these three rates are very similar (see Figure 3.61) therefore an orifice diameter of 15.00 mm has been chosen as the one to be implemented, which would lead to an EGR rate slightly above 25% (actual simulated EGR rate in this configuration is of ca. 26% EGR).

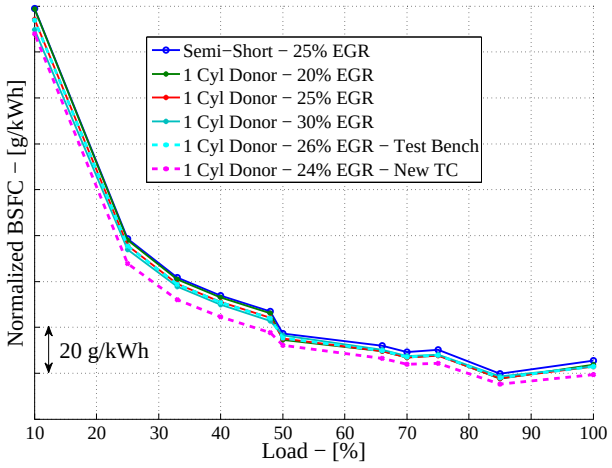

Figure 3.61: Brake Specific Fuel Consumption for the one donor cylinder solution to be implemented on the test engine.

Before setting up this configuration another step has been done, namely the implementation in the simulation program of the new optimized HP turbine map. This new HP turbine specification reflect the closest specification available in the ABB Turbo Systems catalogue to the optimal one that has been simulated in this master thesis (as explained in Section 3.3.2). Through this change in turbine specification the BSFC is reduced (maintaining an EGR rate of about 24%) by -6 g/kWh at full load with respect to the non optimized semi-short configuration actual running on the test engine (see Figure 3.61). Other very important advantage is that through the optimization the peak cylinder pressure is reduced under the maximal allowable value of 180 bar for all load cases (see Figure 3.63). The HP inlet turbine temperature is remained almost the same as the one with 25% EGR, slightly over the desired limit of 540°C for all the Miller cases, but still way under the critical limit of 580°C for all cases (see Figure 3.62). This would mean that this configuration should run for all loads with ca. 25% EGR.

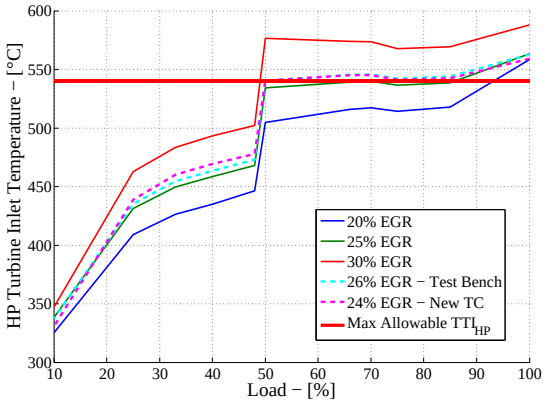

Figure 3.62: Optimization 1 Donor Cylinder Semi-Short Route - HP turbine inlet temperature for the future test bench configuration.

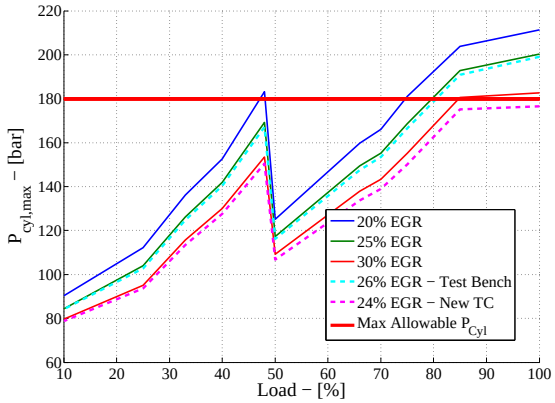

Figure 3.63: Optimization 1 Donor Cylinder Semi-Short Route - Peak cylinder pressure for the future test bench configuration.

This configuration will be now tested experimentally on the engine and the results should then be compared with the simulation results for a validation purpose.

3.4 NO_x Analysis

At the end a brief look at the NO_x emissions model implement in GT-POWER. This model should be calibrated for each engine separately based on measurements data. The calibration process has been carried out by changing only the NO_x calibration multiplier. This value (as already explained in Section 2.1.3) will scale the overall NO_x emissions depending on the output, no change in the oxidation rates or in the activation energies is done. The NO_x emissions multiplier's value that gives the best results compared to the measurement points is of 0.55.

In the following Sections the results of the simulated NO_x emissions are showed in case of different variables variation. The results are generated using the engine model with semi-short EGR path implemented.

3.4.1 Load Variation

The Figure 3.64 shows the simulation's results for the three different EGR rates (20%, 25% and 30%) that were compared with the measurements data (available only for 20% and 25% EGR). The simulations could not compute NO_x emissions for all the loads, therefore a calibration was very difficult for the lack of corresponding measurements points.

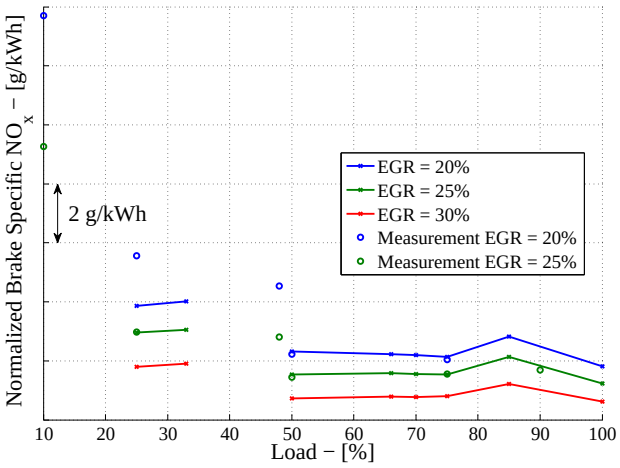

Figure 3.64: Brake Specific NO_x emissions for Load variation.

The measurements and the simulations show that NO_x emissions decreases with the increase of EGR rate. This benefit is higher at lower loads. The pollutant emissions decreases generally for increasing load, apart for load points where an higher rail injection pressure is used (for example at the 85% load case) which increases the NO_x emissions again.

3.4.2 EGR Rate Variation

The variation of EGR rate at three different loads (25%, 50% and 75%) shows a pretty much linear relation. Figure 3.65 shows that a simple calibration of the NO_x

model with the only modification of the overall multiplier is not the optimal way in order to reproduce and estimate the emissions over a wide range of loads and EGR rates. The actual NO_x model is calibrated in order to get the best results for 25% EGR and 50% load.

3.4.3 O_2 Concentration Variation

Because the EGR rate is not the most reliable value, the oxygen concentration in the intake manifold can be used as an indicator of the presence of EGR flow. For absence of EGR this concentration will be around the oxygen concentration present in the air, therefore around 21%. Increasing EGR the oxygen concentration will drop. Figure 3.66 shows the linear relationship between EGR rate (in this case expressed through oxygen concentration) and the $BSNO_x$ produced by the engine as already seen before. Different slopes of the curves are caused mainly by different start of injection timing and different injection rail pressure for different load points.

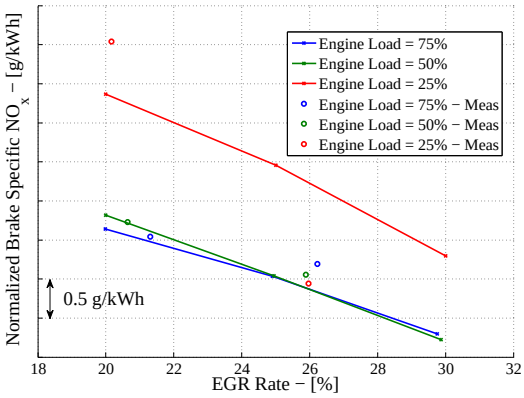

Figure 3.65: Brake Specific NO_x emissions for EGR variation.

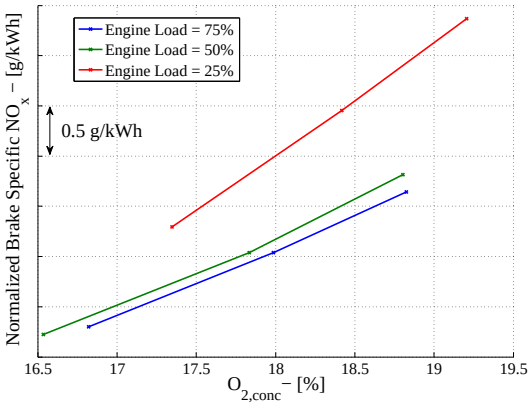

Figure 3.66: Brake Specific NO_x emissions for Oxygen Concentration variation.

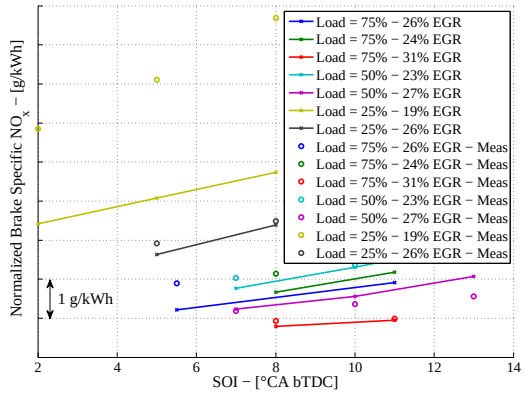

Figure 3.67: Brake Specific NO_x emissions for Start Of Injection variation.

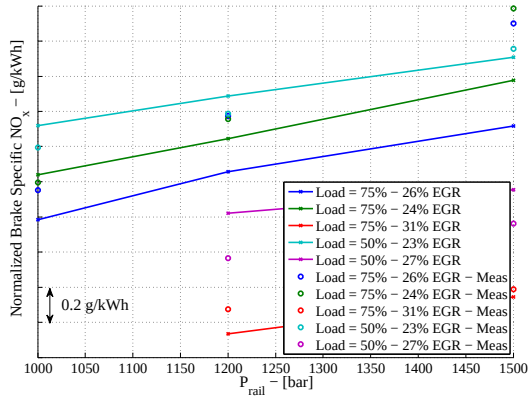

Figure 3.68: Brake Specific NO_x emissions for Rail Pressure variation.

3.4.4 Start Of Injection Variation

For the increase in efficiency of the combustion process the start of injection can be advanced improving a fast combustion. This will cause a, partially very high, increase of NO_x emissions too (as shown in Figure 3.67). This analysis shows a wide variation of SOI for different loads and EGR rates compared with measurements. Again the 50% load and 25% EGR (chosen as calibration point) gives the best match.

3.4.5 Injection Rail Pressure Variation

A way to improve the efficiency is to increase the injection rail pressure leading to a decrease in BSFC. Figure 3.68 shows that there is a price to pay for the reduction of BSFC, namely a slightly increase in NO_x emissions, although the curves are much flatter than the ones for advancing the SOI.

3.4.6 Efficiency Improvement Through Optimization, Advanced SOI And Increased P_{Rail}

All these analysis show that with EGR there is the concrete possibility to drastically reduce NO_x emissions to levels that would accomplish the strict IMO Tier III limits. On the other side the introduction of an EGR system will decrease the quality of the combustion process and thus the overall efficiency. Figure 3.69 shows exactly this effect, the introduction of an EGR system will shift the NO_x emissions curves (for all three tested loads): to much lower values with expected reduction between -5 g/kWh and -12 g/kWh; and to higher BSFC values, increase calculated between 10 g/kWh and (for lower load points) up to 40 g/kWh.

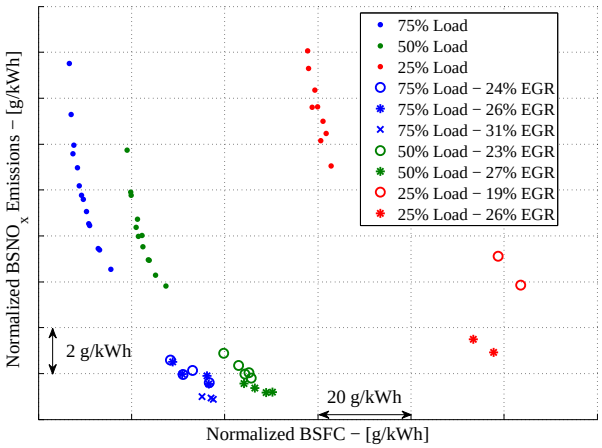

Figure 3.69: Brake Specific NO_x emissions reduction through the adoption of EGR.

The rematch of the turbocharger specifications and the optimization process will reduce the BSFC maintaining almost unchanged the NO_x emissions values. Simulation results compared to the measurements (see Figure 3.70) gives the same values for the NO_x emissions but partly different values for the BSFC (an underestimation

on the BSFC is expected, especially at higher loads). This difference has to be kept in mind for a valuation in absolute terms, but for a comparison is not important until two simulations results are compared to each other. Only the optimization process will drastically reduce the BSFC for the EGR cases, reduction is estimated to be in the order of ca. -5 g/kWh.

Another way to regain some of the lost efficiency is to tune the start of injection and the injection rail pressure. Higher rail pressure and very advanced SOI are desired to reduce BSFC. These two ways will again made the combustion process more efficient, lowering thus the fuel consumption, but increasing the NO_x emissions as shown in the two previous Sections 3.4.4 and 3.4.5. Figure 3.70 shows that the adoption of extreme values for these two tuning parameters will reduce NO_x in this case only maximal -0.5 to -2 g/kWh depending on the load point and on the EGR rate case.

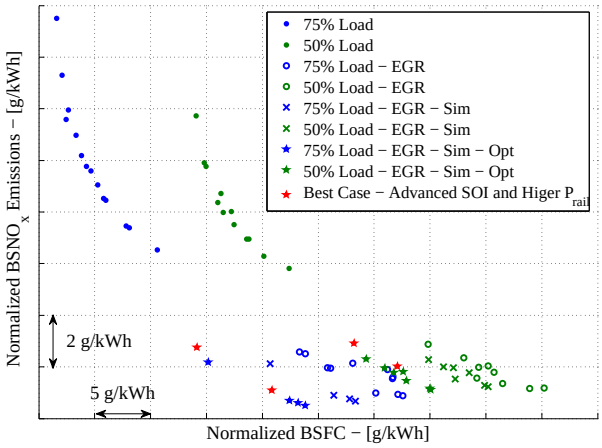

Figure 3.70: Brake Specific NO_x emissions after optimization.

Although a brake specific fuel consumption for the optimized best case EGR configuration equal to the one for the case without EGR is not reached, the BSFC increase is maintained limited to $5 - 10$ g/kWh with respect to an important brake specific NO_x reduction of $4 - 14$ g/kWh (for both BSFC and NO_x depending on the actual EGR rate).

Concluding it was shown that EGR is a valid technology useful to obtain a drastic reduction of NO_x emissions at the cost of a limited increase of brake specific fuel consumption.

Chapter 4

Conclusion

The during the six months of this master thesis fulfilled tasks are here summarized, analyzing the most important findings, pointing out their importance.

The project is motivated by the need of a technology in order to reduce NO_x emissions for large medium speed diesel engines, normally used for marine purposes, which in year 2016 will be subjected to stricter regulations, the IMO Tier III NO_x limit. A solution to this challenging goal is given by the implementation of an Exhaust Gas Recirculation (EGR) system, based on the principle that increasing inert gases (in this case the already burned exhaust gases) will reduce the combustion temperature (especially the peak temperature), thus reducing the main formation part of the thermal NO_x

The reached scope of this project was to simulate and evaluate different EGR paths applied on a 6-cylinder, two-stage turbocharged Wärtsilä medium speed diesel engine. Through 1-D simulations five EGR configurations were examined:

- Semi-Short Route
- 1 Donor Cylinder Semi-Short Route
- 2 Donor Cylinders Short Route
- EGR Blower Short Route
- EGR Turbocharger Short Route

For simulation time reasons the fully detailed engine model has been then simplified to a Fast Running Model (FRM) leading to a radical increase in computational speed. After recalibration, this model has been taken as the basis to create the various models with different EGR configurations and EGR rates (between 10% and 30% by mass).

4.1 Discussion Of EGR Setups

For each EGR configuration an optimizing process has been carried out in order to compare not only every EGR technology, but also the best of each setup achievable in terms of BSFC. All the configurations were compared with each other, with their optimized case and with the case without EGR.

The results are shown in the Table 4.1, where the full load BSFC, the 75% load BSFC are compared with the case without EGR as a reference. In this table also the two constrain variables, inlet turbine temperature and maximal cylinder pressure, are present. The results for the EGR setups are all simulated with 25% EGR rate.

Configuration	**ΔBSFC$_{100\%}$ [g/kWh]**	**ΔBSFC$_{75\%}$ [g/kWh]**	**TTI$_{max}$ [°C]**	**P$_{cyl,max}$ [bar]**
NO EGR	*0.0*	*0.0*	*510.4*	*168.5*
Semi-Short	+10.9	+12.1	541.7	199.2
Semi-Short Opt	+3.3	+5.6	574.9	***162.3***
1 Donor	+8.3	+9.7	560.0	200.9[1]
1 Donor Opt	+3.2	+5.3	572.1	163.0[1]
2 Donor	+11.8	+12.8	533.1	207.8[2]
2 Donor Opt	+4.2	+5.2	***502.6***	187.6[2]
EGR Blower Opt	***+2.0***	***+3.6***	550.6	167.7
EGR TC Opt	+3.6	+3.9	538.8[3]	173.4
1 Donor Test Bench	+8.3	+9.7	562.7	199.1[1]
1 Donor Test Bench Opt	+4.8	+6.3	559.1	176.6[1]

Table 4.1: Comparison of the simulated EGR technologies (25% EGR).

In Table 4.2 shows an evaluation of each EGR technology with respect to key parameters like cost, reliability, complexity of the system. An overall grade, taking into account the BSFC behavior, has been then given to each EGR path.

The analysis carried out for the EGR Semi-Short Route configuration is very promising. After a rematch of the turbocharging components the throttling losses present in the non-optimized model can be drastically lowered. The efficiency of a semi-short EGR solution can be optimized regaining in BSFC up to 7.6 g/kWh at full load, i.e. remaining only 3.3 g/kWh higher than the case without EGR. While the cylinder peak pressure is not problematic, the HP inlet temperature is

[1] Occurring at the donor cylinder.
[2] Occurring at the donor cylinder Nr.2.
[3] Occurring at the EGR TC turbine inlet.

Configuration	Complexity	Durability	Cost	Overall
Semi-Short	🟢	🟡	🟢	🟢
1 Donor Cylinder	🟡	🟡	🟡	🟡
2 Donor Cylinders	🟡	🟢	🟡	🟡
EGR Blower	🟡	🟡	🔴	🟡
EGR TC	🔴	🔴	🔴	🔴

Table 4.2: Evaluation of the simulated EGR technologies.

here a limiting constrain to further optimized the model (almost reaching the limit of 580°C). Simplicity of the system is the main advantage of this system. Only drawbacks of this configuration are the durability question, challenged by the high temperatures in the exhaust and on the fact that EGR flows through the HP compressor, which may cause problems due to condensation or to deposits in case of combustion of heavy fuels.

For the 1 Donor Cylinder Semi-Short Rout EGR configuration can be said that it gives, in case of an optimization, equivalent results as the semi-short route optimized. This apply to the BSFC values but also for the values regarding the HP turbine inlet temperature and the maximal cylinder peak pressure. For the solution presented in this report the EGR rate is limited downwards by the physical fact that one cylinder (at least) will always pump EGR flow to the intake producing a minimal value of 16.67%. This limitation counts as a disadvantage with respect to the semi-short route, where a desired EGR rate can be set acting on the EGR valve. The system itself is not much more complicate than that in the simple semi-short case, the physical separation of the exhaust manifold and the pressure differences that the EGR valve placed between the two exhaust manifolds should withstand rises some questions on the reliability. The fact that one cylinder is running with extremely different conditions compared to the others will cause unbalances that, after a long time, will not be beneficial to the engine. The same problems of a semi-short connection of EGR mentioned for the semi-short case are here also present. Overall, because the results are similar to the semi-short route case, this solution is not preferred with respect to the semi-short.

The 2 Donor Cylinders Short Route EGR configuration would be advantageous with respect to the single donor cylinder solution under many aspects: the BSFC simulated is always lower (apart for full load, minimally for Miller cases, while remarkably for other cases) compared with the single donor cylinder and the semi-short route configuration. Like the single donor cylinder this configuration needs an EGR valve between two exhaust manifolds and will produce some unbalancing in the engine run. The EGR rate is this time limited above by the full flow exiting two cylinders, i.e. 33.3% EGR. Important to be mentioned is that in this case the maximal cylinder peak pressure with 187.6 bar will exceed the limit. The fact that

the thermal stress is lower on this solution and that no EGR with a short route configuration will flow through the compressor wheel (which eliminate a possible problematic) rends the two donor cylinders EGR path a valid and competitive technology. An issue in this case is the increased maximal cylinder temperature for the donor cylinders and the unbalance of the engine (both also present in the single donor cylinder), which will certainly reduce the life of the engine.

The adoption of an opposite EGR Blower in a Short Route configuration permits to reduce the BSFC (also through the increase in turbocharging efficiency) by -1.3 g/kWh at full load with respect to the semi-short route and thus the smallest increase with respect to the case without EGR of 2.0 g/kWh. The limiting HP turbine inlet temperature shows also benefits, because all values remains lower than the ones for the optimized semi-short route case. The cylinder peak pressure is like for the other solution almost at the limit but without reaching it. This solution represents the best under many aspects, the BSFC is reduced drastically, the thermal stress is high but still not critical and lower than in other configurations. Disadvantages are mainly that this is one of the most expensive solution to be implemented, due to the electrical motor need by the blower (which is not yet fully developed) or by the space costing gearbox configuration is mechanically driven. Although in this case a short connection of the EGR path is used the exhaust gases must flow through a compressor wheel which will then carry all the problems explained before for the HP compressor. The more complicate and cost intensive solution represented by the EGR blower would then be discarded promoting the semi-short route solution.

For the last tested EGR Turbocharger Short Route EGR configuration a very interesting fact has been found: the optimization process tends to equalize the intermediate pressure with the exhaust pressure, for this limiting case the best efficiency is registered. But for the limiting case where this two pressures are equal, then the EGR TC will have to pump the exhaust gases to the intake manifold, doing exactly the same pressure ratio of the HP turbocharger. Then a much simpler solution, without loosing any efficiency, would be to simply connect the exhaust manifold to the intermediate stage manifold, i.e. use the semi-short route configuration, making unnecessary an additional EGR TC. The BSFC increase with respect to the case without EGR is of about 3.6 g/kWh at full load (similar to the semi-short case). More advantages are shown for lower loads. Thermal stress is reduced compared to the semi-short case, but the mechanical one is on the other hand increased slightly. This configuration shows overall good behaviors in terms of BSFC, thermal and mechanical stress, but the high costs caused by an additional turbocharger, the maintenance of this unit, the complex control strategy, the increased space needed for the devices and the pipings compared to a simple semi-short route will reduce the attractiveness of this solution.

Concluding, to be mentioned is the impact of EGR to the two constrain variables, HP turbine inlet temperature and maximal cylinder peak pressure.

Reducing the EGR rate will increase the flow through the turbines increasing consequently the boos pressure and simultaneously reducing the quantity of inert gases in the intake manifold. All this will cause an augmented peak pressure that could easily overcome the maximum allowable.

Opposite, if the EGR rate is increased the amount of exhaust gases flowing through the turbines is reduced, lowering consequently the boost pressure, which has as a consequence the increase in HP turbine inlet temperature to values over the acceptable ones.

4.2 Discussion Of EGR Technology's Choice

The choice of EGR technology is very important, this research should help to understand which advantages and disadvantages has each technology, making easier the selection of the appropriate one.

From the point of view of the results obtained two technologies are recommended:

- Semi-Short Route.
- EGR Blower Short Route.

The first one has the biggest advantage in its simplicity of implementation. The optimization process showed that this EGR path is equivalent to the thermodynamically optimal solution of the EGR turbocharger, which is much more complex. The fuel consumption penalty of 3.3 g/kWh at full load is significant but still one of the lowest with respect to all configurations tested.
The second one shows the lowest fuel consumption reached under the tested EGR configurations with only 2.0 g/kWh at full load. Although the electrical motor for the blower is still a challenging task under investigation this would be a promising future solution for EGR.

The choice of one EGR technology is also very depending on the efficiency of each single components of the system as should be shown briefly in this example.

The simplified overall system efficiency is given by Equation 4.2 for the case of the Semi-Short Route EGR path (or the equivalent EGR turbocharger), while by Equation 4.2 for the Blower Short Route (or the donor cylinder solutions).

$$\eta_{overall,Semi-Short} = (1 - EGR) \cdot \eta_{T,HP} \cdot \eta_{C,HP} \quad (4.1)$$

$$\eta_{overall,Blower} = \eta_{eng} \cdot \eta_{mech} \cdot \eta_{Blower} \quad (4.2)$$

If the turbocharging system has an high efficiency and the engine a rather low fuel-to-power conversion efficiency, then the semi-short route will give higher overall efficiencies compared to the same system equipped with a blower or a donor cylinder solution. This is because in this case energy is extracted through a turbine from the exhaust energy and is used by the compressor to generate the wished boost pressure.
If the engine has a high conversion efficiency and the turbocharging system a lower efficiency, then the blower solution will give better overall efficiencies compared to the semi-short system. In this case the energy used by the blower to compress the EGR flow is directly taken from the engine, thus fuel energy is used instead of exhaust energy.

Taking some fictitious values for the efficiencies and an EGR rate of 25% the example is calculated here:

$$\eta_{overall,Semi-Short} = (1 - 0.25) \cdot 0.75 \cdot 0.75 = 42.2\% \quad (4.3)$$

$$\eta_{overall,Blower} = 0.45 \cdot 0.97 \cdot 0.70 = 30.6\% \quad (4.4)$$

For this case the use of exhaust energy would be beneficial because of the high turbocharging efficiency.

Lastly, considerations about switchability, drivability, packaging, technical risks and the other consideration on durability, costs and stress done before should be taken into account during the decision making process.

4.3 Discussion Of NO_x Analysis

NO_x simulation's results were compared for three different EGR rates (20%, 25% and 30%) with the measurements data (available only for 20% and 25% EGR). The simulations could not compute NO_x emissions for all the loads, therefore a calibration of a NO_x model was very difficult for the lack of corresponding measurements points. However the measurements and the simulations show that NO_x emissions decreases linearly with the increase of EGR rate (or the reduction of oxygen concentration in the intake). The pollutant emissions decreases generally for increasing load. Higher rail injection pressure and advanced SOI will reduce the BSFC (increasing the efficiency of the combustion) but increases the NO_x emissions again.

All these analysis show that with EGR there is the concrete possibility to drastically reduce NO_x emissions to levels that would accomplish the strict IMO Tier III limits. On the other side the introduction of an EGR system will decrease the quality of the combustion process and thus the overall efficiency. In order to rend this solution attractive has been shown that a rematch of the turbocharger specifications and an optimization process will reduce the BSFC maintaining almost unchanged the NO_x emissions values.

Only the optimization process will drastically reduce the BSFC for the EGR cases, reduction is estimated to be in the order of ca. -5.0 g/kWh.

Tuning the rail pressure to higher values and advancing the SOI will reduce further the BSFC. The adoption of extreme values for these two tuning parameters will reduce the fuel consumption for the simulated cases of additional -0.5 to -2.0 g/kWh depending on the load point and on the EGR rate.

Although a brake specific fuel consumption for the optimized best case EGR configuration equal to the one for the case without EGR is not reached, the BSFC increase is maintained limited to $5 - 10$ g/kWh with respect to an important brake specific NO_x reduction of $4 - 14$ g/kWh (for both BSFC and NO_x depending on the actual EGR rate).

Chapter 5

Future Work

This research set an important and consistent starting point for future work in the field of EGR technologies simulations and comparisons for NO_x reduction on large diesel engines.

5.1 NO_x Analysis And Modeling

For a lack of time only a simple modeling (scaling) of NO_x emissions has been carried out during the here presented thesis. In the future the NO_x analysis should be made on a wider range of loads and EGR rates compared to the analysis done until now. This will be only possible if the already implemented NO_x model will be correctly and with much more accuracy calibrated. Therefore other new measurements data at different loads and EGR rates will be necessary.

5.2 Combustion Model Implementation And Calibration

The engine simulation models runs for the moment without a combustion model. Instead of that directly the measured heat release rate is implemented for each load point and EGR rate. Obviously this causes an important limitation to the simulation process, only predefined and on the test bench run operating points can be simulated. To decouple test bench runs and simulations a combustion model should be implemented and calibrated through available measurements data and new ones. This task should be simplified by the fact that reliable combustion modeling programs are available at the LAV department of the ETHZ.

5.3 Adaptability To Variations Of EGR

In 2016 the IMO Tier III limitation will apply only at the ECAs, meaning that outside these areas the ship owners would like to drive their engines generating more emissions (matching the IMO Tier II limit) but reducing the BSFC. This fact forces the engine manufacturers to build engines with emission reduction devices (like EGR, SCR, etc.) that can be switched on and off depending on the emission limit of the area in which the ship is actually traveling. Clearly the switch off for an exhaust after-treatment system can be easily done without influencing the engine

run. In case of an EGR system this would causes instead various problems, mainly the shift of turbocharger's operating point outside the maps into surge regions. To avoid damages to the engine and to the turbocharging system the adaptability to EGR rates changes should be analyzed for each configuration. Solutions to this problem than should be highlighted an simulated. Ways to resolve the problem could be given by e.g. Variable Turbine Geometry (VTG) of Variable Valve Timing (VVT).

5.4 Results Validation Through Comparison With Test Bench Measurements Data

Wished would of course also that the already simulated EGR configurations will be tested on the real engine in order to compare the actual values with the simulations results. This is not only very time expensive, but also expensive from the costs point of view. The implementation of every simulated EGR configuration on the test engine will require every time new turbochargers specifications, pipings, controller units and strategies. At least the one donor cylinder case that is now under investigation should be compared with the simulation's results.

5.5 Full Engine Model Simulations

Although during the thesis it was explained and shown that a Fast Running Model (FRM) of the engine can be considered as good as a fully described Full Engine Model (FEM) the five simulated EGR configurations could be implemented as FEM, modifying the model without EGR. This would require a correct topology development for the EGR paths. In a confident way can be said that the results are expected to be very similar to the FRM ones.

In addition developing and therefore further refining of the model's components characteristics or of the physical and empirical models used by the simulation program is wished in order to achieve more accurate results until best simulations results and optimal computational time is reached.

If something has aroused the reader's interest too, then it just need to join a research at the Aerothermochemistry and Combustion Systems Laboratory of the ETHZ.

Bibliography

[1] *http://www.ecfr.gov/cgi-bin/text-idx?SID=30b72b5ddedc72fb724cc2b0075635d5&node=sp40.33.1042.b&rgn=div6*. Code of Federal Regulations - Part 1042 - Control Of Emissions From New and In-Use Marine Compression-Ignition Engines And Vessels, Accessed on 11/09/2014.

[2] *http://www.ccem.ch/science/nox-reduction*. CCEM - Competence Center Energy and Mobility, Accessed on 13/09/2014.

[3] ABB Turbo Systems Ltd. Topology, 2014.

[4] GH Abd-Alla. Using exhaust gas recirculation in internal combustion engines: a review. *Energy Conversion and Management*, 43(8):1027–1042, 2002.

[5] DL Baulch et al. Evaluation of kinetic data for combustion modelling. proposals of the second cec combustion program. *Journal of Phys. Chem. Ref. Data*, 1991.

[6] Donald L Baulch, DD Drysdale, and Anthony Charles Lloyd. *Critical evaluation of rate data for homogeneous, gas-phase reactions of interest in high-temperature systems*, volume 4. Department of Physical Chemistry, the University, 1969.

[7] Fritz Bedford, Chris Rutland, Peter Dittrich, Alois Raab, and F Wirbeleit. Effects of direct water injection on di diesel engine combustion. Technical report, SAE Technical Paper, 2000.

[8] Milton R. Beychok. Nox emission from fuel combustion controlled. *The Oil and Gas Journal*, pages 53–56, March 1973.

[9] CIMAC. Turbocharging efficiencies - definitions and guidelines for measurement and calculation. *CIMAC Recommendation*, 27:1–46, 2007.

[10] E Codan and T Huber. Application of two stage turbocharging systems on large engines. In *10th International Conference on Turbochargers and Turbocharging*, page 55. Elsevier, 2012.

[11] E Codan and C Mathey. Emissions–a new challenge for turbocharging. In *CIMAC Congress*, number 245, 2007.

[12] E Codan and I Vlaskos. Turbocharging medium speed diesel engines with extreme miller timing. In *Proceedings of the 9th Turbocharging Conference, Dresden, Germany, September*, pages 23–24, 2004.

[13] E Codan and J Wüthrich. Turbocharging solutions for egr on large diesel engines. Technical report, ABB Turbo Systems Ltd., 2013.

[14] DEUTZ. *http://www.deutzamericas.com/products/nox.cfm*. DVERT Technology, Accessed on 19/09/2014.

[15] CP Fenimore. Formation of nitric oxide in premixed hydrocarbon flames. In *Symposium (International) on Combustion*, volume 13, pages 373–380. Elsevier, 1971.

[16] Gamma Technologies. *GT-POST Tutorial*, 2013.

[17] Gamma Technologies. *GT-SUITE - Engine Performance Tutorials*, 2013.

[18] Meisam Ahmadi Ghadikolaei. Effect of cylinder air pressure and fuel injection pressure on combustion characteristics of direct injection (di) diesel engine fueled with diesel and gasoline. *International Journal of Application or Innovation in Engineering & Management (IJAIEM)*, 3(1), 2014.

[19] Zhiyu Han, All Uludogan, Gregory J Hampson, and Rolf D Reitz. Mechanism of soot and nox emission reduction using multiple-injection in a diesel engine. Technical report, SAE Technical Paper, 1996.

[20] Wolfgang Held, Axel Koenig, Thomas Richter, and Lothar Puppe. Catalytic nox reduction in net oxidizing exhaust gas. Technical report, SAE Technical Paper, 1990.

[21] Peter L Herzog, Ludwig Bürgler, Ernst Winklhofer, Paul Zelenka, and Wolfgang Cartellieri. Nox reduction strategies for di diesel engines. Technical report, SAE technical paper, 1992.

[22] John B Heywood. *Internal combustion engine fundamentals*, volume 930. Mcgraw-hill New York, 1988.

[23] Dimitrios Theofanis Hountalas, George C Mavropoulos, TC Zannis, and SD Mamalis. Use of water emulsion and intake water injection as nox reduction techniques for heavy duty diesel engines. Technical report, SAE Technical Paper, 2006.

[24] Klaus Hoyer. Nox-reduction - in-cylinder emission reduction in large diesel engines. Technical report, Competence Center Energy and Mobility, 2012.

[25] International Maritime Organization. *http://www.imo.org/OurWork/Environment/PollutionPrevention/AirPollution/Pages/Nitrogen-oxides-(NOx)—Regulation-13.aspx*. IMO - Nitrogen oxides (NOx) - Regulation 13, Accessed on 09/09/2014.

[26] D Janicke, R Pittermann, and M Borrmann. Process design to minimize the trade-off between efficiency and no {sub x} emissions in medium-speed four-stroke diesel engines. 1998.

[27] Kourosh Karimi. *Characterisation of multiple-injection diesel sprays at elevated pressures and temperatures*. PhD thesis, School of Engineering, University of Brighton, 2007.

[28] Ugur Kesgin. Efficiency improvement and nox emission reduction potentials of two-stage turbocharged miller cycle for stationary natural gas engines. *International journal of energy research*, 29(3):189–216, 2005.

[29] Manfred Koebel, Martin Elsener, and Thomas Marti. Nox-reduction in diesel exhaust gas with urea and selective catalytic reduction. *Combustion science and technology*, 121(1-6):85–102, 1996.

[30] Panagiotis Kyrtatos. Exhaust gas emissions: Nox. In *IC-Engines and Propulsion Systems II*, 2012.

[31] Panagiotis Kyrtatos, Klaus Hoyer, Peter Obrecht, and Konstantinos Boulouchos. Recent developments in the understanding of the potential of in-cylinder nox reduction through extreme miller valve timing. In *CIMAC Congress*, number 225, Shanghai, 2013.

[32] Panagiotis Kyrtatos, Klaus Hoyer, Peter Obrecht, and Konstantions Boulouchos. Apparent effects of in-cylinder pressure oscillations and cycle-to-cycle variability on heat release rate and soot concentration under long ignition delay conditions in diesel engines. *International Journal of Engine Research*, 15(3):325–337, 2014.

[33] N Ladommatos, SM Abdelhalim, H Zhao, and Z Hu. The dilution, chemical, and thermal effects of exhaust gas recirculation on diesel engine emissions-part 1: Effect of reducing inlet charge oxygen. Technical report, SAE Technical Paper, 1996.

[34] W Lausch, F Fleischer, and L Maier. Möglichkeiten und grenzen von noxminderungsmaßnahmen bei man-b&w-viertakt-großdieselmotoren. *Motortechnische Zeitschrift MTZ, Bd*, 54, 1993.

[35] George A Lavoie, John B Heywood, and James C Keck. Experimental and theoretical study of nitric oxide formation in internal combustion engines. *Combustion science and technology*, 1(4):313–326, 1970.

[36] Jianwen Li, Jae Ou Chae, SB Park, HJ Paik, JK Park, YS Jeong, SM Lee, and YJ Choi. Effect of intake composition on combustion and emission characteristics of di diesel engine at high intake pressure. Technical report, SAE Technical Paper, 1997.

[37] MAN Diesel & Turbo. *Emission Project Guide - MAN B&W Two-stroke Marine Engines.*

[38] Johnson Matthey. *http://www.greencarcongress.com/2008/03/johnson-matthey.html.* SCRT System Cut NOx Emissions by 84% in Fleet Trial of Retrofitted Class 8 Trucks, Accessed on 17/09/2014.

[39] Federico Millo, Marco Gianoglio Bernardi, and Diego Delneri. Computational analysis of internal and external egr strategies combined with miller cycle concept for a two stage turbocharged medium speed marine diesel engine. Technical report, SAE Technical Paper, 2011.

[40] Stuart Nemser, Donald Stookey, and Joyce Nelson. Diesel engine nox reduction via nitrogen-enriched air. *Fluid/Particle Separation Journal*, 15(1):69–80, 2003.

[41] Konstantin Pattas and G Häfner. Stickoxidbildung bei der ottomotorischen verbrennung. *MOTORTECHN. Z.*, 34(12), 1973.

[42] S Röpke, GW Schweimer, and TS Strauss. Nox formation in diesel engines for various fuels and intake gases. Technical report, SAE Technical Paper, 1995.

[43] Yoshio Sato, Akira Noda, and Takashi Sakamoto. Combustion and nox emission characteristics in a di methanol engine using supercharging with egr. Technical report, SAE Technical Paper, 1997.

[44] Dieter HE Seher, Michael Reichelt, and Stefan Wickert. Control strategy for nox-emission reduction with scr. Technical report, SAE Technical Paper, 2003.

[45] Gregory P Smith, David M Golden, Michael Frenklach, Nigel W Moriarty, Boris Eiteneer, Mikhail Goldenberg, C Thomas Bowman, Ronald K Hanson, Soonho Song, William C Gardiner Jr, et al. Gri-mech 3.0, 1999.

[46] Hansruedi Stebler. *Luft-und brennstoffseitige Maßnahmen zur internen NOx-Reduktion von schnell laufenden direkt eingespritzten Dieselmotoren.* PhD thesis, PhD thesis, Swiss Federal Institute of Technology (ETH), 1998. Diss. ETH, 1998.

[47] Hansruedi Stebler, German Weisser, Hans-Ulrich Hōrler, and Konstantinos Boulouchos. Reduction of nox emissions of di diesel engines by application of the miller-system: an experimental and numerical investigation. Technical report, SAE Technical Paper, 1996.

[48] T Thurnheer, D Edenhauser, P Soltic, D Schreiber, P Kirchen, and A Sankowski. Experimental investigation on different injection strategies in a heavy-duty diesel engine: emissions and loss analysis. *Energy Conversion and Management*, 52(1):457–467, 2011.

[49] Minoru Tsukahara and Yasufumi Yoshimoto. Reduction of nox, smoke, bsfc, and maximum combustion pressure by low compression ratios in a diesel engine fuelled by emulsified fuel. Technical report, SAE technical paper, 1992.

[50] Jürgen Warnatz, Ulrich Maas, and Robert W Dibble. *Combustion: physical and chemical fundamentals, modeling and simulation, experiments, pollutant formation.* Springer, 2006.

[51] C Wik, H Salminen, K Hoyer, C Mathey, S Vgeli, and P Kyrtatos. 2-stage turbo charging on medium speed engines future supercharging on the new lerf-test facility. 14. In *Aufladetechnische Konferenz*, volume 150, 2009.

[52] Ya B Zeldovich. The oxidation of nitrogen in combustion and explosions. *Acta Physicochim. URSS*, 21(4):577–628, 1946.

[53] Ming Zheng, Graham T Reader, and J Gary Hawley. Diesel engine exhaust gas recirculation—-a review on advanced and novel concepts. *Energy conversion and management*, 45(6):883–900, 2004.

[54] Chuanqiang Zhu, Shuyuan Liu, Huan Liu, Juan Yang, Xiaoxing Liu, and Guangwen Xu. Nox emission characteristics of fluidized bed combustion in atmospheres rich in oxygen and water vapor for high-nitrogen fuel. *Fuel*, 2014.

Appendix A

Measurements Overview

In the following pages are listed all the measurements mean values registered trough the test bench runs. During the master thesis the values for BSFC and NO_x emissions are kept secret. Therefore these values are missing in the following tables.

A.1 Variables Description

- Point: engine load percentage.
- AG_CO2: CO_2 in the exhaust per volume.
- AG_NOX: NO_x in the exhaust per volume.
- AG_O2: O_2 in the exhaust per volume.
- BLOW_VAL: flow rate of Blow-By from the cylinder (mass loss).
- GAS_LOSS: estimated energy flow rate in the exhaust gases (exhaust heat loss).
- KS_QMASS: fuel flow rate.
- LUFT_DUR: air flow rate to the engine.
- MD_WELLE: torque.
- N: engine speed.
- OPA_OPAC: exhaust opacity (soot).
- P: engine output power.
- P_1HP, P_1LP, P_2HP, P_2LP, P_3, P_4, P_5, P_6: engine pressures at different locations (as explained in Section 3.1.1).
- P_BARO: ambient pressure.
- PHI: ambient humidity.
- Q_KW_HT: flow rate of high temperature water.
- Q_KW_LT: flow rate of low temperature water.
- T_1HP, T_1LP, T_2HP, T_2LP, T_3, T_4, T_5, T_6: engine temperatures at different locations (as explained in Section 3.1.1).

- T_1HP: for the EGR cases this is now the temperature of the mixed EGR/fresh air. Take note that this temperature can be lower then both the EGR and fresh air stream, because the EGR expands to this pipe over the EGR valve.
- T_LUFT: ambient temperature.
- TE_FO: fuel temperature.
- TWA_HT: exhaust temperature of HT water.
- TWA_LT: exhaust temperature of LT water.
- TWE_HT: inlet temperature of HT water.
- TWE_LT: inlet temperature of LT water.
- W_HTLOSS: energy flow into HT cooling water.
- Power: engine power.
- Fuel Flow: fuel flow rate.
- Mass Flow: air fow rate.
- BMEP: brake mean effective pressure.
- Fuel Cons: specific fuel consumption (measure of efficiency).
- SAC: specific air consumption.
- NOx: Specific NOx.
- TC HP Speed: high pressure turbocharger speed.
- TC LP Speed: low pressure turbocharger speed.
- Injection Timing: injection timing (indicative for SOI, not the correct one).
- Rail P: common rail (injection) pressure.
- File Name: file containing transient results.
- Peak P: measured peak pressure.
- Fuel/inj: fuel injected per injection.
- T_AGR2: temperature at the exit of the EGR cooler (before expansion).
- AGR_CO2: amount of CO_2 in the intake manifold.
- TICOUT: temperature at the exit of the intercooler (before EGR mixing).
- EGR: percentage of EGR calculated from CO_2 ratios in the exhaust and intake.

A.2 Load Variation

A.2.1 Without EGR

Point	AG_CO2	AG_NOX	AG_O2	BLOW_VAL	GAS_LOSS
%	ppm	ppm	ppm	l/min	kW
10	50667.77	———	137357.69	232.32	130.44
25	52067.90	———	127973.40	300.66	218.58
33	52487.86	———	127470.38	337.07	260.22
40	52651.55	———	127468.98	374.64	291.07
48	52618.77	———	127464.93	429.98	330.98
50	65462.78	———	109042.35	403.03	330.74
66	62557.16	———	112381.84	457.71	425.68
70	61804.93	———	113146.32	485.89	443.24
75	61524.17	———	113830.77	504.92	466.36
85	64223.00	———	110248.16	534.32	483.69
100	62298.23	———	112891.34	601.74	579.29

KS_QMASS	LUFT_DUR	MD_WELLE	N	OPA_OPAC	P
kg/h	kg/h	Nm	rpm	-	kW
———	1785.68	1030.0	998	1.327	107.62
———	2787.31	2575.0	999	0.763	269.29
———	3407.37	3400.0	998	0.566	355.39
———	3935.34	4120.0	998	0.623	430.55
———	4624.05	4999.8	999	0.636	523.20
———	3761.47	5150.1	999	2.018	538.65
———	4939.62	6797.6	1000	1.348	711.74
———	5264.63	7209.5	1000	1.175	755.18
———	5653.52	7724.3	1000	1.270	809.10
———	5889.38	8754.1	999	0.746	915.66
———	7363.69	10274.3	998	0.637	1073.25

P_1HP	P_1LP	P_2HP	P_2LP	P_3	P_4
bar	mbar	bar	bar	bar	bar
0.12	-0.87	0.23	0.12	0.24	0.41
0.37	-2.24	0.82	0.37	0.83	0.93
0.54	-3.39	1.17	0.54	1.20	1.26
0.68	-4.50	1.49	0.69	1.52	1.55
0.89	-6.23	1.90	0.89	1.94	1.94
0.82	-4.13	2.32	0.82	2.35	1.56
1.22	-7.13	3.33	1.22	3.36	2.25
1.34	-8.08	3.61	1.34	3.65	2.44
1.47	-9.34	3.95	1.47	3.98	2.68
1.57	-10.14	4.19	1.57	4.22	2.84
2.08	-15.92	5.45	2.08	5.49	3.80

P_5	P_6	P_BARO	PHI	Q_KW_HT	Q_KW_LT
bar	mbar	mbar	%	l/min	l/min
0.13	0.03	967.9	26.0	0.0	113.1
0.32	0.66	967.9	23.6	28.5	100.6
0.46	1.40	967.8	23.6	31.5	115.5
0.59	2.00	967.9	24.6	33.7	130.0
0.77	1.36	967.9	26.5	36.4	149.3
0.60	2.03	968.0	26.2	35.4	134.6
0.93	2.57	968.0	26.4	38.4	160.7
1.02	2.87	968.1	26.9	39.5	167.8
1.15	3.12	968.1	27.1	40.9	177.9
1.22	3.42	968.1	27.6	43.6	185.4
1.75	3.89	968.1	28.2	49.3	218.5

T_1HP	T_1LP	T_2HP	T_2LP	T_3	T_4
°C	°C	°C	°C	°C	°C
36.31	22.72	66.80	36.74	44.68	314.07
45.10	22.95	103.10	60.04	43.83	378.47
46.65	23.07	114.01	73.70	44.31	389.08
47.19	23.04	121.00	84.98	44.73	394.85
47.87	22.64	127.83	98.83	45.16	402.67
47.39	22.84	128.62	93.50	44.42	477.21
48.44	22.95	138.08	118.86	45.83	475.12
48.65	22.49	139.99	124.91	46.30	475.18
48.97	22.73	142.15	132.76	46.79	476.77
49.07	21.91	143.35	136.79	47.14	479.23
50.06	21.94	149.52	163.29	49.23	497.00

T_5	T_6	T_LUFT	TE_FO	TWA_HT	TWA_LT
°C	°C	°C	°C	°C	°C
281.15	261.95	18	17.5	77.5	46.6
322.35	282.18	20	17.5	84.7	46.1
324.32	274.50	20	17.5	85.0	46.7
324.18	265.17	20	17.4	85.1	47.0
327.03	255.41	19	17.3	85.3	47.3
399.53	329.13	19	17.3	85.2	46.6
390.49	301.97	19	17.3	85.5	47.5
389.47	294.93	19	17.3	85.5	47.7
389.96	288.84	19	17.2	85.6	47.9
390.61	285.70	18	17.2	85.8	48.0
405.11	274.34	18	17.2	86.1	48.5

TWE_HT	TWE_LT	W_HTLOSS	Power	Fuel Flow	Mass Flow
°C	°C	kW	%	kg/s	kg/s
84.8	9.7	279.65	10	———	0.496022222
25.7	8.5	369.56	25	———	0.774252778
26.1	7.3	432.64	33	———	0.946491667
26.0	6.5	489.24	40	———	1.093150000
26.1	5.9	561.05	48	———	1.284458333
26.0	6.3	506.53	50	———	1.044852778
26.2	5.7	604.01	66	———	1.372116667
26.2	5.4	634.96	70	———	1.462397222
26.2	5.3	672.63	75	———	1.570422222
26.2	5.3	707.45	85	———	1.635938889
26.2	4.9	837.85	100	———	2.045469444

BMEP	Fuel Cons	SAC	NOx	TC HP Speed	TC LP Speed
Pa	g/kWh	kg/kWh	g/kWh	rpm	rpm
245600	———	16.592	———	27100	13650
614000	———	10.351	———	36950	22200
810718	———	9.588	———	39900	25900
982400	———	9.140	———	41650	28750
1192185	———	8.838	———	43300	31850
1228024	———	6.983	———	42800	30000
1620865	———	6.940	———	45050	35350
1719081	———	6.971	———	45400	36600
1841833	———	6.987	———	45900	38050
2087385	———	6.432	———	46100	38850
2449872	———	6.861	———	47350	43350

Injection Timing	Rail P	File Name	Peak P	Fuel/inj	
°CA BTDC	bar	-	bar	g	
13.0	1200	Test1_002	70.3	———	
5.0	1400	Test1_003	89.1	———	
6.4	1280	Test1_004	107.0	———	
8.0	1200	Test1_005	122.5	———	
10.0	1000	Test1_006	142.2	———	
10.0	1000	Test1_007	102.0	———	
11.0	1000	Test1_008	126.1	———	
11.0	1000	Test1_009	132.8	———	
11.0	1000	Test1_010	139.7	———	
11.0	1500	Test1_011	166.2	———	
5.5	1500	Test1_012	164.5	———	

A.2.2 With 20% EGR

Point	AG_CO2	AG_NOX	AG_O2	BLOW_VAL	GAS_LOSS
%	ppm	ppm	ppm	l/min	kW
10	54380.18	————	122496.67	412.66	102.87
25	60459.02	————	109398.31	436.12	177.42
48	66964.09	————	98732.13	516.62	271.86
50	69294.91	————	94400.20	493.26	281.14
75	70848.17	————	91932.52	574.61	363.50

KS_QMASS	LUFT_DUR	MD_WELLE	N	OPA_OPAC	P
kg/h	kg/h	Nm	rpm	-	kW
————	1513.47	1031.1	1000	1.624	107.81
————	2401.08	2577.9	1000	1.736	269.63
————	3573.30	4950.4	1000	1.268	518.24
————	3356.00	5156.9	1000	6.160	540.53
————	4740.57	7735.2	1000	3.851	810.27

P_1HP	P_1LP	P_2HP	P_2LP	P_3	P_4
bar	mbar	bar	bar	bar	bar
0.10	-0.55	0.43	0.11	0.43	0.88
0.34	-1.64	1.30	0.35	1.29	1.86
0.71	-3.78	2.49	0.72	2.50	3.31
0.94	-3.35	3.26	0.95	3.25	3.21
1.53	-6.78	5.02	1.54	5.02	4.95

P_5	P_6	P_BARO	PHI	Q_KW_HT	Q_KW_LT
bar	mbar	mbar	%	l/min	l/min
0.17	0.41	989.4	20.5	27.5	63.1
0.45	1.55	979.6	26.8	35.8	98.1
0.91	3.66	979.6	26.8	47.5	140.1
0.87	3.50	979.7	25.9	39.4	130.3
1.49	6.62	979.7	26.0	49.4	170.1

T_1HP	T_1LP	T_2HP	T_2LP	T_3	T_4
°C	°C	°C	°C	°C	°C
42.67	26.95	96.67	41.80	55.92	330.39
39.23	28.67	121.98	69.19	55.78	408.83
30.27	28.94	140.32	107.60	56.00	469.12
30.41	29.80	140.07	111.02	55.96	496.72
33.65	29.45	150.65	151.51	56.44	519.56

T_5	T_6	T_LUFT	TE_FO	TWA_HT	TWA_LT
°C	°C	°C	°C	°C	°C
272.19	248.90	26	24.3	84.8	45.6
313.90	268.30	29	32.1	85.3	46.5
349.67	272.95	30	33.7	86.0	47.8
376.75	298.23	30	34.4	85.4	47.2
388.22	273.60	30	34.6	86.2	48.4

TWE_HT	TWE_LT	W_HTLOSS	Power	Fuel Flow	Mass Flow
°C	°C	kW	%	kg/s	kg/s
23.8	24.1	209.58	10	———	0.42040833
24.1	24.0	303.97	25	———	0.66696667
24.4	24.5	427.74	48	———	0.99258333
24.3	24.4	371.85	50	———	0.93222222
24.6	24.4	492.89	75	———	1.31682500

BMEP	Fuel Cons	SAC	NOx	TC HP Speed	TC LP Speed
bar	g/kWh	kg/kWh	g/kWh	rpm	rpm
2.454	———	14.038	———	14300	33400
6.135	———	8.905	———	23700	42900
11.782	———	6.895	———	32900	48400
12.273	———	6.209	———	33100	47500
18.410	———	5.851	———	40500	50200

Injection Timing	Rail P	Peak P	Fuel/inj	T_AGR2	AGR_CO2
°CA BTDC	bar	bar	g	°C	%
13.0	1200	81.2	———	93.2	1.19
5.0	1400	107.4	———	49.4	1.23
10.0	1000	167.2	———	50.4	1.38
10.0	1000	126.5	———	50.3	1.46
11.0	1000	175.2	———	51.6	1.54

TICOUT	EGR	File Name
°C	%	-
45.5	21.88	EGRM73NewTNomH_001
45.2	19.85	EGRM73NewTNom_008
46.1	20.16	EGRM73NewTNom_011
46.0	20.64	EGRM73NewTNom_014
46.2	21.31	EGRM73NewTNom_015

A.2.3 With 25% EGR

Point	AG_CO2	AG_NOX	AG_O2	BLOW_VAL	GAS_LOSS
%	ppm	ppm	ppm	l/min	kW
10	61112.63	———	107945.72	397.27	100.58
25	70444.65	———	93416.75	431.05	176.37
48	72823.07	———	89576.97	506.92	265.82
50	77008.91	———	85318.76	517.55	291.87
75	74551.93	———	89691.34	557.38	370.61
90	75102.20	———	87832.05	618.59	426.23

KS_QMASS	LUFT_DUR	MD_WELLE	N	OPA_OPAC	P
kg/h	kg/h	Nm	rpm	-	kW
———	1345.84	1029.9	1000	2.275	107.66
———	2074.82	2578.1	1000	6.336	269.63
———	3264.99	4949.7	1000	2.753	518.19
———	3089.81	5157.0	1000	20.505	540.01
———	4544.70	7734.4	1000	6.863	810.20
———	5372.98	9279.5	1000	2.077	972.31

P_1HP	P_1LP	P_2HP	P_2LP	P_3	P_4
bar	mbar	bar	bar	bar	bar
0.08	-0.46	0.34	0.09	0.33	0.73
0.31	-1.19	1.07	0.33	1.07	1.55
0.76	-3.15	2.30	0.78	2.30	2.96
0.92	-2.66	3.01	0.93	3.01	2.95
1.59	-5.93	4.85	1.60	4.86	4.73
1.98	-8.32	5.91	1.99	5.91	5.77

P_5	P_6	P_BARO	PHI	Q_KW_HT	Q_KW_LT
bar	mbar	mbar	%	l/min	l/min
0.15	0.30	979.7	26.4	27.3	64.5
0.36	1.14	979.6	27.0	36.0	92.2
0.80	3.13	979.5	26.4	46.0	133.4
0.78	2.84	991.6	14.3	41.4	128.0
1.40	6.03	991.4	14.5	47.9	171.7
1.78	8.13	991.0	16.0	54.7	195.9

T_1HP	T_1LP	T_2HP	T_2LP	T_3	T_4
°C	°C	°C	°C	°C	°C
46.42	28.58	87.05	40.14	56.29	347.68
32.01	28.99	112.43	63.40	55.80	432.11
32.20	29.32	130.44	102.62	55.78	475.20
52.32	27.69	148.42	105.31	55.99	517.75
34.38	26.57	155.78	144.75	56.53	521.37
37.53	26.83	157.74	168.09	56.49	536.79

T_5	T_6	T_LUFT	TE_FO	TWA_HT	TWA_LT
°C	°C	°C	°C	°C	°C
294.76	270.03	29	30.7	84.7	45.2
343.79	300.68	29	32.5	85.4	46.3
360.65	287.93	30	33.9	85.9	47.3
399.99	324.31	24	26.3	85.5	47.1
391.80	283.01	24	26.5	85.8	48.7
403.48	274.07	23	28.8	86.3	49.4

TWE_HT	TWE_LT	W_HTLOSS	Power	Fuel Flow	Mass Flow
°C	°C	kW	%	kg/s	kg/s
24.2	24.5	207.05	10	———	0.37384444
24.5	24.7	289.83	25	———	0.57633889
24.3	24.4	408.2	48	———	0.90694167
24.4	24.6	374.11	50	———	0.85828056
24.3	24.4	491.4	75	———	1.26241667
24.4	24.4	572.61	90	———	1.49249444

BMEP	Fuel Cons	SAC	NOx	TC LP Speed	TC HP Speed
bar	g/kWh	kg/kWh	g/kWh	rpm	rpm
2.451	———	12.501	———	12950	30950
6.136	———	7.695	———	21800	40400
11.780	———	6.301	———	31400	46300
12.274	———	5.722	———	31800	46850
18.408	———	5.609	———	39500	49400
22.085	———	5.526	———	43200	49900

Injection Timing	Rail P	Peak Press	Fuel/inj	T_AGR2	AGR_CO2
°CA BTDC	bar	bar	g	°C	%
13.0	1200	76.5	———	47.0	1.44
5.0	1400	97.6	———	49.8	1.83
10.0	1000	158.5	———	51.4	1.85
10.0	1000	119.3	———	70.7	2.00
11.0	1000	169.2	———	70.3	1.93
5.5	1500	184.8	———	70.4	1.97

TICOUT	EGR	File Name
°C	%	-
49.2	23.07	EGRM73NewTNom_005
46.2	25.55	EGRM73NewTNom_009
46.5	24.99	EGRM73NewTNom_012
46.1	25.97	EGRM73NewTNomH2_005
45.9	25.89	EGRM73NewTNomH2_006
46.1	26.23	EGRM73NewTNomH2_010

A.3 Start Of Injection & Rail Pressure Variation

A.3.1 Without EGR

25% Load

Point	AG_CO2	AG_NOX	AG_O2	BLOW_VAL	GAS_LOSS
%	ppm	ppm	ppm	l/min	kW
25	51472.46	———	129884.20	316.46	221.51
25	50617.17	———	130894.88	314.45	226.42
25	51992.68	———	128946.74	323.09	219.19
25	52249.95	———	128790.26	316.46	217.42
25	51597.29	———	129657.08	315.21	222.22
25	50836.80	———	130799.19	305.42	224.59
25	50179.27	———	131796.00	309.33	228.50
25	50843.93	———	130995.07	310.58	224.88
25	51300.46	———	130017.52	318.19	220.00

KS_QMASS	LUFT_DUR	MD_WELLE	N	OPA_OPAC	P
kg/h	kg/h	Nm	rpm	-	kW
———	2841.65	2574.8	998	0.713	269.17
———	2908.59	2575.0	998	0.700	269.19
———	2790.54	2575.1	998	0.766	269.20
———	2772.99	2575.0	998	0.673	269.19
———	2832.95	2574.9	998	0.584	269.21
———	2887.09	2575.3	998	0.605	269.24
———	2945.38	2575.0	998	0.799	269.21
———	2886.85	2575.0	998	0.816	269.21
———	2817.91	2575.0	998	0.845	269.22

P_1HP	P_1LP	P_2HP	P_2LP	P_3	P_4
bar	mbar	bar	bar	bar	bar
0.38	-2.30	0.83	0.38	0.85	0.94
0.39	-2.41	0.87	0.40	0.89	0.98
0.36	-2.21	0.80	0.37	0.82	0.91
0.36	-2.19	0.80	0.36	0.81	0.91
0.37	-2.28	0.83	0.38	0.85	0.94
0.39	-2.39	0.86	0.39	0.88	0.97
0.41	-2.49	0.89	0.41	0.91	1.00
0.39	-2.39	0.86	0.39	0.88	0.97
0.38	-2.29	0.83	0.38	0.85	0.94

P_5	P_6	P_BARO	PHI	Q_KW_HT	Q_KW_LT
bar	mbar	mbar	%	l/min	l/min
0.33	0.88	982.1	21.9	27.8	101.4
0.34	0.92	982.1	22.4	27.7	106.9
0.32	0.82	982.1	22.5	28.1	107.6
0.32	0.79	982.1	21.4	28.2	106.1
0.33	0.85	982.2	23.1	28.0	106.5
0.34	0.94	982.3	22.1	27.6	103.8
0.35	0.98	982.3	22.2	27.5	106.6
0.34	0.90	982.4	22.2	27.6	108.0
0.33	0.87	982.4	21.7	27.9	109.9

T_1HP	T_1LP	T_2HP	T_2LP	T_3	T_4
°C	°C	°C	°C	°C	°C
46.38	22.74	104.04	59.63	43.41	379.03
46.39	23.18	105.14	61.57	43.72	380.79
46.33	22.82	103.11	58.80	43.87	378.38
46.34	22.81	102.74	58.36	43.67	377.92
46.36	23.09	103.75	59.92	43.66	379.02
46.40	22.54	104.90	60.60	43.42	380.09
46.42	23.08	105.95	62.51	43.62	381.61
46.38	23.09	104.94	61.40	43.78	380.64
46.33	22.73	103.85	59.66	44.03	379.15

T_5	T_6	T_LUFT	TE_FO	TWA_HT	TWA_LT
°C	°C	°C	°C	°C	°C
322.56	283.35	22	15.7	84.5	45.4
323.31	283.14	22	15.7	84.6	45.8
322.78	284.67	22	15.8	84.7	45.9
322.82	284.82	23	15.8	84.7	45.7
322.87	284.14	21	15.8	84.6	45.7
322.86	283.08	22	15.8	84.6	45.5
323.56	282.70	22	15.9	84.5	45.7
323.39	283.47	22	15.9	84.6	45.9
322.95	284.02	23	15.9	84.6	46.2

TWE_HT	TWE_LT	W_HTLOSS	Power	Fuel Flow	Mass Flow
°C	°C	kW	%	kg/s	kg/s
26.8	8.1	363.92	25	———	0.789347222
26.7	8.0	381.54	25	———	0.807941667
26.3	8.2	385.86	25	———	0.775150000
26.7	8.2	380.34	25	———	0.770275000
26.7	8.2	380.13	25	———	0.786930556
26.9	8.2	369.17	25	———	0.801969444
26.8	8.0	378.88	25	———	0.818161111
26.3	7.9	385.93	25	———	0.801902778
25.3	7.9	396.57	25	———	0.782752778

BMEP	Fuel Cons	NOx	TC LP Speed	TC HP Speed	Injection Timing
Pa	g/kWh	g/kWh	rpm	rpm	°CA BTDC
629951	———	———	22200	37000	5.0
630000	———	———	22650	37400	3.0
630024	———	———	21850	36700	7.0
630000	———	———	21750	36600	7.0
629976	———	———	22150	36950	5.0
630073	———	———	22550	37300	3.0
630000	———	———	22950	37600	3.0
630000	———	———	22550	37300	5.0
630000	———	———	22150	36950	7.0

Rail P	Fuel/stroke	
bar	g	
1400	———	
1400	———	
1400	———	
1500	———	
1500	———	
1500	———	
1200	———	
1200	———	
1200	———	

50% Load

Point	AG_CO2	AG_NOX	AG_O2	BLOW_VAL	GAS_LOSS
%	ppm	ppm	ppm	l/min	kW
50	64850.70	———	109398.13	412.91	350.40
50	63019.37	———	112376.30	426.80	362.00
50	62040.29	———	114159.39	437.63	371.41
50	65043.96	———	109312.09	412.64	353.87
50	66835.74	———	106444.48	397.12	347.57
50	65298.84	———	109070.43	406.15	353.19
50	64340.03	———	110765.12	417.17	359.77
50	63302.23	———	112310.04	424.57	364.13
50	64458.12	———	110387.70	414.16	357.97
50	65613.28	———	108629.63	416.55	353.00
50	66900.24	———	106810.38	405.16	347.91
50	68577.14	———	104368.79	398.08	342.99

KS_QMASS	LUFT_DUR	MD_WELLE	N	OPA_OPAC	P
kg/h	kg/h	Nm	rpm	-	kW
———	3758.14	5149.8	999	2.176	538.61
———	3901.77	5149.9	999	2.082	538.68
———	4030.99	5150.1	999	1.836	538.62
———	3711.45	5150.0	999	1.810	538.58
———	3577.62	5150.1	999	1.177	538.57
———	3687.79	5150.0	999	1.130	538.67
———	3790.40	5150.1	999	1.234	538.72
———	3877.74	5150.1	999	1.147	538.59
———	3767.95	5150.0	999	0.713	538.66
———	3674.76	5149.8	999	0.952	538.61
———	3579.94	5150.0	999	0.962	538.65
———	3485.82	5149.9	999	0.973	538.60

P_1HP	P_1LP	P_2HP	P_2LP	P_3	P_4
bar	mbar	bar	bar	bar	bar
0.8	-4.08	2.30	0.80	2.33	1.54
0.85	-4.36	2.43	0.85	2.45	1.63
0.89	-4.66	2.53	0.89	2.55	1.70
0.79	-3.96	2.27	0.80	2.30	1.52
0.75	-3.68	2.17	0.75	2.19	1.44
0.79	-3.90	2.26	0.79	2.28	1.51
0.82	-4.12	2.34	0.82	2.36	1.56
0.85	-4.32	2.41	0.85	2.44	1.61
0.81	-4.07	2.32	0.82	2.35	1.55
0.78	-3.87	2.25	0.78	2.27	1.50
0.75	-3.67	2.17	0.76	2.19	1.45
0.72	-3.47	2.10	0.73	2.12	1.40

P_5	P_6	P_BARO	PHI	Q_KW_HT	Q_KW_LT
bar	mbar	mbar	%	l/min	l/min
0.59	1.92	980.6	24.5	35.5	134.8
0.63	2.08	980.6	24.3	34.9	136.6
0.66	2.05	980.7	24.5	35.1	138.8
0.58	2.23	980.8	24.6	35.2	133.6
0.55	2.11	980.9	24.5	36.0	131.8
0.57	2.29	981.0	24.0	35.4	133.6
0.60	2.36	981.1	24.3	35.0	134.6
0.62	2.43	981.1	24.4	34.9	136.0
0.59	2.38	981.1	24.2	35.2	134.2
0.57	2.29	981.1	24.2	35.5	132.9
0.55	2.25	981.1	24.2	36.0	131.8
0.52	2.21	981.0	24.2	36.7	130.6

T_1HP	T_1LP	T_2HP	T_2LP	T_3	T_4
°C	°C	°C	°C	°C	°C
47.30	23.57	128.06	92.68	44.40	474.33
47.45	22.86	129.28	94.84	44.59	475.41
47.56	23.71	130.55	98.67	44.80	476.36
47.35	23.03	127.56	91.46	44.27	478.02
47.19	23.74	126.15	89.44	44.18	479.48
47.32	22.72	127.09	90.33	44.35	478.10
47.33	23.46	128.16	93.43	44.53	478.10
47.52	22.94	129.11	94.69	44.64	477.24
47.41	22.96	128.09	92.51	44.41	478.09
47.24	22.89	127.03	90.47	44.29	478.65
47.13	22.81	125.95	88.31	44.18	479.34
47.09	22.56	125.07	86.16	44.14	479.79

T_5	T_6	T_LUFT	TE_FO	TWA_HT	TWA_LT
°C	°C	°C	°C	°C	°C
397.02	327.77	20	16.8	85.0	46.5
396.96	328.09	20	16.8	85.0	46.6
397.24	326.65	20	16.8	85.0	46.8
401.3	336.04	20	16.8	85.0	46.3
404.21	341.07	20	16.8	85.1	46.3
401.9	337.84	20	16.8	85.1	46.4
401.07	335.31	20	16.9	85.0	46.5
399.52	332.34	20	16.9	85.0	46.6
401.23	335.49	20	16.9	85.0	46.4
402.68	338.45	20	16.9	85.1	46.3
404.26	341.60	20	17.0	85.1	46.3
405.78	344.60	20	17.0	85.2	46.2

TWE_HT	TWE_LT	W_HTLOSS	Power	Fuel Flow	Mass Flow
°C	°C	kW	%	kg/s	kg/s
26.0	7.0	500.68	50	———	1.043927778
26.1	7.0	504.30	50	———	1.083825000
26.1	6.7	513.98	50	———	1.119719444
26.0	7.0	494.90	50	———	1.030958333
26.1	7.2	491.17	50	———	0.993783333
26.1	7.3	493.89	50	———	1.024386111
26.1	7.4	494.62	50	———	1.052888889
26.1	7.0	501.99	50	———	1.077150000
26.1	6.9	497.62	50	———	1.046652778
26.1	7.0	494.20	50	———	1.020766667
26.1	7.0	492.39	50	———	0.994427778
26.1	7.4	488.85	50	———	0.968283333

BMEP	Fuel Cons	NOx	TC LP Speed	TC HP Speed	Injection Timing
Pa	g/kWh	g/kWh	rpm	rpm	°CA BTDC
1259951	———	———	29950	42800	10.0
1259976	———	———	30450	43050	8.0
1260024	———	———	31100	43350	6.0
1260000	———	———	29550	42550	12.0
1260024	———	———	28950	42200	12.0
1260000	———	———	29500	42500	10.0
1260024	———	———	30400	42950	8.0
1260024	———	———	30800	43200	6.0
1260000	———	———	29850	42700	6.0
1259951	———	———	29450	42450	8.0
1260000	———	———	28950	42200	10.0
1259976	———	———	29650	42600	12.0

Rail P	Fuel/stroke	File Name
bar	g	-
1000	———	Test1_003
1000	———	Test1_004
1000	———	Test1_005
1000	———	Test1_006
1200	———	Test1_007
1200	———	Test1_008
1200	———	Test1_009
1200	———	Test1_010
1400	———	Test1_011
1400	———	Test1_012
1400	———	Test1_013
1400	———	Test1_014

75% Load

Point	AG_CO2	AG_NOX	AG_O2	BLOW_VAL	GAS_LOSS
%	ppm	ppm	ppm	l/min	kW
75	60993.36	———	115136.06	508.74	466.21
75	60112.16	———	116471.45	515.98	475.50
75	62032.82	———	113399.64	502.01	456.27
75	63013.23	———	111964.23	493.84	448.82
75	63749.13	———	110731.23	497.34	446.36
75	62961.92	———	111923.91	503.07	450.68
75	62045.39	———	113665.63	503.86	456.79
75	61216.86	———	115092.47	511.31	466.75
75	62478.28	———	112859.08	500.66	454.51
75	63501.71	———	111292.23	486.89	447.98
75	64398.37	———	110141.97	490.30	443.46
75	65298.33	———	108657.91	496.47	440.56
75	66186.76	———	107142.27	500.76	437.04
75	64485.84	———	109854.56	504.76	443.99

KS_QMASS	LUFT_DUR	MD_WELLE	N	OPA_OPAC	P
kg/h	kg/h	Nm	upm	-	kW
———	5667.06	7724.4	999	1.275	808.30
———	5852.63	7725.2	999	1.440	808.36
———	5521.44	7724.8	999	1.106	808.33
———	5386.11	7725.2	999	1.170	808.35
———	5303.82	7724.9	999	0.834	808.33
———	5400.09	7725.3	999	0.892	808.36
———	5536.37	7725.3	999	1.001	808.39
———	5703.84	7725.0	999	0.969	808.33
———	5481.38	7724.8	999	0.770	808.29
———	5351.59	7725.2	999	0.754	808.35
———	5250.70	7725.6	999	0.828	808.37
———	5162.90	7725.0	999	0.829	808.31
———	5070.62	7724.9	999	0.838	808.31
———	5239.32	7725.2	999	0.808	808.36

P_1HP	P_1LP	P_2HP	P_2LP	P_3	P_4
bar	mbar	bar	bar	bar	bar
1.48	-9.29	3.97	1.48	4.01	2.69
1.53	-9.91	4.11	1.54	4.15	2.79
1.42	-8.78	3.84	1.42	3.87	2.59
1.38	-8.38	3.74	1.38	3.77	2.52
1.35	-8.11	3.66	1.35	3.70	2.46
1.38	-8.41	3.74	1.38	3.78	2.52
1.43	-8.84	3.86	1.43	3.89	2.60
1.48	-9.39	3.99	1.49	4.03	2.70
1.41	-8.69	3.81	1.41	3.85	2.57
1.37	-8.26	3.70	1.37	3.74	2.49
1.33	-7.95	3.62	1.34	3.66	2.43
1.30	-7.69	3.55	1.30	3.58	2.38
1.27	-7.41	3.48	1.27	3.51	2.32
1.33	-7.90	3.62	1.33	3.65	2.43

P_5	P_6	P_BARO	PHI	Q_KW_HT	Q_KW_LT
bar	mbar	mbar	%	l/min	l/min
1.14	3.60	981.1	25.3	40.6	178.3
1.20	3.71	981.1	25.7	41.3	182.1
1.09	3.30	981.2	26.0	40.4	178.2
1.06	3.21	981.1	25.9	40.6	177.3
1.03	3.16	981.1	25.7	40.9	176.2
1.06	3.24	981.2	25.9	40.6	176.4
1.10	3.33	981.2	26.0	40.7	178.4
1.15	3.43	981.3	26.3	41.1	180.6
1.08	3.21	981.4	25.6	40.8	177.8
1.04	3.15	981.4	26.0	40.7	175.8
1.01	3.11	981.4	25.7	41.1	174.7
0.98	2.97	981.5	26.0	41.9	174.1
0.96	2.93	981.5	26.1	43.0	173.2
1.01	3.10	981.6	25.9	41.9	175.0

T_1HP	T_1LP	T_2HP	T_2LP	T_3	T_4
°C	°C	°C	°C	°C	°C
48.82	21.70	141.56	130.00	46.70	473.87
48.99	22.71	142.72	134.84	47.14	476.00
48.86	22.07	141.22	128.11	46.59	473.84
48.72	21.87	140.55	125.51	46.41	473.32
48.69	22.51	140.16	124.50	46.23	474.25
48.70	22.13	140.60	125.82	46.46	473.70
48.85	21.79	141.30	128.05	46.74	473.67
48.93	22.44	142.11	131.73	46.98	475.05
48.79	22.76	141.01	128.14	46.51	474.77
48.70	22.22	140.40	125.12	46.33	473.74
48.64	22.07	139.87	122.98	46.17	473.95
48.59	22.54	139.43	121.84	46.03	474.35
48.54	22.39	138.97	120.01	45.90	474.88
48.63	22.10	139.76	122.77	46.21	474.09

T_5	T_6	T_LUFT	TE_FO	TWA_HT	TWA_LT
°C	°C	°C	°C	°C	°C
387.82	289.84	20	17.0	85.4	47.6
389.38	286.46	20	17.0	85.5	47.9
387.76	290.00	19	17.0	85.4	47.6
387.46	291.96	19	17.1	85.4	47.5
388.54	294.41	19	17.1	85.4	47.4
387.81	292.33	19	17.1	85.4	47.5
387.46	289.67	19	17.2	85.4	47.7
388.38	287.75	19	17.2	85.5	47.8
388.33	291.21	20	17.3	85.4	47.5
387.87	293.14	20	17.3	85.4	47.4
388.32	295.31	20	17.3	85.4	47.3
389.19	297.70	20	17.4	85.5	47.3
389.88	299.98	20	17.4	85.5	47.3
388.56	296.09	20	17.4	85.5	47.5

TWE_HT	TWE_LT	W_HTLOSS	Power	Fuel Flow	Mass Flow
°C	°C	kW	%	kg/s	kg/s
26.2	6.4	657.17	75	———	1.574183333
26.2	6.2	676.58	75	———	1.625730556
26.1	6.2	658.34	75	———	1.533733333
26.1	6.3	653.04	75	———	1.496141667
26.1	6.3	651.37	75	———	1.473283333
26.2	6.3	652.13	75	———	1.500025000
26.2	6.3	659.73	75	———	1.537880556
26.2	6.4	668.27	75	———	1.584400000
26.1	6.7	652.22	75	———	1.522605556
26.1	6.4	648.17	75	———	1.486552778
26.1	6.4	646.03	75	———	1.458527778
26.2	6.4	647.62	75	———	1.434138889
26.2	6.5	648.13	75	———	1.408505556
26.2	6.4	651.17	75	———	1.455366667

BMEP	Fuel Cons	NOx	TC LP Speed	TC HP Speed	Injection Timing
Pa	g/kWh	g/kWh	rpm	rpm	°CA BTDC
1889853	———	———	37800	45800	11.0
1890049	———	———	38400	46000	9.0
1889951	———	———	37200	45650	13.0
1890049	———	———	36800	45500	15.0
1889976	———	———	36500	45450	15.0
1890073	———	———	36800	45550	13.0
1890073	———	———	37300	45700	11.0
1890000	———	———	37850	45850	9.0
1889951	———	———	37150	45650	9.0
1890049	———	———	36700	45450	11.0
1890147	———	———	36300	45350	13.0
1890000	———	———	36000	45300	15.0
1889976	———	———	35650	45150	15.0
1890049	———	———	36250	45250	11.0

Rail P	Fuel/stroke	File Name
bar	g	-
1000	———	Test1_015
1000	———	Test1_016
1000	———	Test1_017
1000	———	Test1_018
1100	———	Test1_019
1100	———	Test1_020
1100	———	Test1_021
1100	———	Test1_022
1300	———	Test1_023
1300	———	Test1_024
1300	———	Test1_025
1300	———	Test1_026
1500	———	Test1_027
1500	———	Test1_028

A.3.2 With EGR

25% Load

Point	AG_CO2	AG_NOX	AG_O2	BLOW_VAL	GAS_LOSS
%	ppm	ppm	ppm	l/min	kW
25	58219.85	———	117716.77	477.11	174.93
25	57268.05	———	118971.06	480.03	180.21
25	59194.50	———	115935.44	472.67	169.87
25	73757.70	———	92063.99	450.59	167.32
25	71611.20	———	95193.74	454.48	174.46

KS_QMASS	LUFT_DUR	MD_WELLE	N	OPA_OPAC	P
kg/h	kg/h	Nm	rpm	-	kW
———	2543.21	2578.0	1000	0.836	269.61
———	2630.09	2577.9	1000	0.877	269.59
———	2461.34	2578.1	1000	0.947	269.60
———	1978.28	2577.8	1000	4.151	269.62
———	2063.16	2578.0	1000	5.778	269.64

P_1HP	P_1LP	P_2HP	P_2LP	P_3	P_4
bar	mbar	bar	bar	bar	bar
0.38	-1.80	1.41	0.40	1.40	2.08
0.41	-1.92	1.49	0.42	1.48	2.19
0.36	-1.68	1.34	0.37	1.33	1.99
0.31	-1.03	1.00	0.32	1.00	1.49
0.34	-1.13	1.09	0.35	1.08	1.60

P_5	P_6	P_BARO	PHI	Q_KW_HT	Q_KW_LT
bar	mbar	mbar	%	l/min	l/min
0.50	1.81	985.3	19.6	35.3	104.6
0.53	1.92	985.3	19.5	35.4	106.8
0.47	1.66	985.2	19.5	35.4	103.6
0.34	1.12	985.2	19.5	36.2	93.0
0.36	1.21	985.2	19.6	35.7	95.6

T_1HP	T_1LP	T_2HP	T_2LP	T_3	T_4
°C	°C	°C	°C	°C	°C
54.22	28.87	132.89	72.17	56.14	399.52
54.72	28.82	135.16	74.73	56.39	403.87
54.78	28.88	131.33	70.28	56.17	395.93
59.66	29.21	121.44	61.48	56.14	427.61
60.54	29.28	123.74	63.68	55.58	431.89

T_5	T_6	T_LUFT	TE_FO	TWA_HT	TWA_LT
°C	°C	°C	°C	°C	°C
302.04	255.32	28	34.4	85.2	46.9
304.13	255.10	29	35.4	85.2	47.1
300.34	255.88	29	36.1	85.2	46.7
341.85	301.19	29	37.3	85.3	46.2
343.46	302.39	29	37.9	85.3	46.5

TWE_HT	TWE_LT	W_HTLOSS	Load	Fuel Flow	Air Flow
°C	°C	kW	%	kg/s	kg/s
24.4	24.4	311.12	25	———	0.706447222
24.4	24.4	316.26	25	———	0.730580556
24.4	24.3	309.27	25	———	0.683705556
24.2	24.3	293.43	25	———	0.549522222
24.5	24.5	295.61	25	———	0.573100000

BMEP	Fuel Cons	BSAC	NOx	TC LP Speed	TC HP Speed
bar	g/kWh	kg/kWh	g/kWh	rpm	rpm
6.136	———	9.433	———	24700	44000
6.135	———	9.756	———	25500	44600
6.136	———	9.130	———	24100	43500
6.135	———	7.337	———	21100	39800
6.136	———	7.652	———	22000	40600

Injection Timing	Rail P	Peak Press	T_AGR2	AGR_CO2	TICOUT
°CA BTDC	bar	bar	°C	%	°C
5.0	1400	112.447	72.4	1.08	46.2
2.0	1400	103.892	73.8	1.07	46.1
8.0	1400	120.325	73.9	1.11	46.0
8.0	1400	104.349	75.2	1.93	46.4
5.0	1400	98.136	76.7	1.88	46.3

EGR	Fuel/stroke	File Name
%	g	-
18.55	———	EGRM73NewTNom30_001
18.68	———	EGRM73NewTNom30_002
18.75	———	EGRM73NewTNom30_003
26.17	———	EGRM73NewTNom30_004
26.25	———	EGRM73NewTNom30_005

50% Load

Point	AG_CO2	AG_NOX	AG_O2	BLOW_VAL	GAS_LOSS
%	ppm	ppm	ppm	l/min	kW
50	74580.02	———	89729.48	511.58	281.31
50	76377.74	———	87054.13	514.08	277.33
50	78570.90	———	83909.60	508.76	272.09
50	81193.46	———	79971.12	502.29	266.50
50	76478.79	———	87383.67	512.01	277.99
50	84428.72	———	74232.27	509.00	285.56
50	90402.52	———	64832.07	498.60	272.38
50	87198.91	———	70215.25	501.00	279.21

KS_QMASS	LUFT_DUR	MD_WELLE	N	OPA_OPAC	P
kg/h	kg/h	Nm	rpm	-	kW
———	3195.93	5156.5	1000	13.335	539.93
———	3098.56	5156.6	1000	11.062	539.96
———	2988.00	5157.1	1000	8.167	539.98
———	2865.33	5156.4	1000	6.699	539.90
———	3118.09	5156.9	1000	———	539.97
———	2862.75	5156.5	1000	17.997	539.93
———	2594.44	5158.0	1000	11.599	540.10
———	2724.44	5157.4	1000	15.075	540.01

P_1HP	P_1LP	P_2HP	P_2LP	P_3	P_4
bar	mbar	bar	bar	bar	bar
0.94	-2.94	3.11	0.95	3.11	3.09
0.90	-2.77	2.99	0.91	2.99	2.97
0.85	-2.57	2.86	0.86	2.86	2.84
0.80	-2.34	2.71	0.81	2.71	2.69
0.91	-2.81	3.02	0.92	3.01	3.00
0.87	-2.34	2.80	0.88	2.79	2.74
0.75	-1.91	2.48	0.76	2.48	2.43
0.81	-2.14	2.64	0.82	2.64	2.59

P_5	P_6	P_BARO	PHI	Q_KW_HT	Q_KW_LT
bar	mbar	mbar	%	l/min	l/min
0.82	3.30	984.9	18.5	38.6	139.2
0.78	3.17	984.9	18.5	39.0	134.7
0.74	2.98	984.9	18.5	39.8	133.5
0.69	2.81	984.8	17.9	40.8	130.1
0.79	3.20	984.6	17.2	39.4	133.0
0.72	2.88	984.4	17.0	40.3	131.7
0.62	2.38	984.4	16.6	41.9	125.8
0.67	2.63	984.4	16.4	41.2	128.4

T_1HP	T_1LP	T_2HP	T_2LP	T_3	T_4
°C	°C	°C	°C	°C	°C
57.32	29.73	151.93	108.34	56.17	508.40
57.71	29.87	150.89	105.54	55.96	508.32
57.70	30.02	149.51	102.51	56.02	508.28
57.15	30.17	147.29	98.82	55.78	507.80
57.80	29.88	151.04	106.04	55.89	508.11
61.57	30.22	149.69	103.63	55.94	534.64
60.93	30.38	146.35	96.09	55.99	536.98
61.51	30.42	148.05	99.67	56.19	536.33

T_5	T_6	T_LUFT	TE_FO	TWA_HT	TWA_LT
°C	°C	°C	°C	°C	°C
389.06	313.08	29	40.3	85.3	47.5
390.37	316.75	29	37.5	85.4	47.3
391.79	320.62	30	32.4	85.4	47.2
393.24	325.18	30	28.3	85.5	47.3
389.98	316.15	30	28.0	85.4	47.6
418.55	345.94	30	29.6	85.5	47.4
424.72	357.86	31	30.2	85.6	47.0
422.03	353.15	31	30.8	85.5	47.3

TWE_HT	TWE_LT	W_HTLOSS	Load	Fuel Flow	Air Flow
°C	°C	kW	%	kg/s	kg/s
24.3	24.4	384.77	50	———	0.887758333
24.3	24.4	378.56	50	———	0.860711111
24.3	24.3	379.50	50	———	0.830000000
24.4	24.4	378.05	50	———	0.795925000
24.3	24.3	380.42	50	———	0.866136111
24.3	24.4	380.28	50	———	0.795208333
24.2	24.2	375.45	50	———	0.720677778
24.3	24.4	377.31	50	———	0.756788889

BMEP	Fuel Cons	BSAC	NOx	TC LP Speed	TC HP Speed
bar	g/kWh	kg/kWh	g/kWh	rpm	rpm
12.272	———	5.919	———	32350	47500
12.273	———	5.738	———	31800	47200
12.274	———	5.534	———	31100	46800
12.272	———	5.307	———	30200	46500
12.273	———	5.775	———	31900	47200
12.272	———	5.302	———	31150	46400
12.276	———	4.804	———	29300	45580
12.275	———	5.045	———	30200	46000

Injection Timing	Rail P	Peak Press	T_AGR2	AGR_CO2	TICOUT
°CA BTDC	bar	bar	°C	%	°C
10.0	1000	123.236	76.9	1.69	46.1
10.0	1200	127.140	76.8	1.76	46.1
10.0	1500	135.310	76.1	1.81	46.1
13.0	1500	144.061	74.7	1.87	45.9
7.0	1500	125.651	76.7	1.76	46.2
7.0	1500	119.494	83.4	2.24	46.2
13.0	1500	137.344	82.9	2.44	46.0
10.0	1500	129.041	83.8	2.32	46.1

EGR	Fuel/stroke	Indi File Name
%	g	-
22.66	———	EGRM73NewTNom30_008
23.04	———	EGRM73NewTNom30_009
23.04	———	EGRM73NewTNom30_010
23.03	———	EGRM73NewTNom30_011
23.01	———	EGRM73NewTNom30_012
26.53	———	EGRM73NewTNom30_013
26.99	———	EGRM73NewTNom30_014
26.61	———	EGRM73NewTNom30_015

75% Load

Point	AG_CO2	AG_NOX	AG_O2	BLOW_VAL	GAS_LOSS
%	ppm	ppm	ppm	l/min	kW
75	74551.93	———	89691.34	557.38	370.61
75	76395.78	———	87017.66	554.42	360.86
75	78182.15	———	83526.69	541.25	355.67
75	74350.55	———	89152.91	558.58	368.48
75	74229.82	———	86432.20	580.32	366.49
75	75687.28	———	83732.66	577.46	355.73
75	76710.99	———	81462.05	559.91	347.47
75	75550.39	———	83503.17	573.27	355.08
75	86844.08	———	66088.11	552.14	373.84
75	88841.83	———	62484.43	537.00	369.46
75	86539.63	———	66069.48	558.29	377.20

KS_QMASS	LUFT_DUR	MD_WELLE	N	OPA_OPAC	P
kg/h	kg/h	Nm	rpm	-	kW
———	4544.70	7734.4	1000	6.863	810.20
———	4334.51	7734.6	1000	3.003	810.17
———	4164.73	7735.5	1000	1.754	810.37
———	4507.19	7734.4	1000	1.697	810.20
———	4516.91	7734.9	1000	6.087	809.40
———	4311.45	7734.9	1000	2.165	809.41
———	4157.23	7734.6	1000	0.654	809.42
———	4306.53	7735.2	1000	0.469	809.47
———	3833.29	7734.8	1000	5.342	809.40
———	3699.84	7735.3	1000	10.548	809.46
———	3854.12	7735.0	1000	15.913	809.39

P_1HP	P_1LP	P_2HP	P_2LP	P_3	P_4
bar	mbar	bar	bar	bar	bar
1.59	-5.93	4.85	1.60	4.86	4.73
1.50	-5.40	4.59	1.51	4.59	4.47
1.42	-4.95	4.37	1.43	4.37	4.26
1.58	-5.84	4.80	1.59	4.80	4.69
1.59	-6.15	4.81	1.60	4.81	4.78
1.50	-5.59	4.57	1.51	4.56	4.53
1.43	-5.21	4.39	1.44	4.38	4.34
1.49	-5.59	4.56	1.50	4.56	4.52
1.47	-4.37	4.17	1.49	4.16	4.02
1.40	-4.09	4.00	1.42	3.99	3.85
1.48	-4.42	4.18	1.49	4.17	4.03

P_5	P_6	P_BARO	PHI	Q_KW_HT	Q_KW_LT
bar	mbar	mbar	%	l/min	l/min
1.40	6.03	991.4	14.5	47.9	171.7
1.30	5.55	991.3	15.0	47.0	168.7
1.23	5.16	991.2	15.6	47.8	165.4
1.38	5.98	991.2	14.5	48.4	172.5
1.41	6.23	973.1	25.7	48.4	186.8
1.32	5.83	973.1	26.3	47.3	181.0
1.25	5.47	973.0	25.8	47.7	175.4
1.32	5.83	973.0	26.0	48.1	176.6
1.16	5.02	972.7	26.0	49.2	173.9
1.10	4.81	972.7	26.9	49.7	170.0
1.16	5.29	972.6	27.5	49.6	172.1

T_1HP	T_1LP	T_2HP	T_2LP	T_3	T_4
°C	°C	°C	°C	°C	°C
34.38	26.57	155.78	144.75	56.53	521.37
37.66	27.13	153.82	140.08	55.94	519.61
37.47	27.65	153.34	136.25	55.99	519.24
37.12	27.07	155.36	143.61	56.35	521.14
55.82	30.28	163.88	151.02	55.97	529.85
55.48	30.81	162.42	145.87	55.39	526.15
53.84	31.02	160.75	141.81	55.73	523.56
54.02	31.12	161.64	146.12	56.19	525.81
65.26	32.09	159.15	143.27	55.92	560.17
65.09	32.78	158.46	140.10	55.98	560.36
66.52	33.01	160.35	143.98	56.17	561.17

T_5	T_6	T_LUFT	TE_FO	TWA_HT	TWA_LT
°C	°C	°C	°C	°C	°C
391.80	283.01	24	26.5	85.8	48.7
391.65	287.39	24	26.8	85.7	48.3
392.48	292.45	24	27.6	85.8	48.2
391.93	283.90	25	28.0	85.9	48.9
398.51	285.60	30	27.6	85.8	49.4
396.58	288.95	31	28.4	85.7	48.5
395.20	291.63	31	29.3	85.8	48.4
396.44	288.99	31	30.3	85.8	49.0
433.64	330.78	31	34.4	85.9	48.5
435.13	335.73	31	36.0	85.9	48.3
434.49	331.31	30	37.2	85.9	48.9

TWE_HT	TWE_LT	W_HTLOSS	Power	Fuel Flow	Mass Flow
°C	°C	kW	%	kg/s	kg/s
24.3	24.4	491.40	75	———	1.262416667
24.2	24.3	479.60	75	———	1.204030556
24.3	24.4	475.81	75	———	1.156869444
24.4	24.5	496.78	75	———	1.251997222
24.3	24.3	530.61	75	———	1.254697222
24.2	24.3	505.16	75	———	1.197625000
24.3	24.3	494.78	75	———	1.154786111
24.4	24.4	505.75	75	———	1.196258333
24.3	24.4	499.38	75	———	1.064802778
24.3	24.3	492.75	75	———	1.027733333
24.4	24.4	503.08	75	———	1.070588889

BMEP	Fuel Cons	BSAC	NOx	TC LP Speed	TC HP Speed
bar	g/kWh	kg/kWh	g/kWh	rpm	rpm
18.408	———	5.609	———	39500	49400
18.408	———	5.350	———	38500	48900
18.410	———	5.139	———	37800	48750
18.408	———	5.563	———	39300	49200
18.409	———	5.581	———	40150	50100
18.409	———	5.327	———	39200	49800
18.408	———	5.136	———	38450	49600
18.410	———	5.320	———	39150	49850
18.409	———	4.736	———	38100	48200
18.410	———	4.571	———	37400	48050
18.409	———	4.762	———	38200	48300

Injection Timing	Rail P	Peak Press	T_AGR2	AGR_CO2	TICOUT
°CA BTDC	bar	bar	°C	%	°C
11.0	1000	169.200	70.3	1.93	45.9
11.0	1200	169.100	69.9	1.96	45.9
11.0	1500	177.500	70.0	2.02	46.0
5.5	1500	156.500	70.0	1.90	46.0
11.0	1000	166.735	77.8	1.80	45.9
11.0	1200	166.452	77.3	1.85	46.1
11.0	1500	177.752	76.1	1.86	45.9
8.0	1500	163.271	76.5	1.84	46.1
8.0	1500	151.506	84.7	2.64	46.0
11.0	1500	164.025	85.6	2.76	46.0
11.0	1200	156.100	87.5	2.70	46.1

EGR	Fuel/stroke	File Name
%	g	-
25.89	———	EGRM73NewTNomH2_006
25.66	———	EGRM73NewTNomH2_007
25.84	———	EGRM73NewTNomH2_008
25.55	———	EGRM73NewTNomH2_009
24.25	———	EGRM73NewTNom30_017
24.44	———	EGRM73NewTNom30_018
24.25	———	EGRM73NewTNom30_019
24.35	———	EGRM73NewTNom30_020
30.40	———	EGRM73NewTNom30_021
31.07	———	EGRM73NewTNom30_022
31.20	———	EGRM73NewTNom30_023

Appendix B

Simulation Models Layout

In the following pages a list is given with all the working models used throughout this master thesis and presented in this report. Then for each major configuration a picture of the GT-POWER simulation program's Project Map shows the engine layout and (in case of an EGR Setup) highlights the EGR path.

B.1 Depict Of Simulation Models

- Full Engine Model:
  - Without EGR:
    W20_Two-st_M73_1000_all-V72_v2-V74.gtm
  - Semi-Short Route EGR:
    W20_Two-st_M73_1000_all-V72_v2-V74 - EGR_real_v6.gtm
- Fast Running Model:
  - Semi-Short Route EGR:
    - Standard:
      FRM - EGR - v8_set.gtm
    - Optimized:
      FRM - EGR - v9c_set.gtm
    - Constant P_{boost} Analysis:
      FRM - EGR - No5.gtm
    - Constant TTI Analysis:
      FRM - EGR - No6.gtm
  - 1 Donor Cylinder Semi-Short Route EGR:
    - Standard:
      FRM - EGR - 1CylDonor - v3_hpt1.gtm
    - Optimized:
      FRM - EGR - 1CylDonor - v3.gtm
    - M80 Cam:
      FRM - EGR - 1CylDonor - v3 M80_hpt1.gtm
    - M80 Cam Optimized:
      FRM - EGR - 1CylDonor - v3 M80.gtm

- 2 Donor Cylinders Short Route EGR:
  - Standard:
    FRM - EGR - 2CylDonor - v3_hpt1.gtm
  - Optimized:
    FRM - EGR - 2CylDonor - v3.gtm

- Short Route EGR Blower:
  - Externally Driven Optimized:
    FRM - EGR - Blower - No1_1.gtm
  - Crankshaft Driven Optimized:
    FRM - EGR - Blower - No2_3.gtm
  - Crankshaft Driven for Constant P_{boost} Analysis:
    FRM - EGR - Blower - No3_1.gtm
  - Crankshaft Driven for Constant TTI Analysis:
    FRM - EGR - Blower - No4_2.gtm

- Short Route EGR Turbocharger Optimized:
  FRM - EGR - TC - New Specs - Opt 50.gtm

- Test Bench Configuration:
  - Semi-Short Route:
    FRM - EGR - v8_set - Test Bench - New TC Maps.gtm
  - 1 Donor Cylinder Semi-Short Route:
    FRM - EGR - 1CylDonor - v3_hpt1 - Test Bench - New TC Maps.gtm

- Semi-Short Route for NO_x Analysis:
  - EGR Rate Variation:
    FRM - EGR - v8_set_NOx_20.gtm
    FRM - EGR - v8_set_NOx_25.gtm
    FRM - EGR - v8_set_NOx_30.gtm
  - Load Variation:
    FRM - EGR - v8_set_NOx_P25.gtm
    FRM - EGR - v8_set_NOx_P33.gtm
    FRM - EGR - v8_set_NOx_P40.gtm
    FRM - EGR - v8_set_NOx_P48.gtm
    FRM - EGR - v8_set_NOx_P50.gtm
    FRM - EGR - v8_set_NOx_P75.gtm
    FRM - EGR - v8_set_NOx_P85.gtm
    FRM - EGR - v8_set_NOx_P100.gtm
  - SOI and P_{rail} Variation:
    FRM - EGR - v8_set - SOI Variation_2_GOOD Meas.gtm
  - SOI and P_{rail} Variation Optimized:
    FRM - EGR - v9_set - SOI Variation_2_GOOD Meas.gtm

B.2 Full Engine Model Without EGR

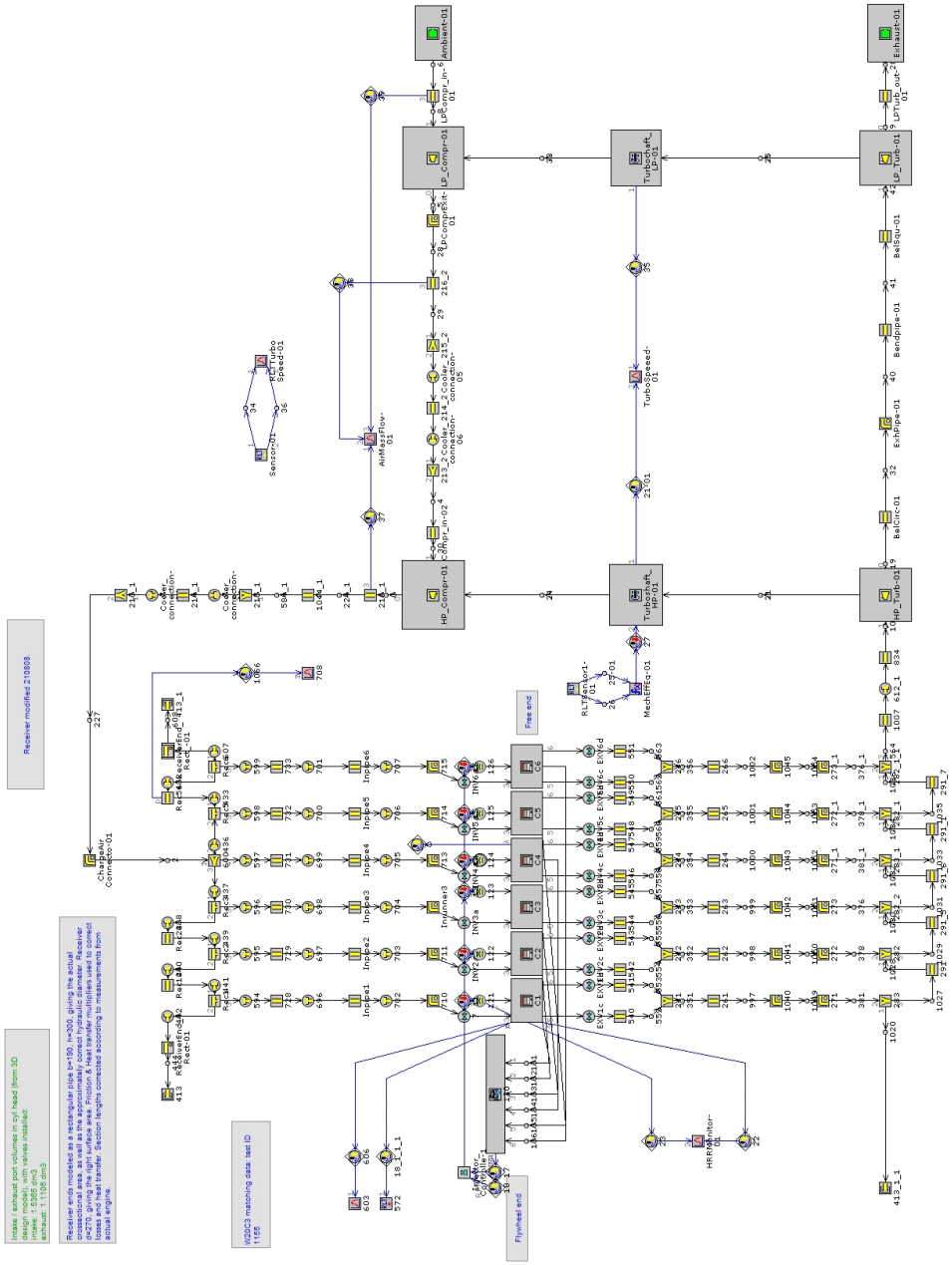

B.3 Full Engine Model With Semi-Short Route EGR

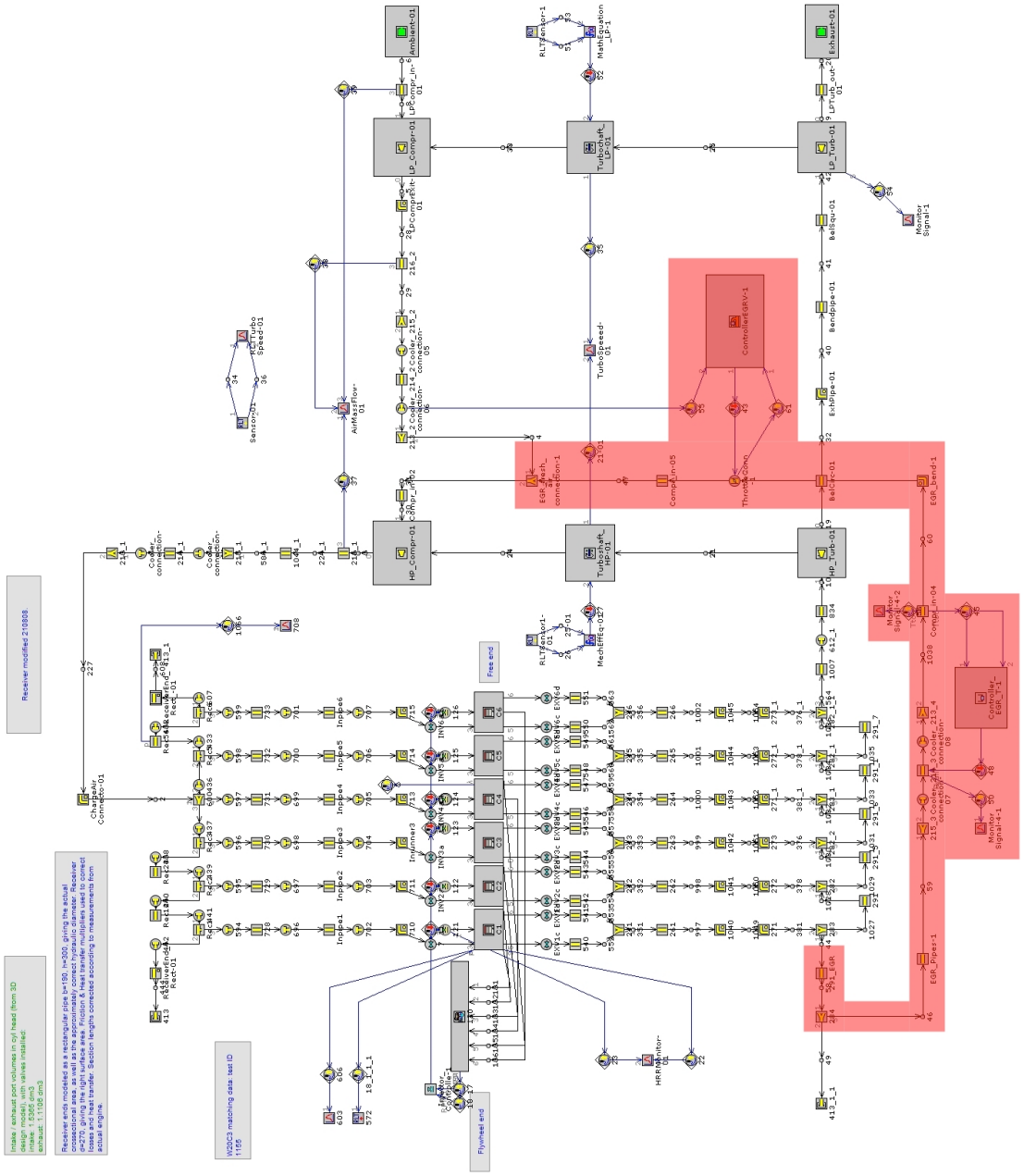

B.4 Fast Running Model With Semi-Short Route EGR

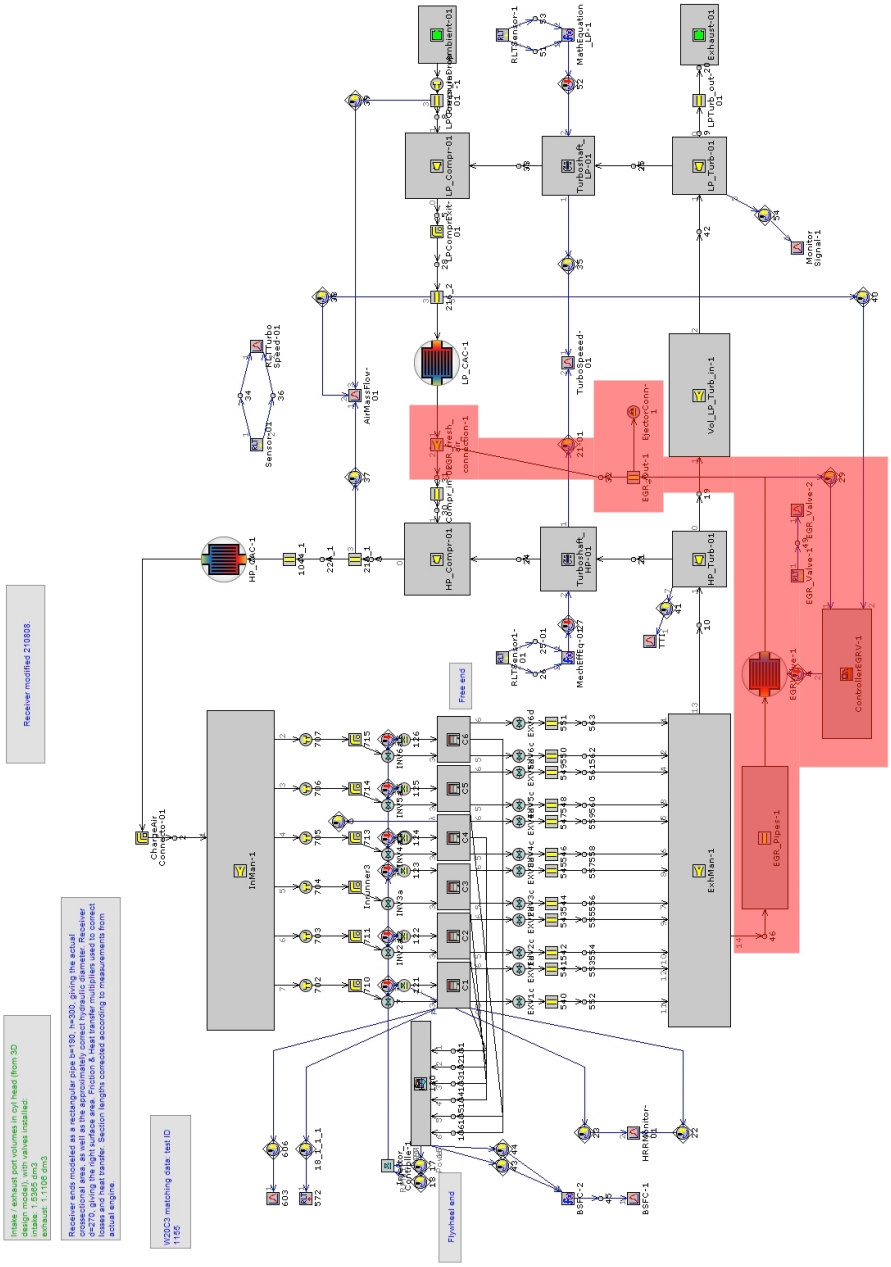

B.5 Fast Running Model With 1 Donor Cylinder Semi-Short Route EGR

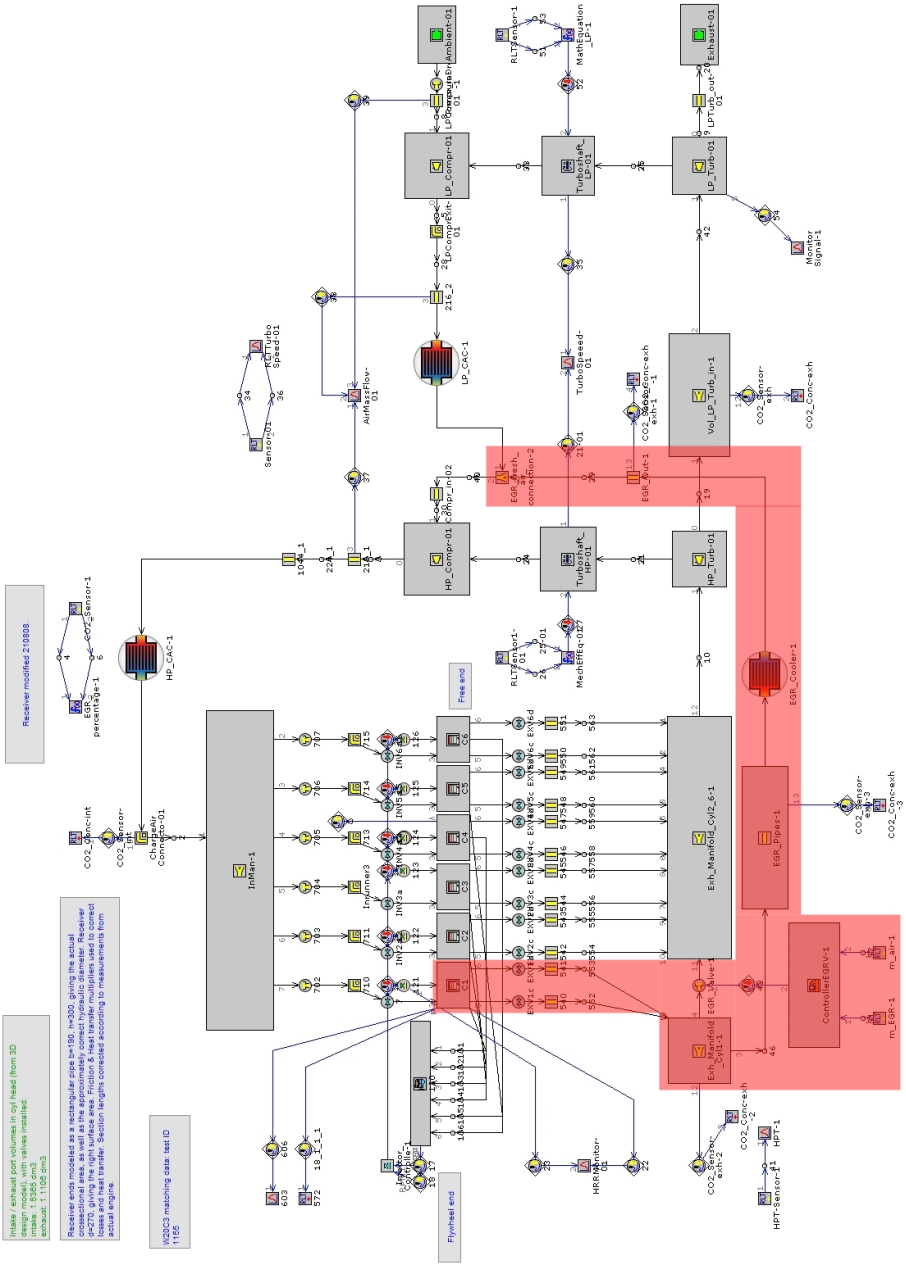

B.6 Fast Running Model With 2 Donor Cylinders Short Route EGR

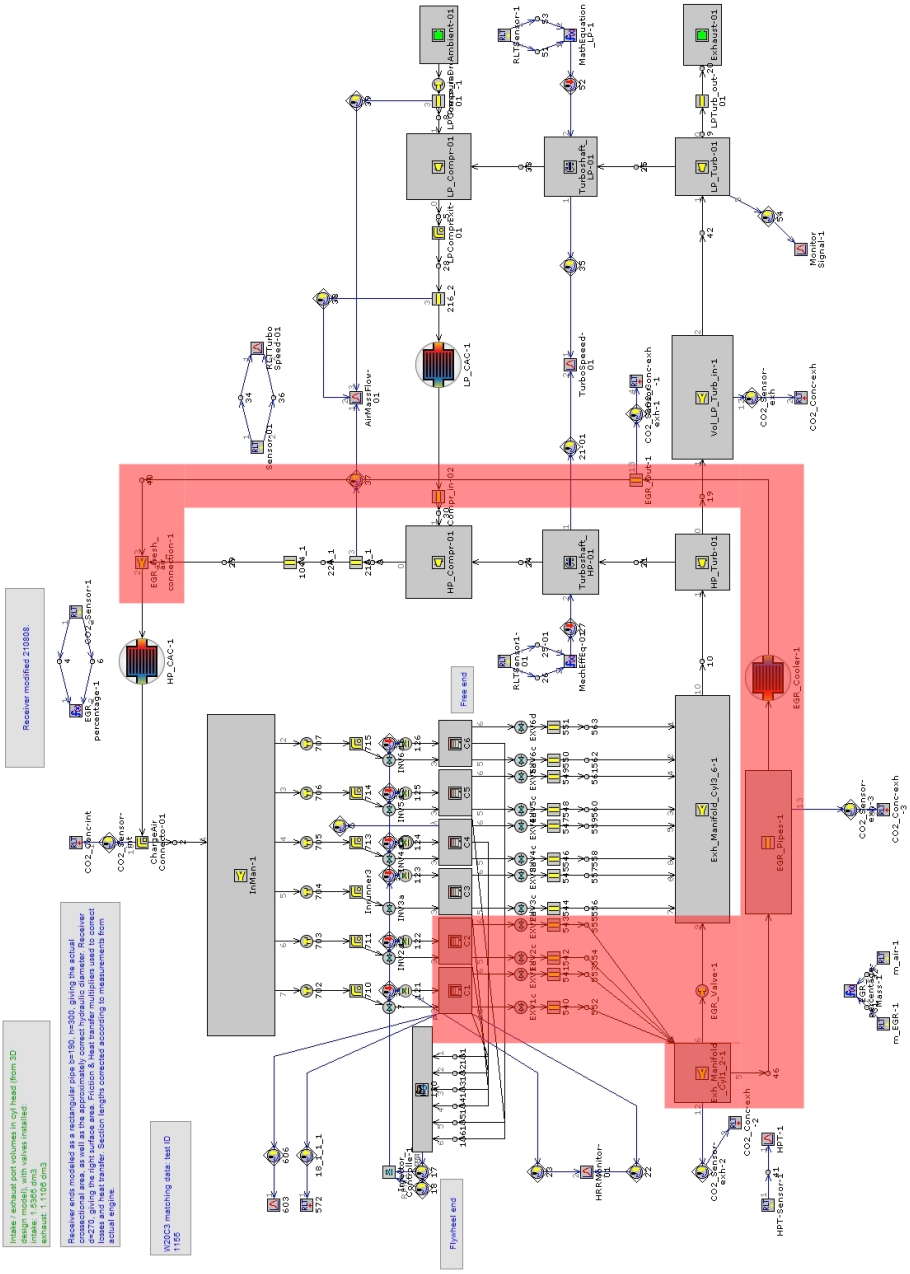

B.7 Fast Running Model With Short Route EGR Blower

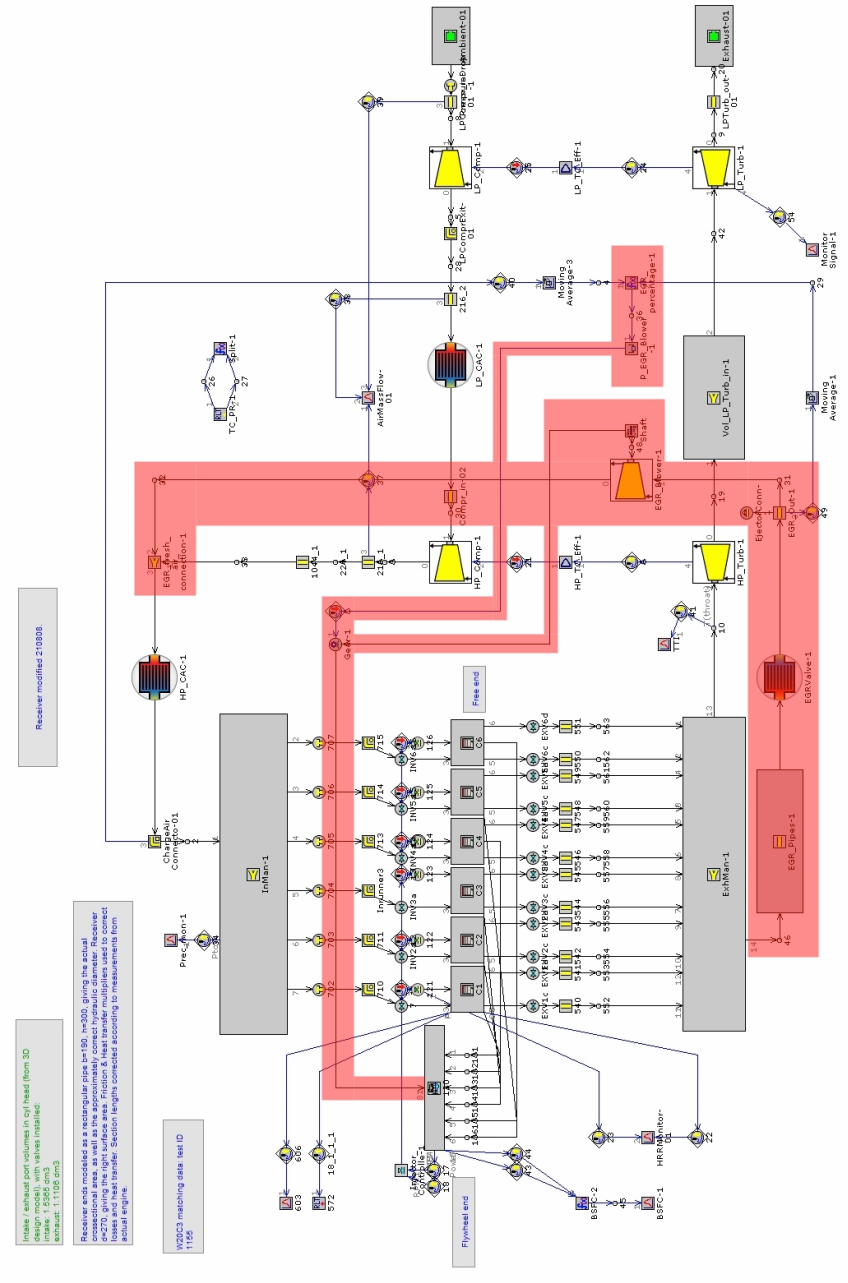

B.8 Fast Running Model With Short Route EGR Turbocharger

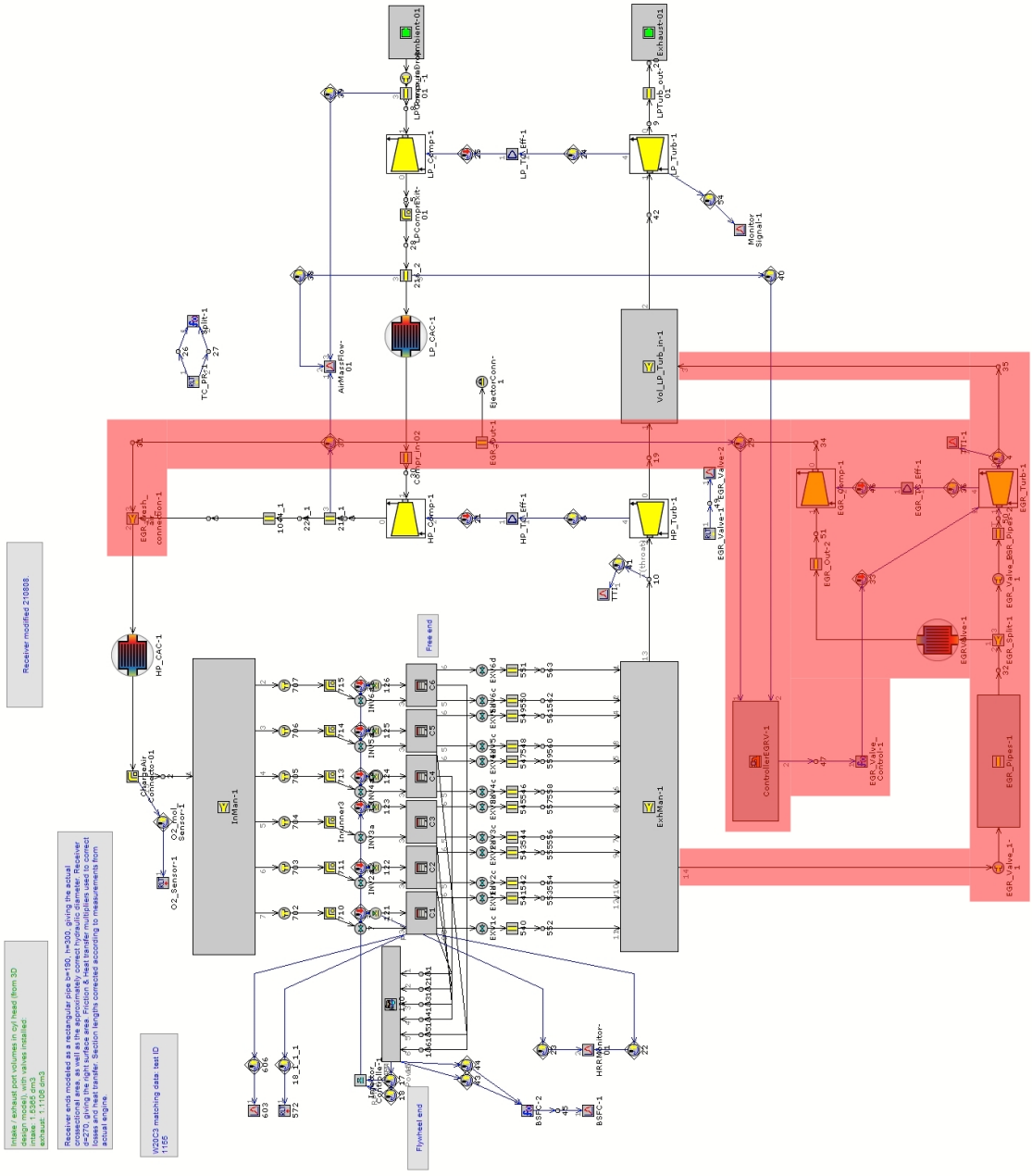

Appendix C

Various Figures

In the following pages are listed different figures created in the various steps of the master thesis utilized then for the detailed analysis done in this project.

C.1 Calibration

C.1.1 Semi-Short Route

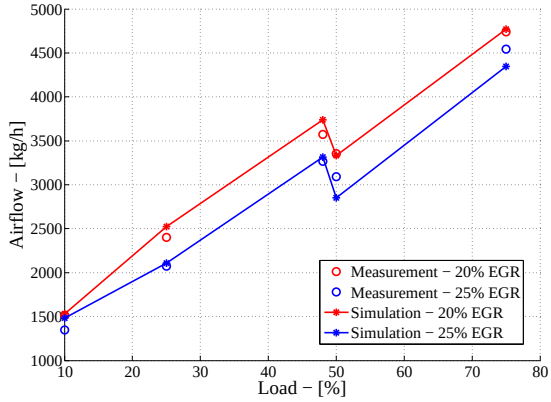

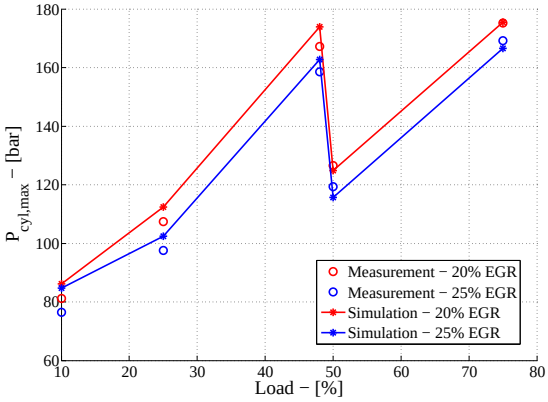

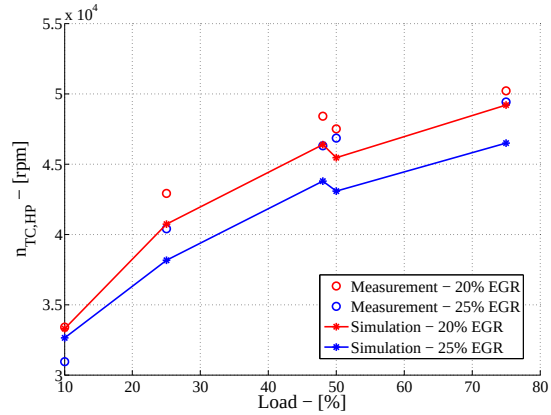

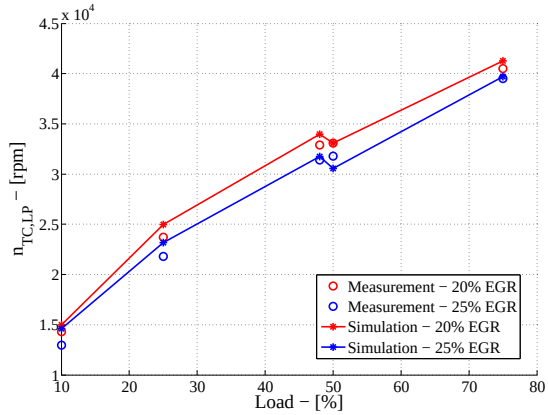

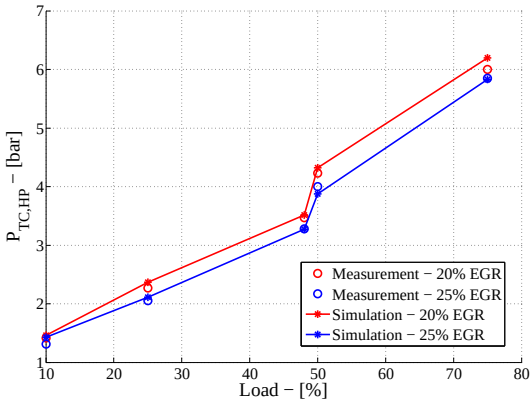
P_TC,HP − [bar]
Load − [%]
Measurement − 20% EGR
Measurement − 25% EGR
Simulation − 20% EGR
Simulation − 25% EGR

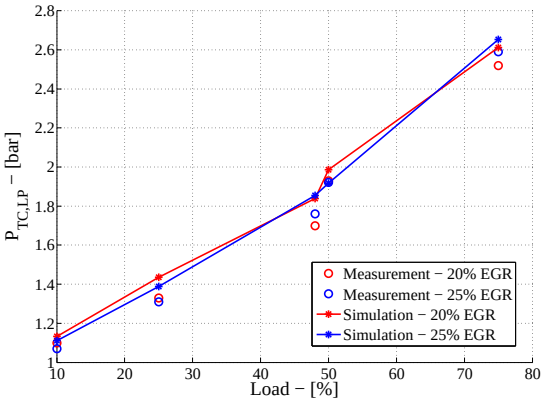
P_TC,LP − [bar]
Load − [%]
Measurement − 20% EGR
Measurement − 25% EGR
Simulation − 20% EGR
Simulation − 25% EGR

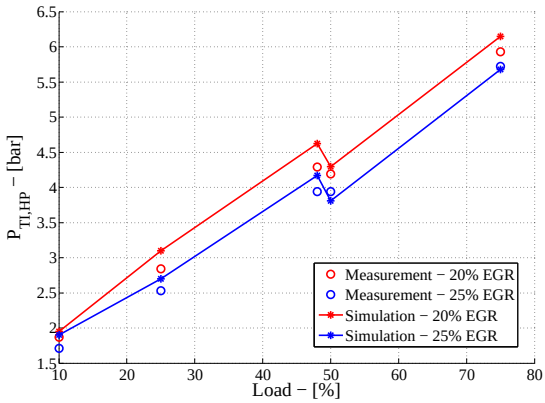
P_TI,HP − [bar]
Load − [%]
Measurement − 20% EGR
Measurement − 25% EGR
Simulation − 20% EGR
Simulation − 25% EGR

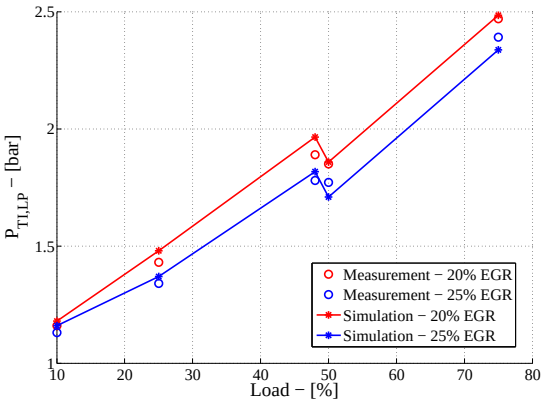
P_TI,LP − [bar]
Load − [%]
Measurement − 20% EGR
Measurement − 25% EGR
Simulation − 20% EGR
Simulation − 25% EGR

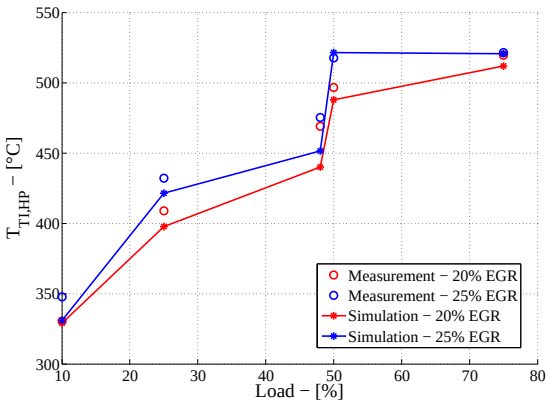
T_TI,HP − [°C]
Load − [%]
Measurement − 20% EGR
Measurement − 25% EGR
Simulation − 20% EGR
Simulation − 25% EGR

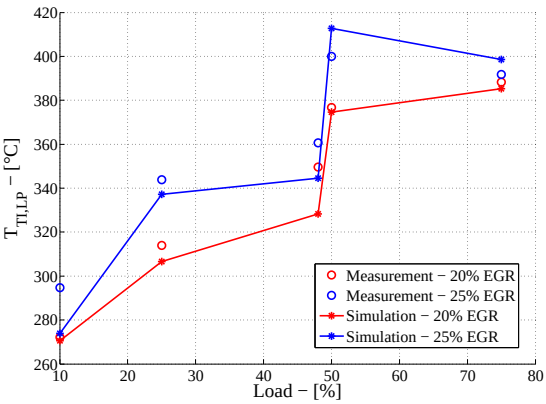
T_TI,LP − [°C]
Load − [%]
Measurement − 20% EGR
Measurement − 25% EGR
Simulation − 20% EGR
Simulation − 25% EGR

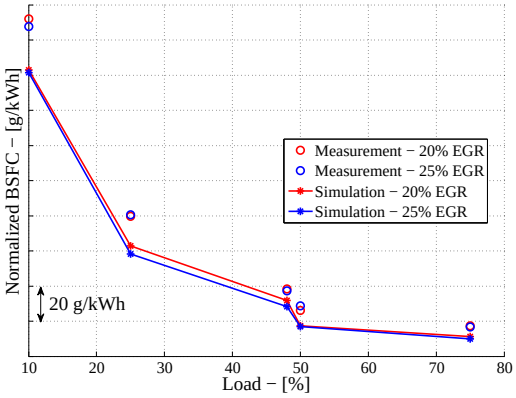
Normalized BSFC − [g/kWh]
Load − [%]
Measurement − 20% EGR
Measurement − 25% EGR
Simulation − 20% EGR
Simulation − 25% EGR
20 g/kWh
10
20
30
40
50
60
70
80

C.2 Optimization Process Results

C.2.1 Semi-Short Route

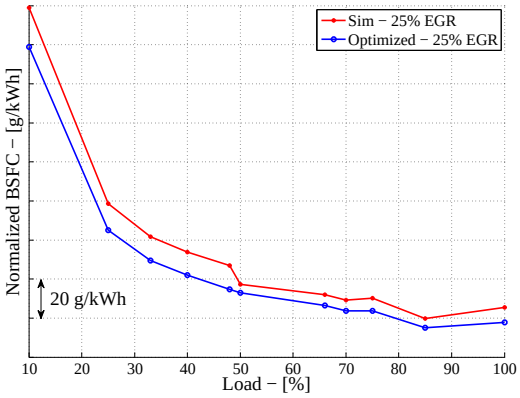

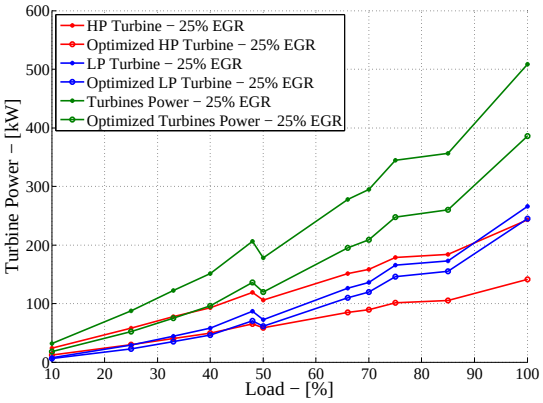

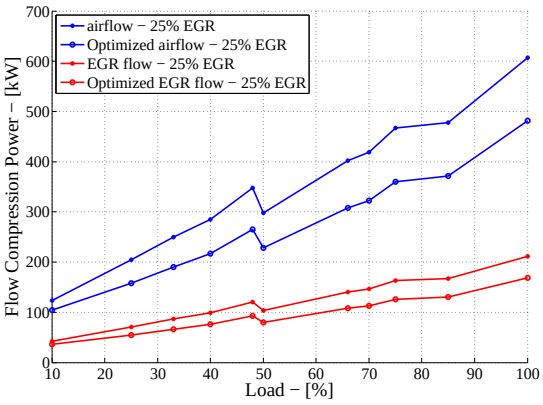

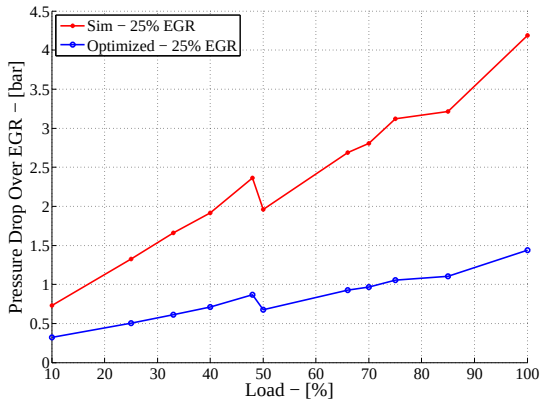

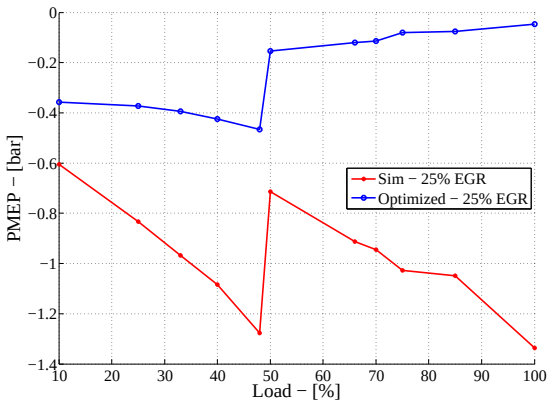

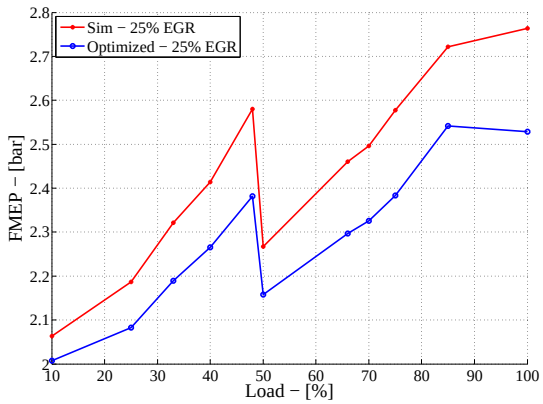

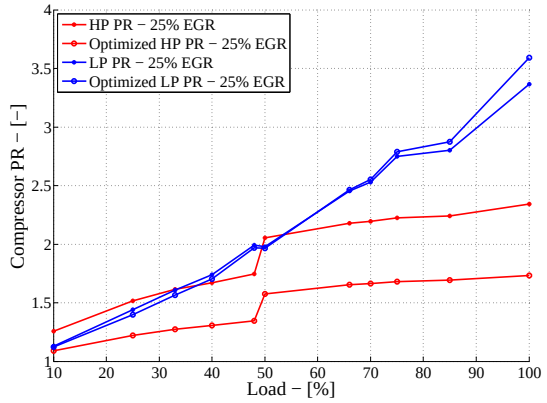
HP PR − 25% EGR
Optimized HP PR − 25% EGR
LP PR − 25% EGR
Optimized LP PR − 25% EGR
Compressor PR − [−]
Load − [%]

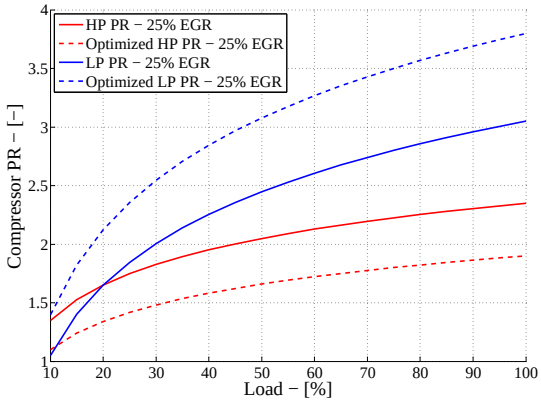
HP PR − 25% EGR
Optimized HP PR − 25% EGR
LP PR − 25% EGR
Optimized LP PR − 25% EGR
Compressor PR − [−]
Load − [%]

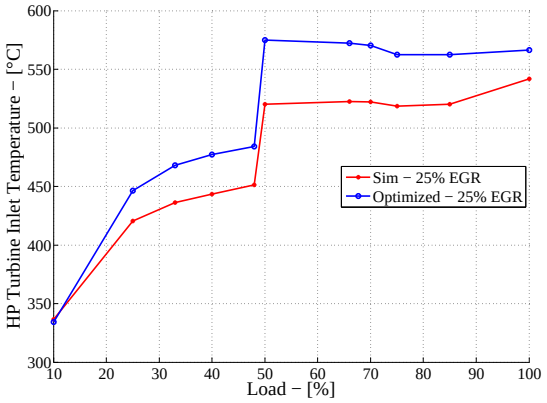
Sim − 25% EGR
Optimized − 25% EGR
HP Turbine Inlet Temperature − [°C]
Load − [%]

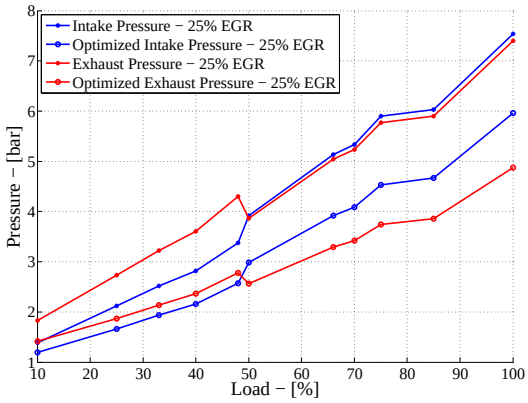
Intake Pressure − 25% EGR
Optimized Intake Pressure − 25% EGR
Exhaust Pressure − 25% EGR
Optimized Exhaust Pressure − 25% EGR
Pressure − [bar]
Load − [%]

C.3 Comparison Between EGR Configurations

C.3.1 No EGR vs. Semi-Short Route

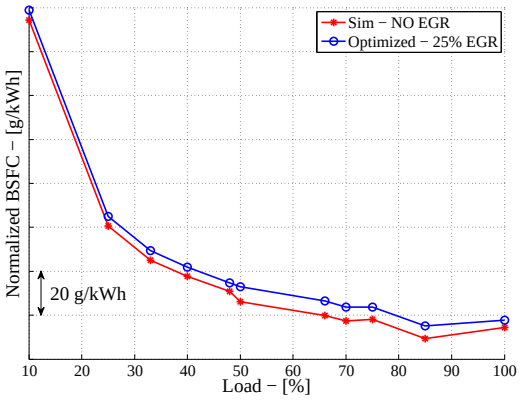

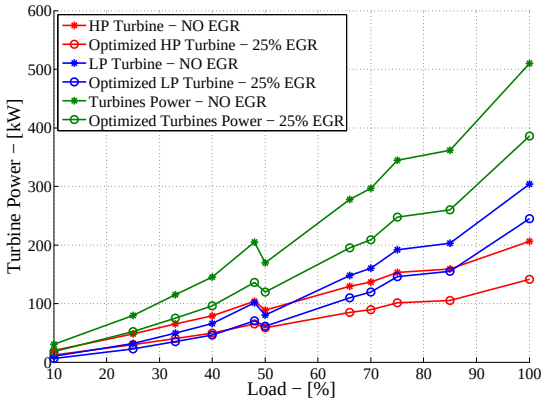

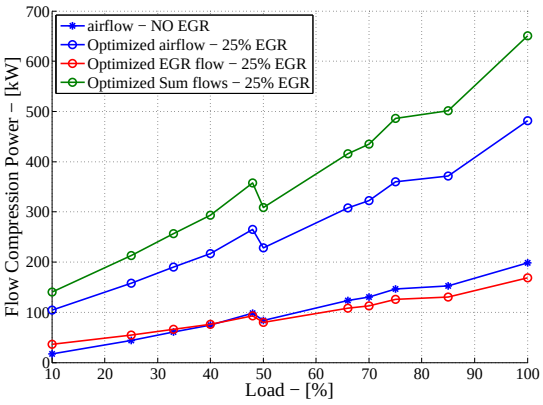

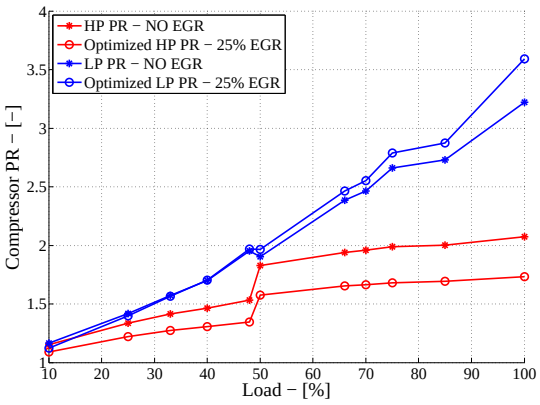

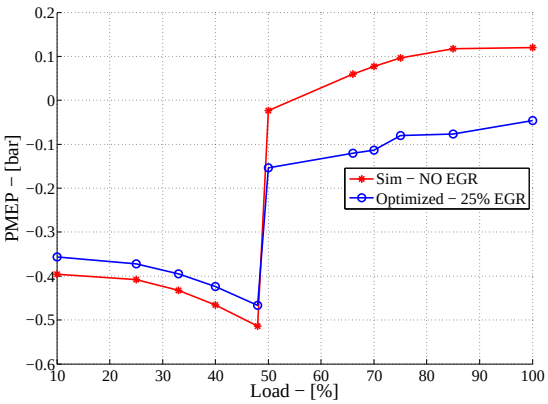

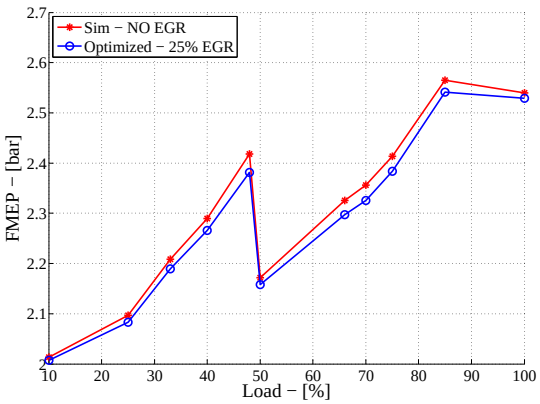

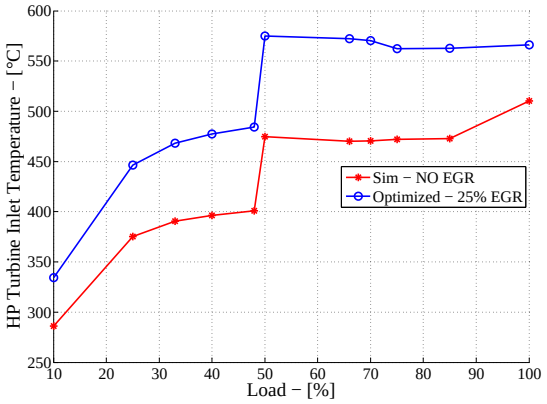

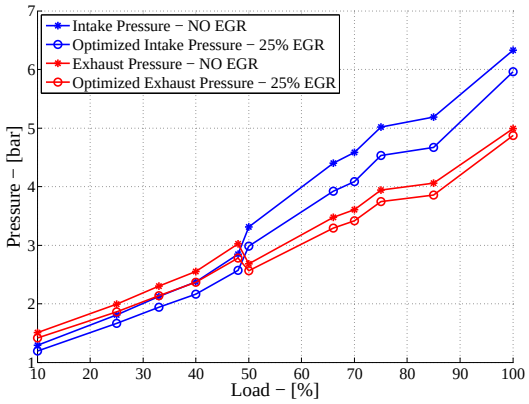

C.3.2 Semi-Short Route vs. 1 Donor Cylinder Semi-Short Route Before Optimization

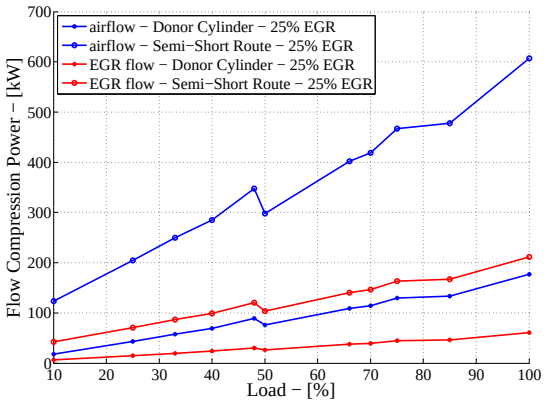

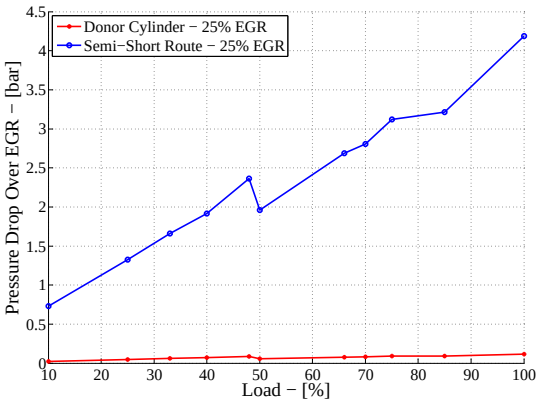

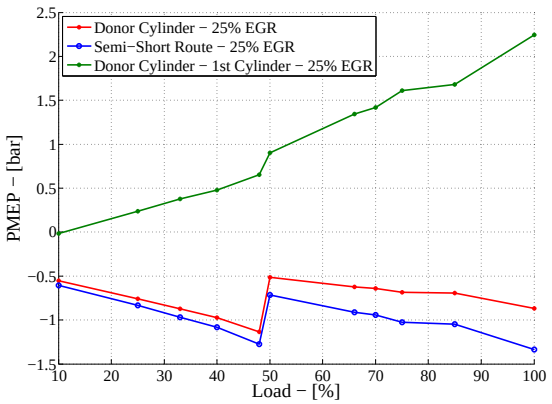

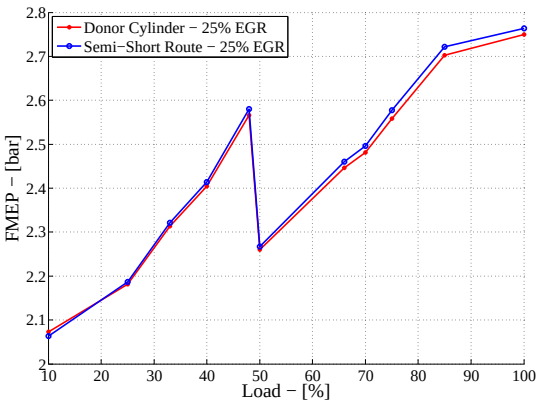

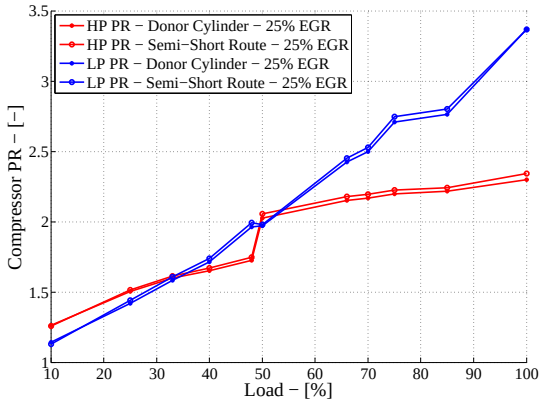
HP PR − Donor Cylinder − 25% EGR
HP PR − Semi−Short Route − 25% EGR
LP PR − Donor Cylinder − 25% EGR
LP PR − Semi−Short Route − 25% EGR
Compressor PR − [−]
Load − [%]

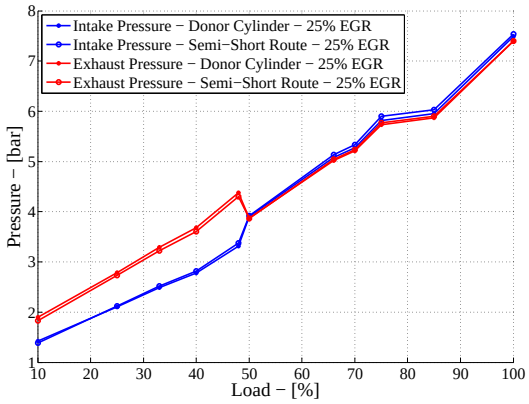
Intake Pressure − Donor Cylinder − 25% EGR
Intake Pressure − Semi−Short Route − 25% EGR
Exhaust Pressure − Donor Cylinder − 25% EGR
Exhaust Pressure − Semi−Short Route − 25% EGR
Pressure − [bar]
Load − [%]

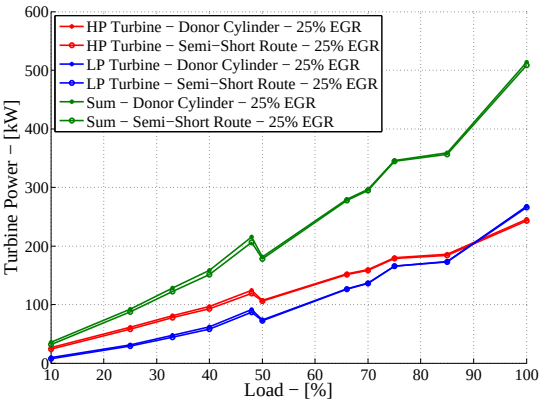
HP Turbine − Donor Cylinder − 25% EGR
HP Turbine − Semi−Short Route − 25% EGR
LP Turbine − Donor Cylinder − 25% EGR
LP Turbine − Semi−Short Route − 25% EGR
Sum − Donor Cylinder − 25% EGR
Sum − Semi−Short Route − 25% EGR
Turbine Power − [kW]
Load − [%]

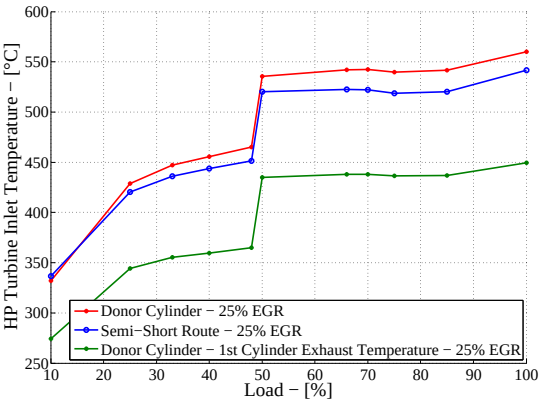
Donor Cylinder − 25% EGR
Semi−Short Route − 25% EGR
Donor Cylinder − 1st Cylinder Exhaust Temperature − 25% EGR
HP Turbine Inlet Temperature − [°C]
Load − [%]

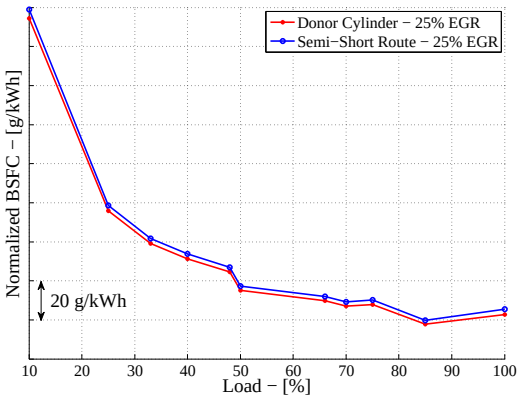
Donor Cylinder − 25% EGR
Semi−Short Route − 25% EGR
Normalized BSFC − [g/kWh]
20 g/kWh
Load − [%]

C.3.3 Semi-Short Route vs. 1 Donor Cylinder Semi-Short Route After Optimization

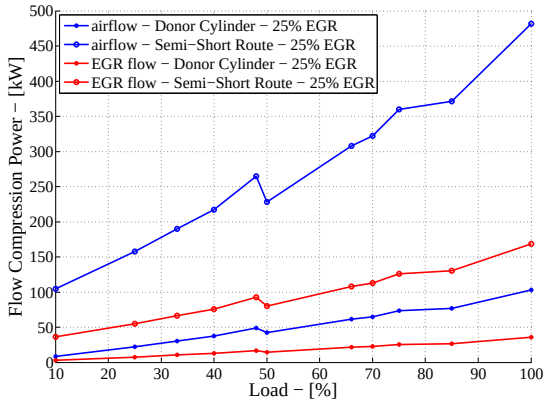

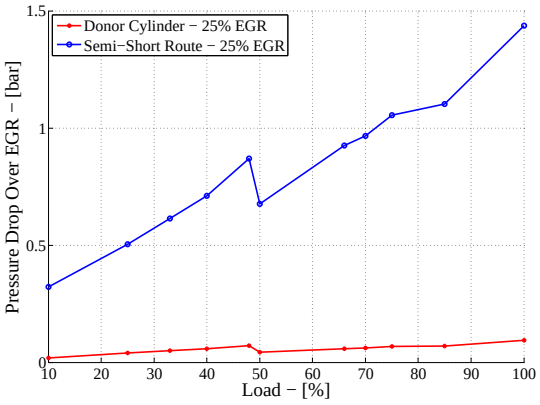

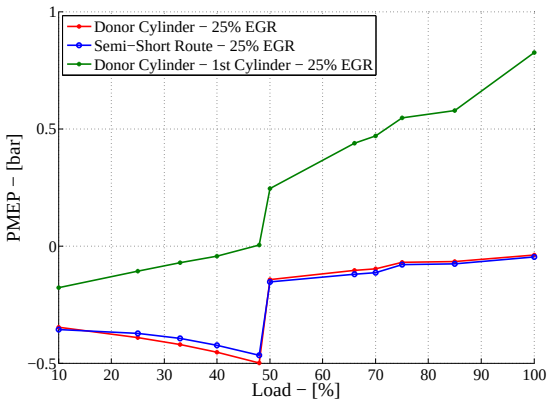

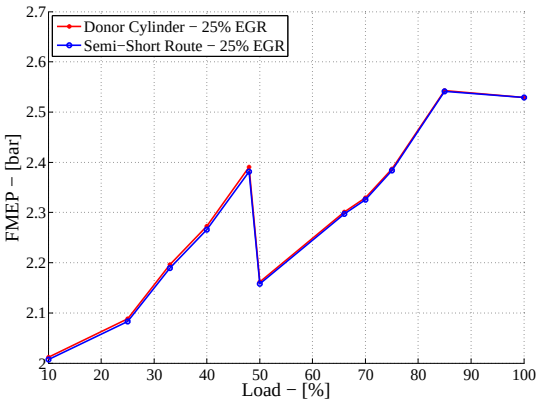

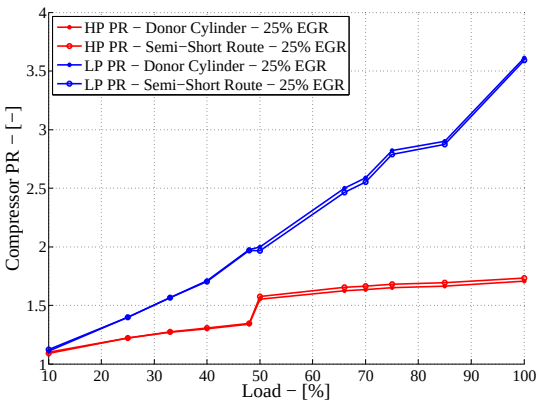

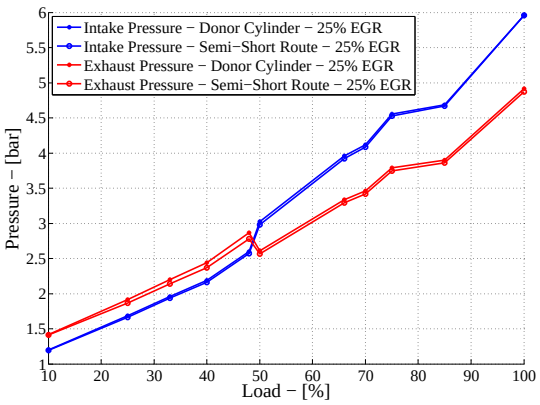

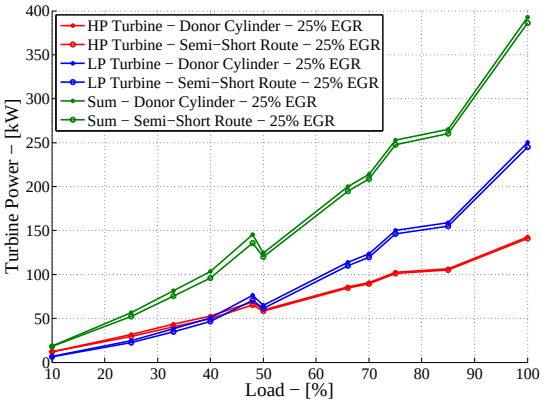

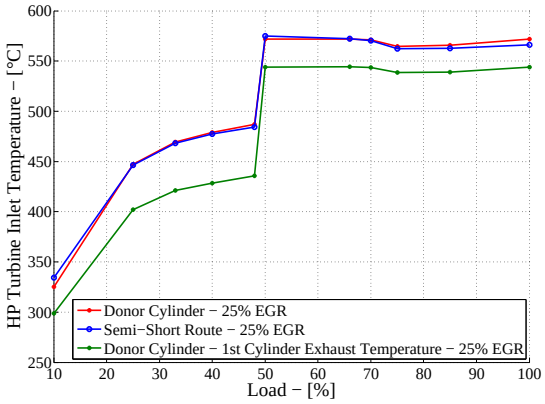

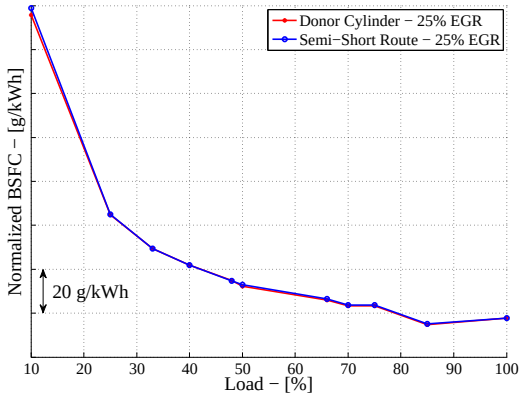

C.3.4 Semi-Short Route vs. 1 Donor Cylinder Semi-Short Route M80 Cam Before Optimization

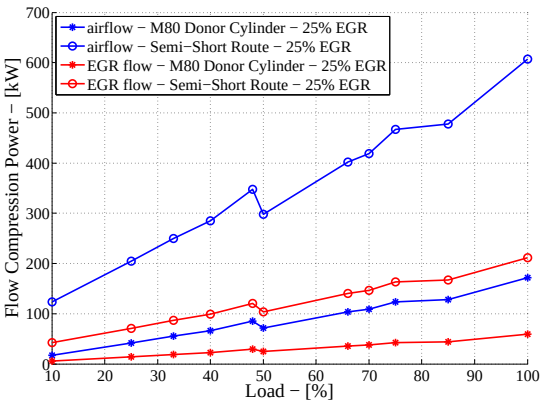

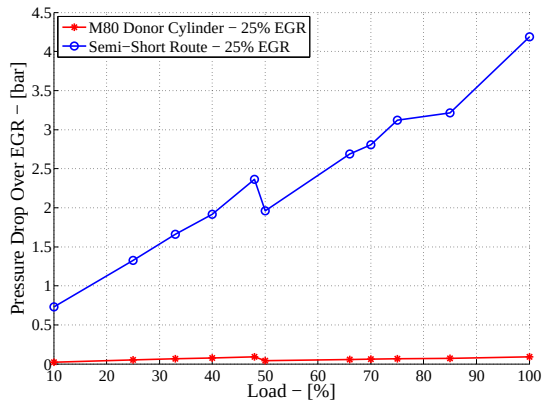

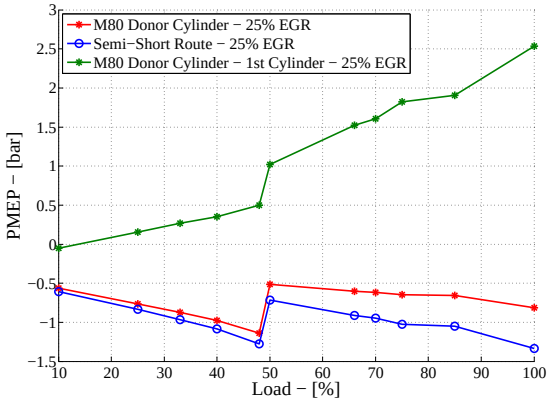
M80 Donor Cylinder − 25% EGR
Semi−Short Route − 25% EGR
M80 Donor Cylinder − 1st Cylinder − 25% EGR
PMEP − [bar]
Load − [%]

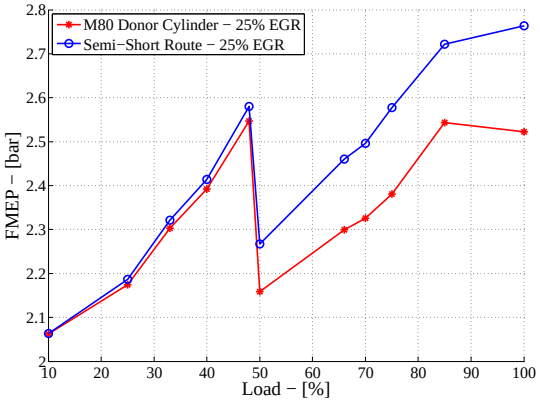
M80 Donor Cylinder − 25% EGR
Semi−Short Route − 25% EGR
FMEP − [bar]
Load − [%]

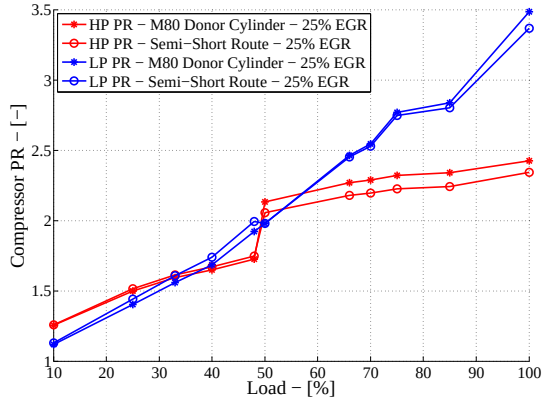
HP PR − M80 Donor Cylinder − 25% EGR
HP PR − Semi−Short Route − 25% EGR
LP PR − M80 Donor Cylinder − 25% EGR
LP PR − Semi−Short Route − 25% EGR
Compressor PR − [−]
Load − [%]

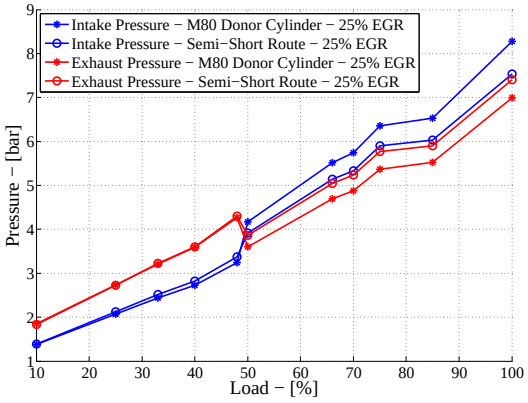
Intake Pressure − M80 Donor Cylinder − 25% EGR
Intake Pressure − Semi−Short Route − 25% EGR
Exhaust Pressure − M80 Donor Cylinder − 25% EGR
Exhaust Pressure − Semi−Short Route − 25% EGR
Pressure − [bar]
Load − [%]

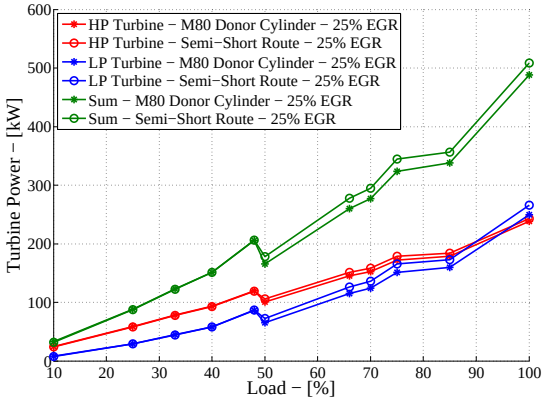
HP Turbine − M80 Donor Cylinder − 25% EGR
HP Turbine − Semi−Short Route − 25% EGR
LP Turbine − M80 Donor Cylinder − 25% EGR
LP Turbine − Semi−Short Route − 25% EGR
Sum − M80 Donor Cylinder − 25% EGR
Sum − Semi−Short Route − 25% EGR
Turbine Power − [kW]
Load − [%]

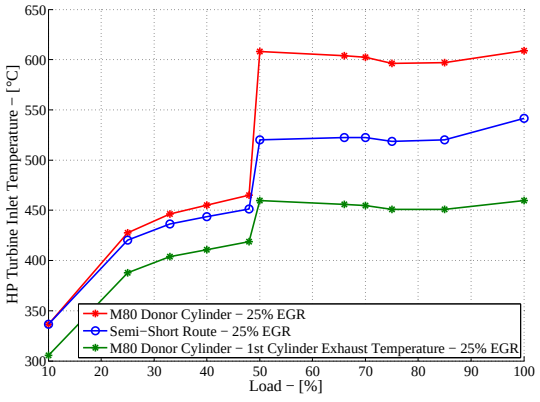
M80 Donor Cylinder − 25% EGR
Semi−Short Route − 25% EGR
M80 Donor Cylinder − 1st Cylinder Exhaust Temperature − 25% EGR
HP Turbine Inlet Temperature − [°C]
Load − [%]

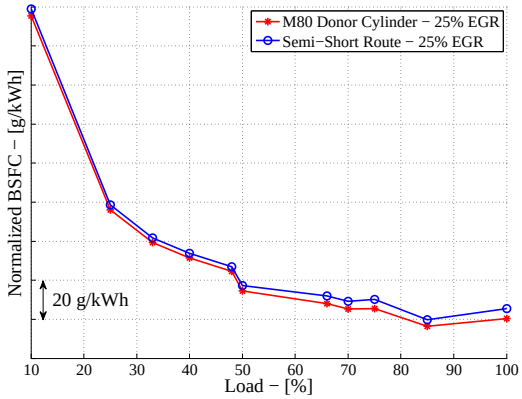

C.3.5 1 Donor Cylinder Semi-Short Route M73 Cam vs. M80 Cam Before Optimization

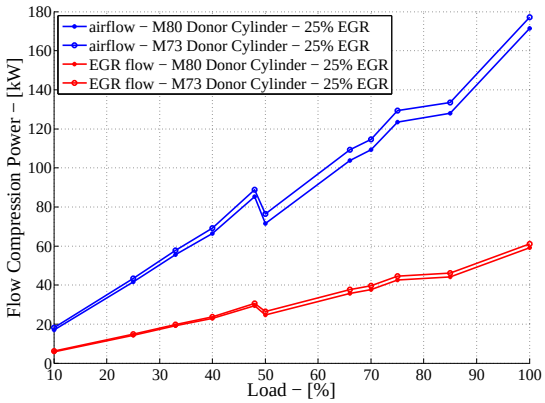

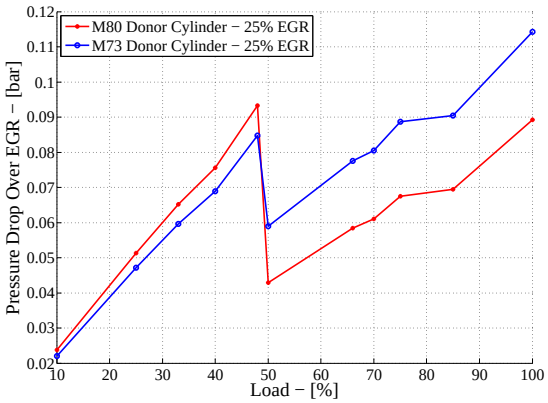

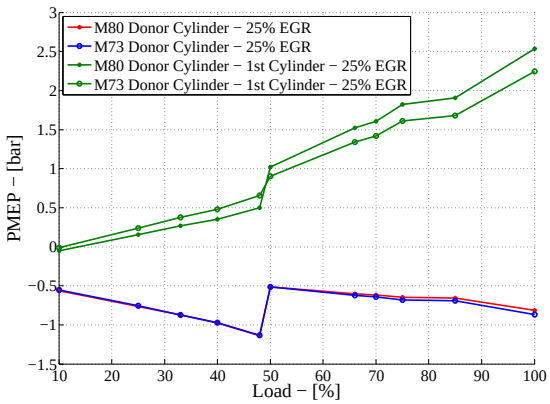

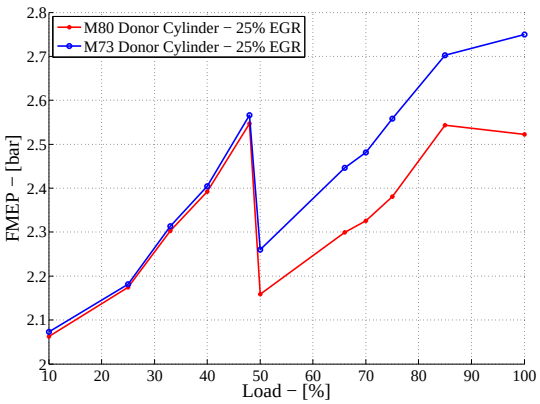

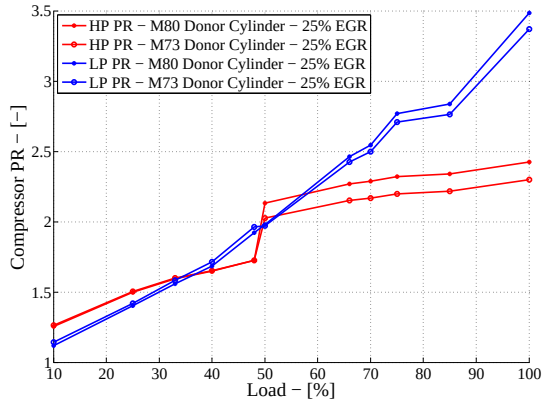
HP PR − M80 Donor Cylinder − 25% EGR
HP PR − M73 Donor Cylinder − 25% EGR
LP PR − M80 Donor Cylinder − 25% EGR
LP PR − M73 Donor Cylinder − 25% EGR
Compressor PR − [−]
Load − [%]

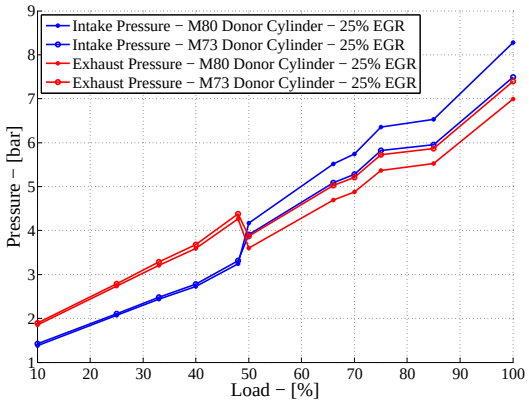
Intake Pressure − M80 Donor Cylinder − 25% EGR
Intake Pressure − M73 Donor Cylinder − 25% EGR
Exhaust Pressure − M80 Donor Cylinder − 25% EGR
Exhaust Pressure − M73 Donor Cylinder − 25% EGR
Pressure − [bar]
Load − [%]

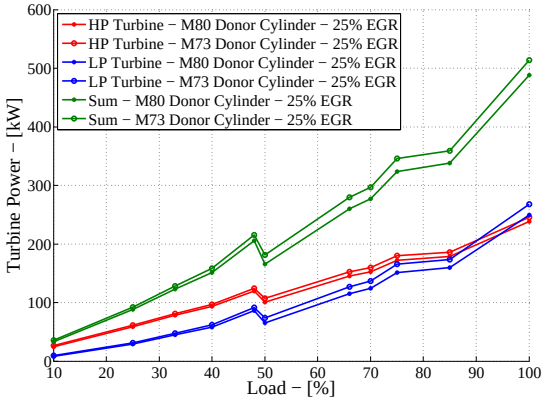
HP Turbine − M80 Donor Cylinder − 25% EGR
HP Turbine − M73 Donor Cylinder − 25% EGR
LP Turbine − M80 Donor Cylinder − 25% EGR
LP Turbine − M73 Donor Cylinder − 25% EGR
Sum − M80 Donor Cylinder − 25% EGR
Sum − M73 Donor Cylinder − 25% EGR
Turbine Power − [kW]
Load − [%]

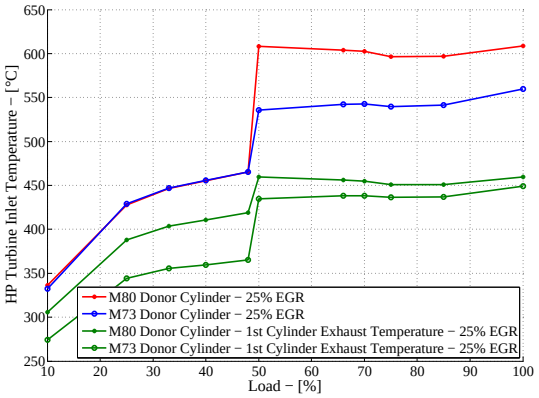
M80 Donor Cylinder − 25% EGR
M73 Donor Cylinder − 25% EGR
M80 Donor Cylinder − 1st Cylinder Exhaust Temperature − 25% EGR
M73 Donor Cylinder − 1st Cylinder Exhaust Temperature − 25% EGR
HP Turbine Inlet Temperature − [°C]
Load − [%]

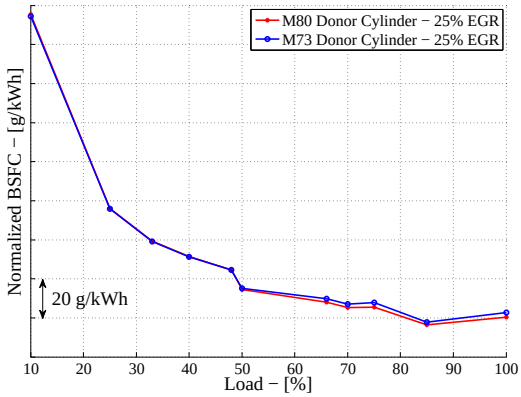
M80 Donor Cylinder − 25% EGR
M73 Donor Cylinder − 25% EGR
Normalized BSFC − [g/kWh]
20 g/kWh
Load − [%]

C.3.6 Semi-Short Route vs. 1 Donor Cylinder Semi-Short Route M80 Cam After Optimization

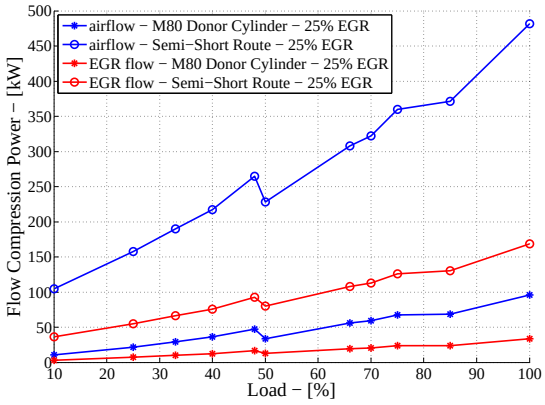

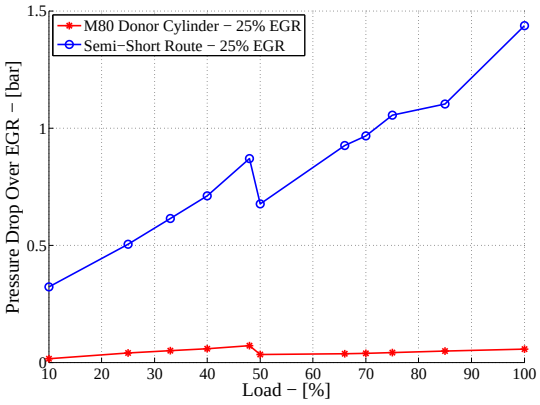

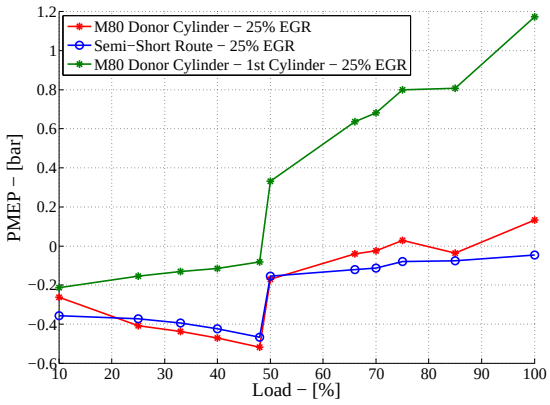

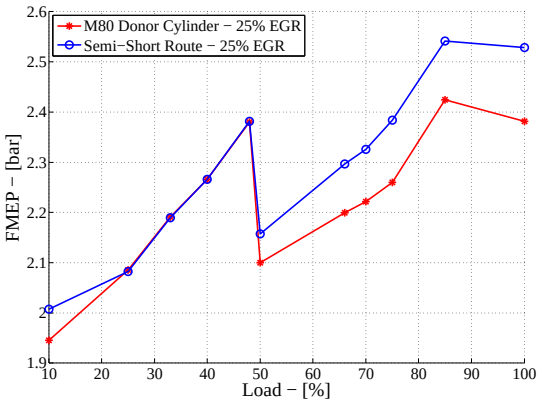

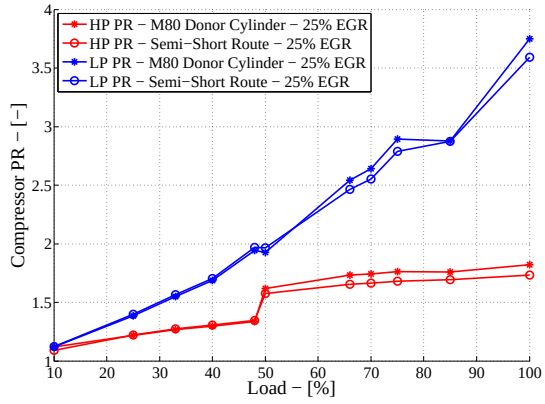

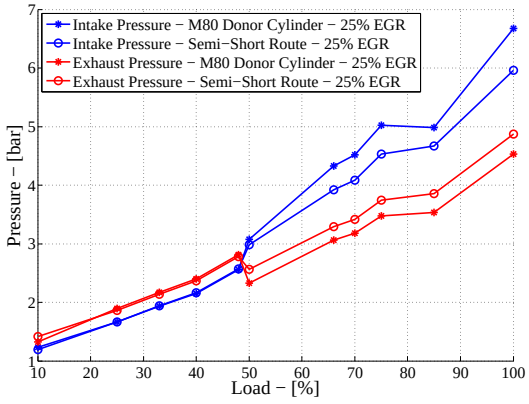

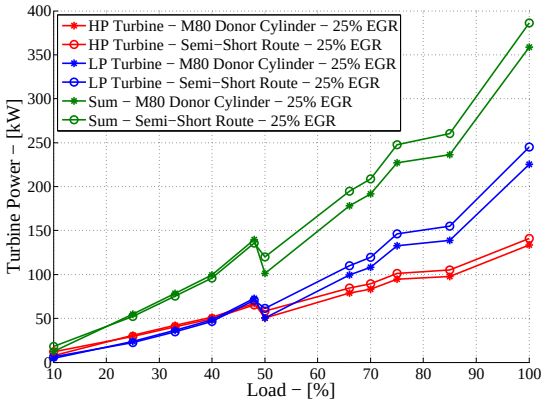

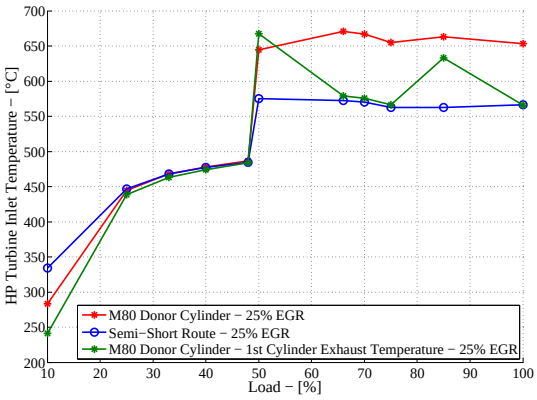

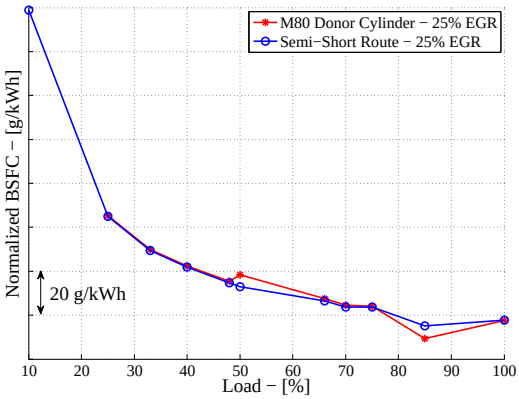

C.3.7 1 Donor Cylinder Semi-Short Route M74 Cam vs. M80 Cam After Optimization

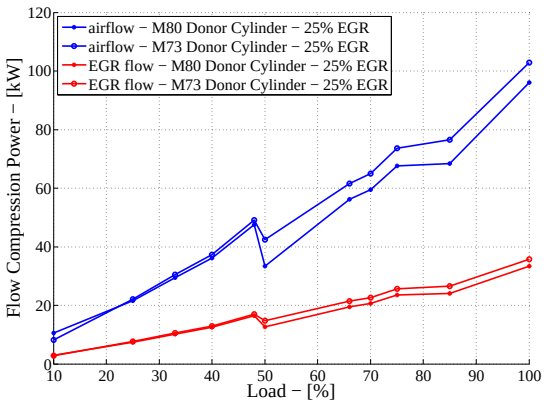

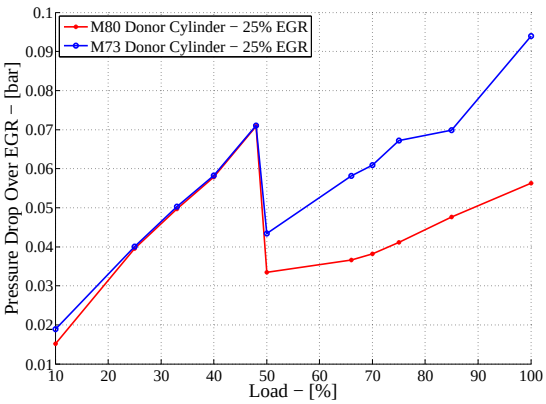

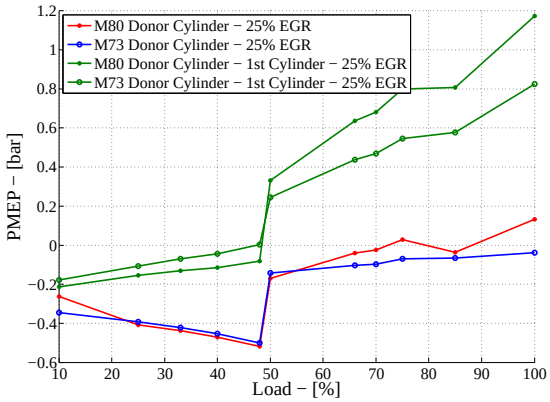
M80 Donor Cylinder − 25% EGR
M73 Donor Cylinder − 25% EGR
M80 Donor Cylinder − 1st Cylinder − 25% EGR
M73 Donor Cylinder − 1st Cylinder − 25% EGR
PMEP − [bar]
Load − [%]

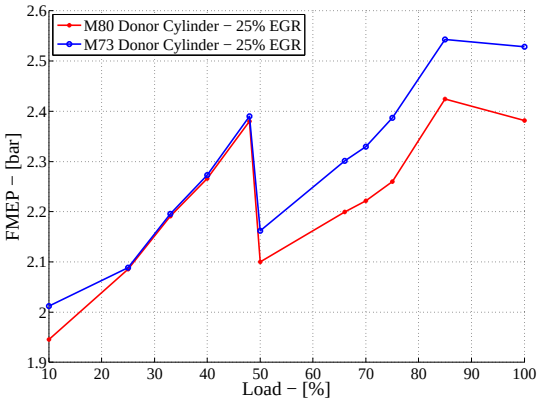
M80 Donor Cylinder − 25% EGR
M73 Donor Cylinder − 25% EGR
FMEP − [bar]
Load − [%]

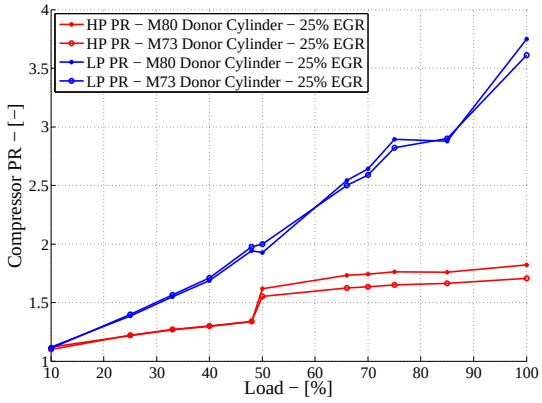
HP PR − M80 Donor Cylinder − 25% EGR
HP PR − M73 Donor Cylinder − 25% EGR
LP PR − M80 Donor Cylinder − 25% EGR
LP PR − M73 Donor Cylinder − 25% EGR
Compressor PR − [−]
Load − [%]

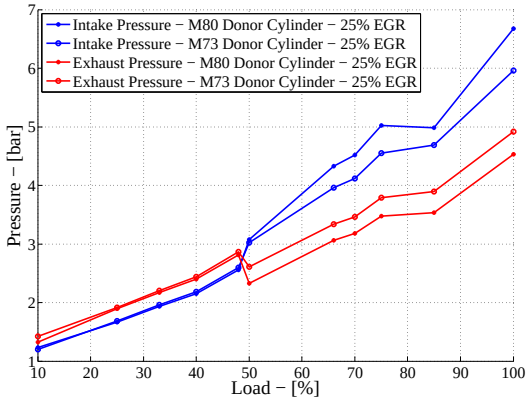
Intake Pressure − M80 Donor Cylinder − 25% EGR
Intake Pressure − M73 Donor Cylinder − 25% EGR
Exhaust Pressure − M80 Donor Cylinder − 25% EGR
Exhaust Pressure − M73 Donor Cylinder − 25% EGR
Pressure − [bar]
Load − [%]

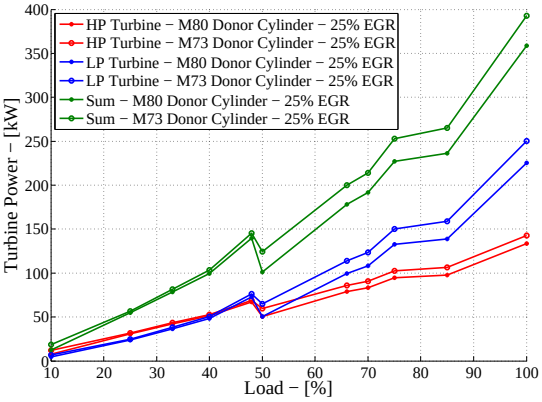
HP Turbine − M80 Donor Cylinder − 25% EGR
HP Turbine − M73 Donor Cylinder − 25% EGR
LP Turbine − M80 Donor Cylinder − 25% EGR
LP Turbine − M73 Donor Cylinder − 25% EGR
Sum − M80 Donor Cylinder − 25% EGR
Sum − M73 Donor Cylinder − 25% EGR
Turbine Power − [kW]
Load − [%]

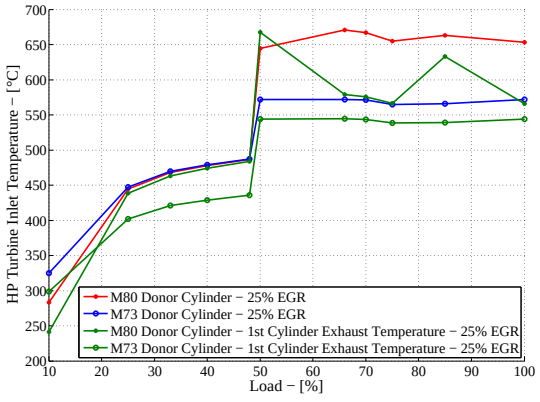
M80 Donor Cylinder − 25% EGR
M73 Donor Cylinder − 25% EGR
M80 Donor Cylinder − 1st Cylinder Exhaust Temperature − 25% EGR
M73 Donor Cylinder − 1st Cylinder Exhaust Temperature − 25% EGR
HP Turbine Inlet Temperature − [°C]
Load − [%]

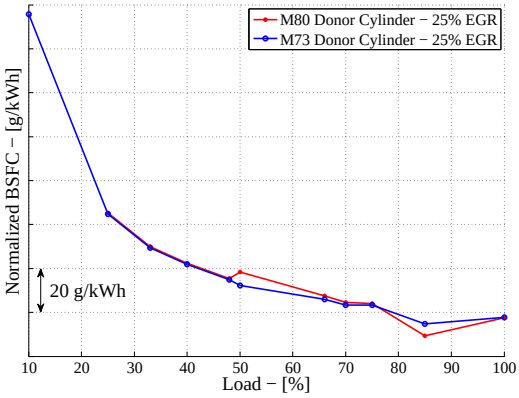

C.3.8 1 Donor Cylinder Semi-Short Route vs. 2 Donor Cylinders Short Route Before Optimization

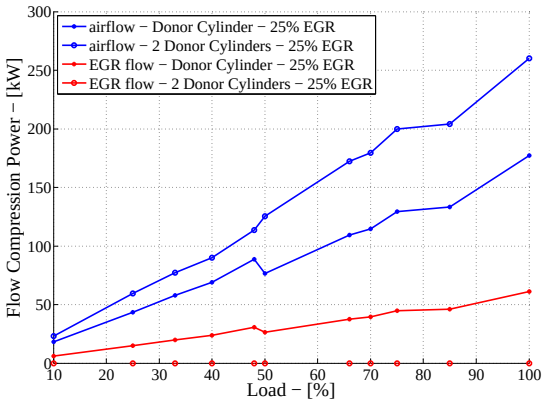

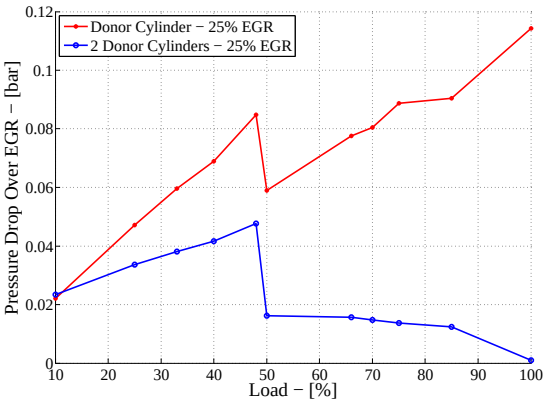

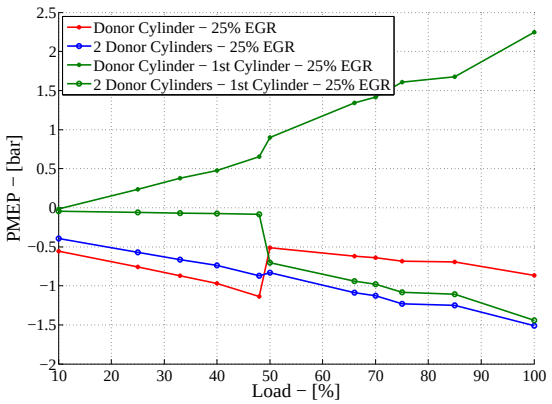

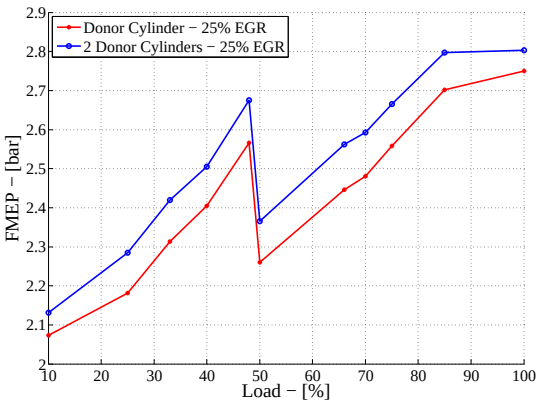

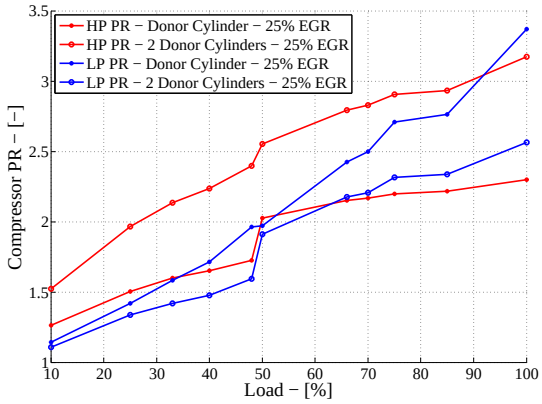
HP PR − Donor Cylinder − 25% EGR
HP PR − 2 Donor Cylinders − 25% EGR
LP PR − Donor Cylinder − 25% EGR
LP PR − 2 Donor Cylinders − 25% EGR
Compressor PR − [−]
Load − [%]

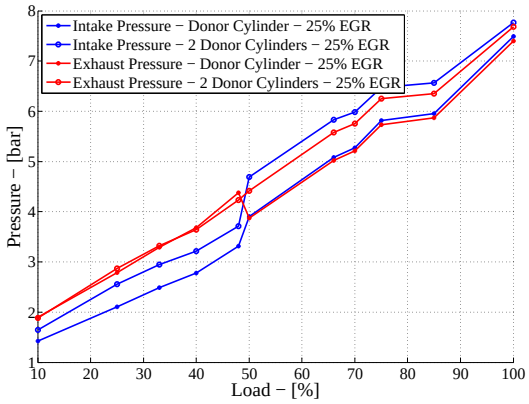
Intake Pressure − Donor Cylinder − 25% EGR
Intake Pressure − 2 Donor Cylinders − 25% EGR
Exhaust Pressure − Donor Cylinder − 25% EGR
Exhaust Pressure − 2 Donor Cylinders − 25% EGR
Pressure − [bar]
Load − [%]

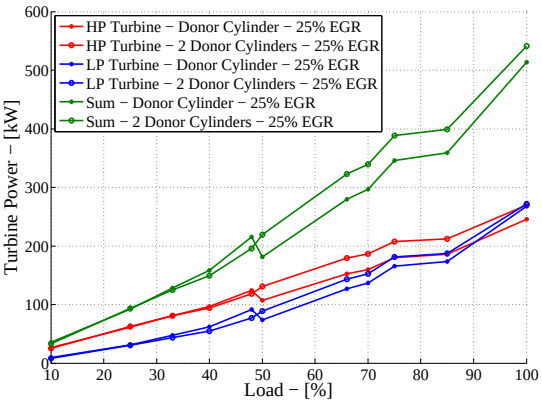
HP Turbine − Donor Cylinder − 25% EGR
HP Turbine − 2 Donor Cylinders − 25% EGR
LP Turbine − Donor Cylinder − 25% EGR
LP Turbine − 2 Donor Cylinders − 25% EGR
Sum − Donor Cylinder − 25% EGR
Sum − 2 Donor Cylinders − 25% EGR
Turbine Power − [kW]
Load − [%]

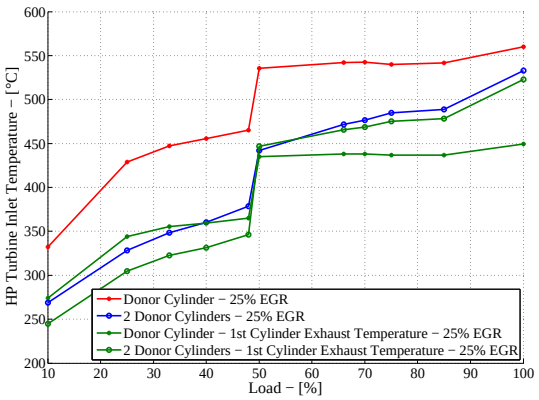
Donor Cylinder − 25% EGR
2 Donor Cylinders − 25% EGR
Donor Cylinder − 1st Cylinder Exhaust Temperature − 25% EGR
2 Donor Cylinders − 1st Cylinder Exhaust Temperature − 25% EGR
HP Turbine Inlet Temperature − [°C]
Load − [%]

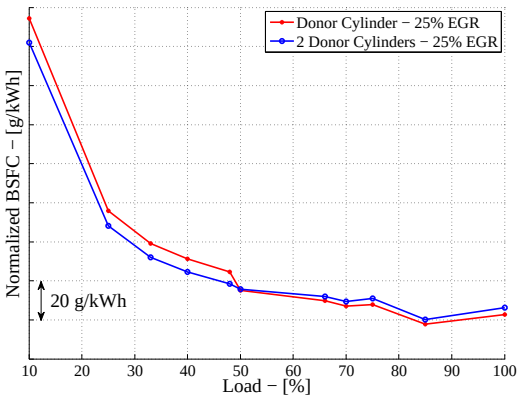
Donor Cylinder − 25% EGR
2 Donor Cylinders − 25% EGR
Normalized BSFC − [g/kWh]
20 g/kWh
Load − [%]

C.3.9 1 Donor Cylinder Semi-Short Route vs. 2 Donor Cylinders Short Route After Optimization

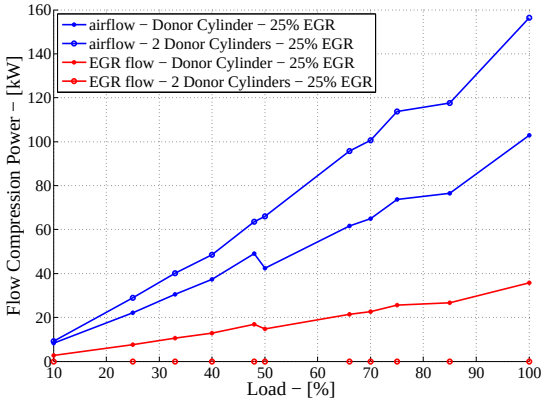

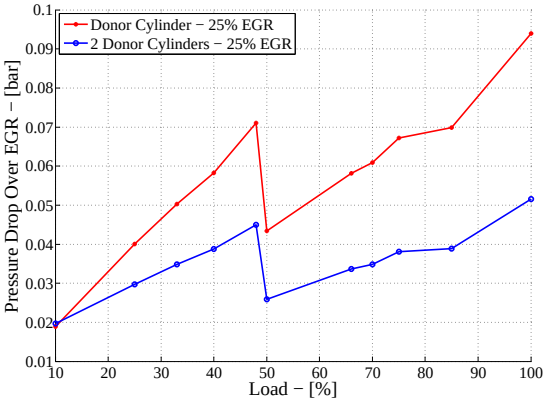

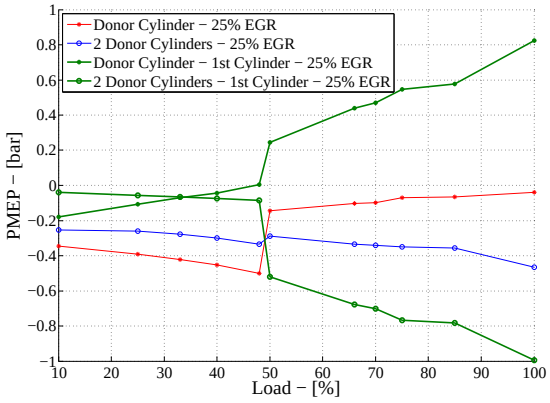

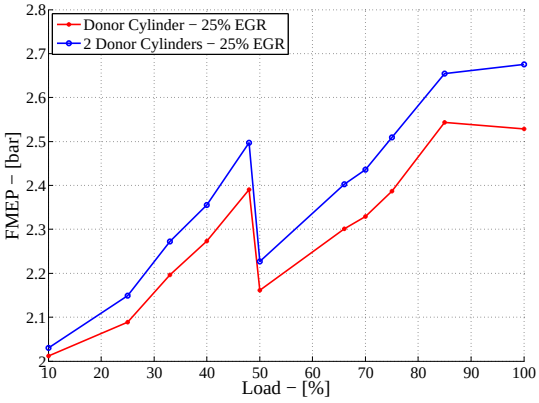

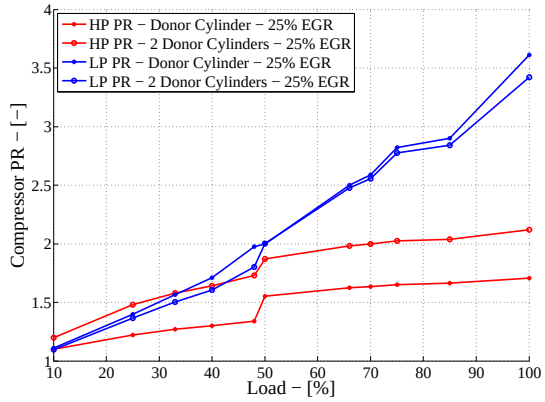

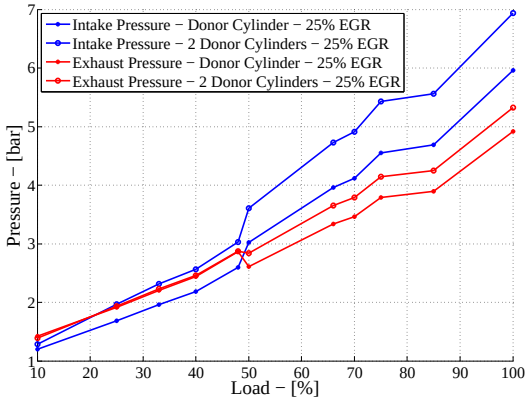

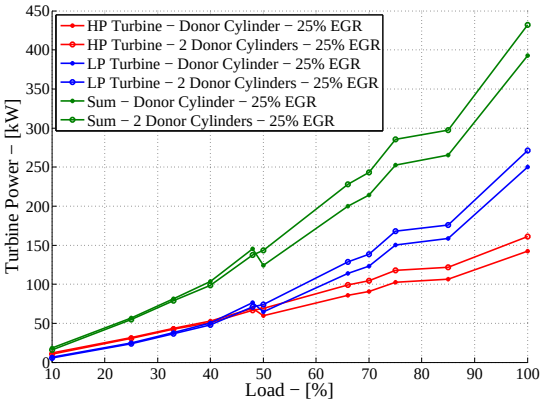

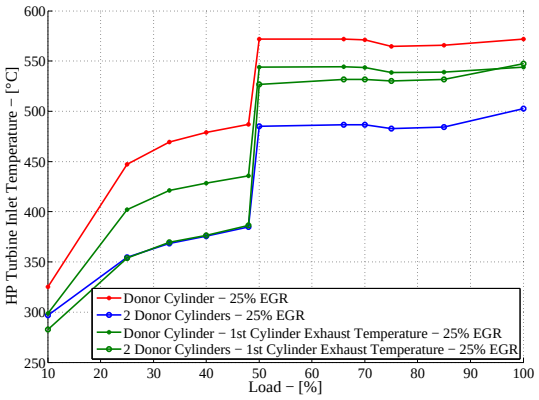

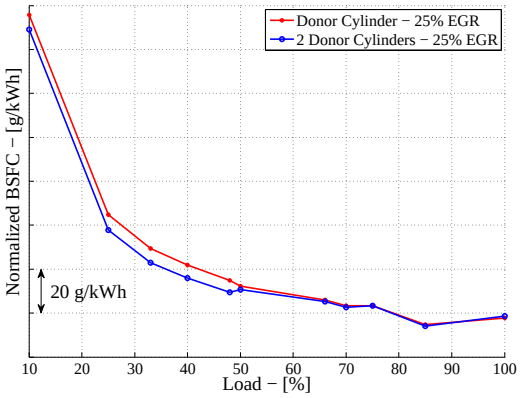

C.3.10 No EGR vs. Semi-Short Route vs. 1 Donor Cylinder Semi-Short Route M73 Cam vs. M80 Cam vs. 2 Donor Cylinders Short Route After Optimization

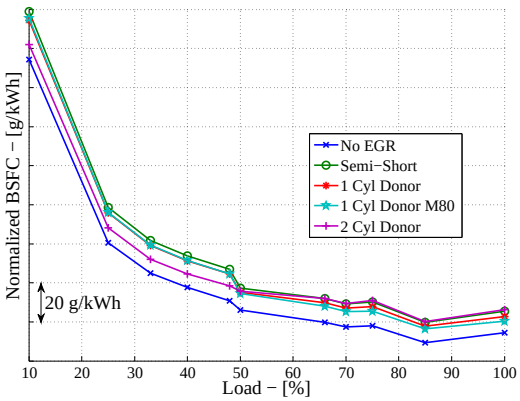

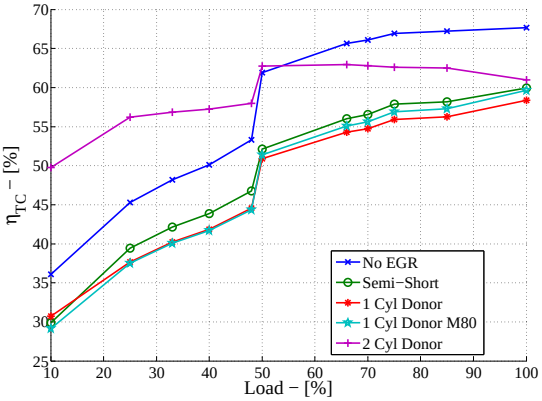

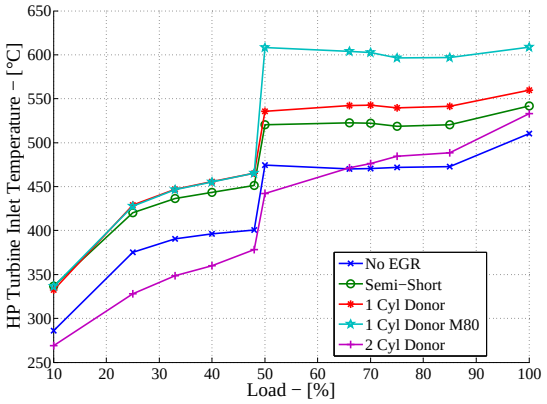

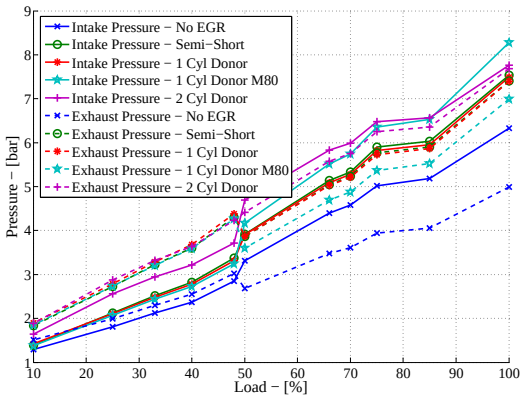

C.3.11 EGR Blower Short Route Externally Driven vs. Crankshaft Driven After Optimization

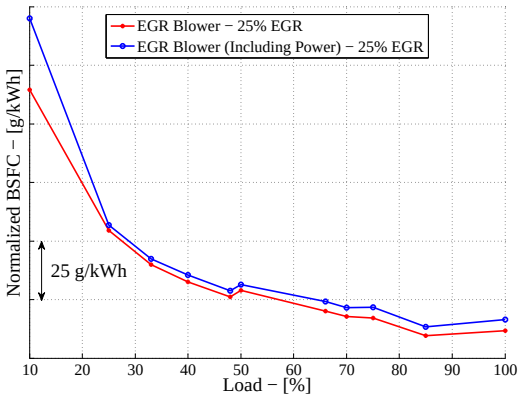

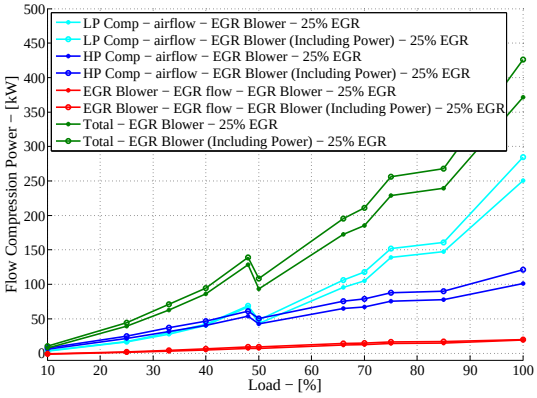

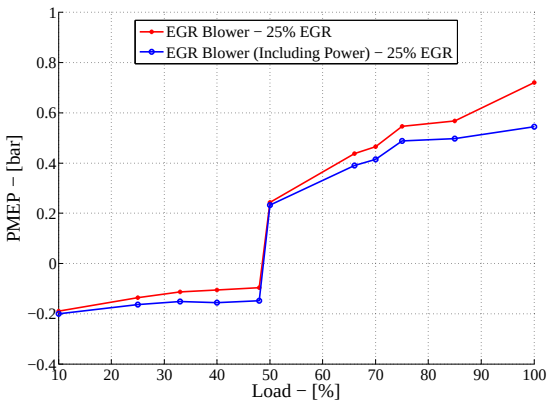

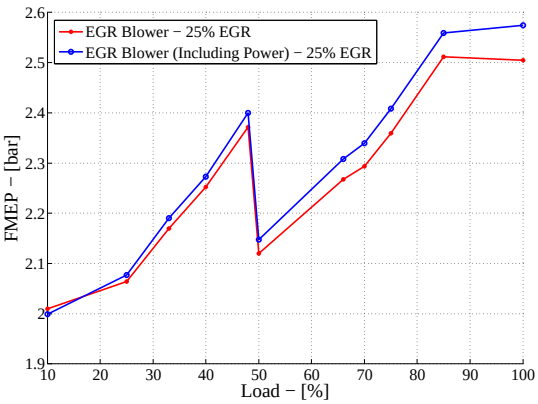

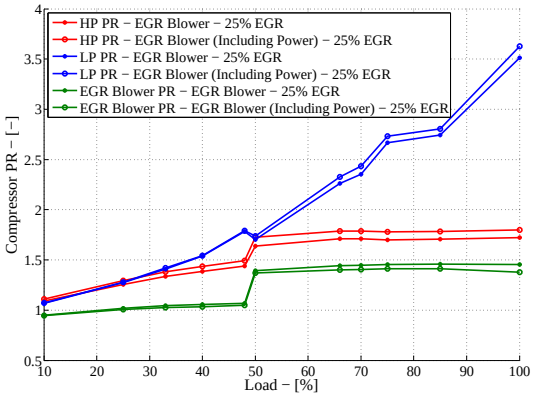
HP PR − EGR Blower − 25% EGR
HP PR − EGR Blower (Including Power) − 25% EGR
LP PR − EGR Blower − 25% EGR
LP PR − EGR Blower (Including Power) − 25% EGR
EGR Blower PR − EGR Blower − 25% EGR
EGR Blower PR − EGR Blower (Including Power) − 25% EGR
Compressor PR − [−]
Load − [%]

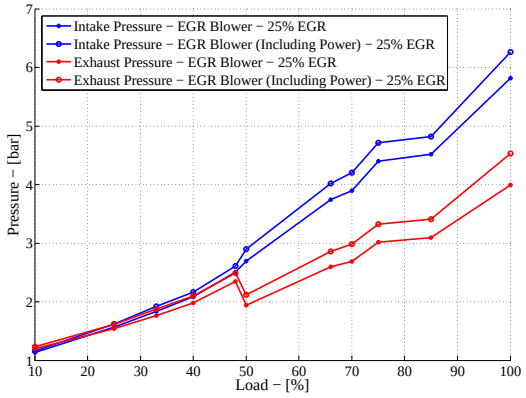
Intake Pressure − EGR Blower − 25% EGR
Intake Pressure − EGR Blower (Including Power) − 25% EGR
Exhaust Pressure − EGR Blower − 25% EGR
Exhaust Pressure − EGR Blower (Including Power) − 25% EGR
Pressure − [bar]
Load − [%]

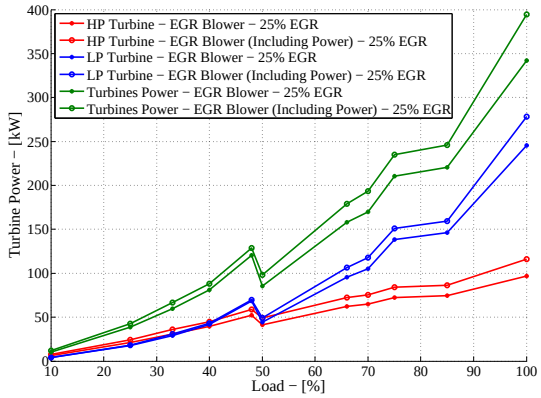
HP Turbine − EGR Blower − 25% EGR
HP Turbine − EGR Blower (Including Power) − 25% EGR
LP Turbine − EGR Blower − 25% EGR
LP Turbine − EGR Blower (Including Power) − 25% EGR
Turbines Power − EGR Blower − 25% EGR
Turbines Power − EGR Blower (Including Power) − 25% EGR
Turbine Power − [kW]
Load − [%]

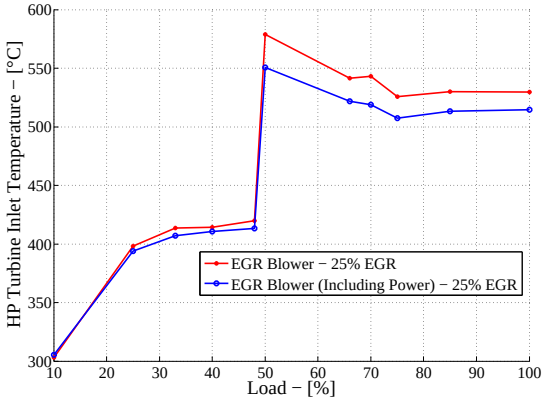
EGR Blower − 25% EGR
EGR Blower (Including Power) − 25% EGR
HP Turbine Inlet Temperature − [°C]
Load − [%]

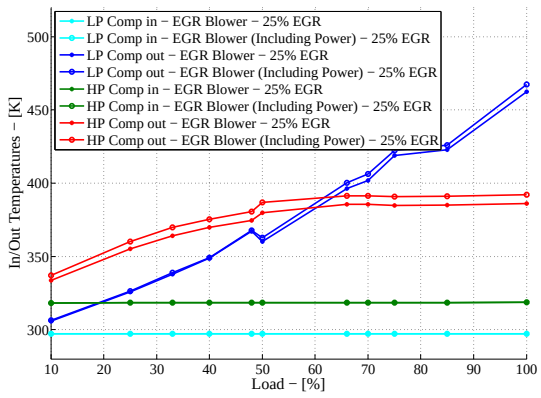
LP Comp in − EGR Blower − 25% EGR
LP Comp in − EGR Blower (Including Power) − 25% EGR
LP Comp out − EGR Blower − 25% EGR
LP Comp out − EGR Blower (Including Power) − 25% EGR
HP Comp in − EGR Blower − 25% EGR
HP Comp in − EGR Blower (Including Power) − 25% EGR
HP Comp out − EGR Blower − 25% EGR
HP Comp out − EGR Blower (Including Power) − 25% EGR
In/Out Temperatures − [K]
Load − [%]

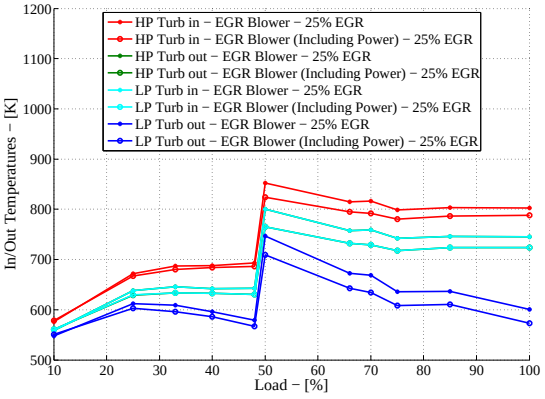
HP Turb in − EGR Blower − 25% EGR
HP Turb in − EGR Blower (Including Power) − 25% EGR
HP Turb out − EGR Blower − 25% EGR
HP Turb out − EGR Blower (Including Power) − 25% EGR
LP Turb in − EGR Blower − 25% EGR
LP Turb in − EGR Blower (Including Power) − 25% EGR
LP Turb out − EGR Blower − 25% EGR
LP Turb out − EGR Blower (Including Power) − 25% EGR
In/Out Temperatures − [K]
Load − [%]

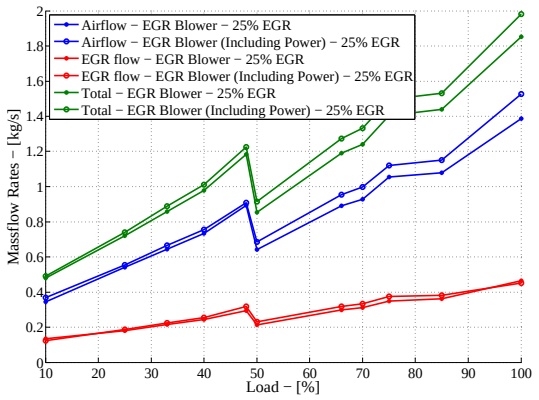

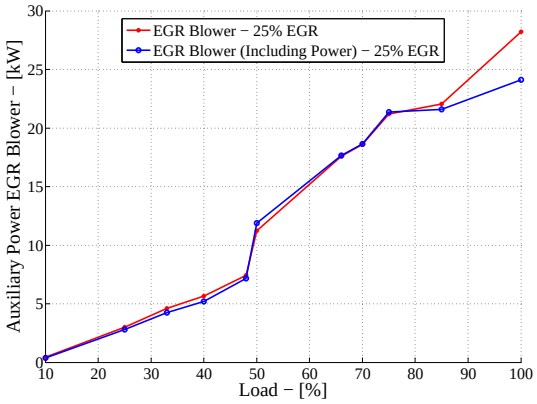

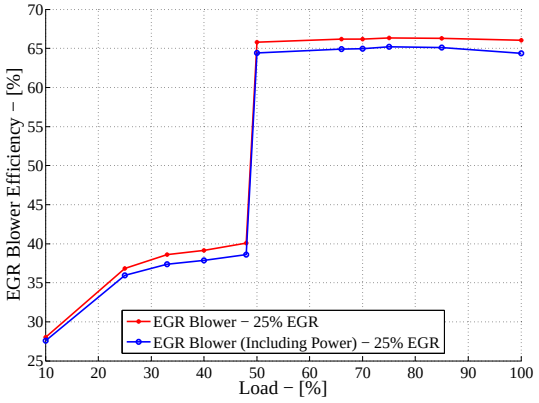

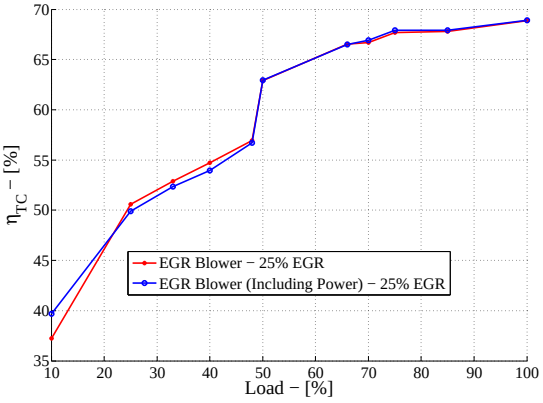

C.3.12 No EGR vs. Semi-Short Route vs. 1 Donor Cylinder Semi-Short Route M73 Cam vs. M80 Cam vs. 2 Donor Cylinders Short Route vs. EGR Blower Short Route Externally Driven vs. Crankshaft Driven After Optimization

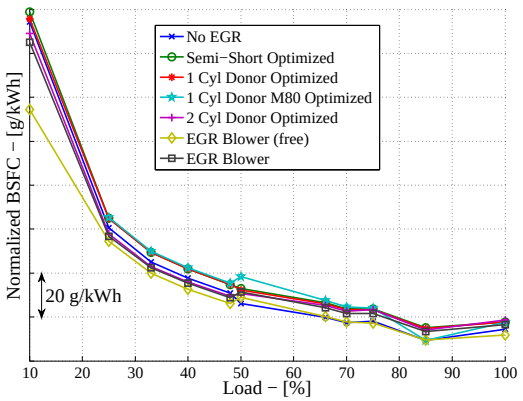

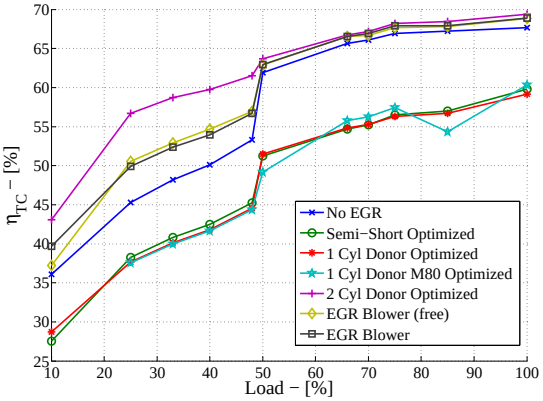

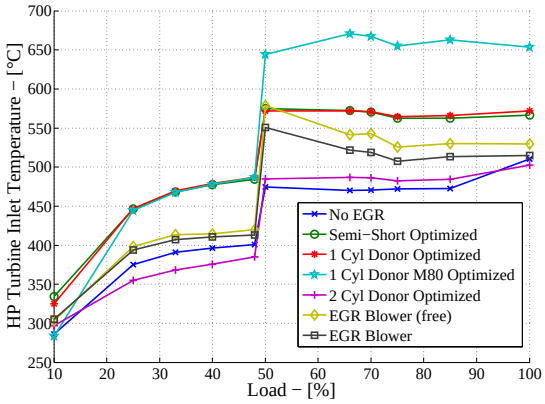

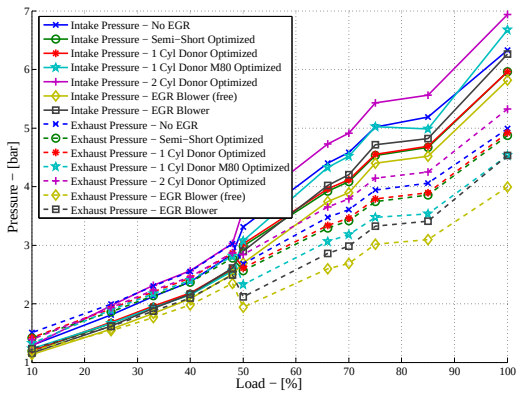

C.3.13 Semi-Short Route vs. EGR TC Short Route After Optimization

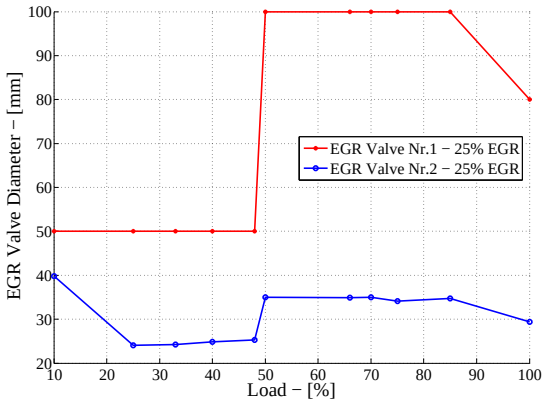

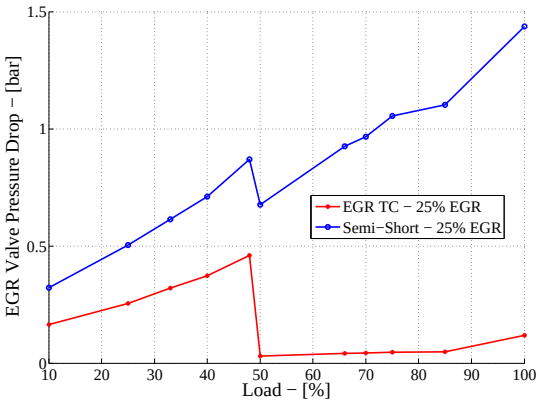

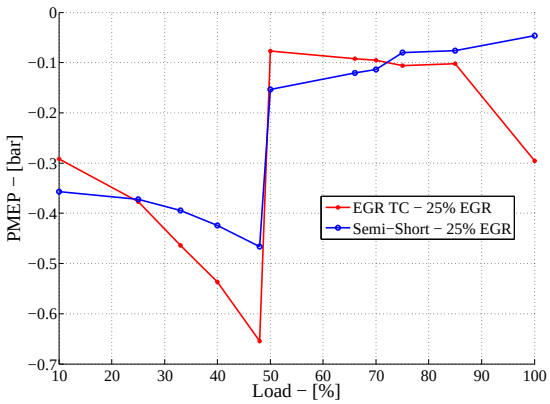

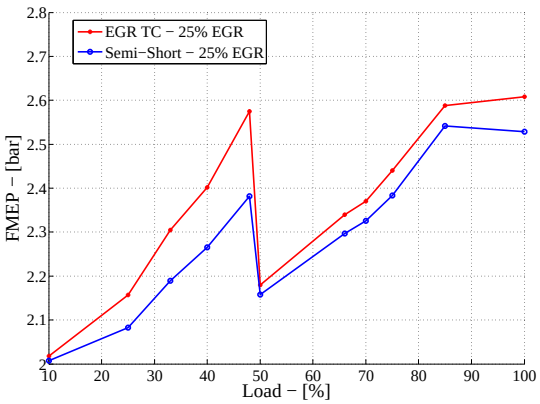

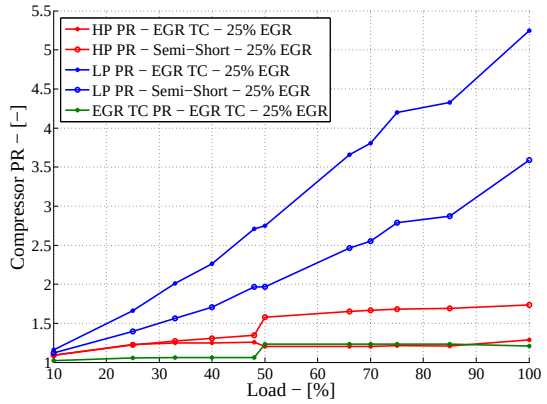
HP PR − EGR TC − 25% EGR
HP PR − Semi−Short − 25% EGR
LP PR − EGR TC − 25% EGR
LP PR − Semi−Short − 25% EGR
EGR TC PR − EGR TC − 25% EGR
Compressor PR − [−]
Load − [%]

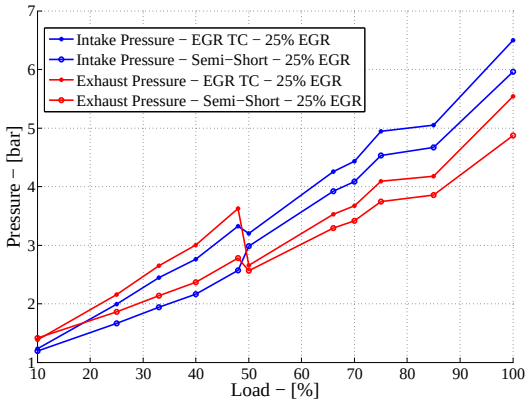
Intake Pressure − EGR TC − 25% EGR
Intake Pressure − Semi−Short − 25% EGR
Exhaust Pressure − EGR TC − 25% EGR
Exhaust Pressure − Semi−Short − 25% EGR
Pressure − [bar]
Load − [%]

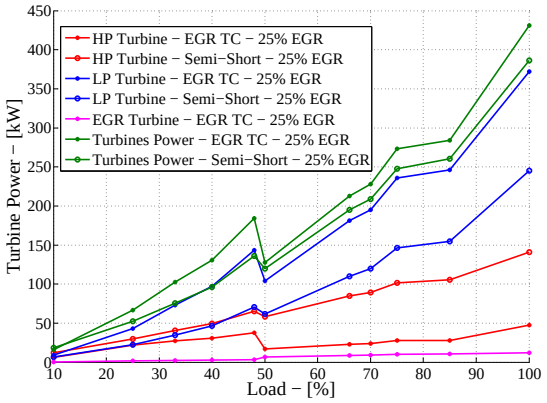
HP Turbine − EGR TC − 25% EGR
HP Turbine − Semi−Short − 25% EGR
LP Turbine − EGR TC − 25% EGR
LP Turbine − Semi−Short − 25% EGR
EGR Turbine − EGR TC − 25% EGR
Turbines Power − EGR TC − 25% EGR
Turbines Power − Semi−Short − 25% EGR
Turbine Power − [kW]
Load − [%]

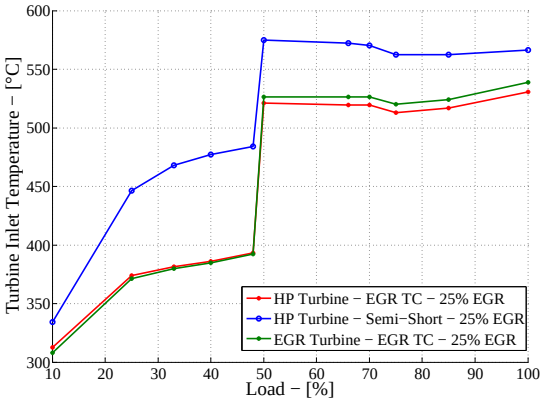
HP Turbine − EGR TC − 25% EGR
HP Turbine − Semi−Short − 25% EGR
EGR Turbine − EGR TC − 25% EGR
Turbine Inlet Temperature − [°C]
Load − [%]

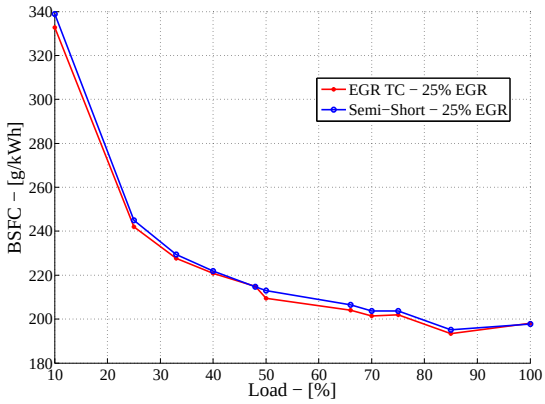
EGR TC − 25% EGR
Semi−Short − 25% EGR
BSFC − [g/kWh]
Load − [%]

C.4 Constant Intake Pressure And HP Turbine Inlet Temperature Analysis

C.4.1 Semi-Short Route

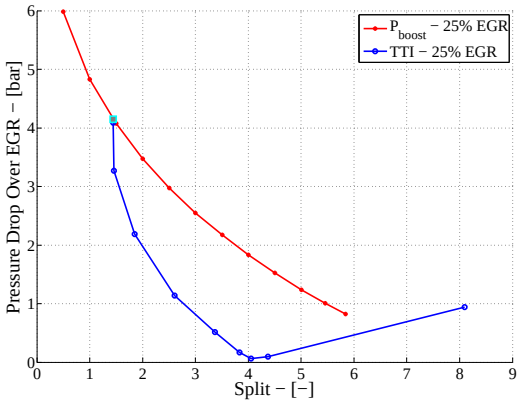

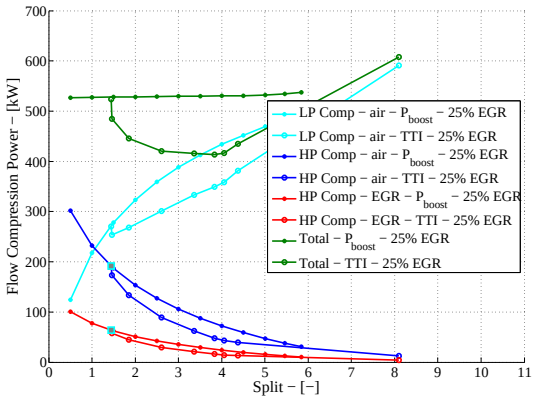

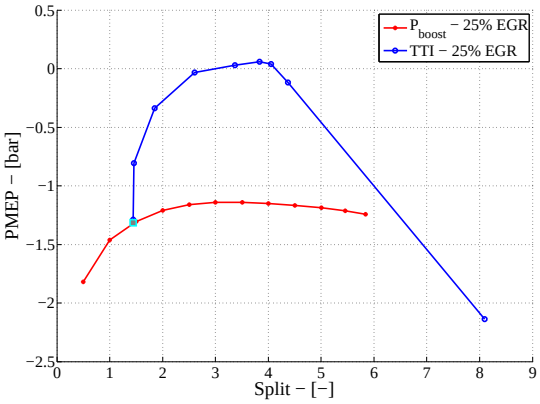

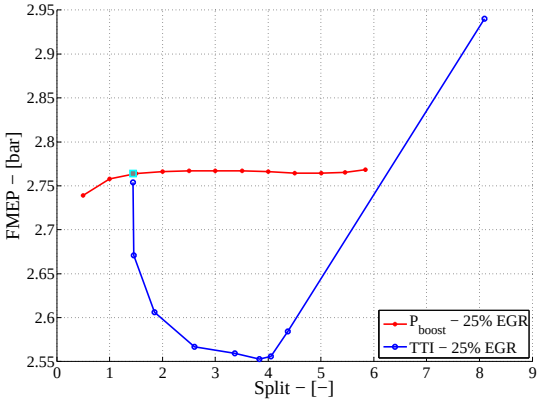

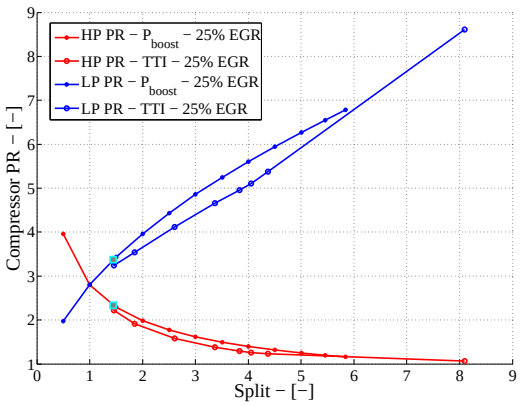

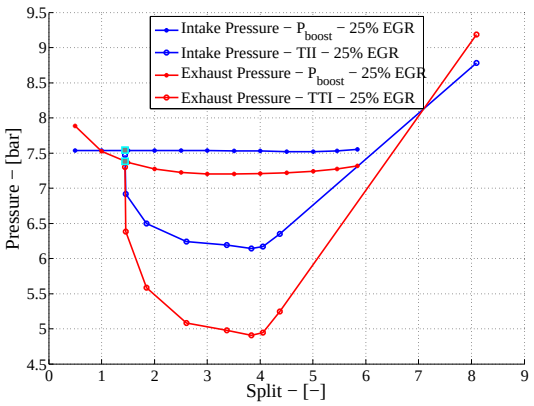

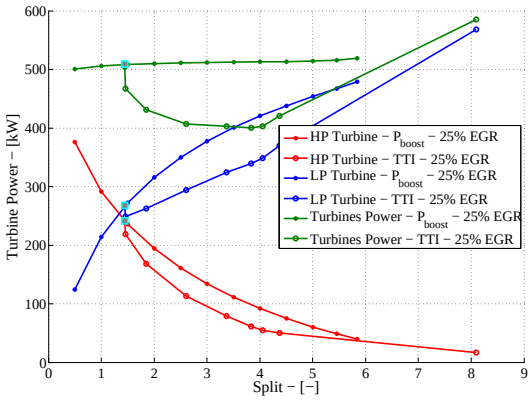
Turbine Power − [kW]
Split − [−]
HP Turbine − P_boost − 25% EGR
HP Turbine − TTI − 25% EGR
LP Turbine − P_boost − 25% EGR
LP Turbine − TTI − 25% EGR
Turbines Power − P_boost − 25% EGR
Turbines Power − TTI − 25% EGR

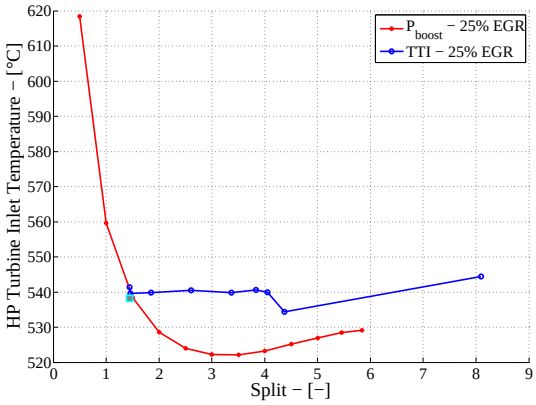
HP Turbine Inlet Temperature − [°C]
Split − [−]
P_boost − 25% EGR
TTI − 25% EGR

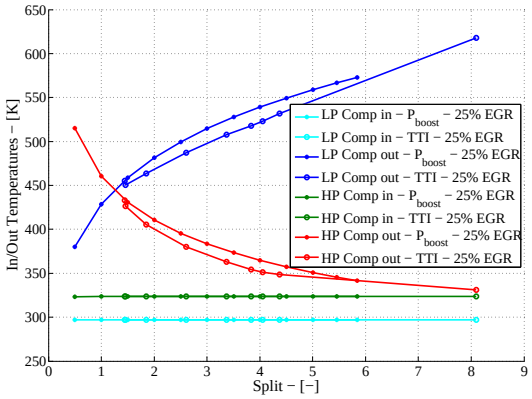
In/Out Temperatures − [K]
Split − [−]
LP Comp in − P_boost − 25% EGR
LP Comp in − TTI − 25% EGR
LP Comp out − P_boost − 25% EGR
LP Comp out − TTI − 25% EGR
HP Comp in − P_boost − 25% EGR
HP Comp in − TTI − 25% EGR
HP Comp out − P_boost − 25% EGR
HP Comp out − TTI − 25% EGR

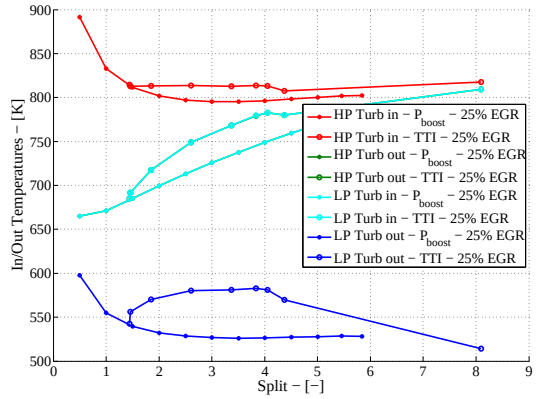
In/Out Temperatures − [K]
Split − [−]
HP Turb in − P_boost − 25% EGR
HP Turb in − TTI − 25% EGR
HP Turb out − P_boost − 25% EGR
HP Turb out − TTI − 25% EGR
LP Turb in − P_boost − 25% EGR
LP Turb in − TTI − 25% EGR
LP Turb out − P_boost − 25% EGR
LP Turb out − TTI − 25% EGR

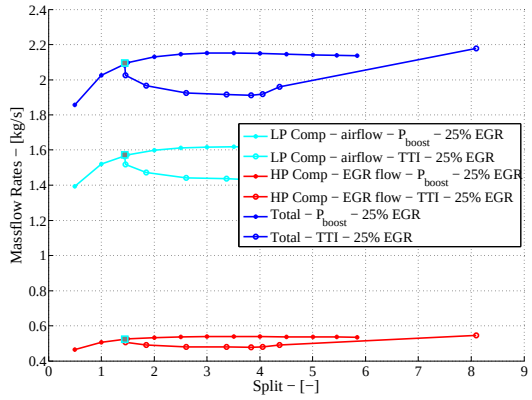
Massflow Rates − [kg/s]
Split − [−]
LP Comp − airflow − P_boost − 25% EGR
LP Comp − airflow − TTI − 25% EGR
HP Comp − EGR flow − P_boost − 25% EGR
HP Comp − EGR flow − TTI − 25% EGR
Total − P_boost − 25% EGR
Total − TTI − 25% EGR

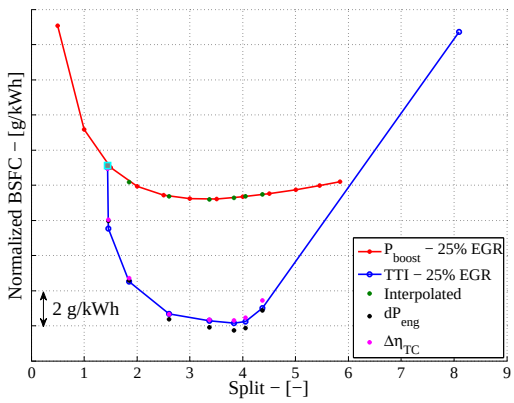
Normalized BSFC − [g/kWh]
Split − [−]
2 g/kWh
P_boost − 25% EGR
TTI − 25% EGR
Interpolated
dP_eng
Δη_TC

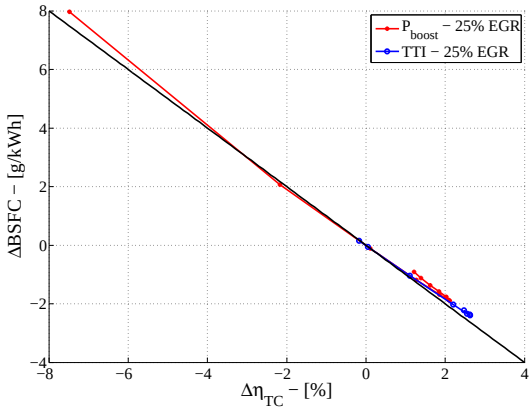

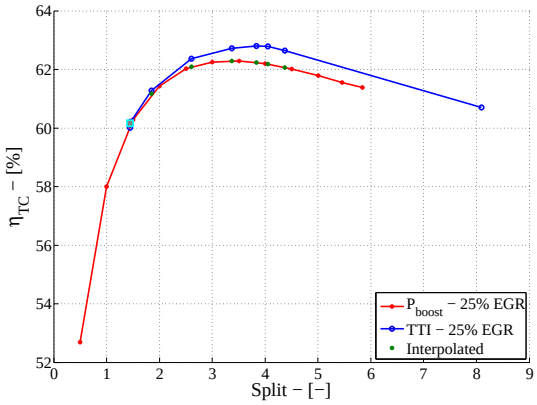

C.4.2 EGR Blower Short Route

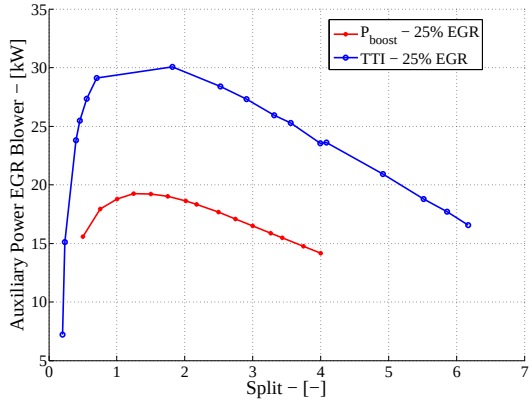

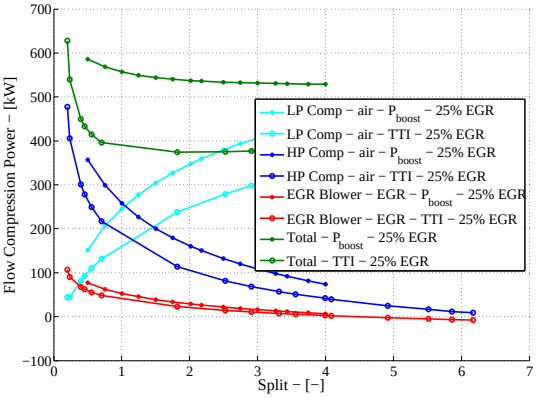

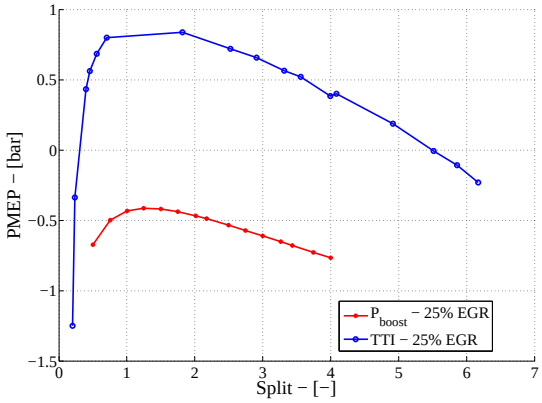

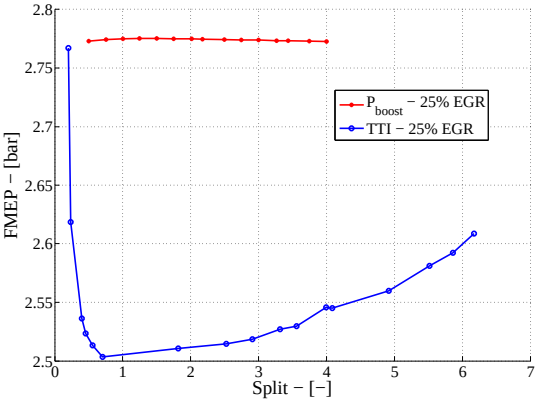

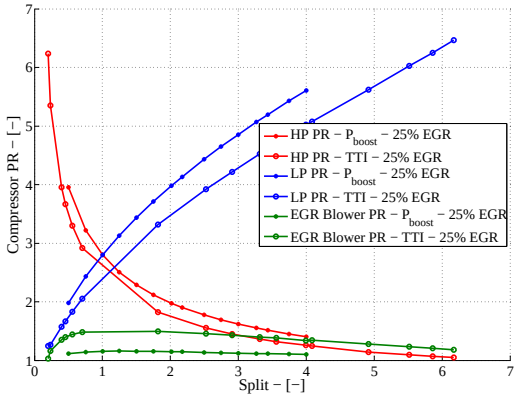
Compressor PR − [−]
Split − [−]
HP PR − P_boost − 25% EGR
HP PR − TTI − 25% EGR
LP PR − P_boost − 25% EGR
LP PR − TTI − 25% EGR
EGR Blower PR − P_boost − 25% EGR
EGR Blower PR − TTI − 25% EGR

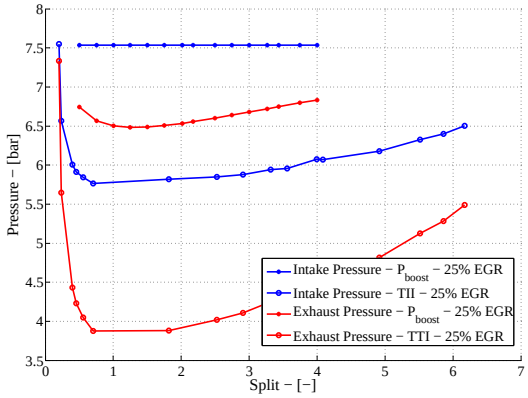
Pressure − [bar]
Split − [−]
Intake Pressure − P_boost − 25% EGR
Intake Pressure − TII − 25% EGR
Exhaust Pressure − P_boost − 25% EGR
Exhaust Pressure − TTI − 25% EGR

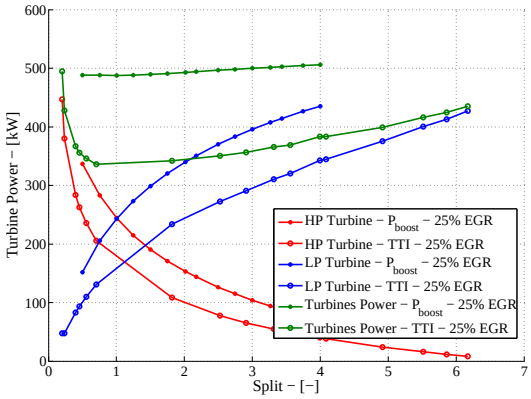
Turbine Power − [kW]
Split − [−]
HP Turbine − P_boost − 25% EGR
HP Turbine − TTI − 25% EGR
LP Turbine − P_boost − 25% EGR
LP Turbine − TTI − 25% EGR
Turbines Power − P_boost − 25% EGR
Turbines Power − TTI − 25% EGR

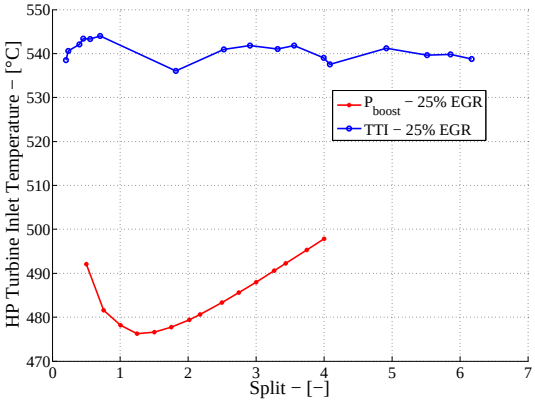
HP Turbine Inlet Temperature − [°C]
Split − [−]
P_boost − 25% EGR
TTI − 25% EGR

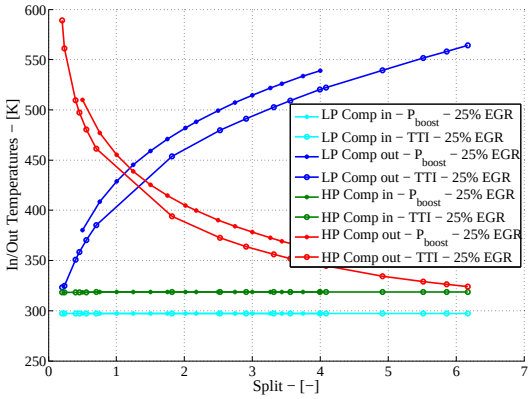
In/Out Temperatures − [K]
Split − [−]
LP Comp in − P_boost − 25% EGR
LP Comp in − TTI − 25% EGR
LP Comp out − P_boost − 25% EGR
LP Comp out − TTI − 25% EGR
HP Comp in − P_boost − 25% EGR
HP Comp in − TTI − 25% EGR
HP Comp out − P_boost − 25% EGR
HP Comp out − TTI − 25% EGR

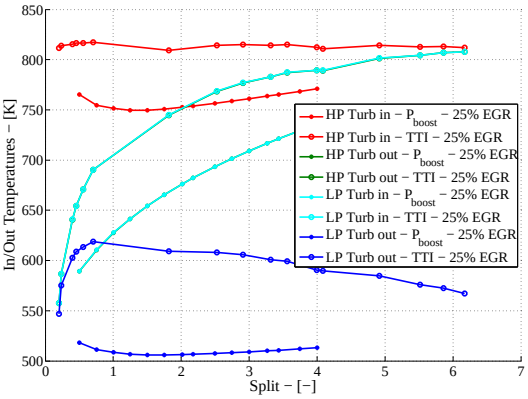
In/Out Temperatures − [K]
Split − [−]
HP Turb in − P_boost − 25% EGR
HP Turb in − TTI − 25% EGR
HP Turb out − P_boost − 25% EGR
HP Turb out − TTI − 25% EGR
LP Turb in − P_boost − 25% EGR
LP Turb in − TTI − 25% EGR
LP Turb out − P_boost − 25% EGR
LP Turb out − TTI − 25% EGR

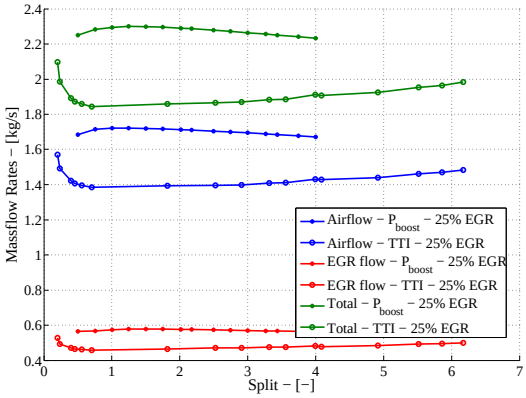

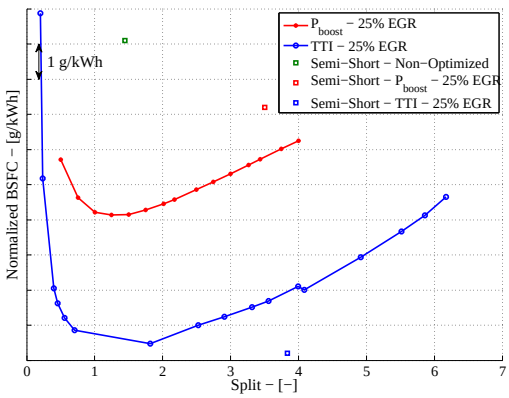

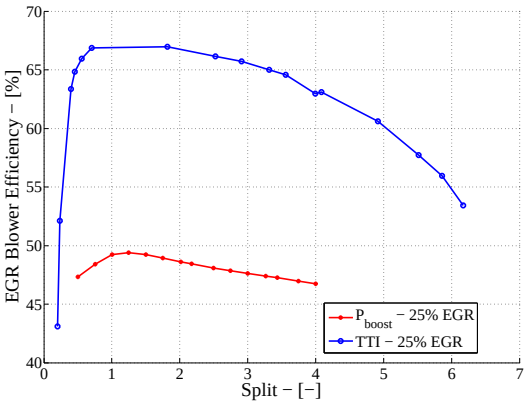

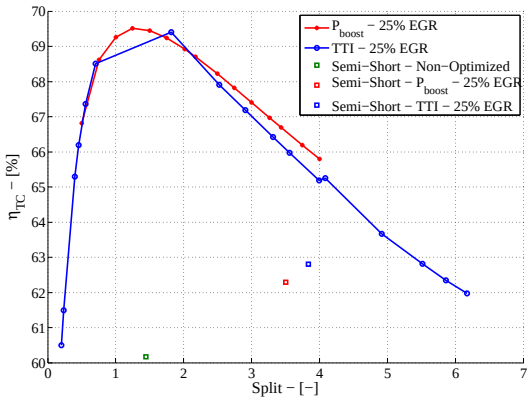

C.4.3 Semi-Short Route vs. EGR Blower Short Route

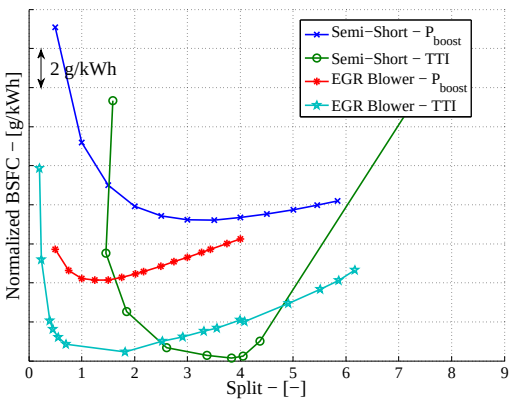

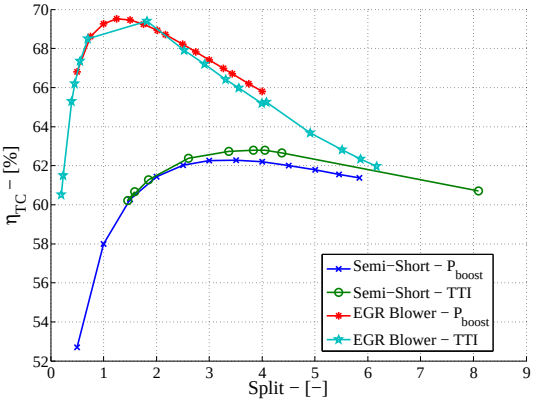

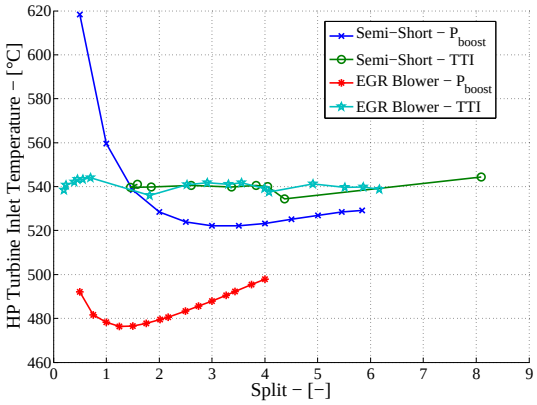
HP Turbine Inlet Temperature − [°C]
Split − [−]
Semi−Short − P boost
Semi−Short − TTI
EGR Blower − P boost
EGR Blower − TTI

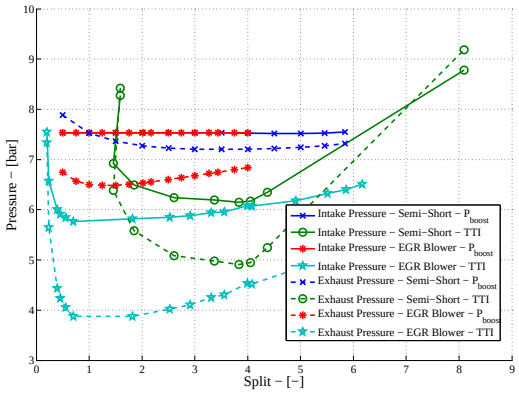
Pressure − [bar]
Split − [−]
Intake Pressure − Semi−Short − P boost
Intake Pressure − Semi−Short − TTI
Intake Pressure − EGR Blower − P boost
Intake Pressure − EGR Blower − TTI
Exhaust Pressure − Semi−Short − P boost
Exhaust Pressure − Semi−Short − TTI
Exhaust Pressure − EGR Blower − P boost
Exhaust Pressure − EGR Blower − TTI

C.5 HP Turbine Inlet Temperature Analysis

C.5.1 EGR Blower Short Route

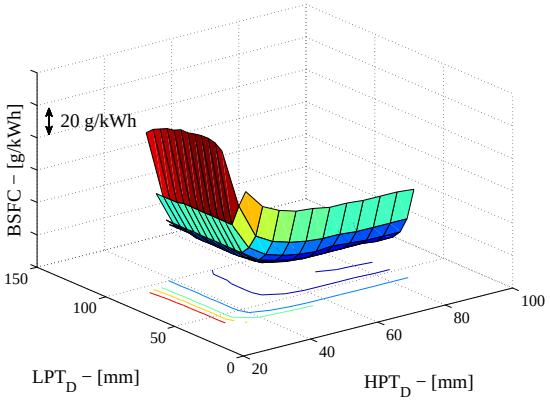

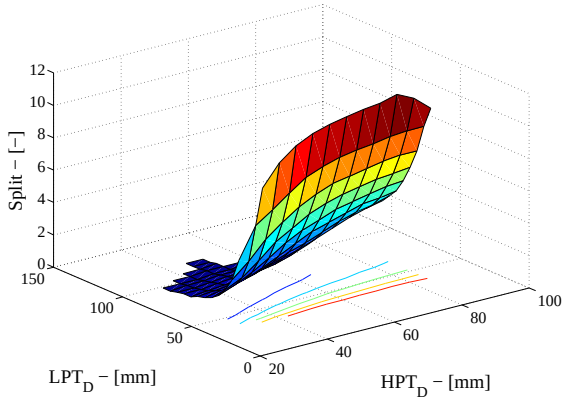

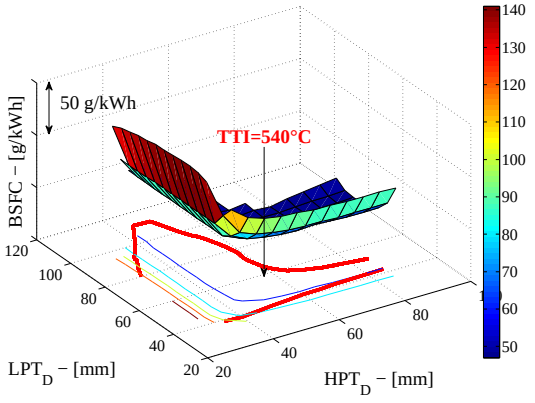

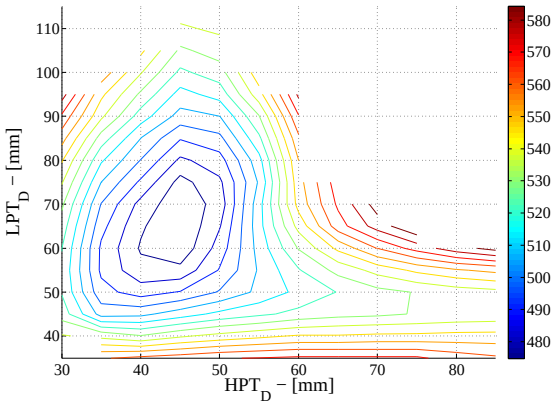

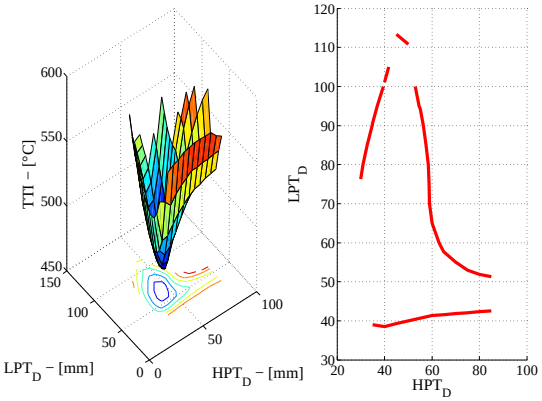

C.6 Future Test Bench Configuration Analysis

C.6.1 1 Donor Cylinder Semi-Short Route Throttle Diameters Proposal

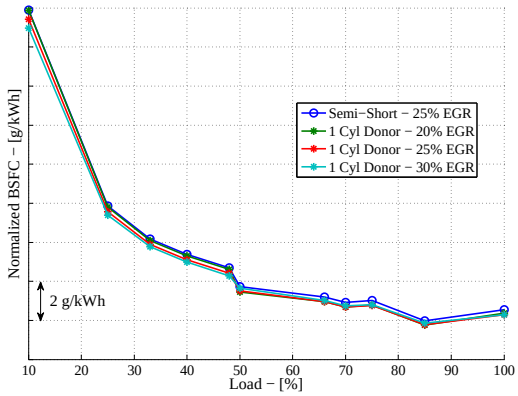

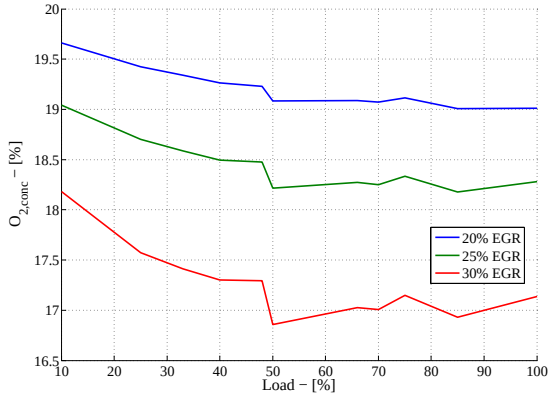

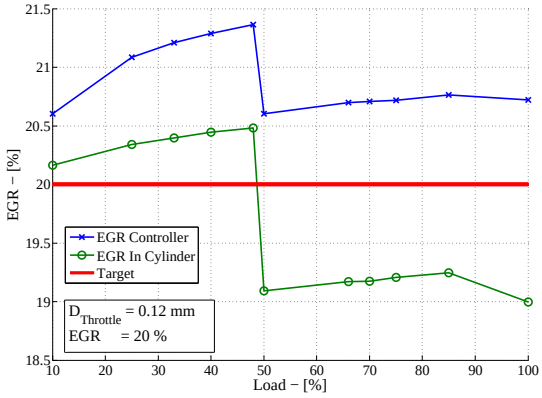

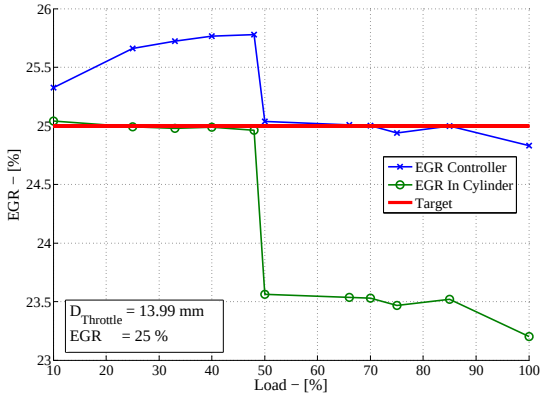

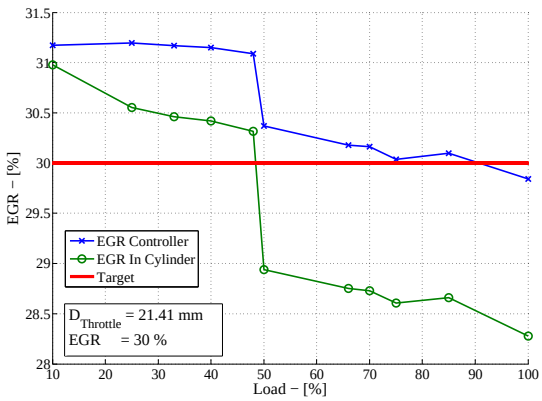

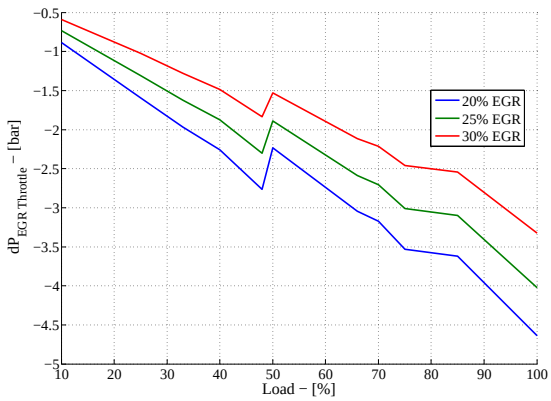

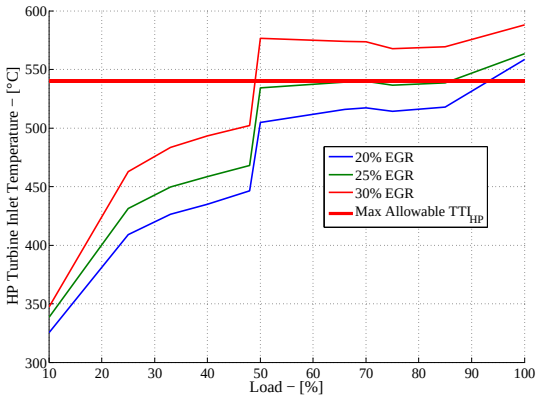

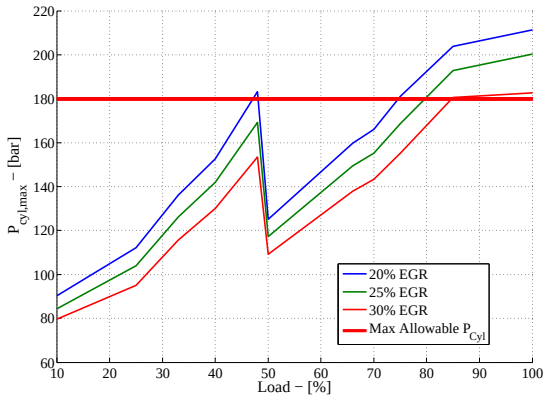

C.6.2 1 Donor Cylinder Semi-Short Route Chosen Throttle Diameter

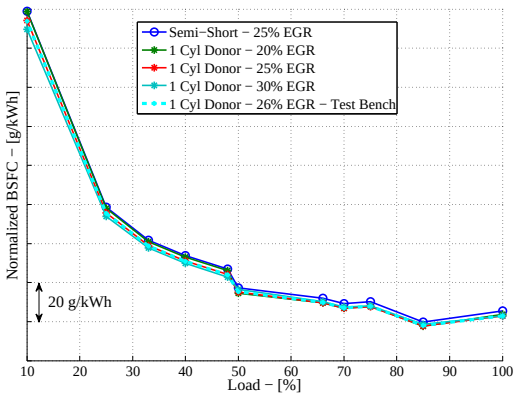

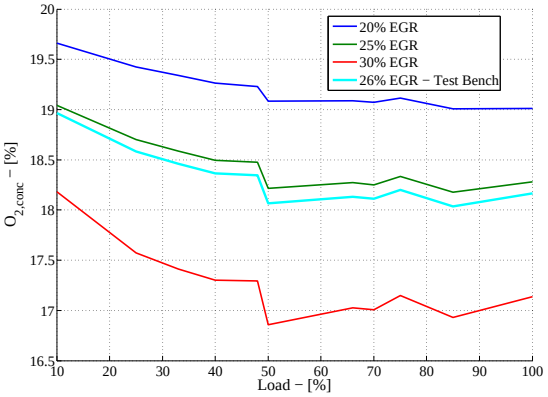

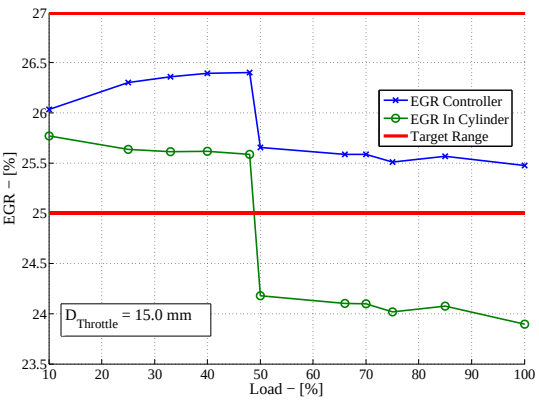

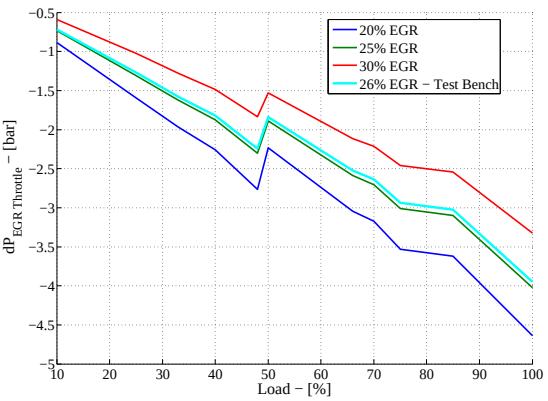

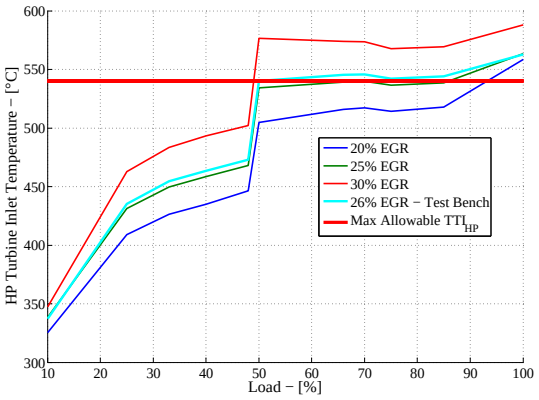

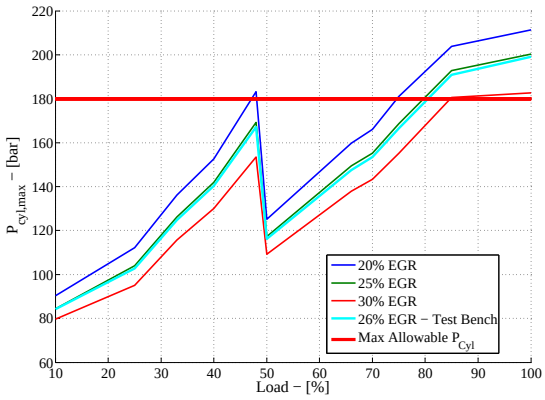

C.6.3 1 Donor Cylinder Semi-Short Route Chosen Throttle Diameter And New TC Specifications vs. Semi-Short Route Optimized

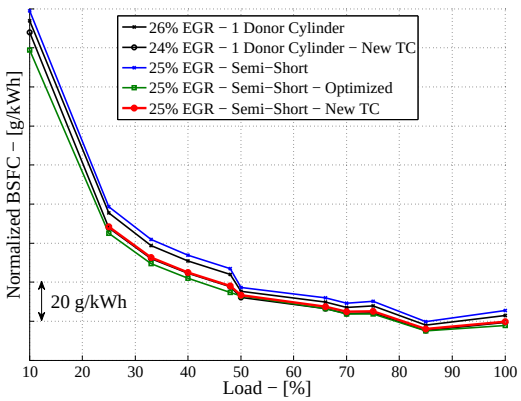

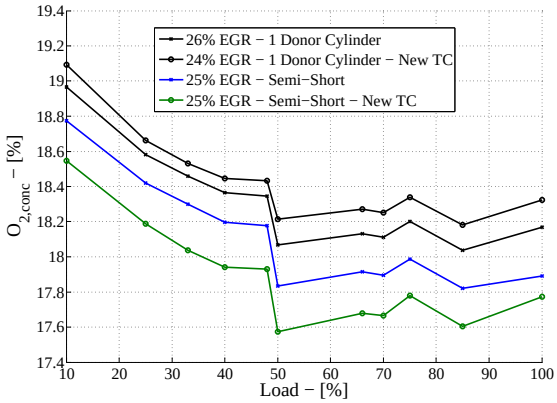

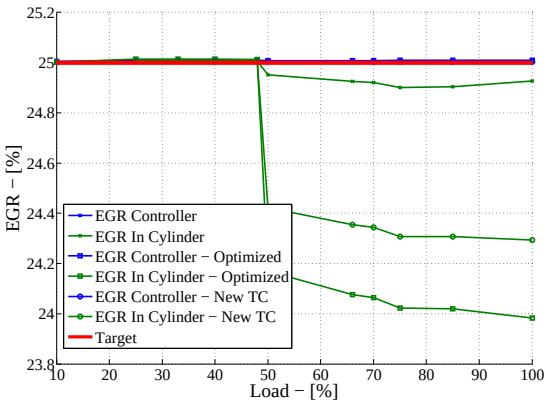

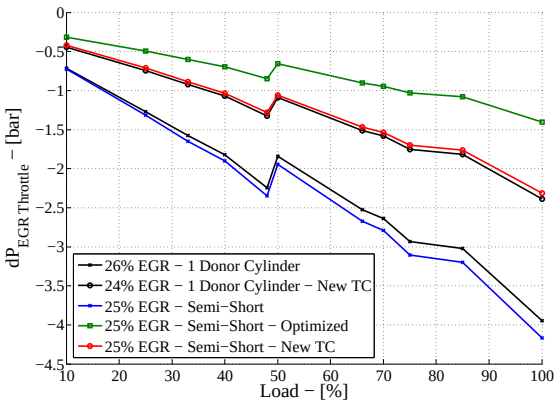

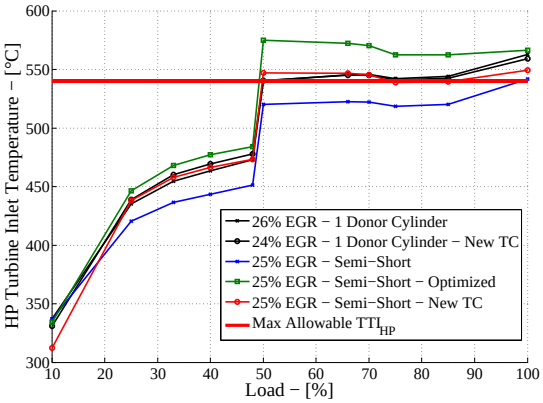
HP Turbine Inlet Temperature − [°C]
Load − [%]
26% EGR − 1 Donor Cylinder
24% EGR − 1 Donor Cylinder − New TC
25% EGR − Semi−Short
25% EGR − Semi−Short − Optimized
25% EGR − Semi−Short − New TC
Max Allowable TTI_HP

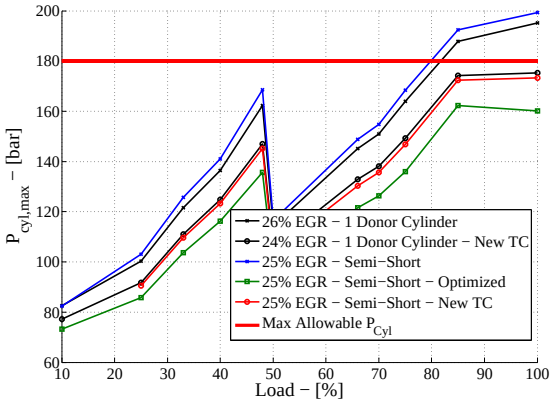
P cyl,max − [bar]
Load − [%]
26% EGR − 1 Donor Cylinder
24% EGR − 1 Donor Cylinder − New TC
25% EGR − Semi−Short
25% EGR − Semi−Short − Optimized
25% EGR − Semi−Short − New TC
Max Allowable P_Cyl

C.7 NO_x Analysis

C.7.1 Calibration

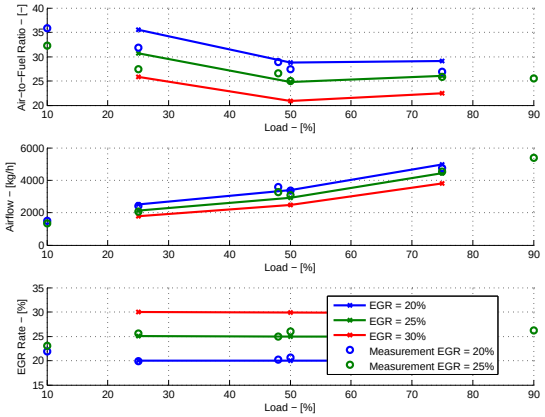

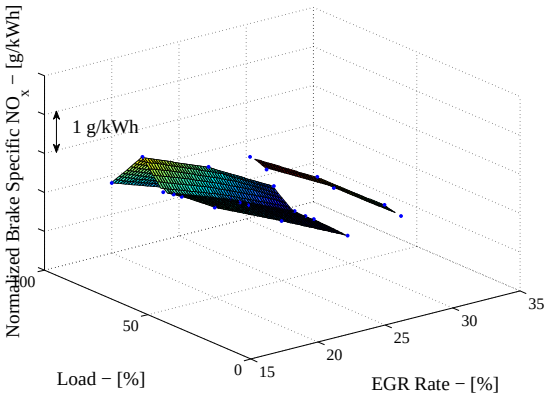

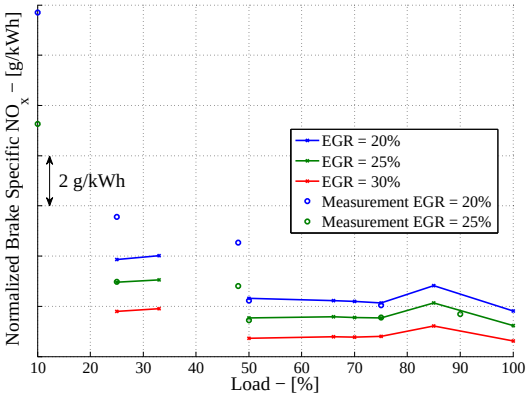

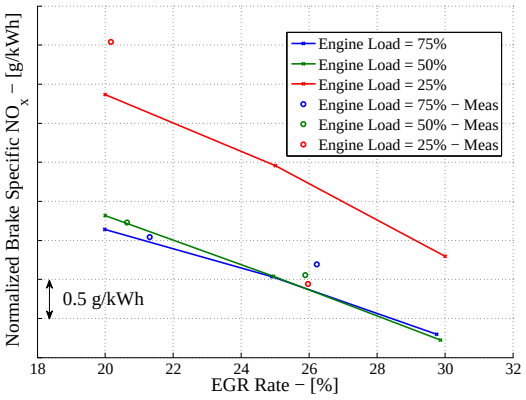

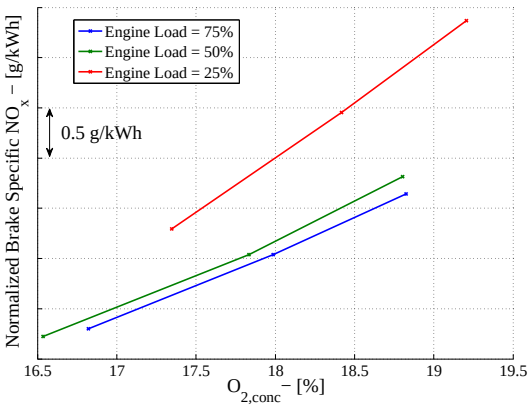

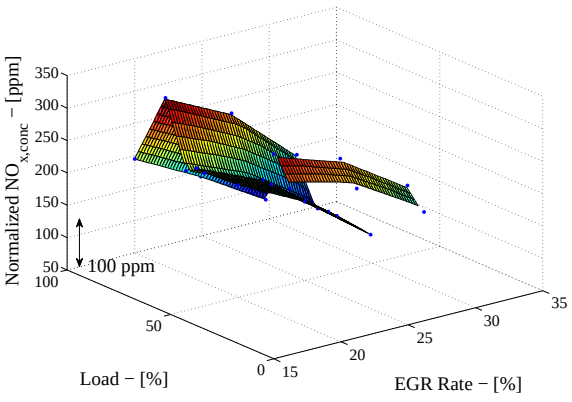

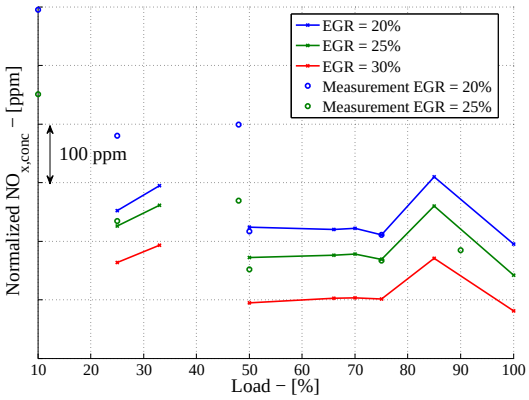

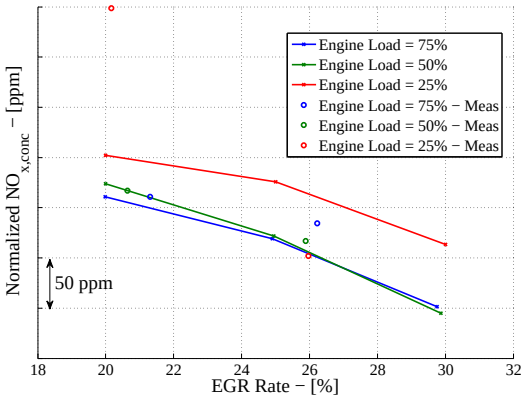

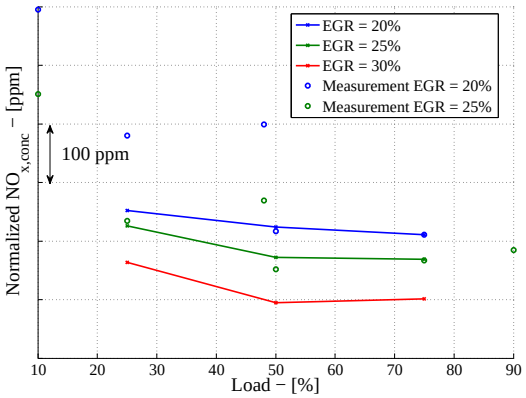

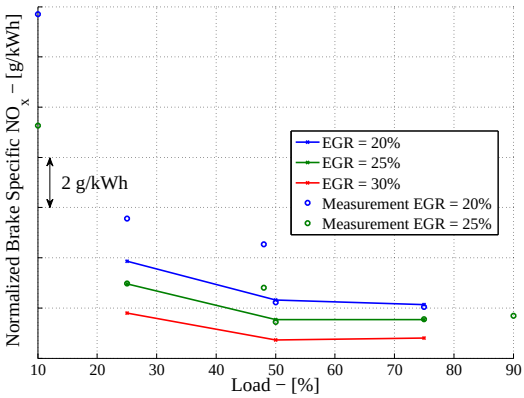

C.7.2 Start Of Injection And Rail Pressure Variation

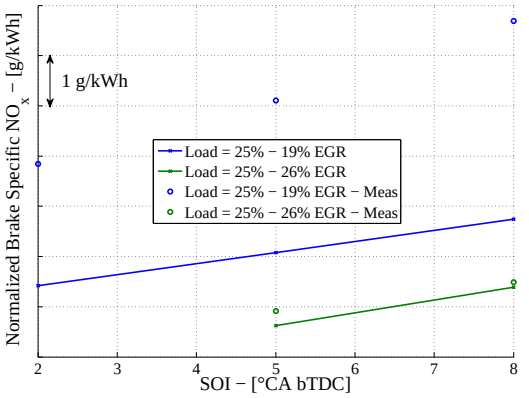

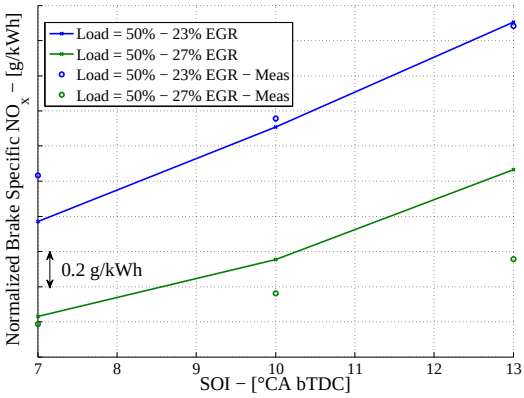

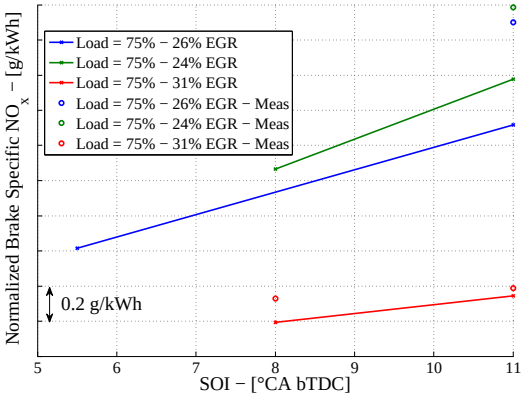
Load = 75% − 26% EGR
Load = 75% − 24% EGR
Load = 75% − 31% EGR
Load = 75% − 26% EGR − Meas
Load = 75% − 24% EGR − Meas
Load = 75% − 31% EGR − Meas
0.2 g/kWh
Normalized Brake Specific NO x − [g/kWh]
SOI − [°CA bTDC]

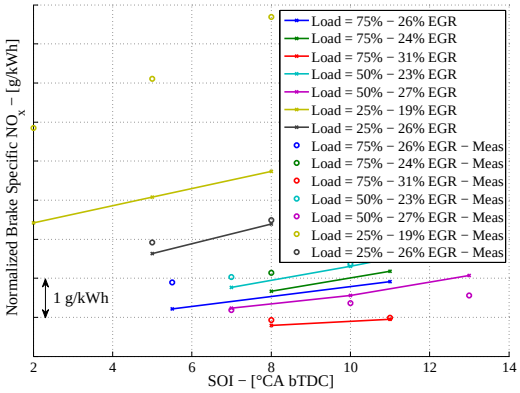
Load = 75% − 26% EGR
Load = 75% − 24% EGR
Load = 75% − 31% EGR
Load = 50% − 23% EGR
Load = 50% − 27% EGR
Load = 25% − 19% EGR
Load = 25% − 26% EGR
Load = 75% − 26% EGR − Meas
Load = 75% − 24% EGR − Meas
Load = 75% − 31% EGR − Meas
Load = 50% − 23% EGR − Meas
Load = 50% − 27% EGR − Meas
Load = 25% − 19% EGR − Meas
Load = 25% − 26% EGR − Meas
1 g/kWh
Normalized Brake Specific NO x − [g/kWh]
SOI − [°CA bTDC]

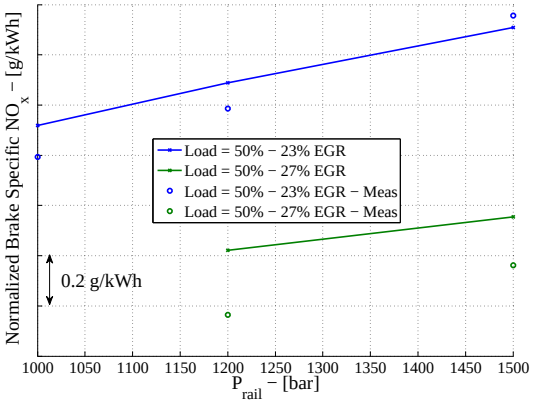
Load = 50% − 23% EGR
Load = 50% − 27% EGR
Load = 50% − 23% EGR − Meas
Load = 50% − 27% EGR − Meas
0.2 g/kWh
Normalized Brake Specific NO x − [g/kWh]
P rail − [bar]

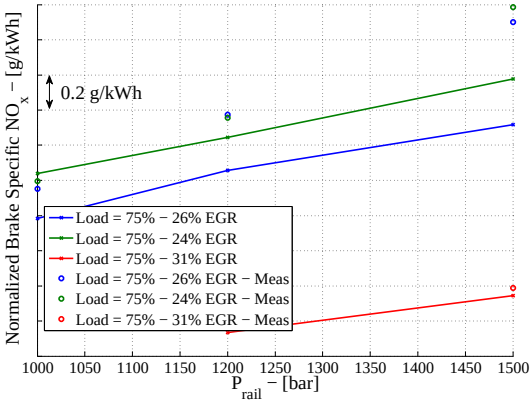
0.2 g/kWh
Load = 75% − 26% EGR
Load = 75% − 24% EGR
Load = 75% − 31% EGR
Load = 75% − 26% EGR − Meas
Load = 75% − 24% EGR − Meas
Load = 75% − 31% EGR − Meas
Normalized Brake Specific NO x − [g/kWh]
P rail − [bar]

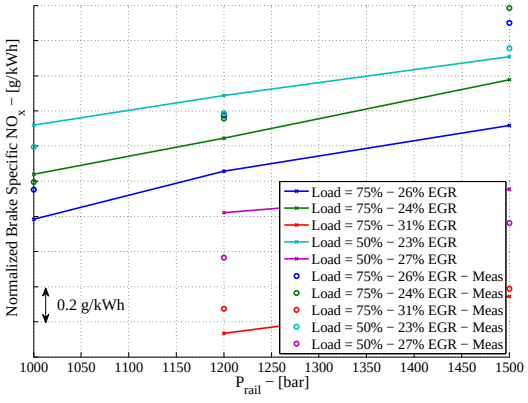
Load = 75% − 26% EGR
Load = 75% − 24% EGR
Load = 75% − 31% EGR
Load = 50% − 23% EGR
Load = 50% − 27% EGR
Load = 75% − 26% EGR − Meas
Load = 75% − 24% EGR − Meas
Load = 75% − 31% EGR − Meas
Load = 50% − 23% EGR − Meas
Load = 50% − 27% EGR − Meas
0.2 g/kWh
Normalized Brake Specific NO x − [g/kWh]
P rail − [bar]

C.7.3 BSFC vs. BSNO$_x$ Trade-Off

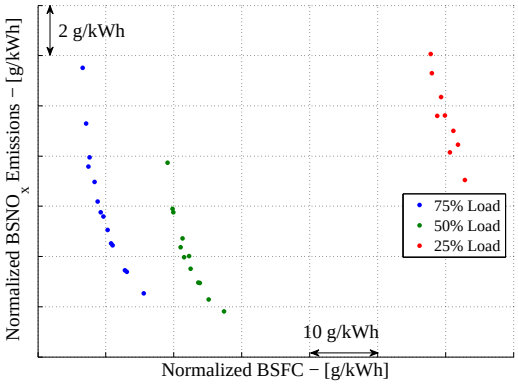

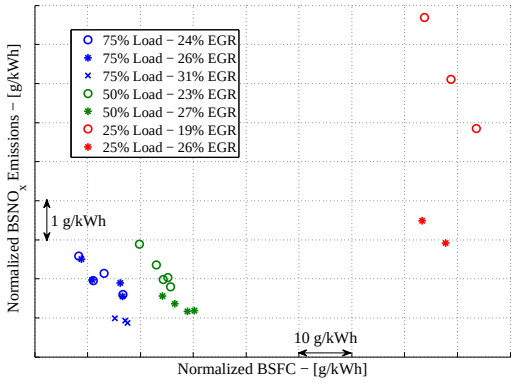

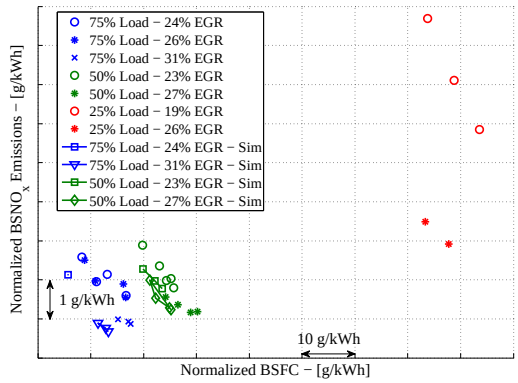

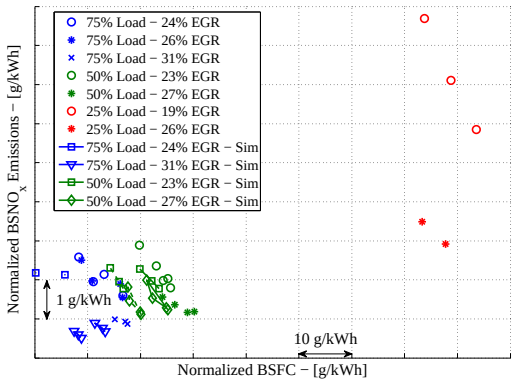

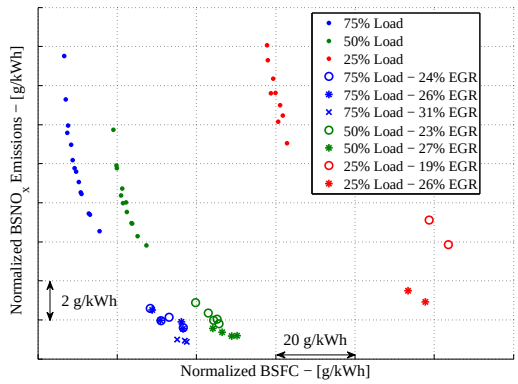

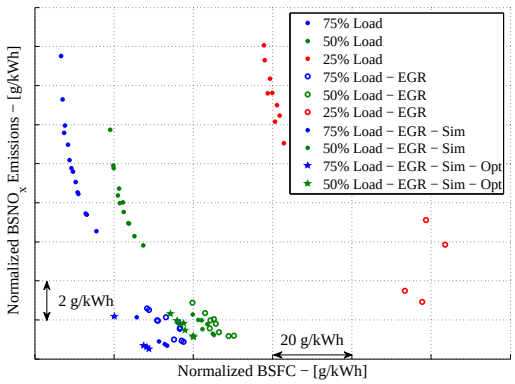

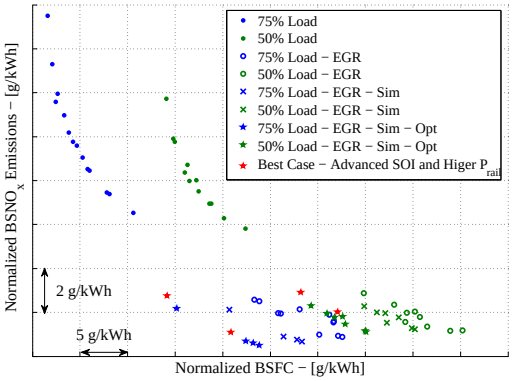
75% Load
50% Load
75% Load − EGR
50% Load − EGR
75% Load − EGR − Sim
50% Load − EGR − Sim
75% Load − EGR − Sim − Opt
50% Load − EGR − Sim − Opt
Best Case − Advanced SOI and Higer P rail
Normalized BSNO x Emissions − [g/kWh]
2 g/kWh
5 g/kWh
Normalized BSFC − [g/kWh]

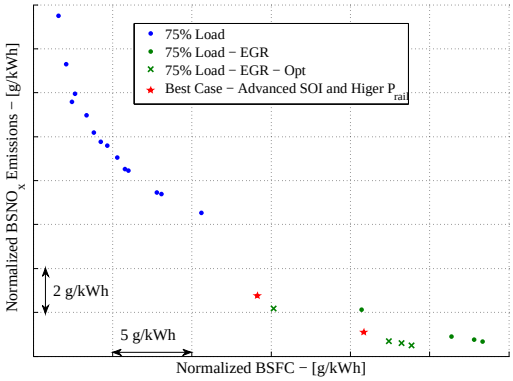
75% Load
75% Load − EGR
75% Load − EGR − Opt
Best Case − Advanced SOI and Higer P rail
Normalized BSNO x Emissions − [g/kWh]
2 g/kWh
5 g/kWh
Normalized BSFC − [g/kWh]

C.8 EGR Setups Evaluation

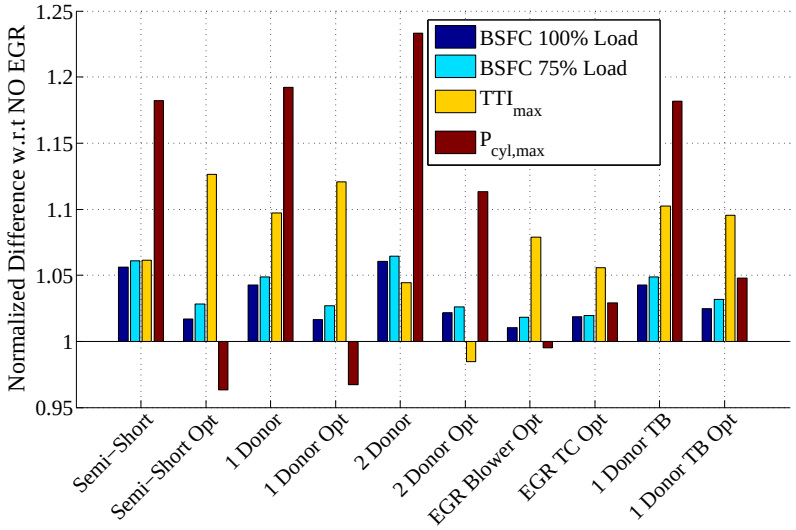

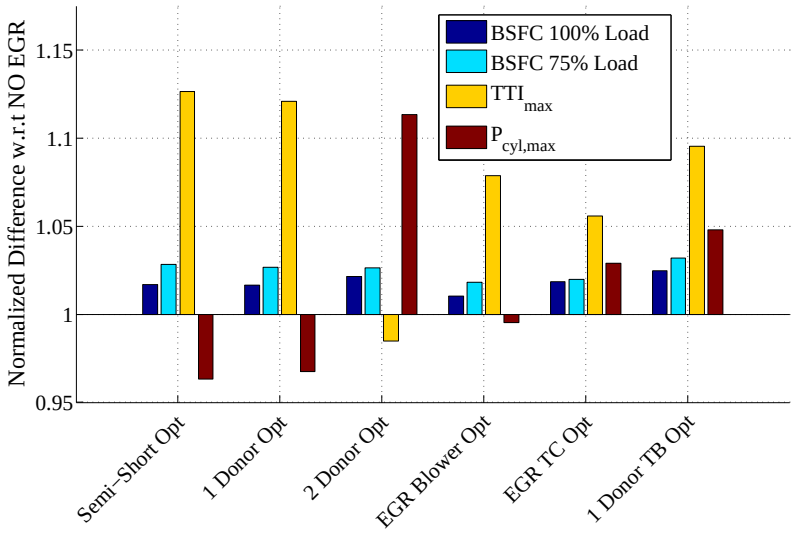

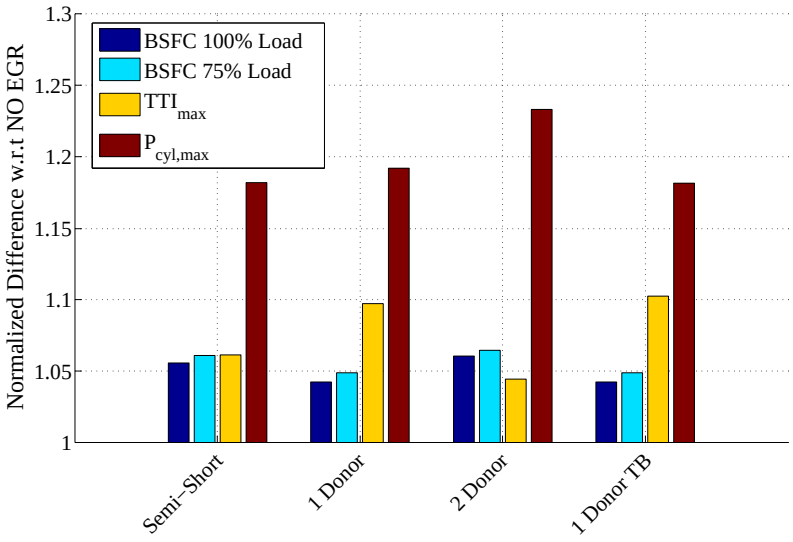
Normalized Difference w.r.t NO EGR
1.3
1.25
1.2
1.15
1.1
1.05
1
BSFC 100% Load
BSFC 75% Load
TTI max
P cyl,max
Semi−Short
1 Donor
2 Donor
1 Donor TB